








EX LIBRIS  
UNIVERSITATIS  
ALBERTENSIS

---

The Bruce Peel  
Special Collections  
Library





Digitized by the Internet Archive  
in 2025 with funding from  
University of Alberta Library

<https://archive.org/details/0162014938250>











**University of Alberta**

**Library Release Form**

**Name of Author:** Michelle Kenny

**Title of Thesis:** Optimization and Control Studies for Ammonia Production

**Degree:** Master of Science

**Year this Degree Granted:** 2001

Permission is hereby granted to the University of Alberta Library to reproduce single copies of this thesis and to lend or sell such copies for private, scholarly or scientific research purposes only.

The author reserves all other publication and other rights in association with the copyright in the thesis, and except as herein before provided, neither the thesis nor any substantial portion thereof may be printed or otherwise reproduced in any material form whatever without the author's prior written permission.







**University of Alberta**

**Optimization and Control Studies for Ammonia Production**

by

Michelle Kenny



A thesis submitted to the Faculty of Graduate Studies and Research in partial  
fulfillment of the requirements for the degree of Master of Science

in

Process Control

Department of Chemical and Materials Engineering

Edmonton, Alberta

Fall 2001





**University of Alberta**

**Faculty of Graduate Studies and Research**

The undersigned certify that they have read, and recommend to the Faculty of Graduate Studies and Research for acceptance, a thesis entitled Optimization and Control Studies for Ammonia Production submitted by Michelle Kenny in partial fulfillment of the requirements for the degree of Master of Science in Process Control.





# ABSTRACT

The need for nitrogen fertilizer is expected to significantly increase over the next twenty years<sup>[40]</sup>. Optimization and control may provide chemical manufacturers a means to support, in part, these increased demands. This thesis explores automation prospects and technologies to exploit these opportunities in the ammonia synthesis loop at Saskferco Products Inc. Existing research in this field is not exhaustive and it is not apparent the most appropriate control technologies have been implemented.

To accomplish these objectives, a dynamic first principles process model is developed and fit to plant data. Using a rigorous nonlinear optimizer, the optimal operation of the unit is evaluated. Enforcement of the optimal converter bed inlet temperatures is successfully accomplished using linear PID and LQR controllers. Results clearly identify the opportunity for improved ammonia conversion, with 70 % of these benefits achievable using a subset of the unit optimizer and conventional controller methods.





# CONTENTS

<b>1. INTRODUCTION</b>	<b>1</b>
1.1. Process Description.....	2
1.2. Process Considerations.....	4
1.3. Process Automation .....	4
1.4. Thesis Scope.....	5
1.5. Thesis Conventions .....	6
<b>2. AMMONIA PROCESS MODEL</b>	<b>7</b>
2.1. Characteristics of Conversion .....	8
2.2. Constitutive Relationships .....	11
2.2.1. Process Inputs and Conditioning.....	11
2.2.2. Chemical Reactions.....	12
2.2.3. Reaction Kinetics.....	13
2.2.4. Heat of Reaction .....	14
2.2.5. Redlich-Kwong-Soave Equation of State.....	14
2.2.6. Steam Calculations .....	15
2.2.7. Heat Transfer .....	16
2.2.8. Flow Through Valves and Process.....	17
2.2.9. Vessel Hold-Up .....	19
2.3. Material & Energy Balances .....	20
2.4. Model Implementation.....	22
2.5. Model Validation .....	22
2.6. Discussion .....	28
<b>3. PARAMETER UPDATES USING HISTORICAL DATA</b>	<b>31</b>
3.1. Parameter Selection.....	31
3.2. Least Squares Regression Formulation.....	33
3.2.1. Sum of Squares.....	34
3.2.2. Recursive Least Squares.....	35
3.3. Results .....	37
3.4. Discussion .....	39
<b>4. PROCESS OPERATION OPTIMIZATION</b>	<b>41</b>
4.1. Optimization Problem Formulation .....	41
4.2. Sensitivity Analysis.....	42
4.3. Optimization Studies.....	45
4.3.1. Normal Operation.....	45
4.3.2. Changing Process Conditions.....	48
4.3.3. Degraded Catalyst .....	52
4.4. Summary of Results .....	53
<b>5. CONTROLLER SYNTHESIS</b>	<b>55</b>
5.1. State Space Analysis .....	56
5.2. BFW Level Implementation.....	58
5.3. Multi-Loop PID Control .....	61
5.3.1. Multi-Loop Design .....	61
5.3.2. Multi-Loop Tuning.....	62
5.3.3. Multi-Loop Results.....	64
5.4. Linear Multi-Variable Control .....	75
5.4.1. MVC Design.....	75
5.4.2. MVC Tuning .....	76





5.4.3. MVC Results .....	77
5.5. Discussion .....	85
<b>6. SUMMARY AND CONCLUSIONS</b>	<b>88</b>
6.1. Area of Study .....	88
6.2. Results .....	89
6.3. Conclusions .....	90
6.4. Recommendations .....	91
<b>7. BIBLIOGRAPHY</b>	<b>92</b>
<b>A. PLANT DATA</b>	<b>96</b>
<b>B. GAS CONSTANTS AND EQUATIONS</b>	<b>116</b>
<b>C. MATLAB, SIMULINK AND MAPLE CODE</b>	<b>118</b>
<b>D. PROCESS MODEL</b>	<b>122</b>
D.1 Calculations .....	122
D.2 Results .....	123
<b>E. PARAMETER UPDATE RESULTS</b>	<b>129</b>
E.1 Dependent Variables .....	129
E.2 Intermediate Variables .....	130
E.3 Results .....	130
<b>F. PROCESS OPTIMIZATION</b>	<b>133</b>
<b>G. CONTROLLER SYNTHESIS RESULTS</b>	<b>136</b>
G.1 Controller Variables .....	136
G.2 Open Loop Responses .....	138
G.3 State Space Matrices .....	141



# LIST OF TABLES

Table 2-1	Operating Conditions .....	8
Table 2-2	Plant Input Variables .....	11
Table 2-3	Fitted Parameters .....	23
Table 2-4	Catalyst Specifications .....	24
Table 3-1	Catalyst Manufacturer Parameter Calculations for R1B1 .....	32
Table 3-2	Model Parameters with Calculated Optimum Temperature .....	33
Table 3-3	Variable and Parameter Results for Parameter Update Problem .....	38
Table 4-1	R1B1 Impact of Temperature Deviation from Optimum .....	45
Table 4-2	Winter vs. Summer Optimal Operation .....	52
Table 4-3	Ammonia Conversion: Optimal Performance Comparisons .....	54
Table 5-1	PID Pairing .....	62
Table 5-2	PID Tuning .....	63
Table 5-3	Comparative Controller Behaviour with $MV_4$ Saturated .....	86
Table 5-4	Comparative Controller Behaviour with $MV_1$ Saturated .....	86
Table 5-5	Comparative Controller Characteristics .....	87
Table A-1	Plant Data .....	96
Table B-1	Gas Component Properties .....	116
Table B-2	Gas Component Shomate Constants from 298 K to 1400K .....	116
Table C-1	Process Simulation Files .....	118
Table C-2	RKS EOS Calculations .....	120
Table C-3	Catalyst Effectiveness Parameter Update Files .....	120
Table C-4	Process Optimization Files .....	121
Table C-5	State Space Matrices .....	121
Table C-6	Process Control Simulations .....	121
Table E-1	Parameter Update Constraint Variables .....	129
Table F-1	Dependent Variables per Equality Equations .....	133
Table G-1	State Space Variables .....	136
Table G-2	Manipulated Variables .....	136
Table G-3	Control Variables .....	137
Table G-4	Disturbance Variables .....	137
Table G-5	Local Value of $A(x,u,w)$ Matrix .....	141
Table G-6	Local Value of $B(x,u,w)$ Matrix .....	142
Table G-7	C Matrix .....	143
Table G-8	Local Value of $G(x,u,w)$ Matrix .....	144
Table G-9	Local Value of $A(x,u,w)$ Matrix – Reduced and Scaled .....	145
Table G-10	Local Value of $B(x,u,w)$ Matrix – Reduced and Scaled .....	146
Table G-11	C Matrix – Reduced and Scaled .....	146





# LIST OF FIGURES

Figure 1-1	Ammonia Plant Overview .....	1
Figure 1-2	Process Diagram .....	3
Figure 2-1	Equilibrium Constant vs. Conversion Temperature .....	9
Figure 2-2	Frequency Factor vs. Conversion Temperature .....	9
Figure 2-3	Effect of Ammonia Concentration on Reaction Rate .....	10
Figure 2-4	Ammonia Conversion vs. Inlet Temperature to R1B1 .....	10
Figure 2-5	Knife Gate Valve Area .....	17
Figure 2-6	Valve Output Characteristics .....	17
Figure 2-7	Gas-Gas Exchanger Fitted Data .....	24
Figure 2-8	Gas-Gas Exchanger Results .....	25
Figure 2-9	Converter One Bed One Fitted Data .....	25
Figure 2-10	Converter One Bed One Results .....	26
Figure 2-11	Overall Ammonia Conversion Fitted Data .....	26
Figure 2-12	Overall Ammonia Conversion Results .....	27
Figure 2-13	Waste Heat Boiler Steam Fitted Data .....	27
Figure 2-14	Waste Heat Boiler Steam Production Results .....	28
Figure 2-15	Synthesis Gas Feed .....	29
Figure 2-16	Synthesis Gas Hydrogen to Nitrogen Ratio in Feed Stream .....	29
Figure 2-17	Synthesis Gas Inert Composition in Feed Stream .....	30
Figure 2-18	Synthesis Gas Ammonia Recycle in Feed Stream .....	30
Figure 3-1	Impact of Changing Model Parameters on Ammonia Reaction .....	32
Figure 3-2	R1B1 Dynamic Parameter Update .....	37
Figure 3-3	R1B1 Conversion Temperature Error .....	37
Figure 3-4	Overall Ammonia Production Error .....	38
Figure 3-5	R1B1 Parameter Update vs. Inlet H/N Ratio .....	40
Figure 4-1	R1B1 Conversion vs. Inlet Temperature, Varying Pressure .....	43
Figure 4-2	R1B1 Conversion vs. Inlet Temperature, Varying H/N Ratio <sup>3</sup> .....	44
Figure 4-3	R1B1 Conversion vs. Inlet Temperature, Varying $y_{NH_3}$ in Feed <sup>3</sup> .....	44
Figure 4-4	R1B1 Conversion vs. Inlet Temperature, Varying $h_x$ Parameter <sup>3</sup> .....	45
Figure 4-5	Optimal Temperature Profile, Normal Operation—Unit Optimization .....	46
Figure 4-6	Optimal Ammonia Production, Normal Operation—Unit Optimization .....	47
Figure 4-7	R2 Optimal Temperature Profile, Normal Operation—R2 Optimization .....	47
Figure 4-8	Optimal $NH_3$ Production, Normal Operation—R2 Optimization .....	48
Figure 4-9	Summer vs. Winter Operation, H/N Ratio .....	49
Figure 4-10	Summer vs. Winter Operation, Synthesis Gas .....	49
Figure 4-11	Summer vs. Winter Operation, Process Inerts .....	50
Figure 4-12	Summer vs. Winter Operation, Synthesis Gas Pressure .....	50
Figure 4-13	Summer vs. Winter Operation, Conversion .....	51
Figure 4-14	Optimal Temperature Profile, Summer Operation .....	51
Figure 4-15	Optimal Ammonia Production, Summer Operation .....	52
Figure 5-1	Waste Heat Boiler Level Open Loop Test .....	59
Figure 5-2	WHB Level Closed Loop Step Test .....	59
Figure 5-3	WHB Level Closed Loop Disturbance Test .....	60
Figure 5-4	WHB Level Open to Closed Loop Test .....	60
Figure 5-5	CV <sub>1</sub> Step, PID, MV <sub>4</sub> Saturated .....	65
Figure 5-6	CV <sub>2</sub> Step, PID, MV <sub>4</sub> Saturated .....	66
Figure 5-7	CV <sub>3</sub> Step, PID, MV <sub>4</sub> Saturated .....	67
Figure 5-8	CV <sub>1</sub> Step, PID, MV <sub>1</sub> Saturated .....	69
Figure 5-9	CV <sub>2</sub> Step, PID, MV <sub>1</sub> Saturated .....	70
Figure 5-10	CV <sub>3</sub> Step, PID, MV <sub>1</sub> Saturated .....	71
Figure 5-11	CV <sub>2</sub> Step Down, Split Range Controller .....	73
Figure 5-12	CV <sub>2</sub> Step Up, Split Range Controller - CV Response .....	74





Figure 5-13	CV <sub>2</sub> Step, Modified LQR, MV <sub>1</sub> Saturated .....	78
Figure 5-14	CV <sub>1</sub> Step, Final LQR, MV <sub>4</sub> Saturated .....	79
Figure 5-15	CV <sub>2</sub> Step, Final LQR, MV <sub>4</sub> Saturated .....	80
Figure 5-16	CV <sub>3</sub> Step, Final LQR, MV <sub>4</sub> Saturated .....	81
Figure 5-17	CV <sub>1</sub> Step, Final LQR, MV <sub>1</sub> Saturated .....	82
Figure 5-18	CV <sub>2</sub> Step, Final LQR, MV <sub>1</sub> Saturated .....	83
Figure 5-19	CV <sub>3</sub> Step, Final LQR, MV <sub>1</sub> Saturated .....	84
Figure C-1	Simulink Block Diagram .....	119
Figure D-1	Converter One Preheat Exchanger Fitted Data .....	124
Figure D-2	Converter One Preheat Exchanger Results .....	124
Figure D-3	Converter One Bed Two Fitted Data .....	125
Figure D-4	Converter One Bed Two Results .....	125
Figure D-5	Converter Two Fitted Data .....	126
Figure D-6	Converter Two Results .....	126
Figure D-7	Waste Heat Boiler I Fitted Data .....	127
Figure D-8	Waste Heat Boiler I Results .....	127
Figure D-9	Waste Heat Boiler II Fitted Data .....	128
Figure D-10	Waste Heat Boiler II Results .....	128
Figure E-1	R1B2 Dynamic Parameter Update .....	131
Figure E-2	R2 Dynamic Parameter Update .....	131
Figure E-3	R1B2 Conversion Temperature Error .....	132
Figure E-4	R2 Conversion Temperature Error .....	132
Figure G-1	CV <sub>1</sub> Step, Open Loop .....	138
Figure G-2	CV <sub>2</sub> Step with MV <sub>1</sub> , Open Loop .....	139
Figure G-3	CV <sub>2</sub> Step Up with MV <sub>4</sub> , Open Loop .....	139
Figure G-4	CV <sub>2</sub> Step Down with MV <sub>4</sub> , Open Loop .....	140
Figure G-5	CV <sub>3</sub> Step, Open Loop .....	140



# LIST OF SYMBOLS

$\omega$	Accentric factor
$f$	Fugacity, bar
$v$	Molar Volume, m <sup>3</sup> /mol
$\sigma$	RKS Reduced Volume Shift
$\phi$	Fugacity Coefficient
$\tau$	PID Tuning Time Constant, minutes
$\lambda$	Relative Gain Array
$\alpha$	RKS Attractive Parameter
$\sigma^2$	Estimate Variance
$\rho$	Density, kg/m <sup>3</sup>
$\Omega_a$	RKS EOS coefficient, $\Omega_a = 0.42748$
$\Omega_b$	RKS EOS coefficient, $\Omega_b = 0.08664$
$\Delta E_k$	Activation Energy Term for Reverse Reaction ( $k_-$ ), J/mol N <sub>2</sub>
$\Delta E_{k_-}$	Activation Energy for Reverse Reaction ( $k_-$ ), J/mol N <sub>2</sub>
$\Delta L_{MIX}$	Pipe Mixing Length for Bypass Valves, $\Delta L_{MIX} = 1$ m
$\Delta P_{RXN}$	Pressure Loss in Each Converter Bed, $\Delta P_{RXN} = 0.1$ MPa
$\frac{\Delta V_{SG}}{\Delta P_{SG}}$	Synthesis Gas Orifice Meter Pressure Differential Scaling Term
$\Phi$	Parameter Update Matrix
$a$	RKS Intermediate Mix Calculation, J m <sup>3</sup> /mol <sup>2</sup>
$a_{C,i}$	RKS Pure Component Calculation at Critical Conditions, J.m <sup>3</sup> /mol <sup>2</sup>
$\tilde{A}$	Shomate Constant
$A$	RKS Intermediate Mix Calculation at Reduced Conditions (Appendix B)
$\mathbf{A}$	State Space Matrix for Process States (Chapter 5)
$A_e$	Exchanger Heat Transfer Area, m <sup>2</sup>
$A_i$	RKS Pure Component Calculation of Component i at Reduced Conditions
$A_v$	Pipe or Valve Flow Area, mm <sup>2</sup>
$A_x$	Cross sectional area of vessel, m <sup>2</sup>
$b$	RKS Intermediate Mix Calculation at Critical Conditions, m <sup>3</sup> /mol
$b_i$	RKS Pure Component Calculation at Critical Conditions, m <sup>3</sup> /mol





<b><math>\tilde{B}</math></b>	Shomate Constant
<b>B</b>	RKS Intermediate Mix Calculation at Reduced Conditions (Chapter B)
<b>B</b>	State Space Matrix for Input Variables (Chapter 5)
$B_i$	RKS Pure Component Calculation at Reduced Conditions
$c$	RKS Intermediate Mix Calculation at Critical Conditions, $m^3/mol$
$c_i$	RKS Pure Component Calculation at Critical Conditions, $m^3/mol$
<b><math>\tilde{C}</math></b>	Shomate Constant
<b>C</b>	RKS Intermediate Mix Calculation At Reduced Conditions (Appendix B)
<b>C</b>	State Space Matrix for Output Variables (Chapter 5)
$C_i$	RKS Pure Component i Calculation At Reduced Conditions (Appendix B)
$C_p$	Heat Capacity, kJ/mol/K
<b><math>\tilde{D}</math></b>	Shomate Constant
$e$	Error
<b><math>\tilde{E}</math></b>	Shomate Constant
<b>E</b>	Energy, MJ
$f$	Heat Transfer Correction Term (Chapter 2)
$f$	Optimization Model Objective Function, kmol $NH_3/hr$ (Chapter 5)
$f_{VOID}$	Converter Catalyst Voidage Fraction
$f_x$	Fraction of Flow
<b><math>\tilde{F}</math></b>	Shomate Constant
<b>F</b>	Synthesis Gas Flow, kmol/s (Chapter 2)
<b>F</b>	Calculated Process Variables (Chapter 3)
$g$	Gravitational Constant, $m/s^2$
$g_x$	Vessel Integral Time Correction Term
<b>G</b>	Vessel Holdup of Synthesis Gas, kmol (Chapter 2)
<b>G</b>	State Space Matrix for Disturbance Variables (Chapter 5)
$G_w$	Vessel Holdup of Boiler Feed Water, kg
$h$	Constraint Equality Equation for Optimization and Parameter Updates (Chapters 3 and 4)
$h$	Enthalpy, kJ/mol (Chapter 2)
$h_R$	Residual Enthalpy, J/mol
$h_t$	Height of Level, m
$h_x$	Forward Reaction Parameter Estimate



H	Enthalpy, kJ/kg
HV	Hand Valve Position, % Output
HX	Heat of Reaction, J/mol N <sub>2</sub>
J	LQR Cost Function/Performance Index
k	Reaction Frequency Factor, kmol NH <sub>3</sub> /hr/m <sup>3</sup> of catalyst/bar (Chapters 2 and 4)
k	Attractive Parameter between Components (Appendix B)
ko	Frequency Factor Constant, kmol NH <sub>3</sub> /hr/m <sup>3</sup> of catalyst/bar
K	RKS EOS Intermediate Calculation (Appendix B)
<b>K</b>	Gain Matrix (Chapter 5)
K <sub>p</sub>	Overall Equilibrium Constant, bar <sup>-2</sup> (Chapter 2)
L	Level, % (Chapter 2)
<b>L</b>	Estimator Gain for Kalman Filter (Chapter 5)
LV	Level Valve Position, % Output
m	Temkin constant, m = 0.46
M	Mass Flow, kg/s or tonne/hr
<b>MWT</b>	Gas Components' Molar Masses, g/mol
<b>n</b>	Moles in the Vessel, kmol
<b>N</b>	LQR Weighting Matrix for Input and Output Variables
<b>O</b>	Observability Matrix
<b>p</b>	RKS EOS Attractive Parameter Calculation Coefficient
P	Pressure, Paa, MPaa or reduced (Chapter 2)
<b>P</b>	Controllability Matrix (Chapter 5)
Q	Heat Transfer Across the Exchanger, MW (Chapter 2)
<b>Q</b>	LQR Weighting Matrix for Output Variables (Chapter 5)
r	Valve Bore Radius, mm
<b>rxn_coeff</b>	Vector of Stoichiometric Coefficients, = [ +1    -0.5    -1.5       0       0       0] = [ NH <sub>3</sub> N <sub>2</sub> H <sub>2</sub> He    Ar    CH <sub>4</sub> ]
R	Ideal Gas Constant, R = 8.314 J/mol/K (Chapter 2)
<b>R</b>	LQR Weighting Matrix for Input Variables (Chapter 5)
R <sub>xN</sub>	Rate of the Overall Reaction, kmol NH <sub>3</sub> /h
<b>S</b>	Riccati Matrix
t	Time, seconds or minutes
T	Temperature, K, mK, °C, reduced or differential





<b>u</b>	Manipulated variable or parameter
<b>U</b>	Exchanger Heat Transfer Coefficient, W/m <sup>2</sup> /K
<b>v</b>	Linear Velocity, m/s
<b>V</b>	Flow of Synthesis Gas Entering Unit at STP, 1000 standard m <sup>3</sup> /h
<b>Vol</b>	Volume, m <sup>3</sup>
<b>w</b>	Disturbance Variables
<b>W</b>	Weighting Matrix: Inverse of Covariance Matrix
<b>x</b>	State Space Variables
<b>X</b>	Half the Width of the Valve Position At Height Y, mm
<b>y</b>	Vector of Mole Fractions, mol/mol (Chapter 2 and Appendix B)
	$= [y_{\text{NH}_3} \quad y_{\text{N}_2} \quad y_{\text{H}_2} \quad y_{\text{He}} \quad y_{\text{AR}} \quad y_{\text{CH}_4}]$
	$= [y_1 \quad y_2 \quad y_3 \quad y_4 \quad y_5 \quad y_6]$
<b>y</b>	Optimization Variables (Chapter 4)
<b>y</b>	Measured Process or Output Variables (Chapter 5)
<b>Y</b>	Height of the Valve Opening, mm
<b>Z</b>	Compressibility Factor



# LIST OF ACRONYMS

BFW	Boiler Feed Water
CBD	Continuous Blowdown
CPUTime	Processing Time based on AMD Athlon 500 MHz processor with 512 MB RAM, minutes
CV	Control Variable
Dev'n	Deviation
DV	Disturbance Variable
EOS	Equation of State
H:N or H/N	Reactant Hydrogen to Nitrogen Mole Ratio
HOLDUP	Vessel Holdup Volume
ODE	Ordinary Differential Equation
LSR	Least Squares Regression
LQR	Linear Quadratic Regulator
LQGR	Linear Quadratic Gaussian Regulator
MIMO	Multiple Input Multiple Output
MP	Medium Pressure
MPC	Multi-Variable Predictive Control
MV	Manipulated Variable
MVC	Multi-Variable Controller
PID	Proportional Integral Derivative Control
R1	Ammonia Converter One
R1B1	Ammonia Converter One, Bed One
R1B2	Ammonia Converter One, Bed Two
R1PH	Ammonia Converter One, Preheat Exchanger
R2	Ammonia Converter Two
RLS	Recursive Least Squares
RKS	Redlich-Kwong-Soave
SISO	Single Input Single Output
SG	Synthesis Gas
WHB I	Waste Heat Boiler One
WHB II	Waste Heat Boiler Two
WHB	Waste Heat Boiler





## LIST OF SUBSCRIPTS

+	Forward Reaction
–	Reverse Reaction Properties
(a)	Refers to the component absorbed onto the catalyst
298.15°	Reference Temperature
ACT	Actual, Measured Value
AR	Argon
ATM	Atmospheric Pressure
AVG	Average
BY	Valve Bypass Stream
BY1	Bypass Stream One
BY2	Bypass Stream Two
BFW	Boiler Feed Water
BFW-B	Waste Heat Boiler II Bottom Area Boiler Feed Water
BFW-M	Waste Heat Boiler II Middle Area Boiler Feed Water
BFW-T	Waste Heat Boiler II Top Area Boiler Feed Water
C	Property Critical Constants (Chapter 2, Appendix B)
C	Controller Properties (Chapter 5)
CALC	Model Calculation
CBD	Continuous Blowdown
CH <sub>4</sub>	Methane
CORR	Corrected for temperature, pressure and/or composition
D	Derivative
ERR	Error
f <sub>298</sub>	Formation at 298 K
G/G	Gas-Gas Exchanger
H <sub>2</sub>	Hydrogen
HE	Helium
Holdup	Vessel Holdup Capacity
i	Component i [NH <sub>3</sub> , N <sub>2</sub> , H <sub>2</sub> , He, Ar CH <sub>4</sub> ] or counter
I	Integral
IG	Ideal Gas Property
IN	Inlet Stream



j	Component j [NH <sub>3</sub> , N <sub>2</sub> , H <sub>2</sub> , He, Ar CH <sub>4</sub> ] or counter
k <sub>-</sub>	Reverse Reaction, NH <sub>3</sub> Decomposition, Property
m	Mean
MIX	Mix Property (length)
mK	milli-Kelvin (units)
n	Process Sample Set, Time Period Reference
N2	Nitrogen
NEW	New Process Characteristics
NH3	Ammonia
OLD	Previous Process Conditions
OUT	Outlet Stream
OP	Valve Output/Position
P	Processes Properties
PLANT	Measured process variable
R	Reduced Property
R1	Ammonia Converter One
R1B1	Ammonia Converter One, Bed One
R1B2	Ammonia Converter One, Bed Two
R1PH	Converter One Preheat
R2	Ammonia Converter Two
REF	Reference, Design Value
RES	Residual Property
RNG	Range of Values
RXN	Ammonia Reaction Property
SG	Synthesis Gas
SHELL	Shell Side of Heat Exchanger
SHELL-B	WHB II Shell Bottom Heat Transfer Area of Vessel
SHELL-M	WHB II Shell Middle Mix Area of Vessel
SHELL-T	WHB II Shell Top Mix Area of Vessel
STD	Standard Deviation
STEAM	Steam from Waste Heat Boilers
STP	Standard Temperature and Pressure
TUBE	Tube Side of Heat Exchanger
VALVE	Valve Property





VESSEL	Reference to Exchanger or Converter Vessel
WHBI	Waste Heat Boiler One
WHBII	Waste Heat Boiler Two



## LIST OF SUPERSCRIPTS

o	Pure Components
*	Optimal Solution
^	Estimated Variable
·	Rate Equation, units/time





# CHAPTER 1

## INTRODUCTION

Farmers around the world currently use 87 million tonnes of nitrogen fertilizer per year<sup>[31]</sup>, which is produced from approximately 400 ammonia plants<sup>[22]</sup>. Extrapolating farming trends to the year 2020, the mean forecast for global nitrogen fertilization is an increase of 60 % from present amounts<sup>[40]</sup>.

As agricultural requirements continue to expand, demand to increase nitrogen fertilizer supply will inevitably push producers to consider growth opportunities within existing plant facilities. Advanced process control will play a role in meeting this demand. While opportunities exist throughout the ammonia process, this thesis focuses on control of the ammonia synthesis unit.

This thesis explores the control and optimization of the ammonia synthesis loop at Saskferco Products Inc. By maximizing reactor conversions, increased production can potentially be achieved. Improved conversion directly impacts synthesis gas recycle and energy consumption per tonne of product.

**Figure 1-1 Ammonia Plant Overview**

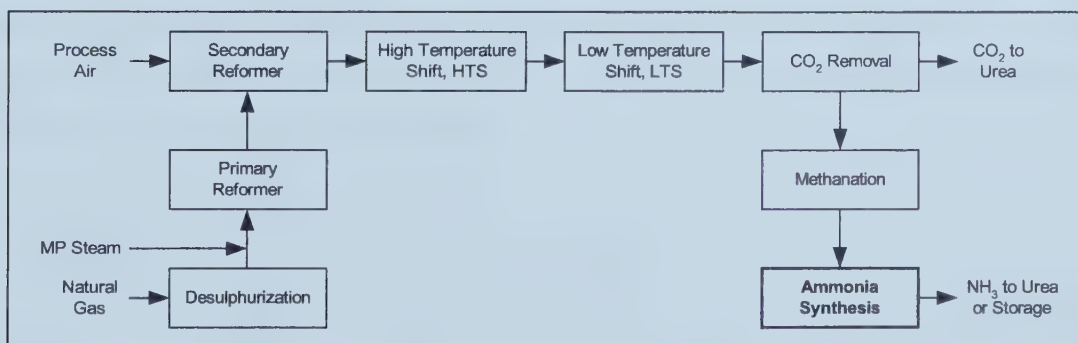


Figure 1-1 provides an overview of the ammonia plant units. An effective controller in this unit would require in-depth process knowledge for model development, reconciliation of plant and model data, parameter updates and an on-line optimization directive.

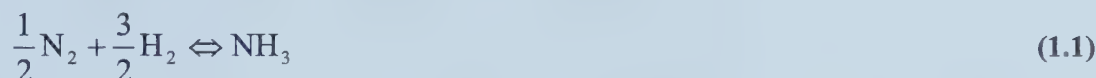
This chapter is intended to provide an overview of the dynamics of the ammonia synthesis process. Work done in this field to date is discussed, establishing the opportunity for additional research and the basis of this thesis.



## 1.1. Process Description

The synthesis of ammonia from hydrogen and nitrogen over an iron catalyst, commonly known as the Haber process, is an industrially important reaction<sup>[25]</sup>. The Haber process has been well characterized. This section reviews the basic principles of the ammonia synthesis as it applies to industry.

Ammonia synthesis is exothermic and after the reaction has been established, it is self-sustaining. The reaction mechanism is governed by the reaction in Equation 1.1.



The process studied in this thesis is based on the operation of Saskferco Products Inc. in Belle Plaine, Saskatchewan, Canada<sup>1</sup>. Saskferco is one of the largest single train nitrogen fertilizer plants in the world, producing approximately 1,850 tonnes per day of anhydrous ammonia and 2,850 tonnes per day of granular urea. Figure 1-2 shows the process flow diagram of the ammonia synthesis unit studied.

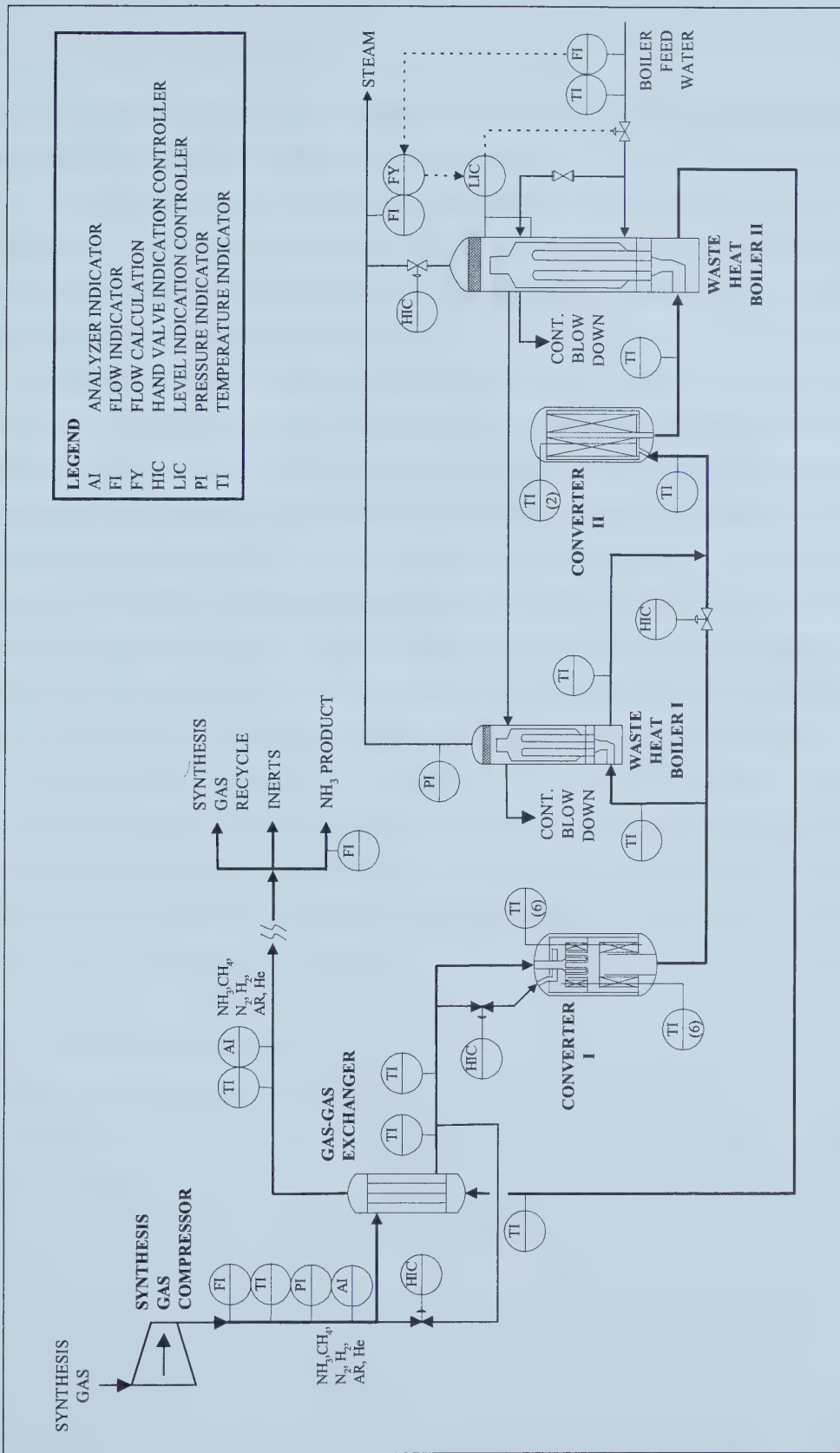
High-pressure synthesis gas is fed to the unit from the synthesis gas compressor. Conversion occurs over three beds of iron based catalyst. Reactant gas is cooled between beds to improve conversion. Heat is removed from the unit through the generation of high-pressure steam in the waste heat boilers. The outlet gas, containing approximately 18 % ammonia, exits the unit where the ammonia product is separated from the unreacted components. The unreacted synthesis gas is then recycled back to the converters. Detailed operation of the ammonia converters including, operating conditions, process constraints, instrumentation, existing applications and proposed process changes is reviewed in Chapter 2.

---

<sup>1</sup> References to data and operation of this facility are bound by the Saskferco – University of Alberta secrecy agreement<sup>[17]</sup>.



**Figure 1-2**







## 1.2. Process Considerations

Ammonia synthesis poses several engineering challenges including nonideal and nonlinear behaviour, as well as a moving optimal operation of the unit

The high pressure of commercial operations, dictated by the reaction kinetics provides an interesting case study for thermodynamic nonidealities. In this case, the Redlich-Kwong-Soave equation of state (RKS EOS) is used to account for residual enthalpies, gas compressibility and to calculate the fugacity of the gas reactants.

Although ammonia conversion is favoured by low temperatures, the reaction kinetics of this exothermic reaction are not. This introduces strong process nonlinearities with respect to the overall ammonia conversion and the operating temperature. If the operating temperature is reduced below the optimum, the production of ammonia can drop off rapidly and the potential exists for the reaction to lose its self sustainability. Consequently, reaction temperatures are operated at a safe open loop differential above the optimum. While this increases the reaction rate, it has a negative impact on the equilibrium and subsequently the amount of ammonia produced. Implementation of a linear controller to the ammonia process is simplified by selection of the control variables with the most linear response to the manipulated variables.

Changing feed composition and pressure contribute to a variable optimum reaction temperature. The inerts in the feed stream (methane, argon and helium) lower the reactant partial pressures and the conversion potential. Ammonia in the recycle gas also has a negative impact on the net ammonia production. The ratio of reactants, referred to as the hydrogen to nitrogen (H/N) ratio, also shifts the optimum temperature.

## 1.3. Process Automation

Due to the nonlinear and nonideal nature of the process, outlined above, research and practical application of closed loop control on the ammonia synthesis loop has been limited. Recognizing nitrogen fertilizer as an important aspect of farming and world food production, with growing demand<sup>[40]</sup>, opportunities to improve the efficiency and throughput of existing plant manufacturers should be evaluated.

Saskferco is a state of the art ammonia/urea plant commissioned in 1992. Similar to other ammonia plants, Saskferco currently uses ratio control to manipulate the H/N ratio into the converter. PID control is also available for the inlet temperature of the third reactor bed. However, due to problems with the control valve, and without a mechanism to determine the optimal setpoint, this controller is operated only in manual mode.



Industrial examples of advanced control that encompass all of the reactor beds are less common. Multivariable control implementations on multibed ammonia converters with direct cooling (quench converters) are documented by several control vendors<sup>[19],[22],[28]</sup>. These implementations have recorded benefits between 1 to 2 % of total ammonia production. However, implementation details and the control options that were explored have not been publicized. Information not explicitly addressed in these implementations includes update of parameter estimates, to account for model mismatch, and on-line optimization of the nonlinear process. This thesis addresses these issues for multibed ammonia converters with indirect cooling.

Similar research in this area, which has been the subject of several publications<sup>[11],[13],[25]</sup>, includes the optimal design of the ammonia converter beds.

## **1.4. Thesis Scope**

This thesis attempts to identify the optimization and control opportunities of an existing ammonia synthesis process and the means to achieve these benefits. To date, research into the control options and the supporting tools necessary to properly implement this control has been limited. While multi-variable control (MVC) applications have been successfully put into service, it is not clear that claimed benefits could not have been realized with less complicated control strategies. Additionally, on-line tools needed to realize these benefits have been either overlooked or oversimplified. This thesis provides an evaluation of the optimization problem, complete with parameter updates. Control options such as a simple PID controller and a slightly more complicated MVC are implemented and compared.

Chapter 2 delves into the kinetic and thermodynamic properties of ammonia synthesis. Thermodynamic properties are based on the RKS EOS with the Temkin-Pyshev equation used to describe the synthesis process. Reconciliation of model results with plant data is explored.

Parameter updates, using historical plant data, are explored in Chapter 3. Variations of the least squares approach are evaluated. Using three parameters, four measured variables are predicted. The parameter update results are employed in the optimization model.

Process optimization is discussed in detail in Chapter 4. Potential benefits for various modes of operation are considered. Both process constraints and sensitivities are addressed. Opportunities and potential benefits using a simplified optimization routine are compared to an overall unit optimizer.

Having established the criteria required to achieve effective control, controllability of the system is considered in Chapter 5. Control, manipulated and disturbance variables are determined. The relative gain array (RGA) is used to determine appropriate coupling of these





variables for PID control. Multi-loop PID and a MVC are designed and tested. Performance in both cases is compared.

The thesis provides recommendations to Saskferco to improve the performance of the ammonia synthesis loop through the implementation of parameter updates, optimization and control.

## 1.5. Thesis Conventions

A consistent set of symbols is used throughout each chapter of the thesis. These symbols are defined at the beginning of the document.

Other standard conventions used in the body of the thesis are described. **Plant** refers to the process at Saskferco Products Inc. The term **model** refers to the Matlab and Simulink simulation, developed based on first principles and fit to plant data. **Process** can be used to describe the operation of either the plant or the simulation. **Sample sets** and **shift averages** refer to plant data collected from the process, using 12-hour shift averages.

The process model contains **states**, **inputs** and **parameters**. A state variable arises naturally in the accumulation term of the dynamic material or energy balance<sup>[4]</sup>. It is often a measured value, used to characterize the system. Inputs are the inlet conditions of the process, required for operation. This includes variables that are manipulated to achieve desired performance. Parameters are defined as the constant values or coefficients included in the model calculations. These parameters include chemical and physical values.

**Variables** used for parameter updates and process optimization are broken down into **dependent (tear)** and **independent (manipulated)** variables. Dependent variables are the direct result of operation at a specified set of values for the independent variables. Manipulated variables are independently adjusted to achieve the model objective function.

Controller variables include **control** variables, **manipulated** variables and **disturbance** variables. Control variables are the controller outputs used to regulate the process. Manipulated variables are the controller inputs, used to achieve the desired control variable. In this thesis, the manipulated variables are the control valve positions. Disturbance variables are independent inputs into the process that cannot be manipulated.

The dynamic process model makes several assumptions, such as radial flow through the converter beds and uniform pressure in each vessel. Heat loss to the environment is assumed negligible. Heat transfer characteristics of the vessels and reactor pellets are not modelled.



## CHAPTER 2

### AMMONIA PROCESS MODEL

The process considered in this thesis is based on the operation and design of the ammonia synthesis loop at Saskferco Products Inc in Belle Plaine, Saskatchewan. In the following section, the process is described at normal plant operating conditions.

The ammonia synthesis unit is comprised of a gas-gas heat exchanger, two converters (three reaction beds in total) and two waste heat boilers, as shown in Figure 1-2.

The synthesis gas feed is a mix of fresh make-up gas and unconverted recycle gas. Inert process gases in the synthesis gas are primarily a function of the upstream units. Equipment limitations at high feed rates and summer temperatures have a negative impact on the ability to remove inerts from the recycle gas stream. The main detrimental effect of inerts in the synthesis gas is to reduce the effective partial pressure of the reactants and thus the conversion rate<sup>[25]</sup>. Similar to inert recycle, the amount of recycled ammonia is related to feed throughput and the ambient temperature. In addition to reducing the partial pressure of the reactants, recycled ammonia reduces the net ammonia production potential. The H/N feed mole ratio is controlled to about 3.1 moles of hydrogen per mole of nitrogen using a PID ratio controller. H/N control is not achievable in the summer months due to reduced ambient air density and the saturated output of the air compressor. Production gas leaving the unit is sent to the process chillers for the separation of ammonia, inerts and recycle gas. Table 2-1 summarizes the operating conditions of the plant.

Four bypass valves exist on the unit. The first valve, around the shell of the gas-gas exchanger is kept closed except for start-up conditions. A bypass valve around the preheat exchanger (R1PH) tubes in the first converter (R1) acts as a cold shot to the first reaction bed inlet temperature. This valve can be used to manipulate both the bed one (R1B1) and bed two (R1B2) inlet temperatures and typically remains closed. The valve around the tube side of the first waste heat boiler (WHB I) is used to manipulate the second converter (R2) inlet temperature. The normal operation of this valve is open loop with a valve position of about ninety percent. The boiler feed water (BFW) inlet flow to the second waste heat boiler (WHB II) can be split between the top and the bottom of the shell. Increasing flow to the top of the exchanger reduces the overall heat transfer in this vessel.



**Table 2-1      Operating Conditions**

Operating Parameters	Typical Operating Conditions
$V_{IN,SG}$	799 k-sm <sup>3</sup> /hr
$T_{IN,SG}$	27 °C
$P_{IN,SG}$	18.6 MPag
$y_{IN} = [y_{NH_3} \ y_{H_2} \ y_{N_2} \ y_{He} \ y_{Ar} \ y_{CH_4}]$	[0.02   0.20   0.63   0.01   0.03   0.11]
$T_{G/G,SHELL}$	282 °C
$T_{R1PH,TUBE}$	377 °C
$T_{R1PH,SHELL}$	407 °C
$T_{R1B1}$	511 °C
$y_{R1B1}$	[0.12   0.17   0.55   0.01   0.03   0.12]
$T_{R1B2}$	464 °C
$y_{R1B2}$	[0.17   0.16   0.50   0.01   0.03   0.13]
$T_{WHBI,TUBE}$	345 °C
$T_{WHBI,BY}$	398 °C
$T_{R2}$	442 °C
$y_{R2}$	[0.21   0.14   0.47   0.01   0.03   0.14]
$T_{WHBII,TUBE}$	320 °C
$T_{G/G,TUBE}$	54 °C

In designing a controller using the WHB II BFW valve, it should be noted that large output changes introduce swings into the plant steam header pressure. The consequence of this is a possible loss of control in the BFW level in WHB II and subsequent shutdown of the entire ammonia plant. Due to the small hold-up of BFW in this vessel, a plant trip can occur in less than one minute.

## 2.1.      Characteristics of Conversion

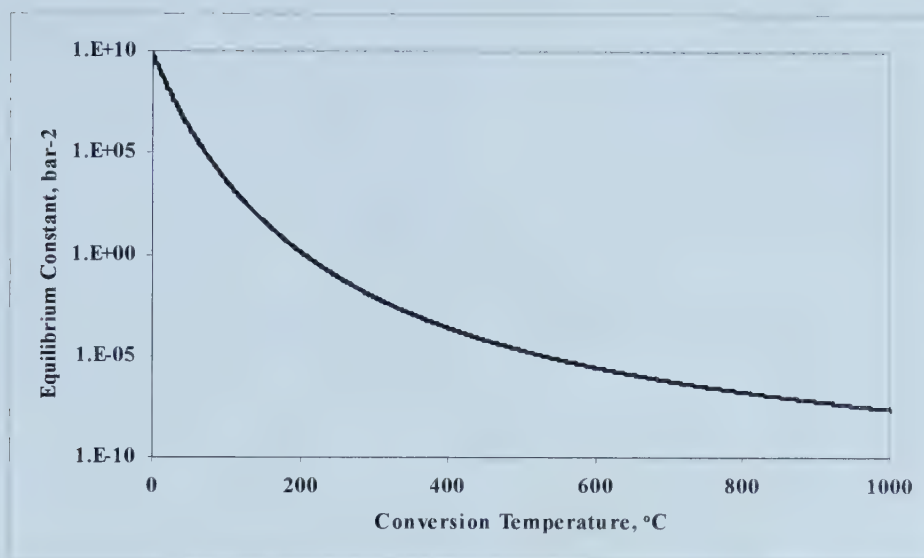
The conversion of ammonia from hydrogen and nitrogen has nonlinear process properties largely due to competing equilibrium and kinetic forces.

The equilibrium favours a low temperature and high pressure. Figure 2-1 shows the decaying exponential relationship between the equilibrium constant for ammonia conversion and the conversion temperature at a pressure of 19 MPa.





**Figure 2-1**      **Equilibrium Constant vs. Conversion Temperature**



The kinetics are accelerated by increased operating temperatures<sup>[1]</sup>. As shown in Figure 2-2 both the forward and reverse reactions occur at a higher rate as the temperature is increased.

**Figure 2-2**      **Frequency Factor vs. Conversion Temperature**

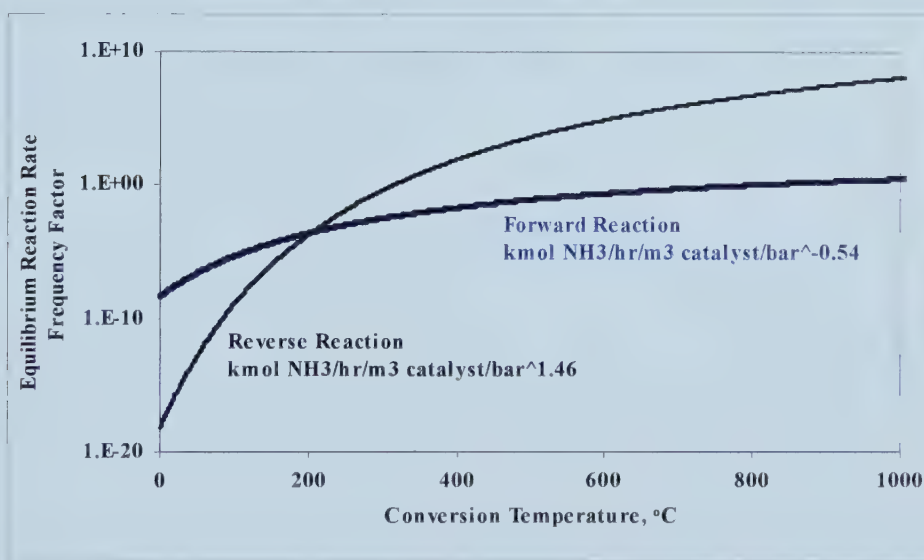


Figure 2-3 illustrates the effect of the ammonia concentration on the equilibrium and optimum temperature curves, using actual plant data.



**Figure 2-3** Effect of Ammonia Concentration on Reaction Rate

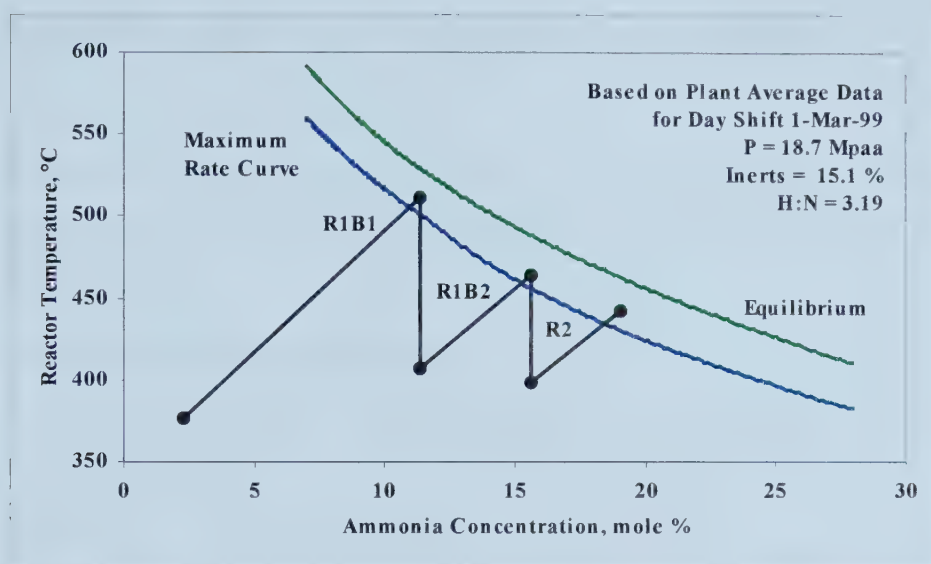
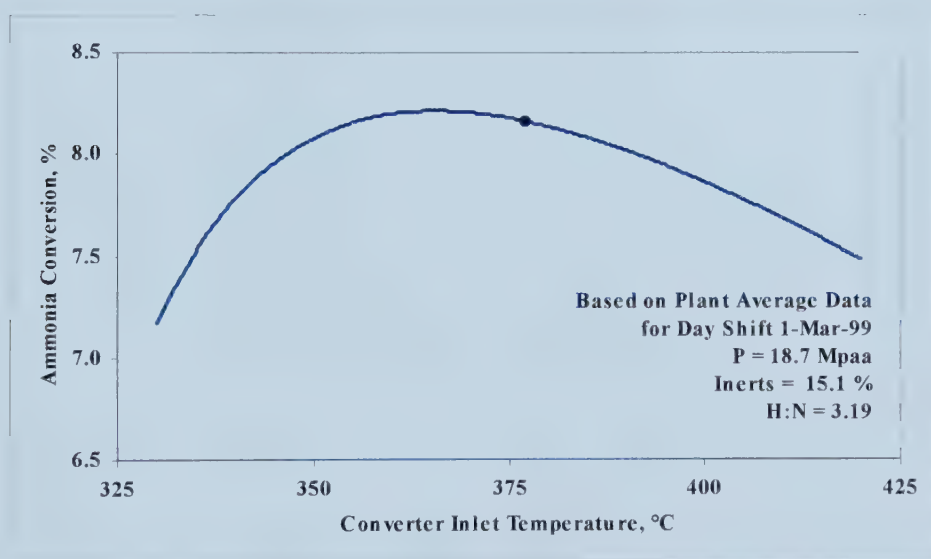


Figure 2-3 shows that Saskferco achieves its optimal ammonia conversion at converter outlet temperatures between 440 °C to 510 °C, depending on the conversion bed and process inlet conditions. The conversion profile based on the inlet temperature to R1B1 may be found in Figure 2-4.

**Figure 2-4** Ammonia Conversion vs. Inlet Temperature to R1B1



The slope of the conversion in Figure 2-4 is notably steeper at temperatures below the optimum conversion temperature. Due to this rapid drop off, operating close to or below the optimum temperature introduces the possibility to lose the reaction as less heat is liberated, resulting in a plant shutdown. Conversely, operating the converter inlet temperature at a safe



margin above the optimum slightly reduces ammonia conversion and provides some latitude for plant disturbances and open loop operation. It is for these reasons that the standard operation of the inlet temperature to the ammonia converters is slightly above optimum.

## 2.2. Constitutive Relationships

This section addresses the constitutive relationships of the ammonia synthesis unit including input conditioning, chemical reactions, thermodynamics of both the synthesis gas and steam and the valve flow characteristics.

### 2.2.1. Process Inputs and Conditioning

The process inputs, including flow, pressure, composition and temperature, Table 2-2, are first converted to the appropriate units.

**Table 2-2 Plant Input Variables**

Variable	Description	Units
$V_{IN,SG}$	Flow of Synthesis Gas Entering Unit at STP	k-sm <sup>3</sup> /hr
$T_{IN,SG}$	Temperature of Synthesis Gas Entering Unit	°C
$P_{IN,SG}$	Pressure of Synthesis Gas Entering Unit	MPag
$Y_{NH3,IN}$	Ammonia Mole Composition Entering	mole fraction
$Y_{N2,IN}$	Nitrogen Mole Composition Entering	mole fraction
$Y_{H2,IN}$	Hydrogen Mole Composition Entering	mole fraction
$Y_{HE,IN}$	Helium Mole Composition Entering	mole fraction
$Y_{AR,IN}$	Argon Mole Composition Entering	mole fraction
$Y_{CH4,IN}$	Methane Mole Composition Entering	mole fraction
$T_{IN,BFW}$	Waste Heat Boiler II BFW Temperature In	°C
$P_{IN,STEAM}$	High Pressure Steam Header Pressure	MPag
$HV_{G/G,SHELL}$	Gas-Gas Exchanger Tube Bypass Valve Output	%
$HV_{R1PH,TUBE}$	Converter One Preheat Tube Bypass Valve Output	%
$HV_{WHBI,TUBE}$	Waste Heat Boiler I Tube Bypass Valve Output	%
$HV_{WHBII,BFW,IN}$	Waste Heat Boiler II BFW Valve Output	%
$HV_{WHBII,BFW-T}$	Waste Heat Boiler II BFW-Split Top Valve Output	%
$HV_{WHBII,STEAM}$	Waste Heat Boiler II Steam Valve Output	%

Flow of synthesis gas into the unit was calculated in the control system using Equation 2.1, which is based on the differential pressure across the orifice meter.

$$V_{IN,SG,OLD} = \Delta P_{SG} \left( \frac{\Delta V_{SG}}{\Delta P_{SG}} \right)_{OLD} \frac{P_{ACT}}{P_{REF}} \frac{T_{REF}}{T_{ACT}} \quad (2.1)$$

The actual calculation for the orifice pressure differential should be as Equation 2.2.

$$V_{IN,SG,NEW} = \Delta P_{SG} \left( \frac{\Delta V_{SG}}{\Delta P_{SG}} \right)_{NEW} \left( \frac{P_{ACT}}{P_{REF}} \frac{T_{REF}}{T_{ACT}} \frac{MWT_{ACT}}{MWT_{REF}} \right)^{0.5} \quad (2.2)$$





Using Equations 2.1 and 2.2, the actual flow of synthesis gas entering the unit is corrected as follows. Equation 2.4 is used to convert the flow rate from volumetric to mass.

$$V_{\text{IN,SG,CORR}} = V_{\text{IN,SG,OLD}} \left( \frac{\Delta P_{\text{SG}}}{\Delta V_{\text{SG}}} \right)_{\text{OLD}} \left( \frac{\Delta V_{\text{SG}}}{\Delta P_{\text{SG}}} \right)_{\text{NEW}} \left( \frac{P_{\text{REF}}}{P_{\text{ACT}}} \frac{T_{\text{ACT}}}{T_{\text{REF}}} \frac{\text{MWT}_{\text{ACT}}}{\text{MWT}_{\text{REF}}} \right)^{0.5} \quad (2.3)$$

$$M_{\text{IN,SG}} = V_{\text{IN,SG,CORR}} \rho_{\text{SG,IN,STP}} \frac{1000}{3600} \quad (2.4)$$

The operating pressure is calculated for the process gas in each vessel, using inlet conditions and assuming a pressure drop of 0.1 MPa across each reactor bed. Inlet compositions are normalized.

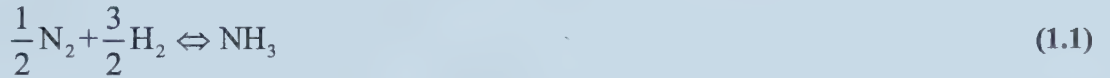
$$P_{\text{R1B1}} = P_{\text{IN,SG}} - \Delta P_{\text{RXN}} + P_{\text{ATM}} \quad (2.5)$$

$$P_{\text{R1B2}} = P_{\text{R1B1}} - \Delta P_{\text{RXN}} \quad (2.6)$$

$$P_{\text{R2}} = P_{\text{R1B2}} - \Delta P_{\text{RXN}} \quad (2.7)$$

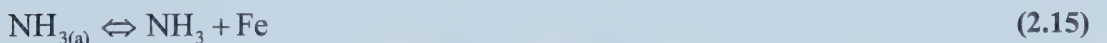
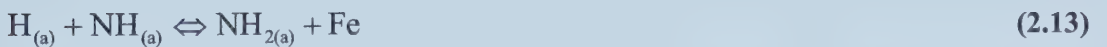
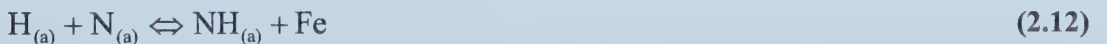
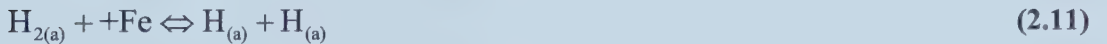
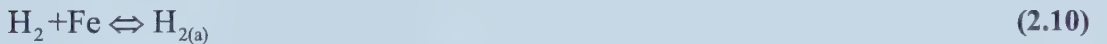
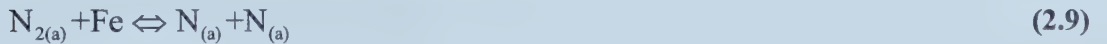
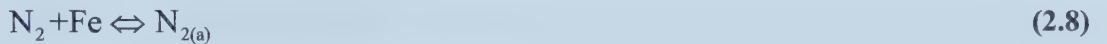
### 2.2.2. Chemical Reactions

The conversion of hydrogen and nitrogen to ammonia is represented as:



This reaction is broken down into the elementary reactions in Equations 2.8 to 2.15<sup>[41]</sup>.

Subscript (a) refers to the component absorbed onto the iron catalyst.





### 2.2.3. Reaction Kinetics

The model studied in this thesis uses the Temkin-Pyshev<sup>[32]</sup> equation to describe the reaction kinetics. The Temkin-Pyshev equation assumes that the rate of the reaction depends on the chemisorption of nitrogen, Equation 2.9.

$$R_{\text{XN}} = \left( k_+ f_{\text{N}_2} \left( \frac{f_{\text{H}_2}^3}{f_{\text{NH}_3}^2} \right)^m - k_- \left( \frac{f_{\text{NH}_3}^2}{f_{\text{H}_2}^3} \right)^{1-m} \right) \text{Vol} \quad (2.16)$$

The equilibrium constant of the ammonia reaction is described by the Equations 2.17 and 2.18<sup>[41]</sup>.

$$K_p(\text{at equilibrium}) = \frac{f_{\text{NH}_3}^2}{f_{\text{N}_2} f_{\text{H}_2}^3} = \frac{k_+}{k_-} \quad (2.17)$$

$$K_p = e^{\left( -27.366 + \frac{12500}{T} + \frac{10 P}{T} \left[ -1.42 + \frac{2100}{T} \right] \right)} \quad (2.18)$$

The frequency factor for the reverse reaction is represented below in Equation 2.19. The forward reaction frequency factor is calculated in Equation 2.20 based on equilibrium conditions with a compensation term, fit to plant data.

$$k_- = (k_{o-}) e^{\left[ \frac{\Delta E_k}{R T} \right]} \quad (2.19)$$

$$k_+ = h x k_- K_p \quad (2.20)$$

From these relationships, the reaction rates, Equations 2.21 to 2.23 are determined as functions of the following variables using Equation 2.16.

$$R_{\text{XN,R1B1}} = f(P_{\text{R1B1}}, T_{\text{R1B1,OUT}}, y_{\text{R1B1}}, \text{Vol}_{\text{R1B1}}, h x_{\text{R1B1}}) \quad (2.21)$$

$$R_{\text{XN,R1B2}} = f(P_{\text{R1B2}}, T_{\text{R1B2,OUT}}, y_{\text{R1B2}}, \text{Vol}_{\text{R1B2}}, h x_{\text{R1B2}}) \quad (2.22)$$

$$R_{\text{XN,R2}} = f(P_{\text{R2}}, T_{\text{R2,OUT}}, y_{\text{R2}}, \text{Vol}_{\text{R2}}, h x_{\text{R2}}) \quad (2.23)$$

Mole fractions are calculated from the reactor composition state variables, Equations 2.24 to 2.26.

$$y_{i, \text{R1B1}} = \frac{n_{i, \text{R1B1}}}{\sum_j n_{j, \text{R1B1}}} \quad (2.24)$$

$$y_{i, \text{R1B2}} = \frac{n_{i, \text{R1B2}}}{\sum_j n_{j, \text{R1B2}}} \quad (2.25)$$



$$y_{i,R2} = \frac{n_{i,R2}}{\sum_j n_{j,R2}} \quad (2.26)$$

#### 2.2.4. Heat of Reaction

The heat of reaction and the activation energy are calculated in Equations 2.27 and 2.28 based on catalyst manufacturer information<sup>[41]</sup>.

$$HX = -R T^2 \left( \frac{\delta \ln K_P}{\delta T} \right)_P \quad (2.27a)$$

$$= -\frac{R}{T} (-12500 T - 4200 P + 14.2 P T) \quad (2.27b)$$

$$\Delta E_{k\_} = \Delta E_K + (1 - m) HX \quad (2.28)$$

Equations 2.29 to 2.31 represent the heat of reaction for each converter bed as functions of Equation 2.27.

$$HX_{R1B1} = f(T_{R1B1}, P_{R1B1}) \quad (2.29)$$

$$HX_{R1B2} = f(T_{R1B2}, P_{R1B2}) \quad (2.30)$$

$$HX_{R2} = f(T_{R2}, P_{R2}) \quad (2.31)$$

#### 2.2.5. Redlich-Kwong-Soave Equation of State

The enthalpies of the synthesis gas streams are calculated using the ideal gas enthalpy with a residual enthalpy term. Due to the high pressure of the process (19 MPa), the residual enthalpy contributes to about five percent of the total calculated enthalpy change.

$$\Delta h = y \Delta h_{IG} + \frac{(hR_{OUT} - hR_{IN})}{1000} \quad (2.32)$$

$$C_P = y C_P^\circ \quad (2.33)$$

The ideal gas heat capacity is calculated from the Shomate<sup>[24]</sup> equation.

$$C_P^\circ = \tilde{A} + \tilde{B} T_{mK} + \tilde{C} T_{mK}^2 + \tilde{D} T_{mK}^3 + \frac{\tilde{E}}{T_{mK}^2} \quad (2.34)$$

$$h^\circ - h_{298.15}^\circ = \tilde{A} T_{mK} + \frac{\tilde{B} T_{mK}^2}{2} + \frac{\tilde{C} T_{mK}^3}{3} + \frac{\tilde{D} T_{mK}^4}{4} - \frac{\tilde{E}}{T_{mK}} + \tilde{F} - \Delta h_{f,298}^\circ \quad (2.35)$$

or

$$\Delta h_{IG} = \tilde{A} (T_{mK,OUT} - T_{mK,IN}) + \tilde{B} \frac{(T_{mK,OUT} - T_{mK,IN})^2}{2} + \tilde{C} \frac{(T_{mK,OUT} - T_{mK,IN})^3}{3} +$$



$$\tilde{D} \frac{(T_{mK,OUT} - T_{mK,IN})^4}{4} - \tilde{E} \left( \frac{1}{T_{mK,OUT}} - \frac{1}{T_{mK,IN}} \right) \quad (2.36)$$

Refer to Tables B-1 and B-2 in Appendix B for the gas properties and constants used to calculate the process enthalpy changes.

The Redlich-Kwong-Soave<sup>[39]</sup> equation of state, Equation 2.37, is used to calculate the synthesis gas compressibility, residual enthalpy and fugacity coefficients. Using a cubic form of this equation, compressibility can be solved. Reference Equation 2.38.

$$P = \frac{RT}{v + c - b} - \frac{a}{(v + c)(v + c + b)} \quad (2.37)$$

$$(Z + C)^3 - (Z + C)^2 + (Z + C)(A - B - B^2) - A \cdot B = 0 \quad (2.38)$$

The residual enthalpy found in Equation 2.39 is calculated using Maple<sup>®</sup><sup>2</sup>. Calculation of the fugacity coefficients<sup>[3]</sup> can be found in Equation 2.40.

$$hR = (Z - 1) R T - \frac{1}{2b} (2k_0 + k_1 \sqrt{T}) \ln \left( 1 + \frac{b}{v + c} \right) \quad (2.39)$$

$$\ln \phi_i = -\ln(Z + C - B) + \frac{B_i}{B} (Z + C - 1) - C_i + \frac{A}{B} \left[ \frac{B_i}{B} - \frac{2}{A} \sum_j y_j \sqrt{A_i A_j} \right] \ln \left( 1 + \frac{B}{Z + C} \right) \quad (2.40)$$

Equations for the RKS constants and intermediate calculations used in Equations 2.39 and 2.40 can be found in Equations B.1 through B.20 of the Appendices.

Re-arranging the gas equation yields the gas density.

$$\rho = \frac{1}{v} (\text{y MWT}) 1000 \quad (2.41a)$$

$$= \left( \frac{P}{Z R T} \right) (\text{y MWT}) 1000 \quad (2.41b)$$

Synthesis gas enthalpy, average heat capacity and average density calculations are listed in Equations D.1 to D.16 of Appendix D as functions of Equations 2.32, 2.33 and 2.41.

## 2.2.6. Steam Calculations

Thermodynamic properties of steam are expressed mathematically by fitting equations to data taken from the steam tables<sup>[37]</sup> over the temperature range considered. The waste heat boiler (WHB) shell temperatures are used to determine the BFW and steam properties including the saturation pressure, enthalpy, heat capacity and densities. These relationships are listed in

<sup>2</sup> © 2000 Waterloo Maple Inc. Maple is a registered trademark of Waterloo Maple Inc.





Equations D.17 to D.21 of Appendix D. The changes in enthalpy across the WHB, attributed to the steam system, are calculated in Equations 2.42 to 2.45.

$$\Delta H_{\text{WHBI,SHELL}} = (M_{\text{WHBI,STEAM}} H_{\text{WHBI,STEAM}} + M_{\text{CBD}} H_{\text{WHBI,BFW}} - M_{\text{WHBI,BFW}} H_{\text{WHBII,SHELL-MID}}) 10^{-3} \quad (2.42)$$

$$\Delta H_{\text{WHBII,BFW-B}} = (M_{\text{WHBII,STEAM}} H_{\text{WHBII,STEAM}} + (M_{\text{WHBI,BFW}} + 2 M_{\text{CBD}}) H_{\text{WHBII,BFW-M}} - M_{\text{WHBII,BFW,IN}} H_{\text{WHBII,BFW,IN}} - \Delta H_{\text{WHBII,BFW-M}} - \Delta H_{\text{WHBII,BFW-T}}) 10^{-3} \quad (2.43)$$

$$\Delta H_{\text{WHBII,BFW-M}} = (M_{\text{WHBII,BFW-T}} H_{\text{WHBII,BFW,IN}} + f_{\text{WHBII,BFW-M}} M_{\text{WHBI,BFW}} H_{\text{WHBII,BFW-B}} - (M_{\text{WHBII,BFW-T}} + f_{\text{WHBII,BFW-M}} M_{\text{WHBI,BFW-B}}) H_{\text{WHBII,BFW-M}}) 10^{-3} \quad (2.44)$$

$$\Delta H_{\text{WHBII,BFW-T}} = ((f_{\text{WHBII,BFW-M}} M_{\text{WHBII,BFW-B}} + M_{\text{WHBII,BFW-T}} - M_{\text{WHBI,BFW}} - M_{\text{CBD}}) H_{\text{WHBII,BFW-M}} + (1 - f_{\text{WHBII,BFW-M}}) M_{\text{WHBI,BFW-B}} H_{\text{WHBII,BFW-B}} - (M_{\text{WHBII,BFW,IN}} - M_{\text{WHBI,BFW}} - M_{\text{CBD}}) H_{\text{WHBII,BFW-T}}) 10^{-3} \quad (2.45)$$

### 2.2.7. Heat Transfer

Heat transfer characteristics for each heat exchanger were provided by Saskferco<sup>[17]</sup>. Using these values, the overall heat transfer is calculated for all heat exchangers.

$$Q_{\text{G/G}} = U_{\text{G/G}} A_{\text{e,G/G}} f_{\text{G/G}} \Delta T_{\text{m,G/G}} 10^{-6} \quad (2.46)$$

$$Q_{\text{R1PH}} = U_{\text{R1PH}} A_{\text{e,R1PH}} f_{\text{R1PH}} \Delta T_{\text{m,R1PH}} 10^{-6} \quad (2.47)$$

$$Q_{\text{WHBI}} = U_{\text{WHBI}} A_{\text{e,WHBI}} f_{\text{WHBI}} \Delta T_{\text{m,WHBI}} 10^{-6} \quad (2.48)$$

$$Q_{\text{WHBII}} = U_{\text{WHBII}} A_{\text{e,WHBII}} f_{\text{WHBII}} \Delta T_{\text{m,WHBII}} 10^{-6} \quad (2.49)$$

The mean temperature difference is based on the operating difference between the hot side and the cold side of the exchanger.

$$\Delta T_{\text{m,G/G}} = \frac{(T_{\text{WHBII,TUBE}} - T_{\text{G/G,SHELL}}) + (T_{\text{G/G,TUBE}} - T_{\text{IN,SG}})}{2} \quad (2.50)$$

$$\Delta T_{\text{m,R1PH}} = \frac{(T_{\text{R1B1}} - T_{\text{R1PH,TUBE}}) + (T_{\text{R1PH,SHELL}} - T_{\text{G/G,BY}})}{2} \quad (2.51)$$

$$\Delta T_{\text{m,WHBI}} = \frac{(T_{\text{R1B2}} - T_{\text{WHBI,SHELL}}) + (T_{\text{WHBI,TUBE}} - T_{\text{WHBII,BFW-M}})}{2} \quad (2.52)$$

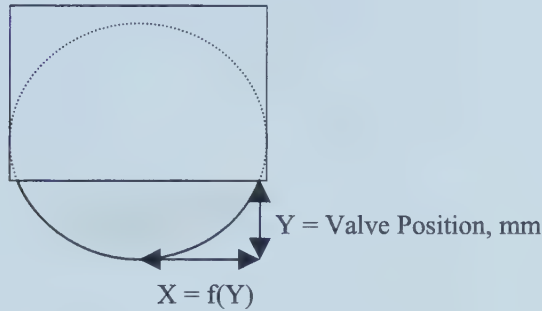
$$\Delta T_{\text{m,WHBII}} = \frac{(T_{\text{R2}} - T_{\text{WHBII,SHELL-B}}) + (T_{\text{WHBII,TUBE}} - T_{\text{WHBII,BFW,IN}})}{2} \quad (2.53)$$



### 2.2.8. Flow Through Valves and Process

The ammonia synthesis unit contains both ball and butterfly valve types. For simplicity all valves are modelled as knife gate valves. From the valve position or output percent (HV) and the valve radius ( $r_{\text{VALVE}}$ ) the area available for flow can be determined.

**Figure 2-5 Knife Gate Valve Area**



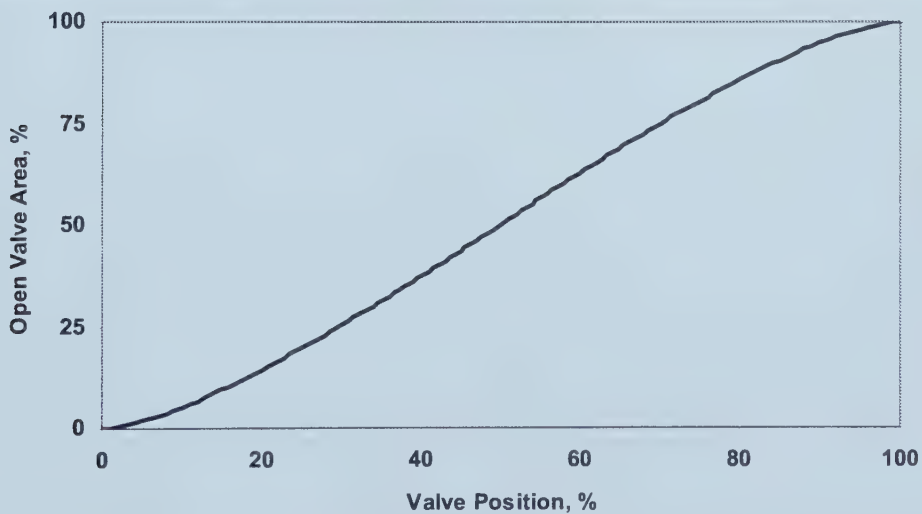
The valve area is calculated as:

$$A_v = 2 \int_0^X Y dX \quad (2.54a)$$

$$= (Y - r_{\text{VALVE}}) X + r_{\text{VALVE}}^2 \text{asin}\left(\frac{HV-50}{50}\right) + \frac{\pi r_{\text{VALVE}}^2}{2} \quad (2.54b)$$

The relationship between the valve output and the flow area exhibits the following characteristics, Figure 2-6.

**Figure 2-6 Valve Output Characteristics**





Available flow area functions, Equations D.22 to D.33, based on Equation 2.54, are listed in Appendix D. Flows to each vessel are then calculated in Equations 2.55 through 2.66 for synthesis gas and Equations 2.67 through 2.72 for BFW and steam.

$$F_{G/G,TUBE} = \frac{M_{IN,SG}}{y_{R2} \text{ MWT}} \quad (2.55)$$

$$F_{G/G,SHELL} = \frac{M_{IN,SG}}{y_{IN} \text{ MWT}} \frac{Av_{G/G,SHELL}}{Av_{G/G,SHELL} + Av_{G/G,BY}} \quad (2.56)$$

$$F_{G/G,BY} = \frac{M_{IN,SG}}{y_{IN} \text{ MWT}} \frac{Av_{G/G,BY}}{Av_{G/G,SHELL} + Av_{G/G,BY}} \quad (2.57)$$

$$F_{R1PH,TUBE} = \frac{M_{IN,SG}}{y_{IN} \text{ MWT}} \frac{Av_{R1PH,TUBE}}{Av_{R1PH,TUBE} + Av_{R1PH,BY}} \quad (2.58)$$

$$F_{R1PH,BY} = \frac{M_{IN,SG}}{y_{IN} \text{ MWT}} \frac{Av_{R1PH,BY}}{Av_{R1PH,TUBE} + Av_{R1PH,BY}} \quad (2.59)$$

$$F_{R1PH,SHELL} = \frac{M_{IN,SG}}{y_{R1B1} \text{ MWT}} \quad (2.60)$$

$$F_{R1B1} = \frac{M_{IN,SG}}{y_{IN} \text{ MWT}} \quad (2.61)$$

$$F_{R1B2} = F_{R1PH,SHELL} \quad (2.62)$$

$$F_{WHBI,TUBE} = \frac{M_{IN,SG}}{y_{R1B2} \text{ MWT}} \frac{Av_{WHBI,TUBE}}{Av_{WHBI,TUBE} + Av_{WHBI,BY}} \quad (2.63)$$

$$F_{WHBI,BY} = \frac{M_{IN,SG}}{y_{R1B2} \text{ MWT}} \frac{Av_{WHBI,BY}}{Av_{WHBI,TUBE} + Av_{WHBI,BY}} \quad (2.64)$$

$$F_{R2} = \frac{M_{IN,SG}}{y_{R1B2} \text{ MWT}} \quad (2.65)$$

$$F_{WHBI,TUBE} = \frac{M_{IN,SG}}{y_{R2} \text{ MWT}} \quad (2.66)$$

$$M_{WHBI,BFW} = Av_{WHBI,BFW} \sqrt{2 g (ht_{WHBI,BFW} - ht_{WHBI,BFW})} \quad (2.67)$$

$$M_{WHBI,BFW,IN} = \rho_{WHBI,BFW,IN} Av_{WHBI,BFW,IN} v_{BFW,IN} \quad (2.68)$$

$$M_{WHBI,STEAM} = \rho_{WHBI,STEAM} Av_{WHBI,STEAM} \sqrt{\frac{2 (P_{WHBI,STEAM} - P_{STEAM})}{\rho_{WHBI,STEAM}}} \quad (2.69)$$

$$M_{WHBI,BFW-T} = M_{WHBI,BFW,IN} \frac{Av_{WHBI,BFW-T}}{Av_{WHBI,BFW-T} + Av_{WHBI,BFW-B}} \quad (2.70)$$





$$M_{\text{WHBI},\text{BFW-B}} = M_{\text{WHBI},\text{BFW-IN}} \frac{A_{\text{V}_{\text{WHBI},\text{BFW-B}}}}{A_{\text{V}_{\text{WHBI},\text{BFW-T}}} + A_{\text{V}_{\text{WHBI},\text{BFW-B}}}} \quad (2.71)$$

$$M_{\text{WHBI},\text{STEAM}} = \rho_{\text{WHBI},\text{STEAM}} A_{\text{V}_{\text{WHBI},\text{STEAM}}} \sqrt{\frac{2 (P_{\text{WHBI},\text{STEAM}} - P_{\text{STEAM}})}{\rho_{\text{WHBI},\text{STEAM}}}} \quad (2.72)$$

### 2.2.9. Vessel Hold-Up

Hold-up in each vessel is determined from the vessel volume<sup>[17]</sup> and gas density. For calculations involving a bypass valve, the mix area is assumed to occur over one metre length of pipe. Again density calculations are expressed as a function of Equation 2.41.

$$G_{\text{G/G,TUBE}} = \frac{\text{Vol}_{\text{G/G,TUBE}} \rho_{\text{G/G,TUBE}} g_{\text{X,HOLDUP}}}{y_{\text{R2}} \text{MWT}} \quad (2.73)$$

$$G_{\text{G/G,SHELL}} = \frac{\text{Vol}_{\text{G/G,SHELL}} \rho_{\text{G/G,SHELL}} g_{\text{X,HOLDUP}}}{y_{\text{IN}} \text{MWT}} \quad (2.74)$$

$$G_{\text{G/G,BY}} = \frac{\pi r_{\text{G/G,SHELL}}^2 \Delta L_{\text{MIX}} 0.5 (\rho_{\text{G/G,BY1}} + \rho_{\text{G/G,BY2}})}{y_{\text{IN}} \text{MWT}} \quad (2.75)$$

$$G_{\text{R1PH,TUBE}} = \frac{\text{Vol}_{\text{R1PH,TUBE}} \rho_{\text{R1PH,TUBE}} g_{\text{X,HOLDUP}}}{y_{\text{IN}} \text{MWT}} \quad (2.76)$$

$$G_{\text{R1PH,BY}} = \frac{\text{Vol}_{\text{R1PH,BY}} 0.5 (\rho_{\text{R1PH,BY1}} + \rho_{\text{R1PH,BY2}})}{y_{\text{IN}} \text{MWT}} \quad (2.77)$$

$$G_{\text{R1PH,SHELL}} = \frac{\text{Vol}_{\text{R1PH,SHELL}} \rho_{\text{R1PH,SHELL}} g_{\text{X,HOLDUP}}}{y_{\text{R1B1}} \text{MWT}} \quad (2.78)$$

$$G_{\text{R1B1}} = \frac{f_{\text{VOID}} \text{Vol}_{\text{R1B1}} \rho_{\text{R1B1}} g_{\text{X,HOLDUP}}}{y_{\text{R1B1}} \text{MWT}} \quad (2.79)$$

$$G_{\text{R1B2}} = \frac{f_{\text{VOID}} \text{Vol}_{\text{R1B2}} \rho_{\text{R1B2}} g_{\text{X,HOLDUP}}}{y_{\text{R1B2}} \text{MWT}} \quad (2.80)$$

$$G_{\text{WHBI,TUBE}} = \frac{\text{Vol}_{\text{WHBI,TUBE}} \rho_{\text{WHBI,TUBE}} g_{\text{X,HOLDUP}}}{y_{\text{R1B2}} \text{MWT}} \quad (2.81)$$

$$G_{\text{WHBLB}} = \frac{\pi r_{\text{WHBI,TUBE}}^2 \Delta L_{\text{MIX}} 0.5 (\rho_{\text{WHBLB-1}} + \rho_{\text{WHBLB-2}})}{y_{\text{R1B2}} \text{MWT}} \quad (2.82)$$

$$G_{\text{R2}} = \frac{f_{\text{VOID}} \text{Vol}_{\text{R2}} \rho_{\text{R2}} g_{\text{X,HOLDUP}}}{y_{\text{R2}} \text{MWT}} \quad (2.83)$$

$$G_{\text{WHBI,TUBE}} = \frac{\text{Vol}_{\text{WHBI,TUBE}} \rho_{\text{WHBI,TUBE}} g_{\text{X,HOLDUP}}}{y_{\text{R2}} \text{MWT}} \quad (2.84)$$



$$Gw_{WHBI,SHELL} = \left( Vol_{WHBI,SHELL} + Ax_{WHBI,SHELL} ht_{WHBI,SHELL} \frac{L_{WHBI,SHELL}}{100} \right) \rho_{WHBI,BFW} g^x_{HOLDUP} \quad (2.85)$$

$$Gw_{WHBI,SHELL-B} = Vol_{WHBI,SHELL-B} \rho_{WHBI,BFW-B} g^x_{HOLDUP} \quad (2.86)$$

$$Gw_{WHBI,SHELL-M} = \left( Vol_{WHBI,SHELL-T} + Ax_{WHBI} ht_{WHBI} \frac{L_{WHBI,SHELL}}{100} \right) \rho_{WHBI,BFW-M} g^x_{HOLDUP} 0.95 \quad (2.87)$$

$$Gw_{WHBI,SHELL-T} = \left( Vol_{WHBI,SHELL-T} + Ax_{WHBI} ht_{WHBI} \frac{L_{WHBI,SHELL}}{100} \right) \rho_{WHBI,BFW-M} g^x_{HOLDUP} 0.05 \quad (2.88)$$

### 2.3. Material & Energy Balances

Process dynamics are modelled for each vessel in the unit. Most of the process ordinary differential equations (ODE) are based on an energy balance<sup>[7]</sup> around the vessel considered, as expressed in Equation 2.89. Mass balances around the converters and the WHBs are also developed. The standard ODE formats for the converters and vessel levels are given by Equations 2.90 and 2.91.

$$\frac{dT}{dt} = \frac{\dot{E}_{IN} - \dot{E}_{OUT}}{C_p G_{Holdup}} \quad (2.89)$$

$$\frac{dn_i}{dt} = \dot{n}_{i,IN} + \dot{n}_{i,RXN} - \dot{n}_{i,OUT} \quad (2.90)$$

$$\frac{dL}{dt} = \frac{\sum_j (M_j)}{Ax ht \rho} 100 \quad (2.91)$$

Equations 2.89 to 2.91 are adapted to the ammonia process under consideration. The state variables for each vessel can be found in Equations 2.92 to 2.112.

$$\frac{d(T_{G/G,TUBE})}{dt} = \frac{-Q_{G/G} - F_{G/G,TUBE} \Delta h_{G/G,TUBE}}{G_{G/G,TUBE} C_{p,G/G,TUBE}} \quad (2.92)$$

$$\frac{d(T_{G/G,SHELL})}{dt} = \frac{Q_{G/G} - F_{G/G,SHELL} \Delta h_{G/G,SHELL}}{G_{G/G,SHELL} C_{p,G/G,SHELL}} \quad (2.93)$$

$$\frac{d(T_{G/G,BY})}{dt} = \frac{-F_{G/G,BY} \Delta h_{G/G,BY1} - F_{G/G,SHELL} \Delta h_{G/G,BY2}}{G_{G/G,BY} (C_{p,G/G,BY1} + C_{p,G/G,BY2})} 0.5 \quad (2.94)$$



$$\frac{d(T_{R1PH,TUBE})}{dt} = \frac{Q_{R1PH} - F_{R1PH,TUBE} f_{R1PH-1} \Delta h_{R1PH,TUBE}}{G_{R1PH,TUBE} C_{P,R1PH,TUBE}} \quad (2.95)$$

$$\frac{dT_{R1PH,BY}}{dt} = \frac{-F_{R1PH,BY} \Delta h_{R1PH,BY1} - F_{R1PH,TUBE} \Delta h_{R1PH,BY2}}{G_{R1PH,BY} (C_{P,R1PH,BY1} + C_{P,R1PH,BY2}) 0.5} \quad (2.96)$$

$$\frac{d(T_{R1PH,SHELL})}{dt} = \frac{-Q_{R1PH} - F_{R1PH,SHELL} f_{R1PH-2} \Delta h_{R1PH,SHELL}}{G_{R1PH,SHELL} C_{P,R1PH,SHELL}} \quad (2.97)$$

$$\frac{d(T_{R1B1})}{dt} = \frac{\frac{HX_{R1B1}}{2 \times 10^3} \frac{R_{XN,R1B1}}{3600} - F_{R1B1} \Delta h_{R1B1}}{G_{R1B1} C_{P,R1B1}} \quad (2.98)$$

$$\frac{d(T_{R1B2})}{dt} = \frac{\frac{HX_{R1B2}}{2 \times 10^3} \frac{R_{XN,R1B2}}{3600} - F_{R1B2} \Delta h_{R1B2}}{G_{R1B2} C_{P,R1B2}} \quad (2.99)$$

$$\frac{d(n_{R1B1})}{dt} = y_{IN} F_{R1B1} + rxn\_coeff R_{XN,R1B1} - y_{R1B1} F_{R1B2} \quad (2.100)$$

$$\frac{d(n_{R1B2})}{dt} = y_{R1B1} F_{R1B2} + rxn\_coeff R_{XN,R1B2} - y_{R1B2} F_{R2} \quad (2.101)$$

$$\frac{d(T_{WHBI,TUBE})}{dt} = \frac{-Q_{WHBI} - F_{WHBI,TUBE} \Delta h_{WHBI,TUBE}}{G_{WHBI,TUBE} C_{P,WHBI,TUBE}} \quad (2.102)$$

$$\frac{dT_{WHBI,BY}}{dt} = \frac{-F_{WHBI,BY} \Delta h_{WHBI,BY1} - F_{WHBI,TUBE} \Delta h_{WHBI,BY2}}{G_{WHBI,BY} (C_{P,WHBI,BY2} + C_{P,WHBI,BY2}) 0.5} \quad (2.103)$$

$$\frac{d(T_{WHBI,SHELL})}{dt} = \frac{Q_{WHBI} - \Delta H_{WHBI,SHELL}}{G_{WHBI,SHELL} C_{P,WHBI,BFW}} \quad (2.104)$$

$$\frac{d(L_{WHBI,SHELL})}{dt} = \frac{M_{WHBI,BFW} - M_{CBD} - M_{WHBI,STEAM}}{Ax_{WHBI} ht_{WHBI} \rho_{WHBI,BFW}} 100 \quad (2.105)$$

$$\frac{d(n_{R2})}{dt} = y_{R1B2} F_{R2} + rxn\_coeff R_{XN,R2} - y_{R2} F_{WHBI,TUBE} \quad (2.106)$$

$$\frac{d(T_{R2})}{dt} = \frac{\frac{HX_{R2}}{2 \times 10^3} \frac{R_{XN,R2}}{3600} - F_{R2} \Delta h_{R2}}{G_{R2} C_{P,R2}} \quad (2.107)$$

$$\frac{d(T_{WHBI,TUBE})}{dt} = \frac{-Q_{WHBI} - F_{WHBI,TUBE} \Delta h_{WHBI,TUBE}}{G_{WHBI,TUBE} C_{P,WHBI,TUBE}} \quad (2.108)$$

$$\frac{d(T_{WHBI,SHELL-B})}{dt} = \frac{Q_{WHBI} - \Delta H_{WHBI,SHELL-B}}{G_{WHBI,SHELL-B} C_{P,WHBI,BFW-B}} \quad (2.109)$$



$$\frac{d(T_{\text{WHBII,SHELL-M}})}{dt} = \frac{\Delta H_{\text{WHBII,SHELL-M}}}{Gw_{\text{WHBII,SHELL-M}} C_{P,\text{WHBII,BFW-M}}} \quad (2.110)$$

$$\frac{d(T_{\text{WHBII,SHELL-T}})}{dt} = \frac{\Delta H_{\text{WHBII,SHELL-T}}}{Gw_{\text{WHBII,SHELL-T}} C_{P,\text{WHBII,BFW-T}}} \quad (2.111)$$

$$\frac{d(L_{\text{WHBII,SHELL}})}{dt} = \frac{M_{\text{WHBII,BFW,IN}} - M_{\text{WHBI,BFW}} - M_{\text{CBD}} - M_{\text{WHBII,STEAM}}}{Ax_{\text{WHBII}} ht_{\text{WHBII}} \rho_{\text{WHBII,BFW-M}}} 100 \quad (2.112)$$

## 2.4. Model Implementation

In an effort to design optimization and control applications for the converter, the process is modelled in Matlab®<sup>3</sup> version 5.3 and Simulink®<sup>3</sup> version 3.0.

Process ODEs are implemented using Matlab standard s-functions. Programming is done in a modular fashion for each vessel. This is done to allow for increased flexibility and ease of use for program testing and modifications. The modular programs are then linked together in Simulink using subsystem blocks. It is also in Simulink that the process inputs, disturbances and time delays are introduced into the model. An overview of the model can be found in Appendix C, Figure C-1.

## 2.5. Model Validation

Model validation is based on existing plant data encompassing process changes. Two data sets were collected from the plant. The first data set, used to fit steady-state model predictions to plant data, is based on twelve hour shift averages for the month of March 1999. The second data set, taken from February 1999, is used to validate these results. This data set excludes data from February 24<sup>th</sup> and 25<sup>th</sup>, since the ammonia plant was not in operation during this time period.

The parameter estimates found using plant data from March are listed in Table 2-3.

---

<sup>3</sup> © 1999 The MathWorks, Inc. Matlab and Simulink are registered trademarks of The MathWorks, Inc.





**Table 2-3 Fitted Parameters**

Parameters	Description	Value	Units
$f_{G/G}$	Gas-Gas Heat Transfer Correction Term	1.1807	--
$f_{R1PH-1}$	R1 Preheat Heat Transfer Correction Term	0.9669	--
$f_{R1PH-2}$	R1 Preheat Heat Transfer Correction Term	1.0603	--
$f_{WHB I}$	WHB I Heat Transfer Correction Term	0.9321	--
$f_{WHB II}$	WHB II Heat Transfer Correction Term	1.0270	--
$hx_{R1B1}$	R1B1 Forward Reaction Parameter Estimate	1.5976	--
$hx_{R1B2}$	R1B2 Forward Reaction Parameter Estimate	1.3337	--
$hx_{R2}$	R2 Forward Reaction Parameter Estimate	1.2604	--
$v_{BFW,IN}$	BFW Velocity to WHB II	2.3907	m/s
$M_{CBD}$	WHB I and II Continuous Blowdown	3.5	kg/s
$gx_{HOLDUP}$	Vessel Hold-up Correction Term	10	--

These values can be classified as follows.

1. Heat Transfer Correction Terms

Parameters  $f$  are calculated using previously defined equations and averaging results for the month of March.

2. Catalyst Effectiveness Parameters

Parameters  $hx$  are fit by minimizing the sum of the square of the error between the model predictions and the process data. Characteristics of this method are described in detail in Chapter 3. Average results for the month of March are used to validate model performance.

3. Average Process Operation

Parameters  $v_{BFW,IN}$  and  $M_{CBD}$  are calculated based on the average operation for March.

4. Dynamic Model Characteristics

A parameter,  $gx_{HOLDUP}$ , is introduced to compensate for changes in energy in the vessel that are not modelled. For example, the first converter bed has a residence time of three seconds based on its gas hold-up capacity. However, the integral time of the exiting temperature is notably larger. This difference is attributed to changes in the stored energy of the vessel (eight inch wall thickness) and the iron catalyst (modelled as 64% of the vessel volume<sup>[41]</sup>).

Other factors commonly fit to experimental data can be found in Table 2-4. In this case, values from catalyst suppliers are used.

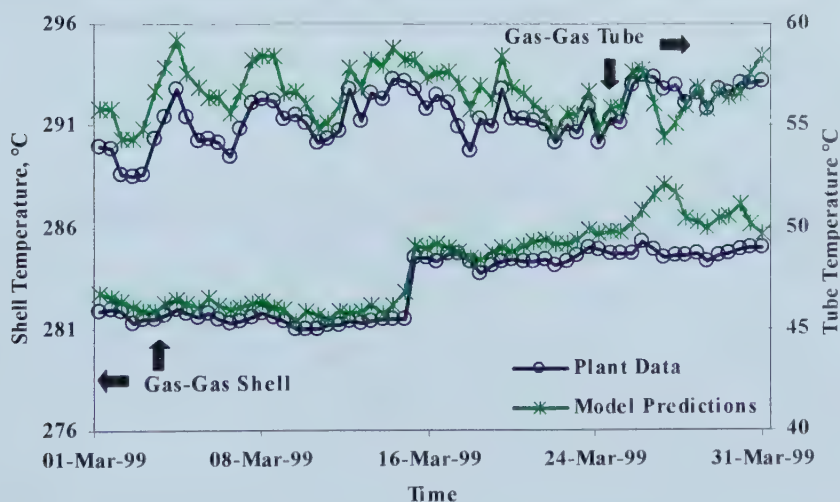


**Table 2-4**      **Catalyst Specifications**

Parameter	Description	Value	Units
m	Temkin Parameter	0.46	--
$\log(k_{(o)})$	Reverse Reaction Factor	14.7102	k-mol NH <sub>3</sub> /hr/m <sup>3</sup> catalyst
$\Delta E_K$	Activation Energy of Reverse Reaction	104.5	J/mol N <sub>2</sub>

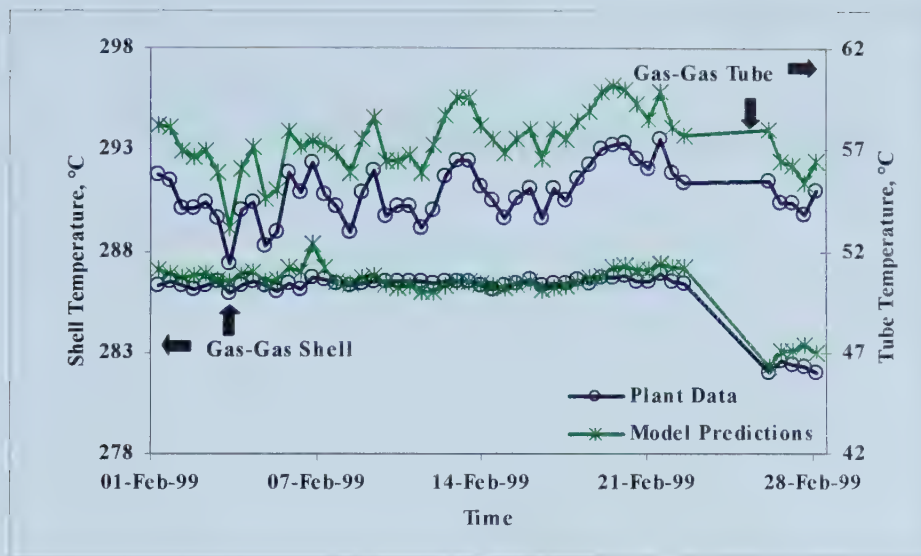
Cross validating parameter estimates using the February data set confirms a good relationship with plant data, over a wide range of operating conditions. Figures 2-7 to 2-14 illustrate the fitted data and results for the gas-gas heat exchanger, R1B1, overall conversion and steam production. These results are demonstrative of the results for other vessels, listed in Appendix D, Figures D-1 to D-10.

Fitted data and results for the gas-gas heat exchanger, Figures 2-7 to 2-8 are typical of the other synthesis gas exchangers modelled. Results are based on a steady state expression of Equations 2.92 and 2.93. Overall the model predictions track well with the plant data. However, in some cases, such as 27-Mar-99, it is noted that the model predictions appear to be directionally incorrect. Additionally, a small consistent offset is observed. By using a single constant parameter in Equation 2.46,  $f_{G/G}$ , to fit the shell and tube exit temperatures, it is not expected for the model predictions to perfectly match plant data, due to noise, possible measurement error and changing inlet conditions.

**Figure 2-7**      **Gas-Gas Exchanger Fitted Data**



**Figure 2-8 Gas-Gas Exchanger Results**



Three parameters,  $h_{x_{R1B1}}$ ,  $h_{x_{R1B2}}$  and  $h_{x_{R2}}$  in Equations 2.21 to 2.23 are used to fit the exit temperature of the three conversion beds and the overall ammonia conversion.

Conversion temperature results for R1B1, based on Equation 2.98, can be observed in Figures 2-9 and 2-10. Unlike the other reactor beds, R1B1 does not have a measured exit temperature. Therefore four bed temperatures are averaged to fit the model predictions. Since the majority of the ammonia conversion occurs in this bed, the largest temperature rise (about +133 °C) is observed across R1B1.

**Figure 2-9 Converter One Bed One Fitted Data**

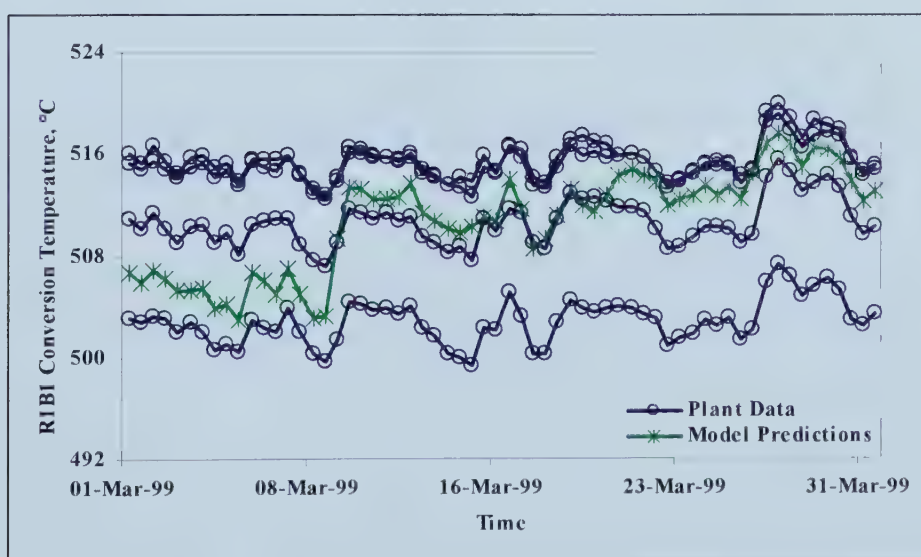
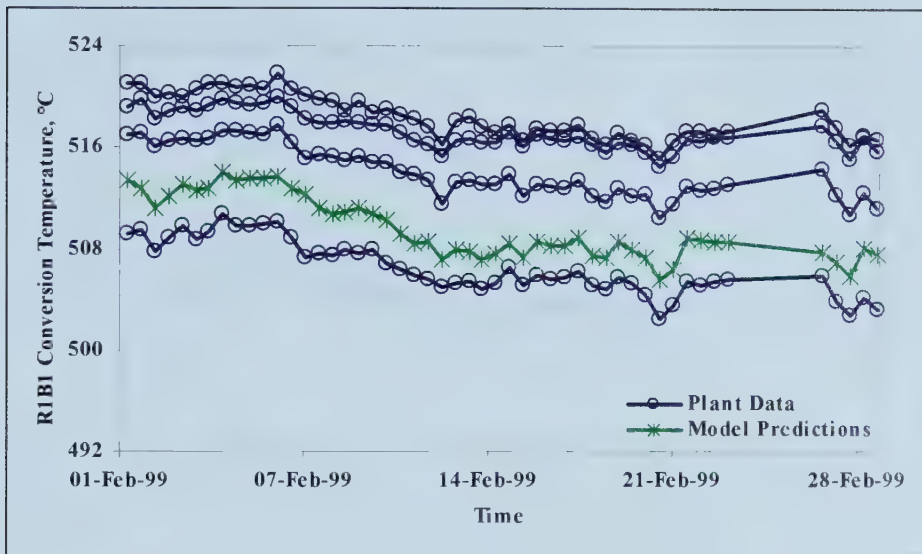




**Figure 2-10** Converter One Bed One Results



Total ammonia conversion is illustrated in Figures 2-11 and 2-12. The most notable characteristic in these figures is the sudden jump in the plant's ammonia conversion from 13.9 % to 15.3 % between 25-Mar-99 to 27-Mar-99. Possible reasons why the model does not predict this spike are discussed in Section 2.6.

**Figure 2-11** Overall Ammonia Conversion Fitted Data

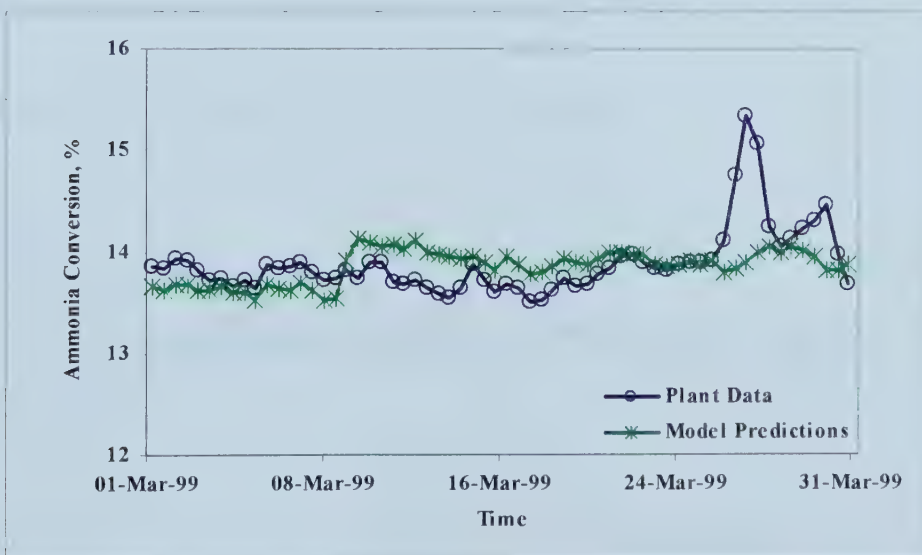
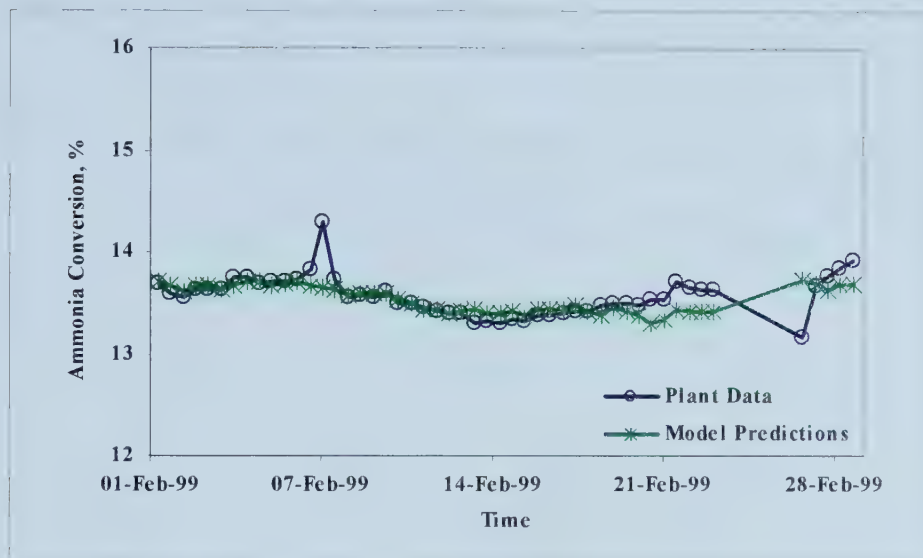






**Figure 2-12 Overall Ammonia Conversion Results**



Lastly results from the steam system are presented in Figures 2-13 and 2-14. Data from WHB I and WHB II are used to determine the correction terms for the overall exchanger heat transfer,  $f_{WHBI}$  and  $f_{WHBII}$ , in Equations 2.48 and 2.49. The average BFW velocity,  $v_{BFW,IN}$ , and the average continuous blow down (CBD),  $M_{CBD}$ , for the month of March are used. Steam production offset for the month of February is largely attributed to using average BFW and CBD rates. Difficulties with directional predictions are a carry-over of problems in modelling upstream vessels.

**Figure 2-13 Waste Heat Boiler Steam Fitted Data**

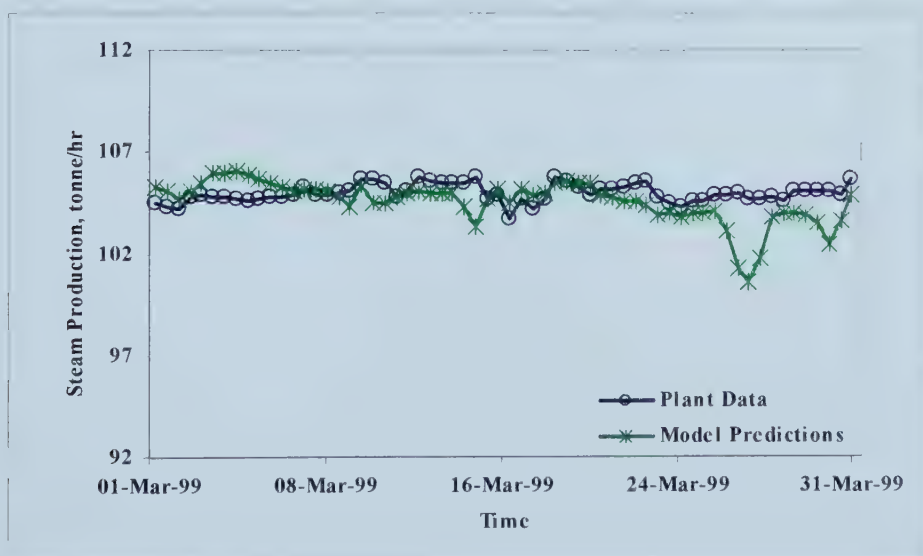
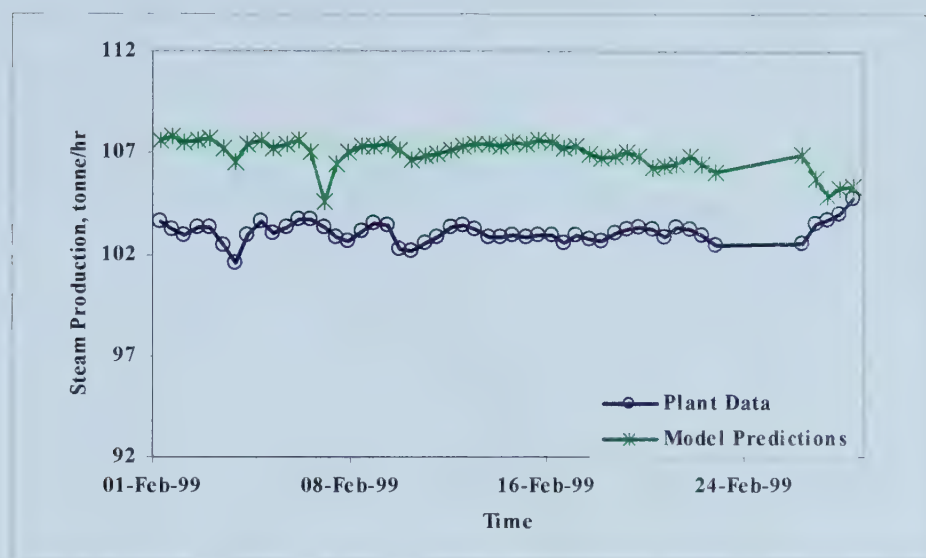




**Figure 2-14**      **Waste Heat Boiler Steam Production Results**



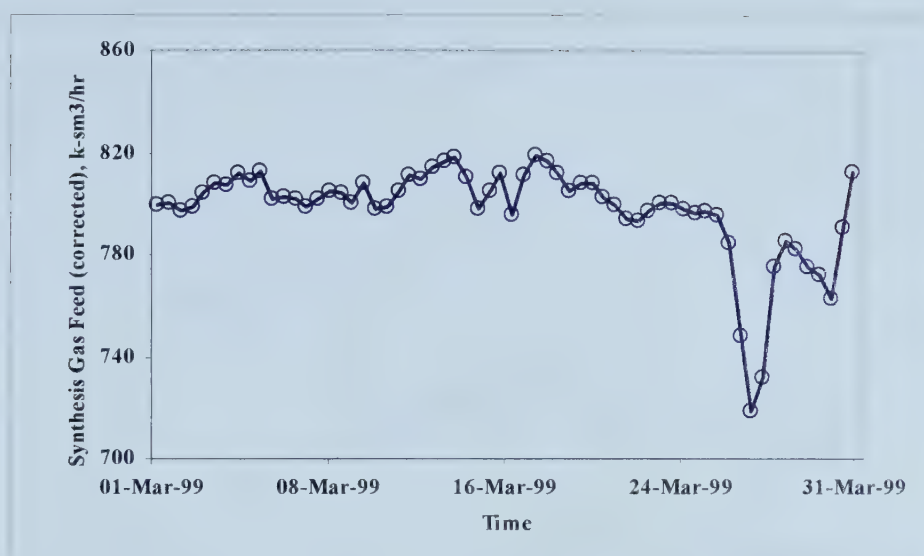
## 2.6. Discussion

In consideration of the nonideal thermodynamic behaviour and kinetics for the synthesis of ammonia, a nonlinear dynamic model of the process is developed. The steady-state performance of the model is compared to existing operations, where eight correction terms are fit using twelve plant measurements.

In general, model results provide an adequate fit to plant data over a wide range of operating conditions, based on 12 hour shift averages. However, a significant discrepancy is observed between plant data and model predictions for ammonia conversion around 27-Mar-01. Inspection of plant disturbances such as synthesis gas feed, Figure 2-15, suggests that the process may be diffusion limited at higher feed rates.

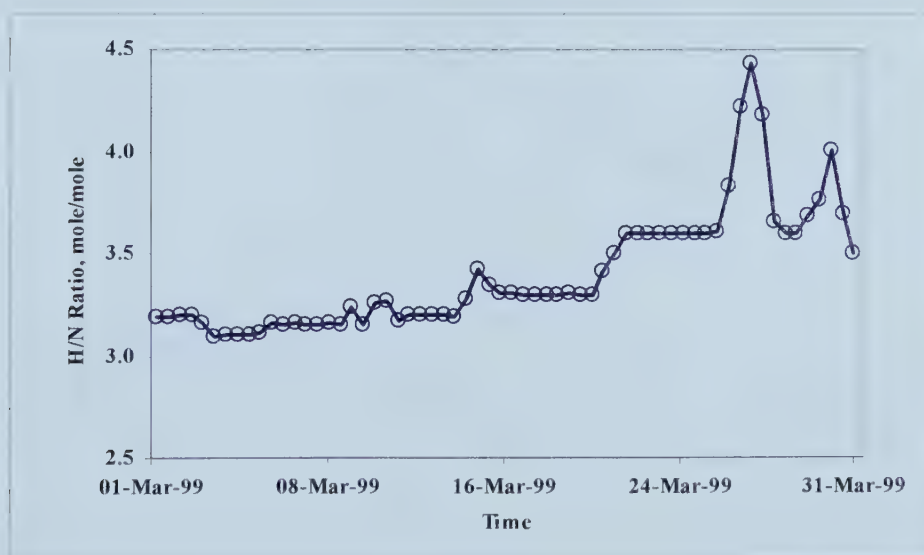


**Figure 2-15**      **Synthesis Gas Feed**



The sudden increase in the H/N ratio at this time, Figure 2-16, may also contribute to model inaccuracy. Interestingly, model results of the rising H/N ratio are contradictory to literature that indicates a negative impact on ammonia conversion at H/N ratios above 2.8<sup>[41]</sup>.

**Figure 2-16**      **Synthesis Gas Hydrogen to Nitrogen Ratio in Feed Stream**



In the converters, the model predicts a sudden increase in the conversion temperature on 9-Mar-99, where none had occurred, Figure 2-9. A sudden drop in inert composition in the feed stream, Figure 2-17, and a rise in the ammonia recycle, Figure 2-18, are also observed at this time. This suggests that a constant catalyst effectiveness term does not adequately account for large changes in process operation. Dynamic update of this parameter is explored in Chapter 3.



The dynamic parameter estimate is used to account for changes in feed rates, H/N ratio, inerts, recycle ammonia, synthesis gas pressure and catalyst activity.

**Figure 2-17      Synthesis Gas Inert Composition in Feed Stream**

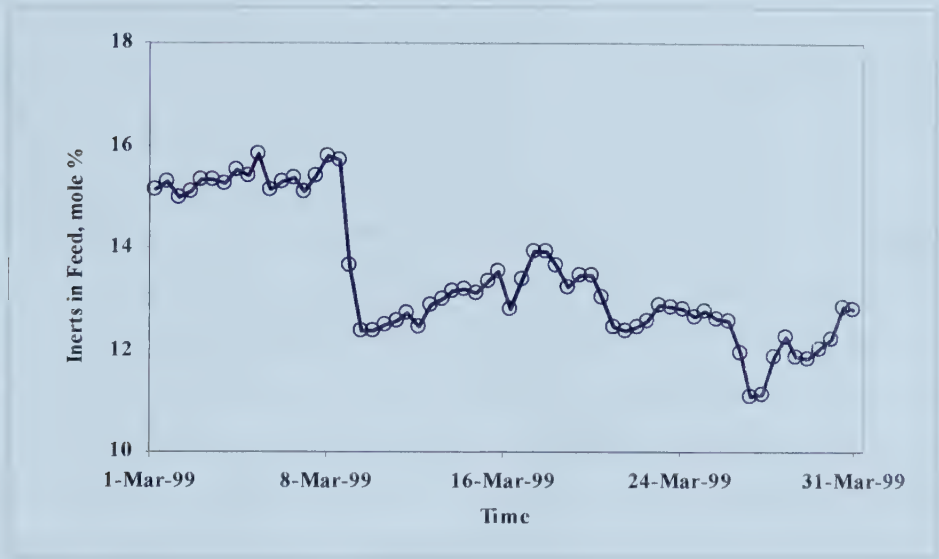
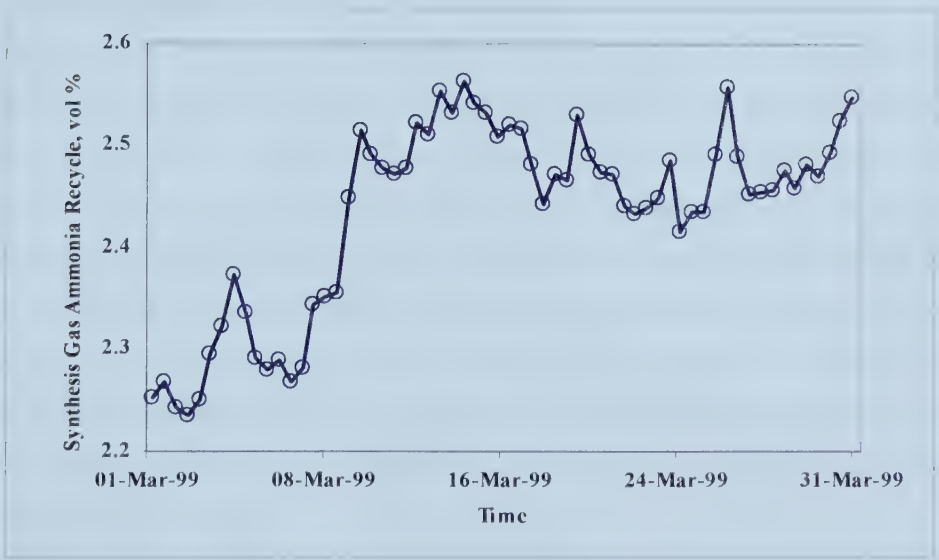


**Figure 2-18      Synthesis Gas Ammonia Recycle in Feed Stream**







## CHAPTER 3

### PARAMETER UPDATES USING HISTORICAL DATA

In an operating plant the catalyst activity and the heat transfer coefficients change due to fouling and variations in process conditions. Knowledge of these parameters and how they vary is an important step in moving the process to its optimal operating conditions<sup>[35]</sup>.

In Chapter 2, several parameters are introduced to fit the model to the process. In this chapter, different ways of using steady-state historical data to update the catalyst effectiveness parameters are investigated. Update of the heat transfer correction terms is not addressed here.

To account for changing catalyst activity and changing equilibrium conditions, an appropriate model parameter must be identified first. Catalyst manufacturers offer specifications relating to their catalyst, as listed in Table 2-4. The possibility of using these values is evaluated. Other possible catalyst effectiveness parameters are also considered. In choosing a suitable parameter, the impact on the reaction curve is evaluated.

Several techniques for updating the parameter identified are studied. These techniques are based on variations of the least squares method, which is the classic approach to estimate model coefficients<sup>[11]</sup>. The intent is to identify the pros and cons of each technique. Results of each technique are expressed in relation to the estimation error, the ability to reject process noise and/or instrumentation error, and the feasibility of each method based on computer resources required to solve the problem. Historical data from Saskferco, based on 12 hour shift averages are used. Due to the fast dynamics of this nonlinear process relative to the process disturbance frequency, it is assumed that the historical process data represents steady-state operation. Ultimately a recommended approach for parameter updates, specific to the process considered, is offered. Correlations between the estimation parameters and process input conditions are investigated and commented on.

#### 3.1. Parameter Selection

The process simulated in Chapter 2 uses the Temkin-Pyshev equation to describe the reaction rate. The catalyst activity parameter to be identified is ultimately incorporated into Equation 2.16. This section considers the published catalyst manufacturer parameters and alternatively a correction factor on the forward reaction as possible candidates to fit model results to plant data.



$$R_{\text{XN}} = \left( k_+ f_{\text{N}_2} \left( \frac{f_{\text{H}_2}^3}{f_{\text{NH}_3}^2} \right)^m - k_- \left( \frac{f_{\text{NH}_3}^2}{f_{\text{H}_2}^3} \right)^{1-m} \right) \text{Vol} \quad (2.16)$$

Manufacturer catalyst parameters include the following:

1. Temkin constant,  $m$ ,
2. Frequency factor for the reverse reaction,  $ko_-$  and
3. Activation energy constant  $\Delta E_k$ , for the reverse reaction

To gain an understanding of the impact of these constants on the model, the optimal value of these parameters is calculated using a single data set. Published and calculated results are listed in Table 3-1. The impact of modifying these parameters on the reaction curve can be viewed in Figure 3-1 and Table 3-2. Most notable, changing these parameters impacts the maximum potential ammonia production with a reduced temperature at which optimal conversion is achieved.

**Table 3-1 Catalyst Manufacturer Parameter Calculations for R1B1**

	$m$	$\log(ko_-)$ kJ/kmol NH <sub>3</sub> /hr/m <sup>3</sup>	$\Delta E_K$ kJ/mol N <sub>2</sub>
<b>Published Values</b>	0.46-0.75	14.7102	104.5-110.8
<b>Calculated <math>m</math></b>	<b>0.50</b>	14.7102	104.5
<b>Calculated <math>\log(ko_-)</math></b>	0.46	<b>15.0917</b>	104.5
<b>Calculated <math>\Delta E_K</math></b>	0.46	14.7102	<b>98.8</b>

**Figure 3-1 Impact of Changing Model Parameters on Ammonia Reaction**

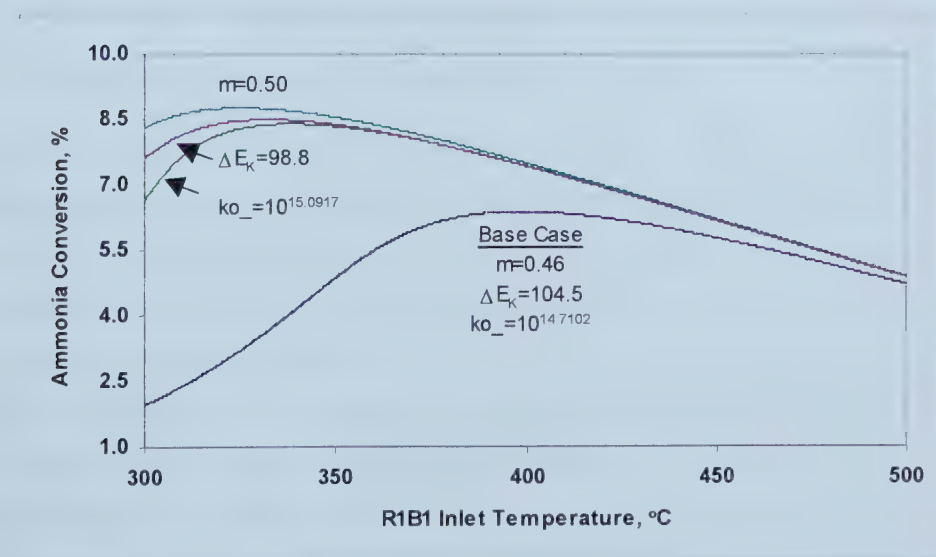




**Table 3-2**      **Model Parameters with Calculated Optimum Temperature**

<b>m</b>	<b>log(ko<sub>-</sub>) kJ/kmol NH<sub>3</sub> /hr/m<sup>3</sup></b>	<b>ΔE<sub>K</sub> kJ/mol N<sub>2</sub></b>	<b>R1B1 T<sub>OPT</sub> °C</b>	<b>R1B1 Conversion %</b>
0.46	14.7102	104.5	399	6.38
<b>0.50</b>	14.7102	104.5	325	8.76
0.46	<b>15.0917</b>	104.5	338	8.39
0.46	14.7102	<b>98.8</b>	332	8.49

The large shift in the reaction curve, observed in Figure 3-1, is considered erroneous and update of the manufacturer parameters is dropped due to its infeasibility. Since this thesis only considers operation within a small range of the reaction curve (within approximately 20 °C for R1B1), it is decided to use published parameters based on the assumption that these values were determined from a broader range of conversion temperatures.

Chapter 2 introduced a term referred to as the catalyst effectiveness parameter, defined in Equation 2.20. The correction factor,  $h_x$ , is used to fit the equilibrium forward reaction rate to the actual forward reaction rate. It is noted that the forward reaction is considered the rate-limiting step.

$$k_+ = h_x k_- K_p \quad (2.20)$$

Subsequent discussion on parameter update techniques and results uses three parameters,  $h_{XR1B1}$ ,  $h_{XR1B2}$  and  $h_{XR2}$  to fit the process model to measured process variables. The remainder of this chapter considers update of  $h_x$  as a dynamic value, sensitive to process disturbances and changes to input conditions.

### 3.2. Least Squares Regression Formulation

The least squares approach yields a solution that minimizes the problem's objective function<sup>[6]</sup>, expressed as a function of the problem error. Two parameter update methods are evaluated in an attempt to find the approach best suited to the ammonia synthesis parameter update problem. These approaches include the sum of squares and recursive least squares. Both methods are based on least squares regression techniques.

The sum of squares is a common approach to estimate model coefficients. The second method, recursive least squares, uses difference equations to calculate the catalyst parameters. The weighting matrix is calculated from the variation in error of the model variables.

The sum of squares algorithm compares results using a single data set and multiple data sets to update the parameter. Multiple data sets potentially increase the robustness of the parameter estimation problem by rejecting or reducing the impact of erroneous or noisy signals.





However, the use of too many data sets dampens the response to current operating conditions. As a compromise, four data sets are used to evaluate this criterion. Four data sets were chosen to allow the estimator to respond to current operating conditions, while weighing historical trends.

The model variables and parameters for the update problem are defined in Equations 3.1 to 3.3.  $\mathbf{y}$  refers to the measured plant variables, scaled appropriately. These variables include the conversion temperature into each reactor bed and the total ammonia production.  $\hat{\mathbf{y}}$  are the estimated variables.  $\mathbf{u}$  are the parameters to be manipulated to meet the objective function.

$$\mathbf{y} = \begin{bmatrix} T_{R1B1,PLANT} \\ T_{R1B2,PLANT} \\ T_{R2,PLANT} \\ (M_{NH3,PLANT}) \cdot 10 \end{bmatrix} \quad (3.1)$$

$$\hat{\mathbf{y}} = \begin{bmatrix} T_{R1B1,CALC} \\ T_{R1B2,CALC} \\ T_{R2,CALC} \\ (M_{NH3,CALC}) \cdot 10 \end{bmatrix} \quad (3.2)$$

$$\mathbf{u} = \begin{bmatrix} hx_{R1B1} \\ hx_{R1B2} \\ hx_{R2} \end{bmatrix} \quad (3.3)$$

The calculated total ammonia production is based on the sum of ammonia produced in each converter, Equation 3.4.

$$M_{NH3,CALC} = (R_{XN,R1B1,CALC} + R_{XN,R1B2,CALC} + R_{XN,R2,CALC}) MWT_{NH3} \cdot 10^{-3} \quad (3.4)$$

### 3.2.1. Sum of Squares

The first formulation is based on minimizing the sum of the squared errors of the three reactor bed temperatures and ammonia production using a single, stationary sample period. The problem solution in this case does not depend on the results of preceding time periods. The objective function is posed in Equation 3.5, with 123 equality constraints referenced in Equation 3.6. Dependent variables referenced in Equation 3.6 are listed in Table E-1 of Appendix E.

#### Case 1a

Minimize:

$$e(\mathbf{y}, \mathbf{u}) = \sum_{i=1}^4 (y_i - \hat{y}_i)^2 \quad (3.5)$$

Subject to:





$$h_j(\mathbf{y}, \mathbf{u}) = 0 \quad j = 1, 2, \dots, 123 \quad (3.6)$$

To ensure reliable and efficient solution of the parameter estimation problem, variables are scaled and equations manipulated to eliminate decision and dependent variables from equation denominators. Constraint equalities use the equations specified in Chapter 2. Deviations from this are as follows.

1. Converter temperatures and reaction rates are solved using steady-state mass and energy balances.
2. For convenience, several intermediate calculations are introduced. These variables are listed in Section E.2 of Appendix E.

Extending Case 1a to include multiple data sets, the objective function and constraint equalities are reposed in Case 1b as shown in Equations 3.7 and 3.8.

#### Case 1b

Minimize:

$$e(\mathbf{y}, \mathbf{u}) = \sum_{n=-3}^0 \left( \sum_{i=1}^4 (y(t_n)_i - \hat{y}_i(t_n))^2 \right) \quad (3.7)$$

Subject to:

$$h_{nj}(\mathbf{y}, \mathbf{u}) = 0 \quad n = -3, -2, \dots, 0; \quad j = 1, 2, \dots, 123 \quad (3.8)$$

Where:  $n$  is the sample period, based on 12 hour shift averages (e.g. at  $t_0 = 25\text{-Mar-99 } 7 \text{ AM}$ ,  $t_{-1} = 24\text{-Mar-99 } 7 \text{ PM}$ ,  $t_{-2} = 24\text{-Mar-99 } 7 \text{ AM}$ ,  $t_{-3} = 23\text{-Mar-99 } 7 \text{ PM}$ .)

### **3.2.2. Recursive Least Squares**

The recursive least squares method is similar to Case 1, in that it uses the sum of the squared error, but with a weighting matrix based on knowledge of the process. Additionally, as a recursive function, results depend on the results of preceding solutions. Equations 3.9 to 3.10 outline the process. Variables are expressed as difference equations, depending on the values of previous time periods to determine the predicted operation for comparison to measured plant variables.

$$\hat{\mathbf{y}} = \Phi \mathbf{u} \quad (3.9)$$

$$\Phi = \frac{\partial \mathbf{F}(\mathbf{y}, \mathbf{u})}{\partial \mathbf{u}} \quad (3.10)$$

The error between the measured and estimated outputs is expressed in Equation 3.11. Equation 3.11 is the cost function to be minimized. From this basis,  $\mathbf{u}$  can be evaluated by solving the Jacobian of Equation 3.11. This yields Equation 3.12<sup>[36]</sup>.

$$\|\mathbf{e}\|^2 = \mathbf{e}^T \mathbf{e} = (\mathbf{y} - \Phi \mathbf{u})^T (\mathbf{y} - \Phi \mathbf{u}) \quad (3.11)$$



$$\mathbf{u} = (\Phi^T \Phi)^{-1} \Phi^T \mathbf{y} \quad (3.12)$$

Introducing a weighting matrix in the objective function, the recursive least squares problem is posed in Equation 3.13<sup>[36]</sup>.

#### Case 2

Minimize:

$$\|\mathbf{e}\|^2 = \mathbf{e}^T \mathbf{W} \mathbf{e} = (\mathbf{y} - \Phi \mathbf{u})^T \mathbf{W} (\mathbf{y} - \Phi \mathbf{u}) \quad (3.13)$$

The parameter update calculation then becomes Equation 3.14. The weighting matrix is set to the inverse of the covariance matrix, Equations 3.15 to 3.16.

$$\mathbf{u} = (\Phi^T \mathbf{W} \Phi)^{-1} \Phi^T \mathbf{W} \mathbf{y} \quad (3.14)$$

$$\mathbf{W} = \frac{1}{\text{diag}(\sigma^2)} \quad (3.15)$$

$$\sigma^2 = \text{var}(\mathbf{e}) \quad (3.16)$$

The parameter update matrix,  $\Phi$ , is a complex function of changing process inputs and outputs. It is recalculated in each parameter update calculation based on the steady-state mass and energy balances around each bed. In determining the matrix function, the change in gas activity, compression factors and residual enthalpies with respect to the update parameters is assumed relatively negligible.

$$\Phi = \begin{bmatrix} \frac{\partial T_{R1B1,CALC}}{\partial (hx_{R1B1})} & \frac{\partial T_{R1B1,CALC}}{\partial (hx_{R1B2})} & \frac{\partial T_{R1B1,CALC}}{\partial (hx_{R2})} \\ \frac{\partial T_{R1B2,CALC}}{\partial (hx_{R1B1})} & \frac{\partial T_{R1B2,CALC}}{\partial (hx_{R1B2})} & \frac{\partial T_{R1B2,CALC}}{\partial (hx_{R2})} \\ \frac{\partial T_{R2,CALC}}{\partial (hx_{R1B1})} & \frac{\partial T_{R2,CALC}}{\partial (hx_{R1B2})} & \frac{\partial T_{R2,CALC}}{\partial (hx_{R2})} \\ \frac{\partial M_{NH_3,CALC}}{\partial (hx_{R1B1})} & \frac{\partial M_{NH_3,CALC}}{\partial (hx_{R1B2})} & \frac{\partial M_{NH_3,CALC}}{\partial (hx_{R2})} \end{bmatrix} \quad (3.17)$$

Since the above equations are all expressed as difference variables, a judicious starting point is required. The absolute value of the parameter updates depends on the previous calculations. At time zero,  $\mathbf{u}_n$  uses the calculated value from the sum of squares approximation, for one sample period.

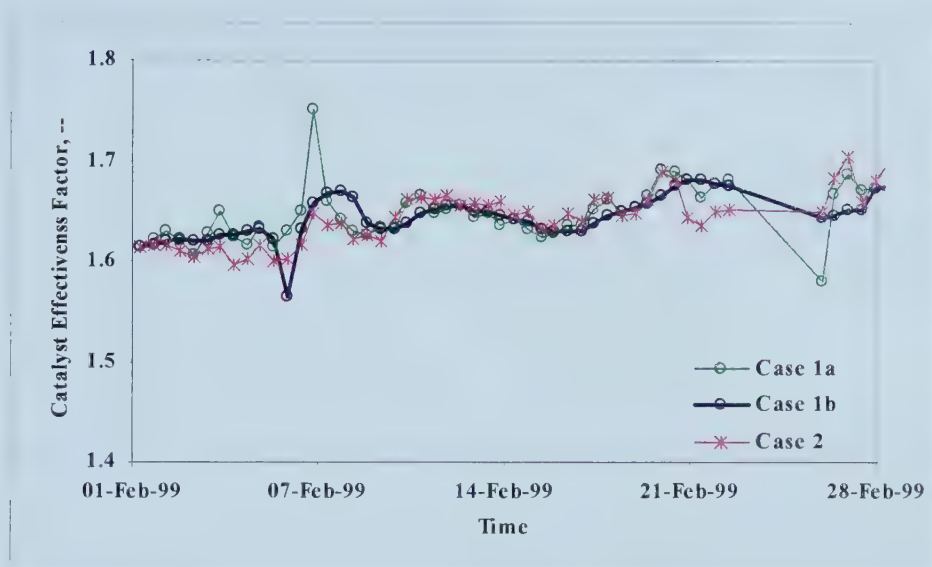
$$\mathbf{u}_n = \mathbf{u}_{n-1} + (\Phi^T \mathbf{W} \Phi)^{-1} \Phi^T \mathbf{W} \mathbf{y} \quad (3.18)$$



### 3.3. Results

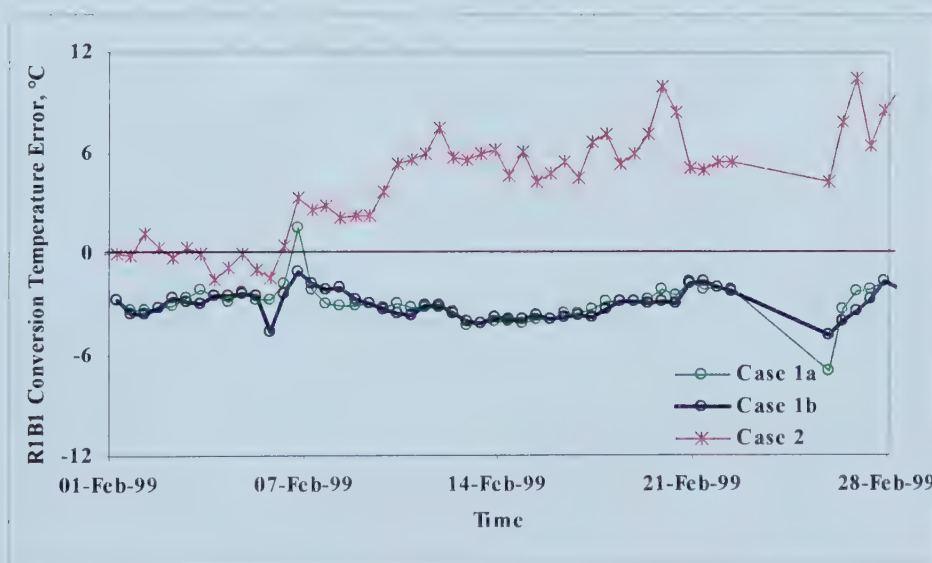
Using historic data for the month of February, parameter updates are solved using the two least squares methods established in Section 3.2. The parameter results for the first converter bed, R1B1, can be found in Figure 3-2.

**Figure 3-2** R1B1 Dynamic Parameter Update



Subsequent model error for R1B1 is plotted in Figure 3-3. Results for R1B2 and R2 can be referenced in Section E.3 of the Appendix in Figures E-1 to E-4.

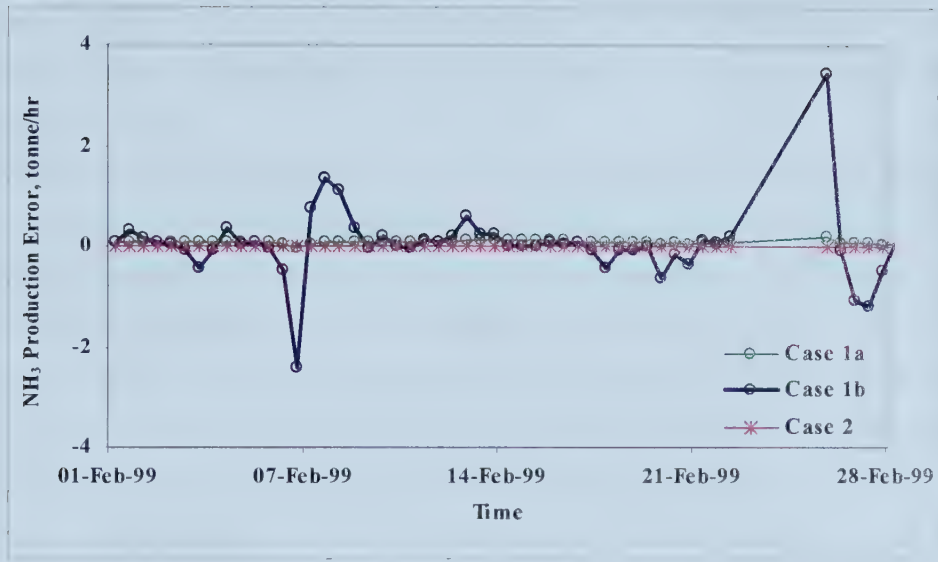
**Figure 3-3** R1B1 Conversion Temperature Error



Overall ammonia production error is illustrated in Figure 3-4.



**Figure 3-4 Overall Ammonia Production Error**



Results are summarized in Table 3-3.

**Table 3-3 Variable and Parameter Results for Parameter Update Problem**

	Case 1a	Case 1b	Case 2
$h_{R1B1,STD}$	0.028	0.022	0.025
$h_{R1B2,STD}$	0.042	0.027	0.020
$h_{R2,STD}$	0.056	0.036	0.013
$T_{R1B1,ERR,AVG}$ (°C)	-2.9	-3.0	4.1
$T_{R1B2,ERR,AVG}$ (°C)	-2.8	-2.9	0.7
$T_{R2,ERR,AVG}$ (°C)	-2.8	-2.8	0.8
$M_{NH3,ERR,AVG}$ (tonne/hr)	0.08	0.04	0.004
$T_{R1B1,ERR,RNG}$ (°C)	-7.0 to 1.5	-4.9 to -1.1	-1.6 to 10.4
$T_{R1B2,ERR,RNG}$ (°C)	-6.8 to 1.5	-4.5 to -0.6	-0.3 to 1.1
$T_{R2,ERR,RNG}$ (°C)	-6.7 to 1.5	-4.0 to -0.2	-0.5 to 1.4
$M_{NH3,ERR,RNG}$ (tonne/hr)	-0.1 to 0.2	-2.4 to 3.5	0 to 0.005
<b>CPUTime</b> <sup>4</sup> (minutes)	5.9	22.4	0.16

<sup>4</sup> Based on AMD Athlon 500 MHz processor with 512 MB RAM.





### 3.4. Discussion

The parameter update problem formulation encompasses process changes of the unit, fitting the process model to measured plant data. Results in all cases track reasonably well with plant data with some discrepancies.

Results for the sum of squares method, using four data sets compared to a single data set, demonstrate less variation in the parameter update value. The estimated response of the process variables is also dampened. The benefit of using multiple data sets is that it allows for rejection of model noise and instrumentation error. The difficulty is that the four time periods are each given equal weighting. The recursive least squares method calculates the weighting matrix based on the variation in error between the measured and calculated variables. With this knowledge of the process, it is able to estimate the measured variables, with the least total error.

Overall, implementation of the sum of squares is relatively intuitive. However, restating constraints without decision or dependent variables in the denominator proved to be an arduous and time consuming task. Subsequent troubleshooting became more difficult based on increased program size. Comparatively, the recursive least squares method is a simple algorithm, and is easy to troubleshoot. Evaluation of the parameter update matrix,  $\Phi$ , is the most difficult aspect of this technique. On-line implementation of this method needs to consider conditioning of the Jacobian and possible singularities, as well as error checking of the variables.

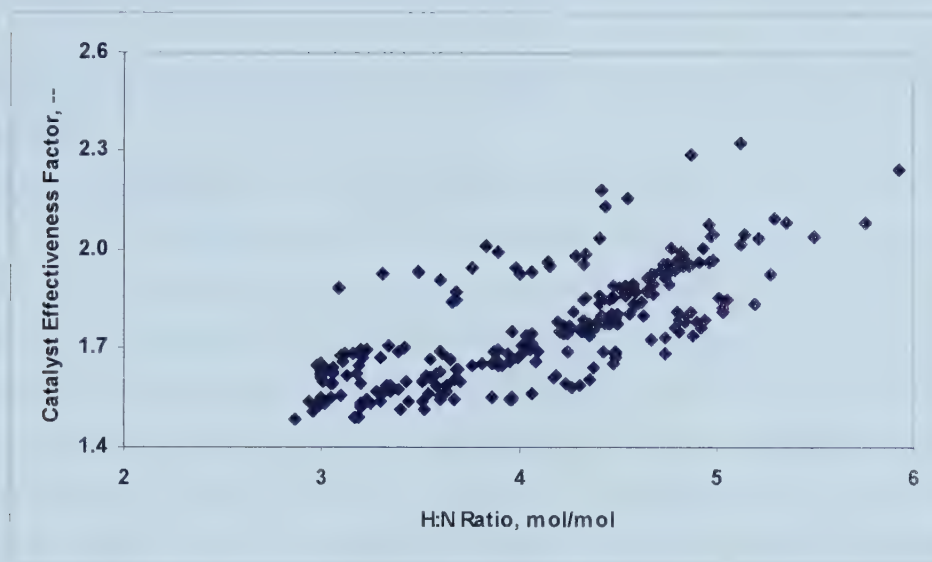
Based on the above evaluations, the preferred implementation is the recursive least squares approach. In general, based on results summarized in Table 3-3, the recursive least squares, Case 2, demonstrates the least overall error. Convergence time in this case is about 36 times less than the next fastest parameter update algorithm. The major drawback of this method is that it depends on reasonable initial conditions. In the above example, the initial value for the sum of squares case is used. As such, a combination of the recursive least squares and sum of squares method would be the most advantageous implementation. The recursive least squares approach could be used for fast, frequent updates, with the slower sum of squares model used to amend the parameter updates on a less frequent basis.

Impact of the process inputs to the parameter update solution is explored to determine if any correlations exist. This is done to gain insight into parameter update sensitivities and potential deficiencies of the process model. Figure 3-5 illustrates the relationship of the case one sum of squares parameter update values to the feed H/N ratio. As observed in this plot, the catalyst effectiveness factor increases directly with increasing H/N ratios. This relationship



suggests that ammonia equilibrium and subsequent conversion at higher H/N ratios is better than supported by the process model. This is consistent with observations at Saskferco<sup>[12]</sup>.

**Figure 3-5** R1B1 Parameter Update vs. Inlet H/N Ratio



Subsequent control and optimization calculations and observations use the sum of squares method with one sample period. This technique is chosen for future studies since it employs uses the same formulation as the process model and control and optimization programs.

While not explored in this chapter, results are also a function of the sample period. The above examples use historic data based on twelve hour averages.



## CHAPTER 4

### PROCESS OPERATION OPTIMIZATION

This chapter investigates the steady-state optimization of the ammonia synthesis loop and the relative benefits.

Generally speaking an increase in overall ammonia conversion from 13.85 % to 13.90 %, based on \$ 50/tonne ammonia netback<sup>[12]</sup>, and operating 300 days per year at constant converter throughput, would increase company profits by approximately \$100 k per year.

The process model and parameter updates developed in Chapter 2 and Chapter 3 are used to formulate an off-line optimizer using historical plant data. The objective function is to maximize conversion of the synthesis gas to ammonia. Impact of increased conversion on the process is twofold. Additional ammonia production can potentially be realized. Secondly, recycled synthesis gas flow will decrease, resulting in reduced energy costs per tonne of product and a more efficient process. For simplicity, this thesis explores the opportunity for increased production.

The performance of the optimizer, given the changing inlet conditions and their impact on the process optimum is addressed as part of the post optimality analysis. Optimization studies with actual plant data are also carried out. Process optimization under normal operating conditions is determined as a baseline. Active constraints are flagged. The results of unit optimization are compared to the simplified optimization of a single converter bed. Additional studies including summer vs. winter operation and operation at reduced catalyst activity are also performed.

#### 4.1. Optimization Problem Formulation

Due to the complexity of the optimization problem 245 equality constraints are devised. The objective function, equalities and inequalities are posed in Equations 4.1 to 4.4. The dependent variables are listed in Appendix F, Table F-1.

Minimize:

$$f(\mathbf{y}) = -\left(R_{\text{XN,R1B1}} + R_{\text{XN,R1B2}} + R_{\text{XN,R2}}\right)^2 \quad (4.1)$$



$$\mathbf{y} = \begin{bmatrix} T_{R1PH,BY} \\ T_{R1PH,SHELL} \\ T_{WHBI,BY} \end{bmatrix} \quad (4.2)$$

Subject to:

$$h_j(\mathbf{y}, \mathbf{u}) = 0 \quad j = 1, 2, \dots, 245 \quad (4.3)$$

$$0 \leq \mathbf{u} \leq 100 \quad \mathbf{u} = \begin{bmatrix} HV_{G/G,SHELL} \\ HV_{R1PH,TUBE} \\ HV_{WHBI,TUBE} \\ HV_{WHBI,STEAM} \end{bmatrix}^T \quad (4.4)$$

Equality constraints are based on the steady-state versions of the mass and energy balances developed in Chapter 2. Several intermediate variables are also introduced for convenience. It is noted that all variables are scaled to solve within a factor of ten and included in the equation numerator only. Four independent variables,  $HV_{G/G,SHELL}$ ,  $HV_{R1PH,TUBE}$ ,  $HV_{WHBI,TUBE}$  and  $HV_{WHBI,STEAM}$  are employed in minimizing the objective function. The objective of the optimizer is to identify feasible controller setpoints within constraints.

## 4.2. Sensitivity Analysis

An optimal solution gained from a deterministic optimization problem may not by itself be entirely useful<sup>[15]</sup> because of uncertainties and possible variations involved in process parameters or models. Post-optimality analysis is necessary to quantitatively ascertain the sensitivity of the optimal results to model parameters<sup>[15]</sup>. In this case, the impact of process disturbances and the catalyst effectiveness parameter on the calculated optimal converter inlet temperature is explored.

Sensitivities are determined using a first order analysis by perturbation. Methods such as a Reduced Hessian Strategy<sup>[15]</sup> exist to evaluate the first order sensitivity of the optimal solution, with potentially significant computational savings. However, in this case, perturbation of model formulated in Section 4.1 is used for expediency.

Figure 4-1 looks at the impact of varying inlet pressure to the first reactor bed. The line traversing the locus of the maxima, often referred to as the “ridge line”, illustrates the optimal operation of bed one, with changing pressure.





**Figure 4-1 R1B1 Conversion vs. Inlet Temperature, Varying Pressure<sup>5</sup>**

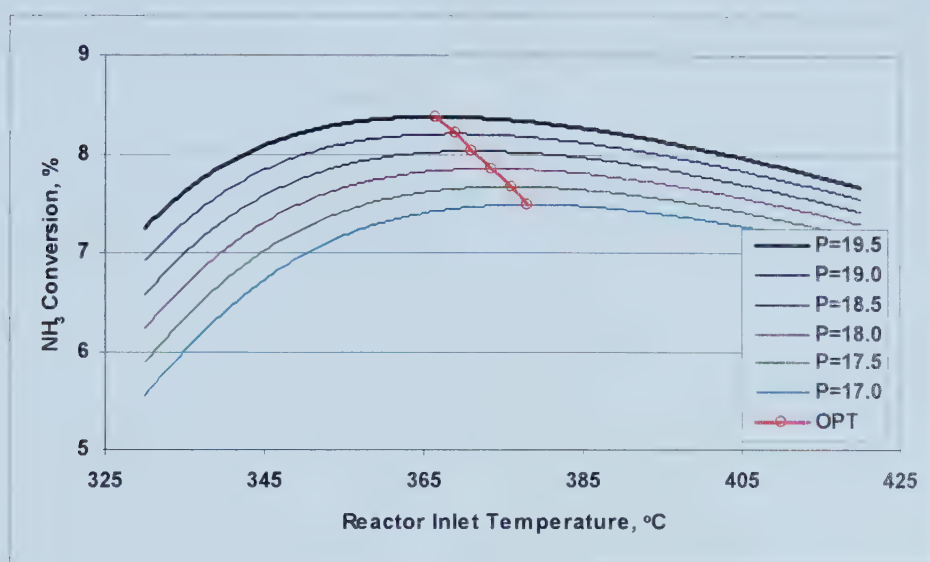


Figure 4-1 highlights a few key points. The equilibrium favours a higher operating pressure. An increase of 1 MPa in bed one, impacts ammonia conversion by approximately 0.36 %. As pressure is reduced, the optimum converter inlet temperature increases. Increasing system pressure by 1 MPa reduces the optimum bed one temperature by approximately 4.6 °C.

The effect of composition on ammonia conversion is often considered in three parts, H/N ratio, ammonia recycle and inerts. Figures 4-2 and 4-3 illustrate the impact of the H/N ratio and ammonia recycle on the optimal operation respectively. It is noted that process inerts have the same directional impact as recycle ammonia.

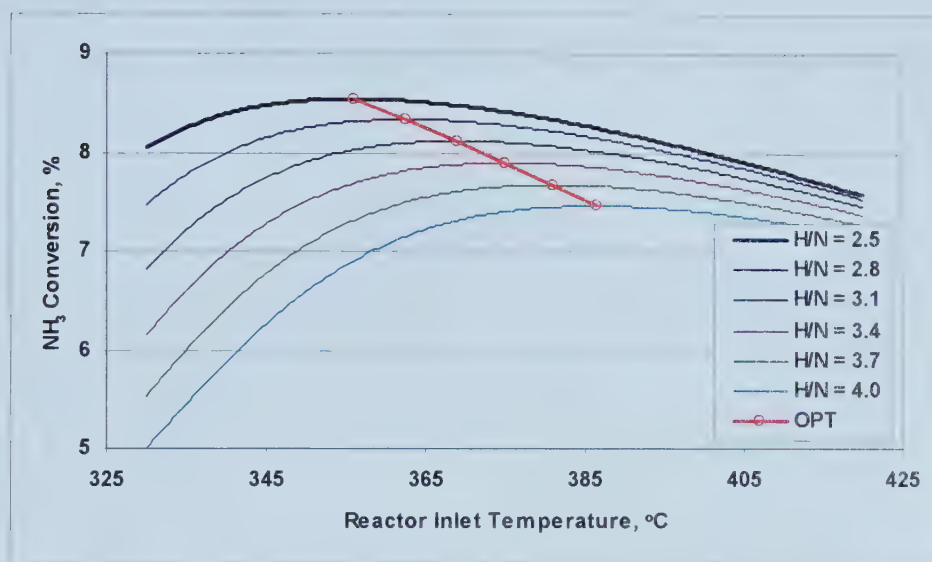
As can be seen in Figure 4-2 a lower H/N ratio is favoured for ammonia conversion, which is consistent with nitrogen being the rate-limiting reagent. However the model does not detect the published optimum H/N ratio of 2.8<sup>[41]</sup>.

<sup>5</sup> Based on the following initial process conditions:

$V_{IN,SG} = 799 \text{ k-sm}^3/\text{hr}$ ,  $P = 18.6 \text{ MPa}$ ,  $y_{NH_3} = 2.25 \%$ ,  $y_{H_2}/y_{N_2} \text{ ratio} = 3.2$ ,  $y_{INERTS} = 15.1 \%$

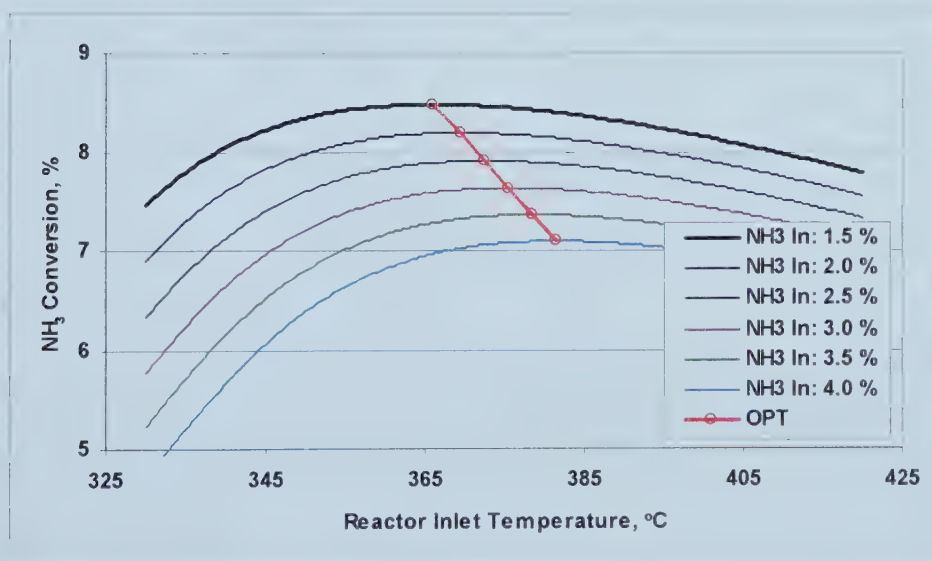


**Figure 4-2** R1B1 Conversion vs. Inlet Temperature, Varying H/N Ratio<sup>5</sup>



Residual ammonia in the feed, as shown in Figure 4-3, impacts the process in two ways. Firstly, it reduces the net ammonia conversion potential. Secondly, it decreases the reactants' partial pressure. A 1 % increase in ammonia recycle reduces conversion potential by about 0.55 % and increases the bed one optimum operating temperature about 6.1 °C. Increased inerts in the synthesis gas feed also reduce the partial pressure of the reactants and shift the reaction equilibrium.

**Figure 4-3** R1B1 Conversion vs. Inlet Temperature, Varying  $y_{\text{NH}_3}$  in Feed<sup>5</sup>

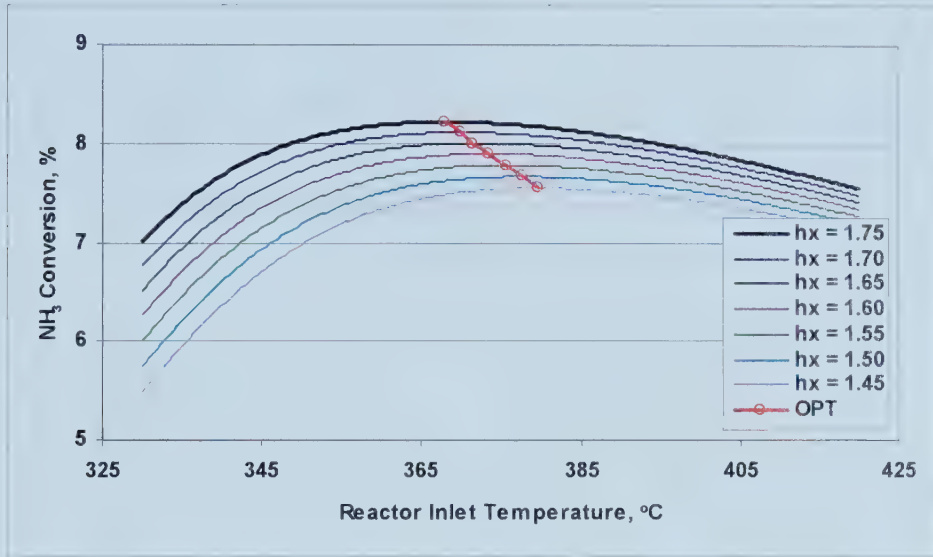


Sensitivity of the optimal solution with the catalyst update parameter,  $h_x$  is demonstrated in Figure 4-4. As expected, predicted ammonia conversion increases with a higher parameter



update value. As determined by the slope of the ridge line, a change in the update parameter of 0.05, shifts the optimal setpoint by  $-1.9^{\circ}\text{C}$ .

**Figure 4-4 R1B1 Conversion vs. Inlet Temperature, Varying  $h_x$  Parameter<sup>5</sup>**



The other interesting point consistent in Figures 4-1 to 4-4 is the insensitivity of the conversion to changes in temperature near the optimal inlet temperature. Using data from Figures 4-1 to 4-4, the average response of ammonia conversion with temperature around the optimal inlet temperature is summarized in Table 4-1.

**Table 4-1 R1B1 Impact of Temperature Deviation from Optimum**

$\Delta T$ Above Optimum $^{\circ}\text{C}$	$\Delta \text{Conversion}$ %
1	$-4 \times 10^{-4}$
5	-0.01
10	-0.04
20	-0.13

### 4.3. Optimization Studies

In this section, the optimal operation is evaluated for different scenarios. Potential benefits are evaluated where applicable. Scenarios to be considered include normal operation, changing process conditions and degraded catalyst activity.

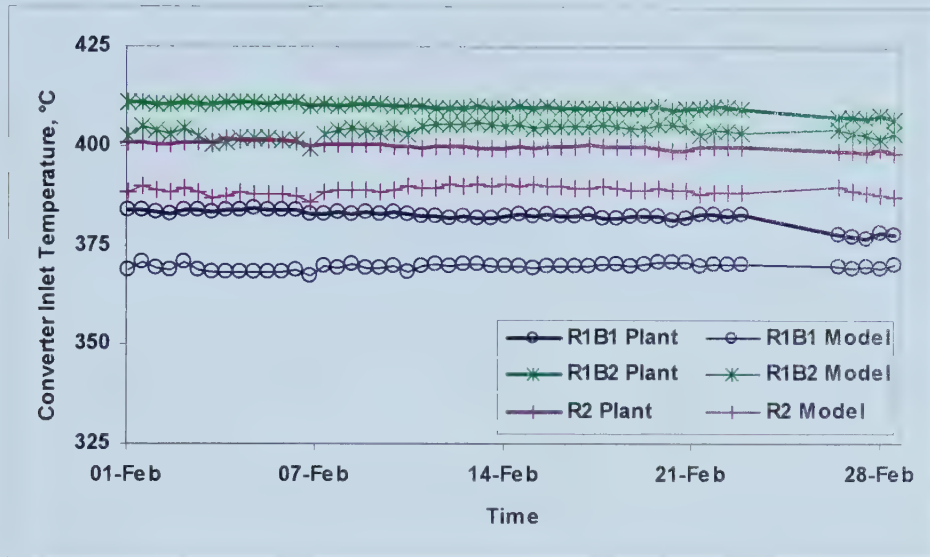
#### 4.3.1. Normal Operation

The optimum operating temperatures for February 1999 are solved for each bed. These values are calculated from the optimization problem formulated in Section 4.1, using historic plant data as



the model inputs. Results are presented in Figure 4-5. Realization of these results requires a suitable control application, discussed further in Chapter 5.

**Figure 4-5 Optimal Temperature Profile, Normal Operation–Unit Optimization**



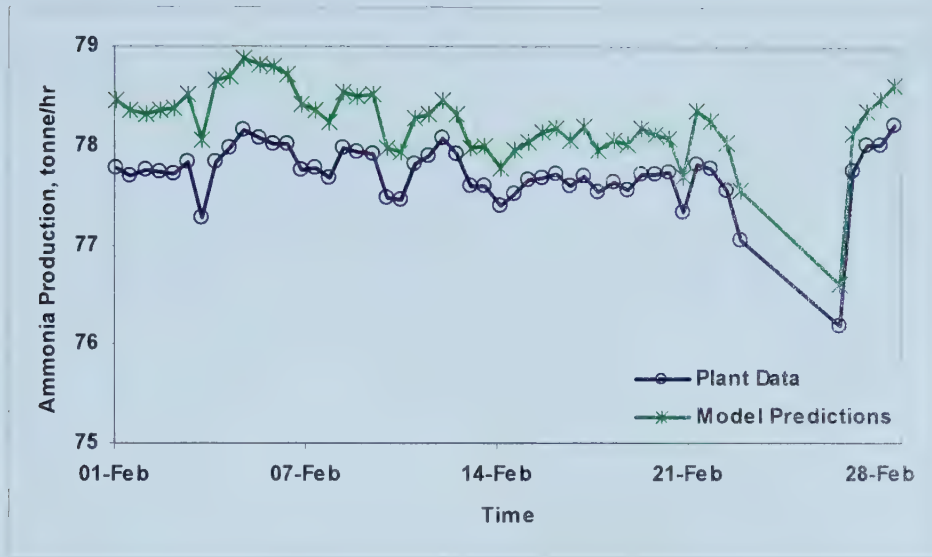
For the month of February, the R1B1 inlet temperature was on average 13 °C above optimal conditions. Similarly, R1B2 and R2 operated on average 6 °C and 11 °C above the optimal setpoint. Interestingly, the variance in the optimal setpoints for R1B1, R1B2 and R2, was only 0.6 °C, 2.3 °C and 0.9 °C. It is noted that the independent variable  $HV_{R1PILTUBE}$  is typically constrained in the closed position.

Figure 4-6 summarizes the change in ammonia production predicted, equivalent to an average of +0.52 tonne/hr. Data from this month suggests that a potential of \$188 k/year could have been achieved by running the plant at its optimal operation. These results are tempered by the results from Chapter 3, which indicated an error of 0.08 tonne/hr between ammonia production predictions and plant data, Table 3-3.





**Figure 4-6** Optimal Ammonia Production, Normal Operation–Unit Optimization



The above case study focuses on optimization of the entire synthesis loop. However, ammonia conversion not achieved in beds one and two can be partially recovered in the third converter bed. As such a simplified approach, optimization of the last converter is evaluated in Figures 4-7 and 4-8. Plant operation of  $T_{R1B1,IN}$  and  $T_{R1B2,IN}$  is assumed to remain constant.

**Figure 4-7** R2 Optimal Temperature Profile, Normal Operation–R2 Optimization

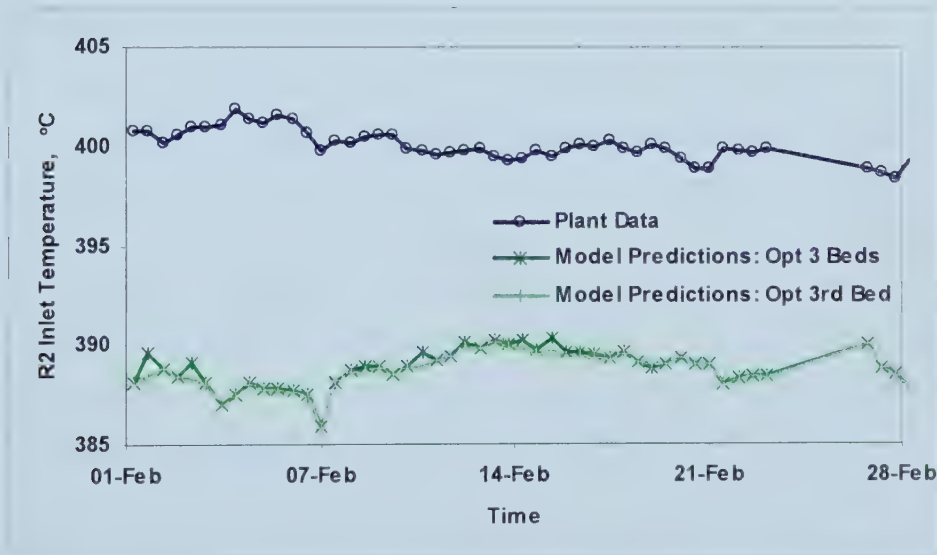
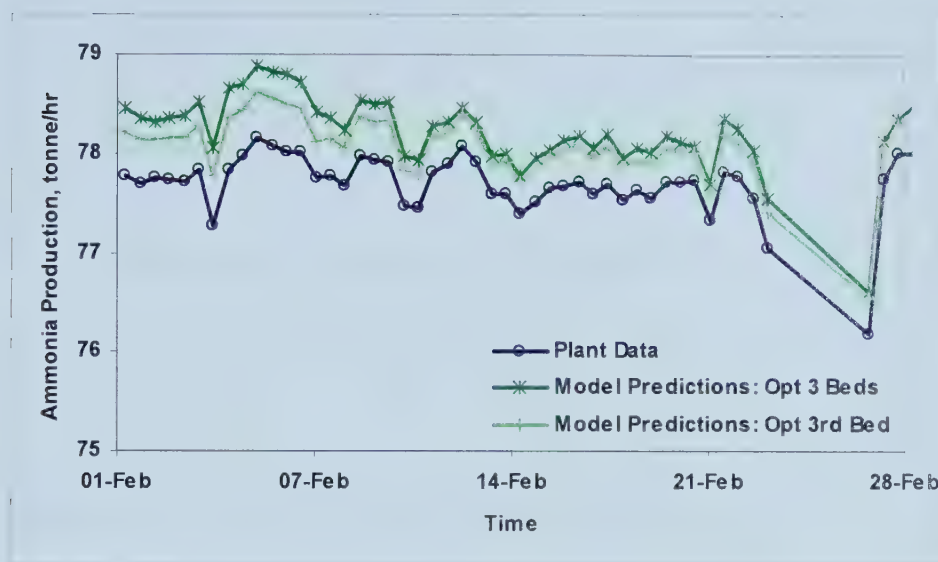


Figure 4-7 compares the optimal operation of converter inlet temperature for the last converter with a unit optimization scheme and a simplified optimizer imposed on the last converter bed. In general, the optimum temperatures for the simplified optimizer are only slightly



colder. Performance of the R2 optimizer is summarized in Figure 4-8, which predicts an average increase in ammonia production of 0.37 tonne/hr.

**Figure 4-8 Optimal NH<sub>3</sub> Production, Normal Operation-R2 Optimization**



In this case, potential returns are approximately \$134 k/year. Expressed in other terms, about 70% of predicted returns can potentially be achieved by optimizing a single loop. The remaining 30 %, or \$ 54 k/year, requires a more complex optimization strategy.

#### 4.3.2. Changing Process Conditions

The above example in section 4.3.1 looked at normal operation of the plant for the month of February. For comparison of winter and summer operations, winter operation is represented by the February data set, with data from July representing the summer months. Due to changing ambient conditions and subsequent process limitations, variation in optimal setpoints is expected.

Most notably, the process operates at a much higher H/N ratio during the summer months, Figure 4-9. During these months, a process limitation exists in getting sufficient air into the system. This increases the H/N ratio in the feed gas. Saskferco often reduces feed rates in an attempt to reduce this saturated control variable. This is shown in Figure 4-10.



**Figure 4-9** Summer vs. Winter Operation, H/N Ratio

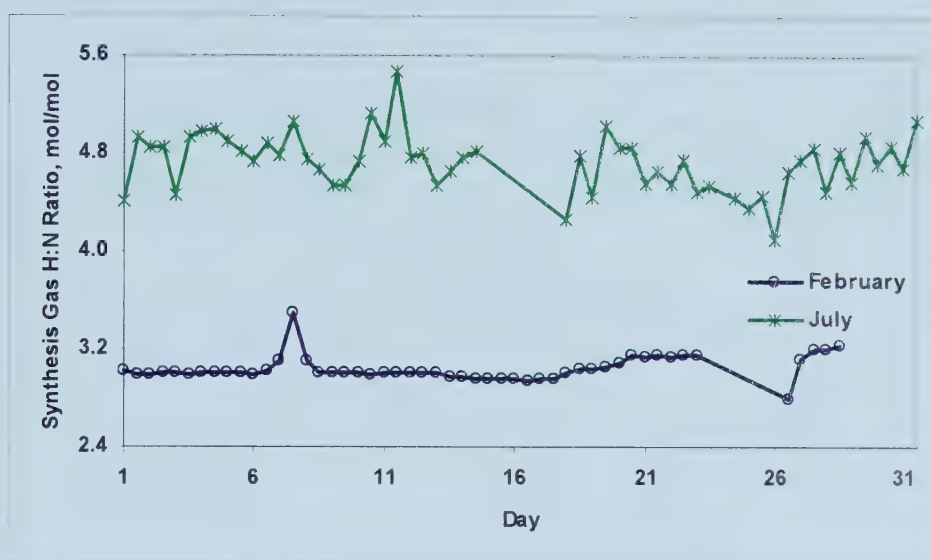
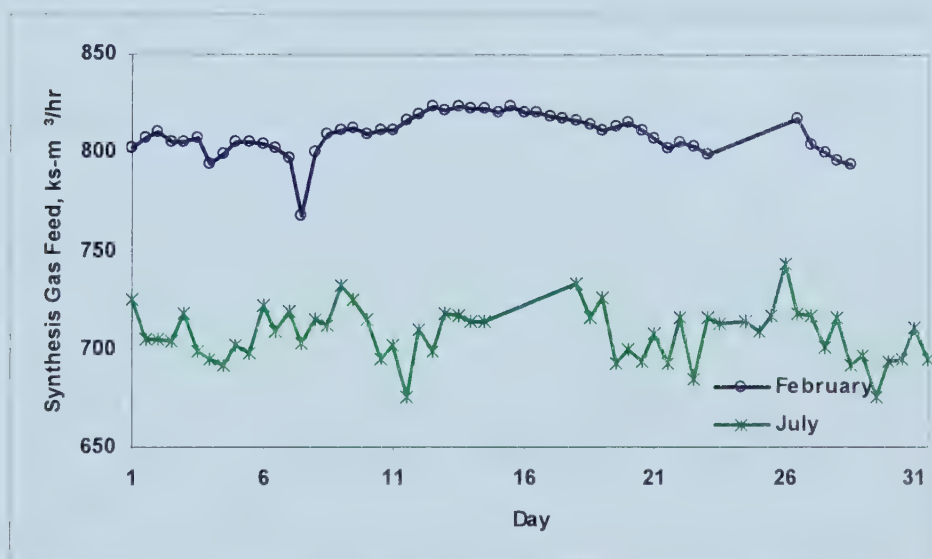


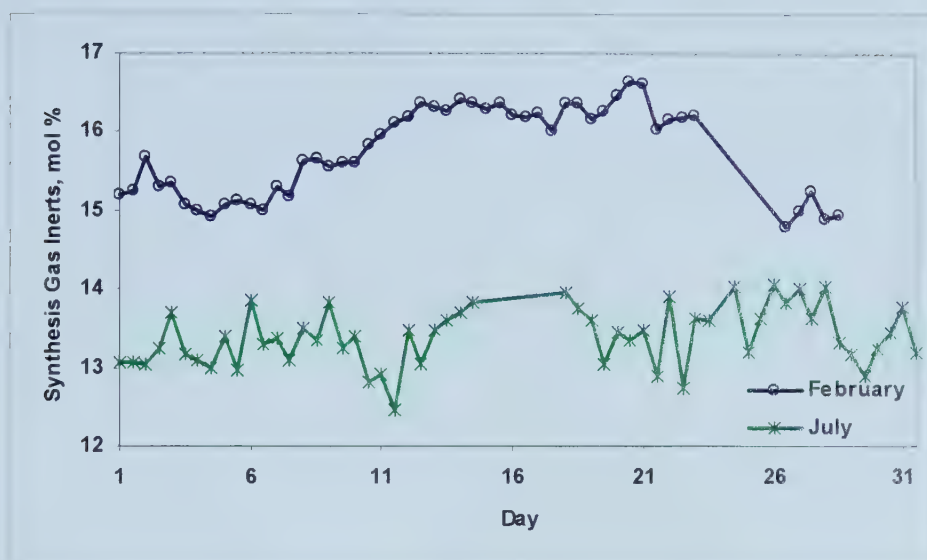
**Figure 4-10** Summer vs. Winter Operation, Synthesis Gas



Removal of ammonia and inerts from the recycle gas is a function of the ambient temperature and process throughput. With the climbing temperatures in the summer, the ammonia coolers do not run as efficiently, increasing the ammonia recycle into the unit. This is offset with the reduced rates, which help to improve the inert removal process. The problem with inerts is further compounded by methane in the fresh feed and a process limitation in the upstream carbon dioxide removal system. Carbon dioxide, which is a poison to the ammonia catalyst, is converted to methane in the methanation unit prior to entering the ammonia synthesis loop. The net effect is reduced inerts in the synthesis gas during the summer months, Figure 4-11.

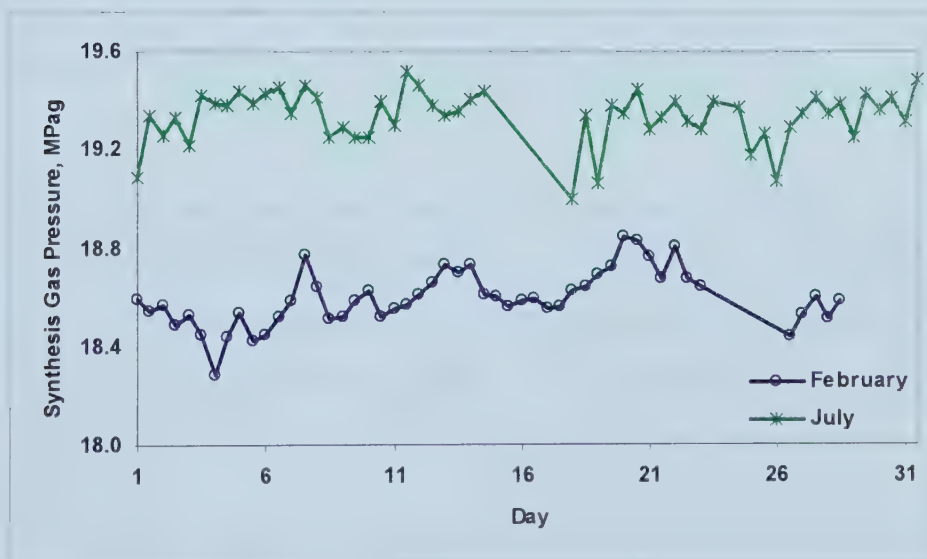


**Figure 4-11** Summer vs. Winter Operation, Process Inerts



The synthesis gas pressure is slightly impacted by changes in the ambient temperature, Figure 4-12. As noted earlier, the equilibrium favours a higher operating pressure as is shown in Figure 4-1.

**Figure 4-12** Summer vs. Winter Operation, Synthesis Gas Pressure

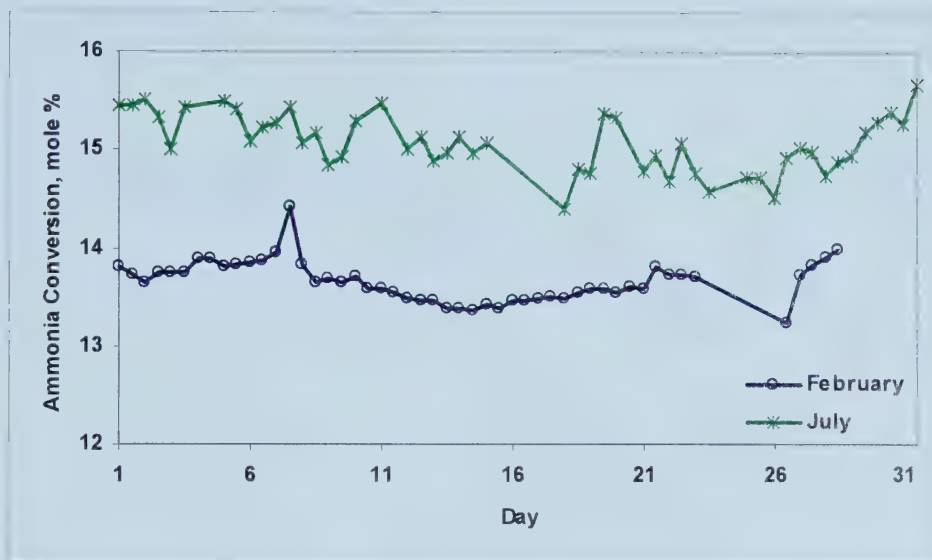


Conversion under these changing operations is represented in Figure 4-13.





**Figure 4-13** Summer vs. Winter Operation, Conversion



The process model parameters are updated for July and then substituted into the optimization model, with the results listed in Figures 4-14 to 4-15. The results indicate slightly colder optimum temperatures compared to winter operation with increased temperature variation in the summer months. Resultant production under optimal conditions reveals an average potential increase of 0.48 tonne/hr.

**Figure 4-14** Optimal Temperature Profile, Summer Operation

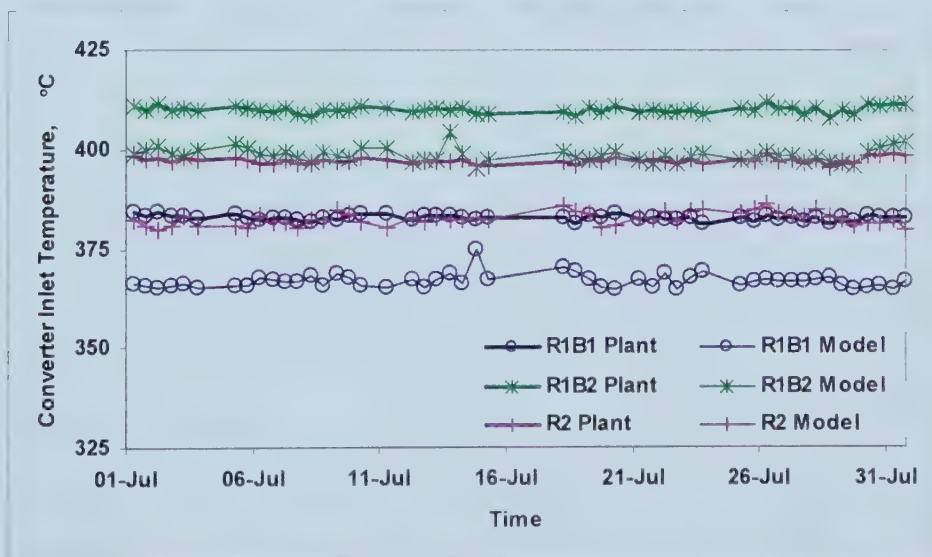
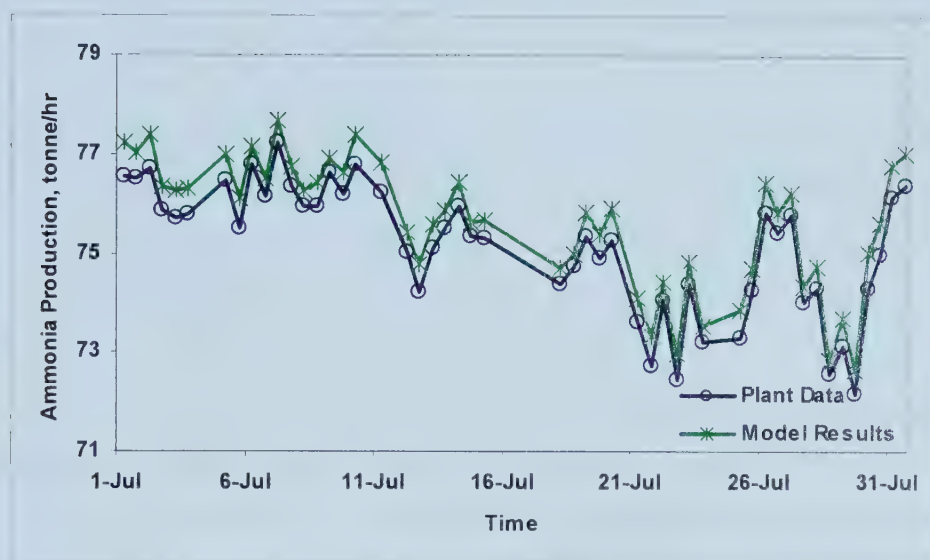




**Figure 4-15 Optimal Ammonia Production, Summer Operation**



Comparison of the July results in Figures 4-14 and 4-15 to February results presented in Figures 4-5 and 4-6 is summarized in Table 4-2.

**Table 4-2 Winter vs. Summer Optimal Operation**

	$T_{R1B1,IN}$ °C	$T_{R1B2,IN}$ °C	$T_{R2,IN}$ °C	$M_{NH_3}$ tonne/hr	Conv. %	Benefit /year
<b>Winter Range (February)</b>	367-371	399-406	386-390	76.6-78.9	13.2-14.4	\$188 k
<b>Summer Range (July)</b>	365-375	395-405	380-386	72.7-77.7	14.4-15.7	\$ 173 k

Table 4-2 contrasts the economics of winter and summer operation. The most notable differences between summer and winter operation are the reduced rates and increased conversion. As demonstrated in Figures 4-9 to 4-13, more variation occurs in the ammonia synthesis loop process during the summer months. This increased variation is reflected in the calculated optimum temperature profile for summer operation. Consolidating summer and winter benefits, indicates an average potential increase of 0.50 tonne/hour or \$180 k/year.

### 4.3.3. Degraded Catalyst

Iron based ammonia synthesis catalyst is an industry standard, with an expected life of up to 10 years. Deactivation may occur as a result of thermal sintering or poisoning. Poisoning by oxygenated components, such as water, carbon monoxide and carbon dioxide is largely reversible, compared to poisons such as sulphur and chlorine that have an irreversible impact on the catalyst activity<sup>[41]</sup>.



This deactivation process effectively reduces the ammonia equilibrium. The reduced equilibrium has a direct impact on the forward reaction, Equation 4.5, and subsequent ammonia production.

$$k_+ \propto K_p \quad (4.5)$$

By including parameter updates in the optimization problem, the impact of catalyst deactivation on the optimizer's performance is reduced. Parameter updates are instituted to fit the process model to plant data. A shift in the ammonia synthesis equilibrium is compensated for in Equation 2.20, allowing the optimizer to be sensitive to a change in catalyst activity.

$$k_+ = h_x \cdot k_- \cdot K_p \quad (2.20)$$

Saskferco was commissioned in 1992. During catalyst reduction, the catalyst in the first bed was exposed to deactivating conditions and permanent damage<sup>[12]</sup>. The result is reduced conversion in the first reactor bed. This increases the potential for ammonia conversion in the third reactor bed, allowing the optimal inlet temperature of bed three to be pushed slightly below design conditions. Replacement of the ammonia synthesis catalyst is anticipated in 2006. After catalyst replacement, it is expected that the optimal inlet temperature for bed three will increase, based on the improved conversion in bed one.

#### 4.4. Summary of Results

This chapter brings together research done in the previous chapters. Using the process model developed in Chapter 2, process optimization is explored. The optimizer's ability to perform in an accurate and reliable fashion is dependent on both the parameter updates and a controller, yet to be identified.

The reaction curve, presented in the sensitivity analysis, reveals a band around the optimum temperature in which conversion indicates a weak relationship to changes in the inlet temperature. Furthermore, while the model is sensitive to changes in the H/N ratio, it does not reflect an optimal H/N point as indicated in literature.

The optimization studies identify the opportunity to increase production of the ammonia plant operation by approximately 0.5 tonne/hr, equivalent to \$180 k/year. It is estimated that 70 % of these results are achievable by optimizing a single converter bed, R2. Optimization results relative to design and normal operation are compiled in Table 4-3.



**Table 4-3      Ammonia Conversion: Optimal Performance Comparisons**

	<b>R1B1 %</b>	<b>R1B2 %</b>	<b>R2 %</b>	<b>Net %</b>
<b>Design<sup>6</sup></b>	7.30	3.59	2.74	13.08
<b>Actual</b>	7.93	3.55	2.68	13.57
<b>Optimum – Unit</b>	7.96	3.56	2.73	13.66
<b>Optimum – R2</b>	7.93	3.55	2.74	13.63

Studies around summer and winter seasons indicate notably different operation. Due to climbing H/N ratios in the summer and increased loop pressure, operations may reduce make-up synthesis gas. Despite the higher H/N ratio, conversion increases. This suggests that the process may be diffusion limited at higher feed rates, such that approach to equilibrium is reduced. The current optimization model assumes a pseudo steady-state and does not account for reactor residence time. It is noted that residence time in the first bed is approximately three seconds. Impacts to equilibrium such as reduced catalyst activity are compensated by parameter updates. This allows optimization calculations to be sensitive to the changing process.

Extension of the optimization model, as an on-line optimizer could be employed given the appropriate computer resources and process information infrastructure. Frequency of the optimization calculations and the necessary parameter updates would need to be explored in more detail.

---

<sup>6</sup> Design numbers are included as a point of interest only. Differences in design and actual conversion in the first bed are attributed to site improvements in the synthesis feed gas composition.





## CHAPTER 5

### CONTROLLER SYNTHESIS

The first step in designing a control system is to define the control objectives appropriately. These objectives depend on the goals of the entire plant and of the design of the associated equipment<sup>[27]</sup>.

The design of the control system must take into consideration the safe and reliable operation of the plant. For example, adequate level control in WHB I and WHB II is essential. While level control may not directly impact ammonia production, it is a critical part of the plant's operation. The safety control system shuts down the ammonia plant on either a high or low level to avoid risk to plant equipment. The level control variable is considered as part of the plant's protection system and is designed as a stand-alone regulatory controller.

In general, the control objective of the process considered in this thesis is to control ammonia production under changing process conditions. To achieve this objective, control of the ammonia conversion in each reactor bed must be realized. Based on the measured plant variables, this can be achieved by controlling either the converter inlet temperatures, outlet temperatures or temperature changes across each reactor bed. For this thesis the inlet temperatures are chosen. Choosing the reactor beds inlet temperatures has several advantages. They are expected to have responses closer to linear than the reactor outlet temperatures or the changes in temperature.

PID and multi-variable control (MVC) algorithms are applied to the control problem. In designing these servo controllers, the variability in the controlled and manipulated variables needs to be considered. To this end, a maximum overshoot of one tonne/hour of steam production per one degree Celsius setpoint change is imposed based on feedback from site operations. Oscillations in steam production inevitably produce oscillations in the steam header pressure. Without operator intervention, this could trigger a shutdown on level in the waste heat boilers. Due to the small volume of hold-up in these vessels, this can occur in less than one minute. Note that the steam header process is not modelled in the process simulation.

The control system should be adaptable to the degrees of freedom available in the process<sup>[27]</sup>. The process being considered has more manipulated variables than the number of control variables. The final controller structure needs to evaluate the effective use of the extra degrees of freedom.



Lastly, due to downstream cooling constraints, the ability to remove ammonia from the recycle synthesis gas is related to the synthesis gas exit temperature from the gas-gas exchanger tubes. This relationship varies with production levels and seasonal conditions. This point is noted for interest only and it is not explored in this thesis.

From this point forward, reference to the process refers to the process model developed in Chapter 2 unless a specific differentiation is made.

## 5.1. State Space Analysis

Excluding measurement noise, the process can be approximated by linear state space as follows<sup>[7]</sup>.

$$\frac{d\mathbf{x}}{dt} = \mathbf{Ax} + \mathbf{Bu} + \mathbf{Gw} \quad (5.6)$$

$$\mathbf{y} = \mathbf{Cx} \quad (5.7)$$

Where:

- $\mathbf{x}$  are the state variables
- $\mathbf{u}$  are the input variables
- $\mathbf{w}$  are the disturbance variables
- $\mathbf{y}$  are the output variables
- $t$  is the time, minutes
- $\mathbf{A}$ ,  $\mathbf{B}$ ,  $\mathbf{G}$  and  $\mathbf{C}$  are the state matrices.

Equations 5.8 to 5.10 define the control, manipulated and disturbance variables. A detailed listing of all the variables, including the thirty-four state variables can be found in the Appendix G, Tables G-1 to G-4. Since level control is considered to be part of the plant's protection system, it is evaluated separately. Level is not included in the state space model.

$$\mathbf{y} = \begin{bmatrix} \text{CV}_1 \\ \text{CV}_2 \\ \text{CV}_3 \end{bmatrix} = \begin{bmatrix} T_{\text{R1B1,IN}} \\ T_{\text{R1B2,IN}} \\ T_{\text{R2,IN}} \end{bmatrix} = \begin{bmatrix} T_{\text{R1PH,BY}} \\ T_{\text{R1PH,SHELL}} \\ T_{\text{WHBI,BY}} \end{bmatrix} \quad (5.8)$$

$$\mathbf{u} = \begin{bmatrix} \text{MV}_1 \\ \text{MV}_2 \\ \text{MV}_3 \\ \text{MV}_4 \end{bmatrix} = \begin{bmatrix} \text{HV}_{\text{G/G,SHELL}} \\ \text{HV}_{\text{R1PH,TUBE}} \\ \text{HV}_{\text{WHBI,TUBE}} \\ \text{HV}_{\text{WHBI,STEAM}} \end{bmatrix} \quad (5.9)$$



$$\mathbf{w} = \begin{bmatrix} F_{\text{GAS,IN}} \\ P_{\text{GAS,IN}} \\ Y_{\text{NH}_3,\text{IN}} \\ Y_{\text{N}_2,\text{IN}} \\ Y_{\text{H}_2,\text{IN}} \\ Y_{\text{H}_2\text{O},\text{IN}} \\ Y_{\text{AR},\text{IN}} \\ Y_{\text{CH}_4,\text{IN}} \\ T_{\text{G/G,SHELL,IN}} \\ T_{\text{WHBII,BFW,IN}} \end{bmatrix} \quad (5.10)$$

To determine the local controllability and observability of the system, the state space matrices are determined by linearizing the process. In developing these matrices, two simplifications are made. The first simplification is that the derivatives of the compressibility factor with respect to the state variables are negligible. This is justified based on the weak relationship between these variables over the range of operation considered. Secondly, when solving the input gain matrix, **B**, the bypass flow areas are modelled as a linear function of the valve opening as defined in Equation 5.11, rather than the more accurate equation given in Equation 2.54b, which yields a gradient of 0 with input values of 0 % or 100 %.

$$A_v = \pi r_{\text{Valve}}^2 \frac{HV}{100} \quad (5.11)$$

$$A_v = (Y - r_{\text{Valve}}) X + r_{\text{Valve}}^2 \arcsin\left(\frac{HV-50}{50}\right) + \frac{\pi r_{\text{Valve}}^2}{2} \quad (2.54b)$$

Steady-state local input values are substituted into the state space functions. The evaluated matrices **A**, **B**, **G** and **C** are listed in Appendix G, Tables G-5 to G-8. From this data, the controllability of the system is explored. The controllability matrix, **P**, defined in Equation 5.12<sup>[6]</sup>, must be full rank to satisfy the criterion for control.

$$\mathbf{P} = [\mathbf{B} \mid \mathbf{AB} \mid \mathbf{A}^2\mathbf{B} \mid \dots \mid \mathbf{A}^{33}\mathbf{B}] \quad (5.12)$$

The rank of **P** is found to be  $3 < 34$ , indicating a non-controllable system. To find a controllable sub-space the eighteen reactor compositions are removed from the state variables to eliminate the near-zero eigenvalues from the **A** matrix. Additionally, the state derivatives are rescaled as necessary. The reduced and rescaled state space matrices are listed in Appendix G, Tables G-9 to G-11. The controllability matrix is then recalculated and found to be a locally controllable system, with a rank of 16.



To allow for state estimation, the observability of the system is evaluated by testing the rank of the observability matrix  $\mathbf{O}$ , Equation 5.13.  $\mathbf{O}$  is also found to be full rank, indicating a locally observable system.

$$\mathbf{O} = \left[ \mathbf{C}^T \mid \mathbf{A}^T \mathbf{C}^T \mid \mathbf{A}^{2T} \mathbf{C}^T \mid \dots \mid \mathbf{A}^{15T} \mathbf{C}^T \right] \quad (5.13)$$

## 5.2. BFW Level Implementation

The level controller, which is required for plant operation, is designed first. The WHB II boiler feed water (BFW) inlet valve is perturbed +/- 10% to see the impact on the levels in both waste heat boilers. Refer to Figure 5-1.

Since the WHB level dynamics are naturally integrating, a proportional controller is implemented to control the level. A gain of one (1 % valve opening/1% level offset) is chosen. Determination of the gain is based on the need to have fast disturbance rejection, while reducing the oscillations in the steam system. Comparatively, the level controller implemented on site has a nonlinear gain ranging from 0.35 to about 1.2, depending on the error and a feedforward term based on the change in steam production and BFW into the vessel.

The level controller is tested for its ability as a servo controller and as a regulatory controller.

Controller response to a setpoint change of 10 % is good, reaching steady-state in about six minutes, with no offset. An overshoot of approximately 2 tonne/hr in steam production occurs. It is noted that setpoint changes in level are not typical. Refer to Figure 5-2.

In order to test the regulatory performance of the controller, a change of 50 % in the upstream gas-gas exchanger bypass valve is introduced. This resulted in a 2 tonne/hr drop in steam production and a steady-state offset of about 1.0 %. Results are shown in Figure 5-3. This level offset is attributed to the change in the steady-state BFW demand and steam production.

In the last test, the loop is temporarily put into manual and the valve opened 10 % before placing back into auto control. This test is performed to simulate operator intervention and the placing of the loop into auto when the process is not at steady-state. The result is again a steady-state offset. Results can be observed in Figure 5-4.

Based on these tests, it is noted that proportional control applied to the WHB level has some limitations as a regulatory controller. Alternatively, a proportional integral controller could be considered. This is rejected, since integral action would introduce more oscillations in the process and the small offset observed is deemed acceptable.





**Figure 5-1** Waste Heat Boiler Level Open Loop Test

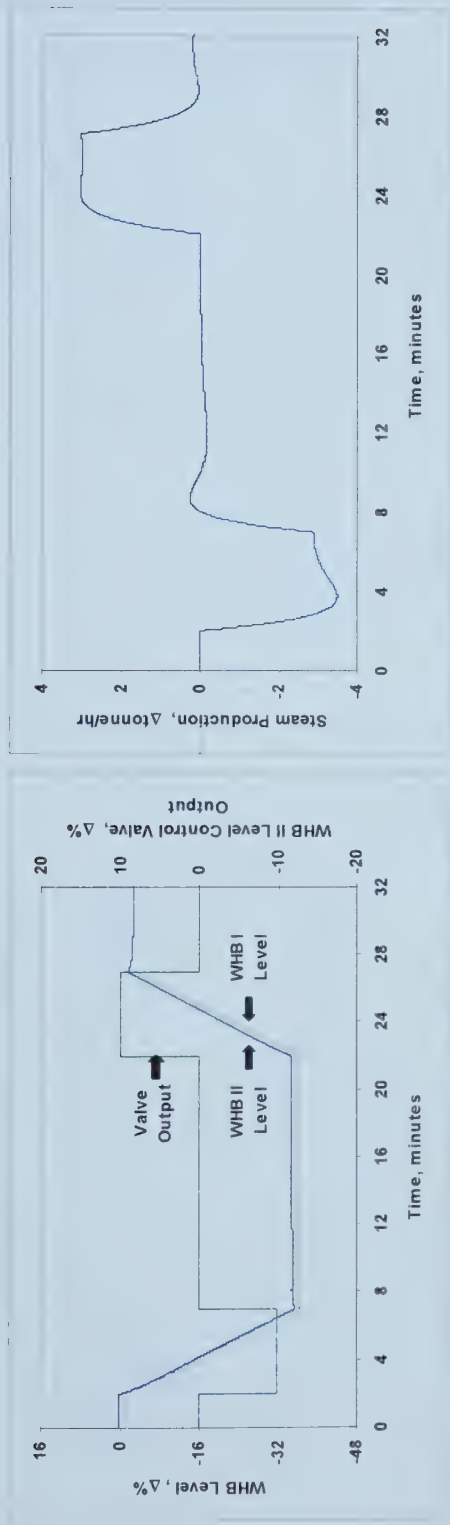


**Figure 5-2** WHB Level Closed Loop Step Test

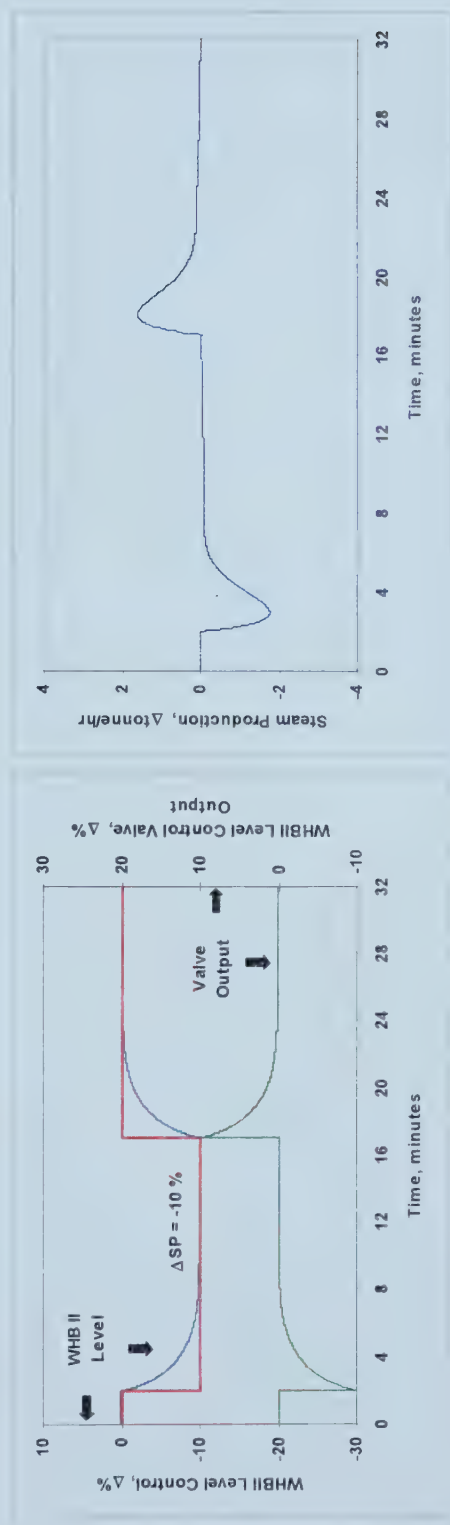




**Figure 5-3** WHB Level Closed Loop Disturbance Test

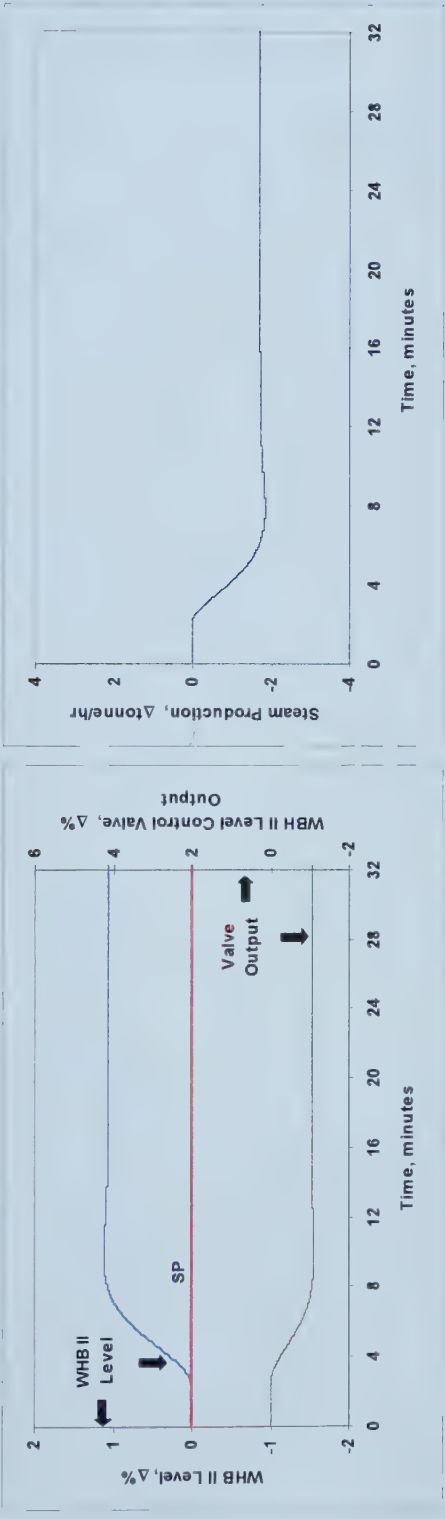
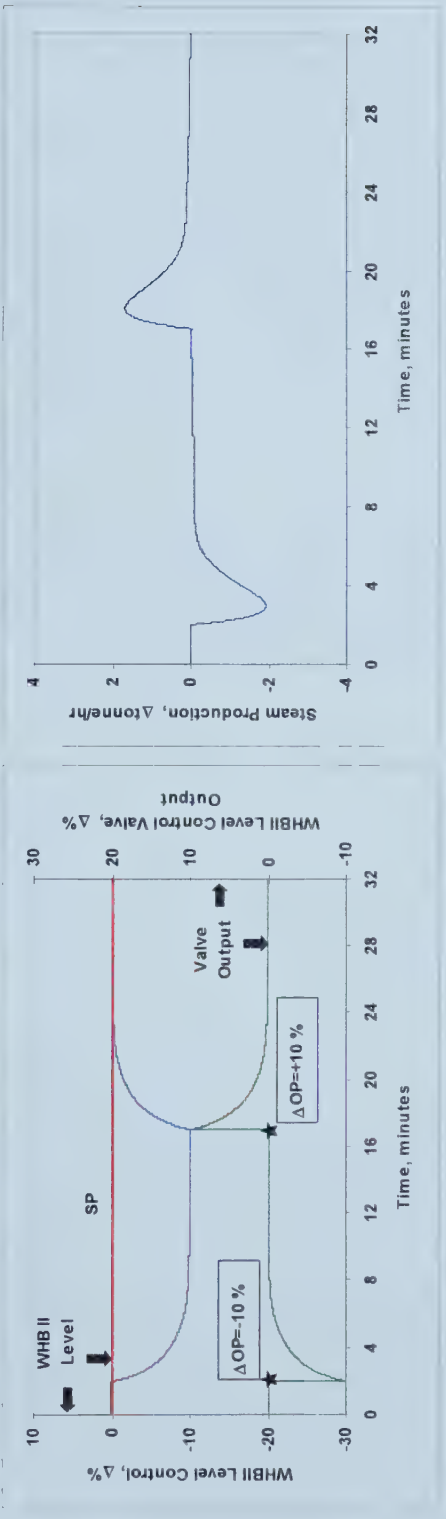


**Figure 5-4** WHB Level Open to Closed Loop Test





### 5.3. Multi-Loop PID Control

PID design is explored as an option for control of the ammonia synthesis loop.

#### 5.3.1. Multi-Loop Design

With a stable process in place, single loop PID pairing between the control variables (CVs) and manipulated variables (MVs) is explored. The pairing of  $T_{R2,IN}$  with  $HV_{WHBI,TUBE}$  would seem obvious due to proximity. However, the pairing of the remaining two control variables is less intuitive due to process interactions. The process gains for each CV relative to available MVs are determined by perturbing each valve +/- 50 %. Refer to Equation 5.14 for the process gain results.

$$\mathbf{K}_p = \begin{bmatrix} -0.079 & -0.109 & 0.068 & 0.033 \\ -0.081 & 0.012 & 0.069 & 0.036 \\ -0.043 & 0.008 & 0.209 & -0.030 \end{bmatrix} \quad (5.14)$$

While the results are informative, the pairing of  $T_{R1B1,IN}$  and  $T_{R1B2,IN}$  is not evident. To provide further insight into the problem, a quantitative measure of the process interaction, the relative gain array (RGA) is calculated. Without closed loop information, the elements of the RGA can be calculated based on Equations 5.15, 5.16 and 5.17<sup>[27]</sup>.

$$\lambda_{ij} = \left( \frac{\partial CV_i}{\partial MV_j} \right)_{MV_k = \text{const}, k \neq j} \left( \frac{\partial MV_j}{\partial CV_i} \right)_{CV_k = \text{const}, k \neq i} \quad (5.15)$$

$$\left( \frac{\partial CV_i}{\partial MV_j} \right)_{MV_k = \text{const}, k \neq j} = \mathbf{K}_{pij} \quad (5.16)$$

$$\left( \frac{\partial MV_j}{\partial CV_i} \right)_{CV_k = \text{const}, k \neq i} = \mathbf{K}_p^{-1}{}_{ji} \quad (5.17)$$

The RGA depends on a square system to yield a unique solution. Accordingly, it is decided to consider  $HV_{G/G,SHELL}$  and  $HV_{WHBII,STEAM}$  in separated RGAs. While both these MVs have different gains, their relative impact on  $T_{R1B1,IN}$  and  $T_{R1B2,IN}$  is similar. Conversely  $HV_{RIPH,TUBE}$  is needed to decouple the control response between  $T_{R1B1,IN}$  and  $T_{R1B2,IN}$ . The local controllability and observability of these two 3x3 systems are acceptable. The RGAs of these two systems with  $HV_{G/G,SHELL}$  and  $HV_{WHBII,STEAM}$  can be found in Equations 5.18 and 5.19, respectively.



$$\lambda_{MV_1, MV_2, MV_3} = \begin{bmatrix} 0.09 & \mathbf{0.90} & -4e-3 \\ \mathbf{1.12} & 0.10 & -0.22 \\ -0.21 & -3e-6 & \mathbf{1.21} \end{bmatrix} \quad (5.18)$$

$$\lambda_{MV_2, MV_3, MV_4} = \begin{bmatrix} \mathbf{0.92} & 0.04 & 0.06 \\ 0.09 & 0.18 & \mathbf{0.73} \\ 1e-3 & \mathbf{0.78} & 0.22 \end{bmatrix} \quad (5.19)$$

Since pairings with a relative gain closest to one have the least amount of transmission interaction, it is decided to pair the CVs as outlined in Table 5-1 below. A split range controller is used to control  $T_{R1B2,IN}$  with  $HV_{G/G,SHELL}$  and  $HV_{WHBII,STEAM}$ . Classic split range control uses a single PID algorithm with two Auto-Manual outputs. This design is modified slightly to use two PID controllers and hence improve controller performance. Additionally implementation of a split range controller allows for  $HV_{G/G,SHELL}$  to be minimized when not required, which is the preferred operation of this valve.

**Table 5-1**      **PID Pairing**

Control Variables	Manipulated Variables			
	$HV_{G/G,SHELL}$	$HV_{R1PH,TUBE}$	$HV_{WHBI,TUBE}$	$HV_{WHBII,STEAM}$
$T_{R1B1,IN}$		X		
$T_{R1B2,IN}$	X			X
$T_{R2,IN}$			X	

The design of the PID controllers includes the saturation of output variables, anti-windup of integral action and derivative action on the control variable to avoid derivative kick.

### 5.3.2. Multi-Loop Tuning

Controller tuning must consider interaction as well as the single-loop feedback process dynamics<sup>[27]</sup>. The open loop response of each CV to the designated MV is observed first. It is noted that all control variables in this process are considered equally important and all have relatively fast dynamics.

The open loop response of  $T_{R1B1,IN}$  to  $HV_{R1PH,TUBE}$  resembles a first order system with fast dynamics and no dead time. Settling time, defined as reaching 98 % of the system response, is about 2 ½ minutes. A small overshoot in steam production is attributed to the change of energy in the system.

A rise time of about ½ minutes is observed in  $T_{R1B2,IN}$  when stepping  $HV_{G/G,SHELL}$ . The overshoot of 22 % in  $T_{R1B2,IN}$  is attributed to the immediate response from the cooled synthesis gas entering the preheater tubes. The slower response, which determines the settling time, 8.3





minutes, is based on the synthesis gas recycling back through the shell side of the preheater. Again, steam production is impacted, with negligible overshoot.

The opening of  $HV_{WHBII,STEAM}$  results in a slight inverse response in  $T_{R1B2,IN}$ . Approximating this behaviour by a first order system yields about a 4 minute deadtime. When  $HV_{WHBII,STEAM}$  is closed, a dead time of approximately 2 minutes is noted, without an inverse response. The dynamics attributed to this MV are significantly slower than the processes observed earlier, with a settling time of 22 ½ minutes. This is a result of the interaction with the steam system and the change in heat distribution between WHB I and WHB II. While steady-state steam production remained relatively constant, opening this MV 50 % results in a -10.2 tonne/hr overshoot in steam production. Comparatively, closing the valve 50 % causes a 12.5 tonne/hr overshoot. As  $HV_{WHBII,STEAM}$  has the largest impact on steam oscillations, it is necessary to detune this control loop to honour the restriction of a maximum overshoot of one tonne/hour of steam production per one degrees Celsius change. Due to the hysteresis observed, both a positive and negative unit step test are required to ensure the control objectives are satisfied.

The impact of  $HV_{WHBI,TUBE}$  on  $T_{R2,IN}$  is almost immediate.  $T_{R2,IN}$  is the mix temperature of the cooled synthesis gas exiting the WHB I tubes and the warmer synthesis gas from R1B2, bypassing WHB I. Closing the WHB I bypass valve immediately decreases the bypass flow and the subsequent mix temperature. The response is tempered as the synthesis gas exiting the WHB I tubes warms slightly as more flow is diverted to this exchanger. The result is a rise time of less than one second and a settling time of approximately 8 minutes. An overshoot in steam production is observed.

Based on this open loop information, determined by perturbing the process model, the controller gains and integral times are evaluated. The controller gains are then detuned to achieve the desired process response. In general, to reach the desired setpoint the controller gains do not change significantly, despite process interactions. However, when the other control objectives are imposed, such as minimizing variation in the manipulated variables and steam production, the control problem becomes more difficult, requiring significant detuning. The final controller tuning values are available in Table 5-2. Open loop results are available graphically in Appendix G, Figures G-1 to G-5.

**Table 5-2      PID Tuning**

	$T_{R1B1,IN}$	$T_{R1B2,IN}$ ( $HV_{G/G,SHELL}$ )	$T_{R1B2,IN}$ ( $HV_{WHBII,STEAM}$ )	$T_{R2,IN}$
$K_C$ (%)	-6.96	-9.26	1.20	3.59
$\tau_I$ (minutes)	0.62	0.20	2.00	0.05
$\tau_D$ (minutes)	0	0	1.40	0



### 5.3.3. Multi-Loop Results

To ensure the control objectives are satisfied, the controllers are implemented and tested on the process using the PID tuning results summarized in Table 5-2. Since the process responds differently, depending which MV is active for the  $T_{R1B2,IN}$  split range controller, two test procedures are performed. In the first test  $HV_{G/G,SHELL}$  is used to control  $T_{R1B2,IN}$ . The second procedure tests the control of  $T_{R1B2,IN}$  with  $HV_{WHBII,STEAM}$ . Additionally, a third test, investigating the split range controller swing over between MVs is performed. For each test procedure, all CVs are perturbed with a unit step change.

#### 5.3.3.1. PID Control with $HV_{G/G,SHELL}$

Performance of the controllers with  $HV_{G/G,SHELL}$  used to control  $T_{R1B2,IN}$  is adequate.  $T_{R1B1,IN}$  satisfies all required criteria as observed in Figure 5-5. No overshoot or steady-state offset is observed in this CV when perturbed with a unit step change. An acceptable overshoot of the manipulated variables is noted. The remaining CVs adequately reject the disturbance, with slight deviations from their setpoints.  $T_{R1B1,IN}$  reaches steady-state in 4.3 minutes.

As illustrated in Figure 5-6, the dynamics of the  $T_{R1B2,IN}$  controller are fast, with a settling time of about  $\frac{1}{2}$  minute. Due to process interaction, the MVs associated to  $T_{R1B1,IN}$  and  $T_{R2,IN}$  are manipulated about  $7\frac{1}{2}\%$  and  $4\%$  respectively to hold their setpoint values.  $T_{R1B1,IN}$  deviates from setpoint by  $0.4\text{ }^{\circ}\text{C}$ . A change in the steady-state steam production and the level with no overshoot is noted.

The  $T_{R2,IN}$  controller response shows almost ideal control performance. Steady-state is reached in less than one minute. Steam production and level are essentially steady and  $T_{R1B1,IN}$  and  $T_{R1B2,IN}$  remain comparatively constant. Results can be observed in Figure 5-7.



**Figure 5-5**  $CV_1$  Step, PID,  $MV_4$  Saturated

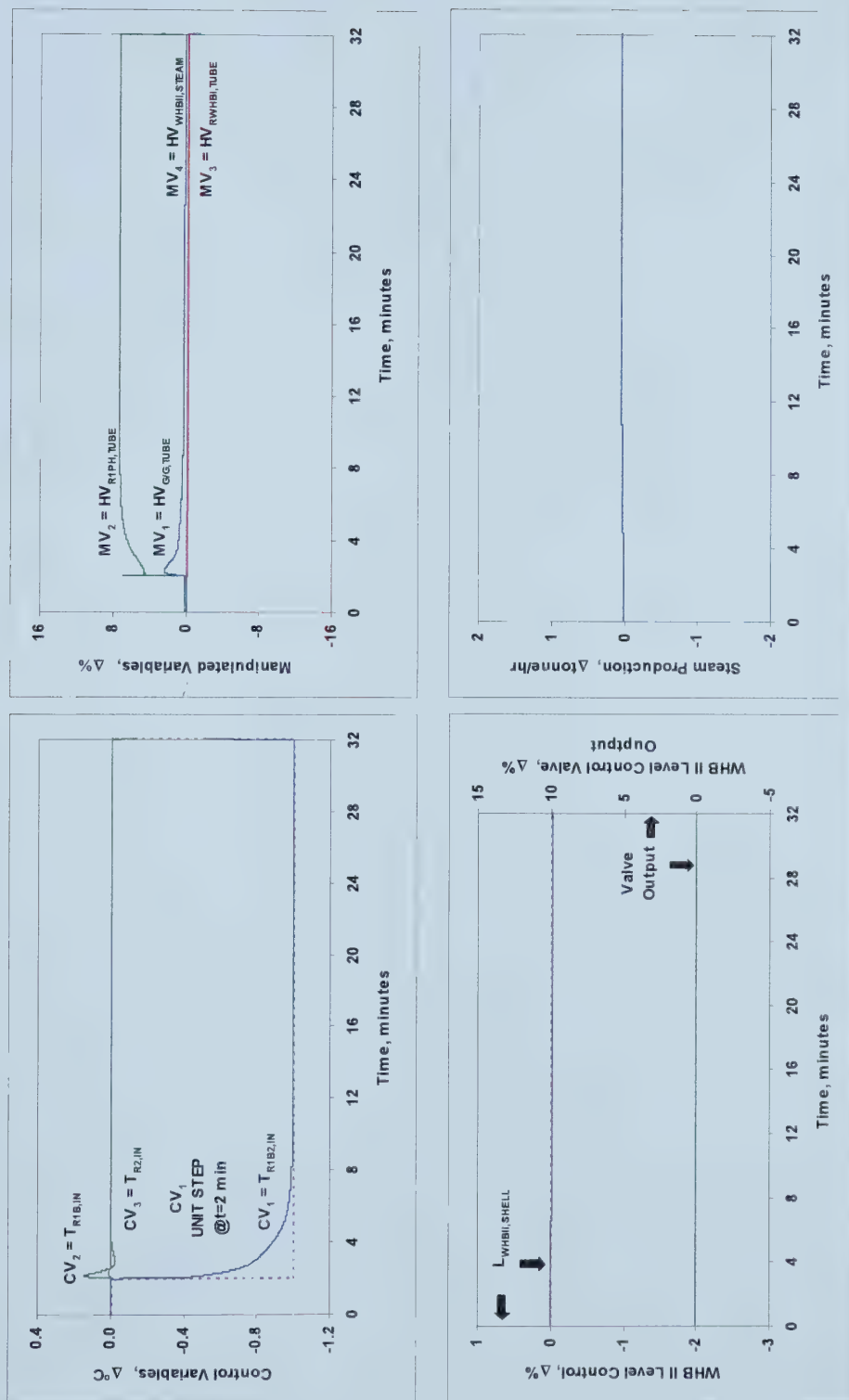




**Figure 5-6**  $CV_2$  Step, PID,  $MV_4$  Saturated

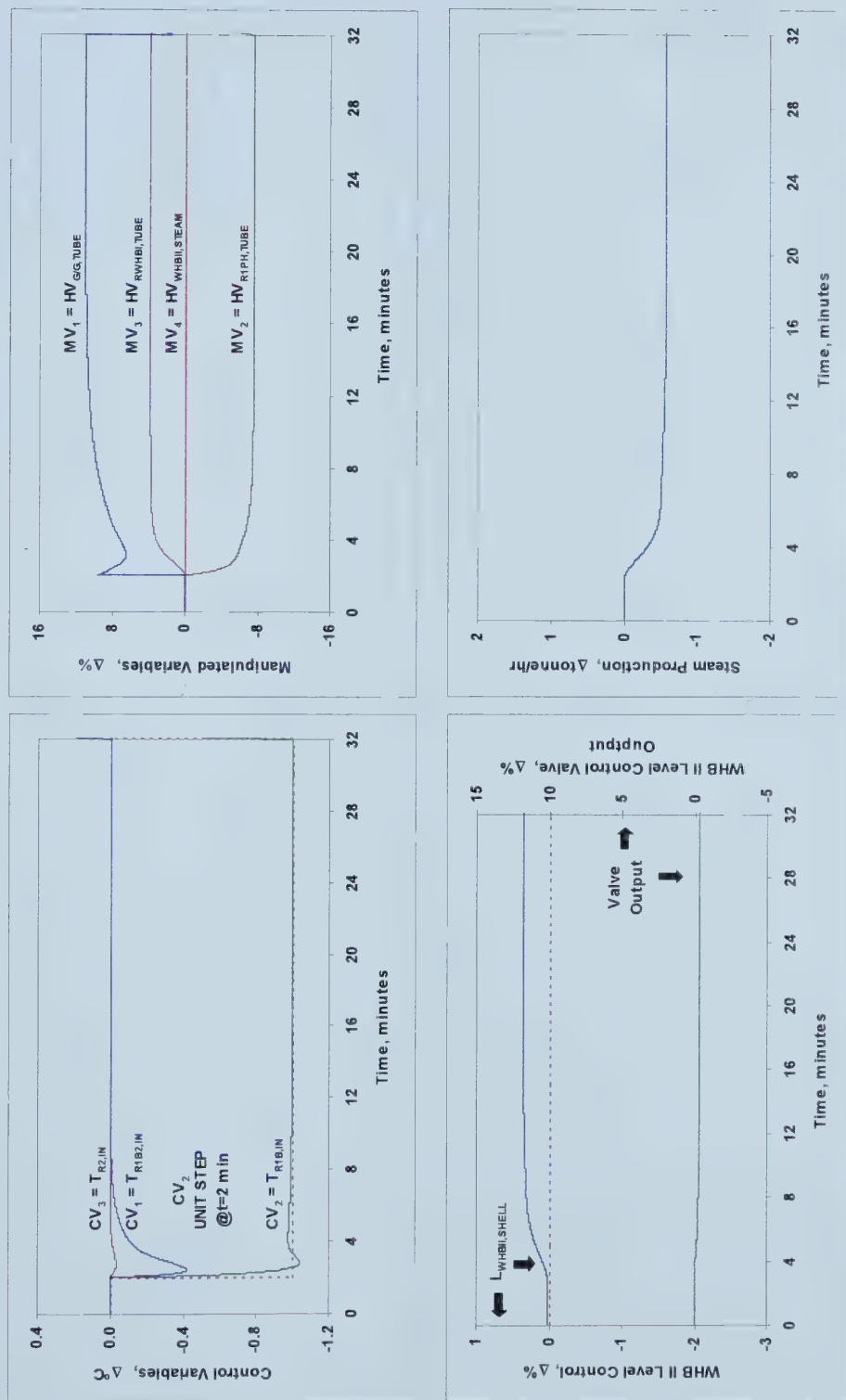
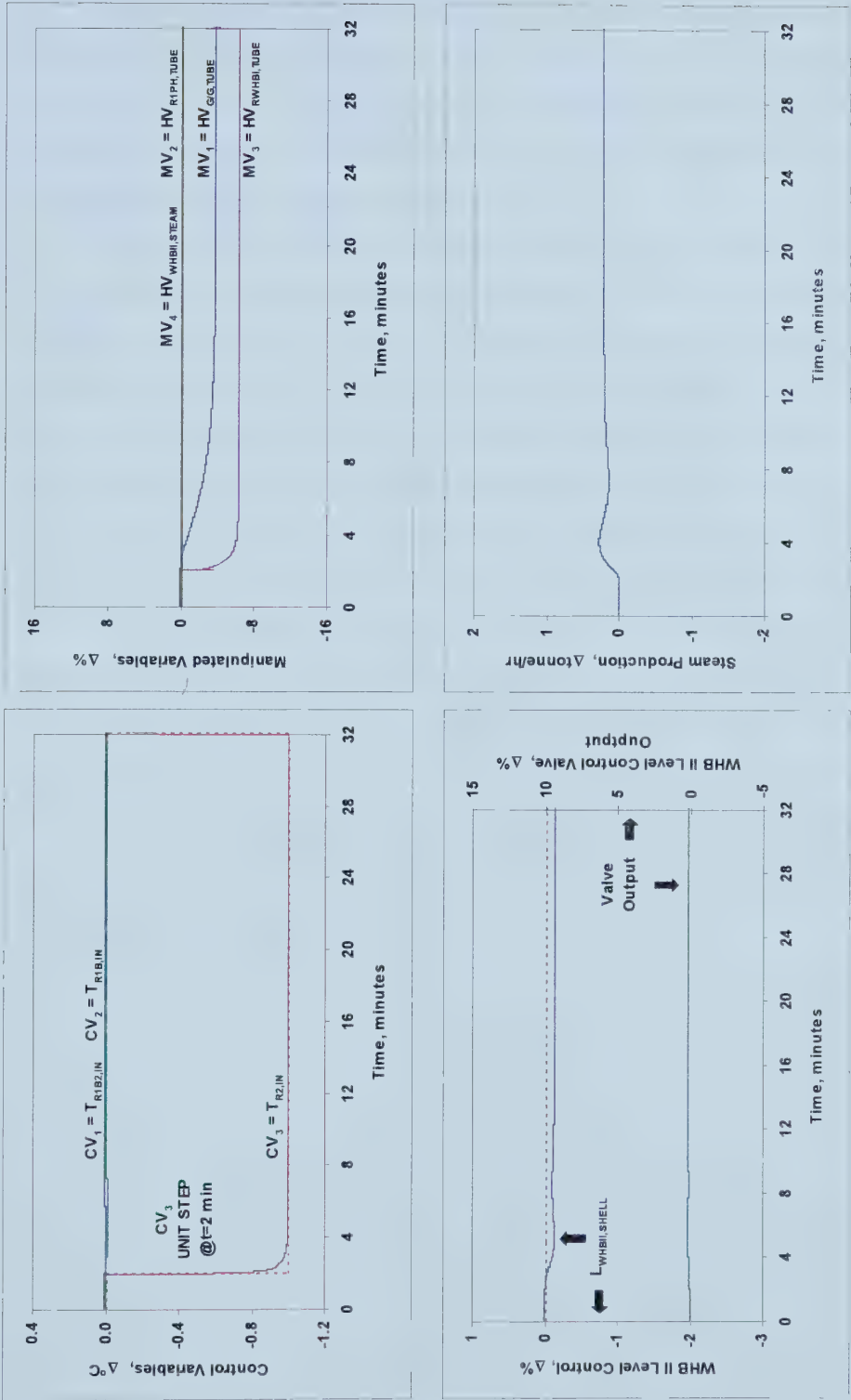






Figure 5-7 CV<sub>3</sub> Step, PID, MV<sub>4</sub> Saturated





### 5.3.3.2. PID Control with $HV_{WHBII,STEAM}$

Results in this case met the design criteria, but the overall performance is diminished.

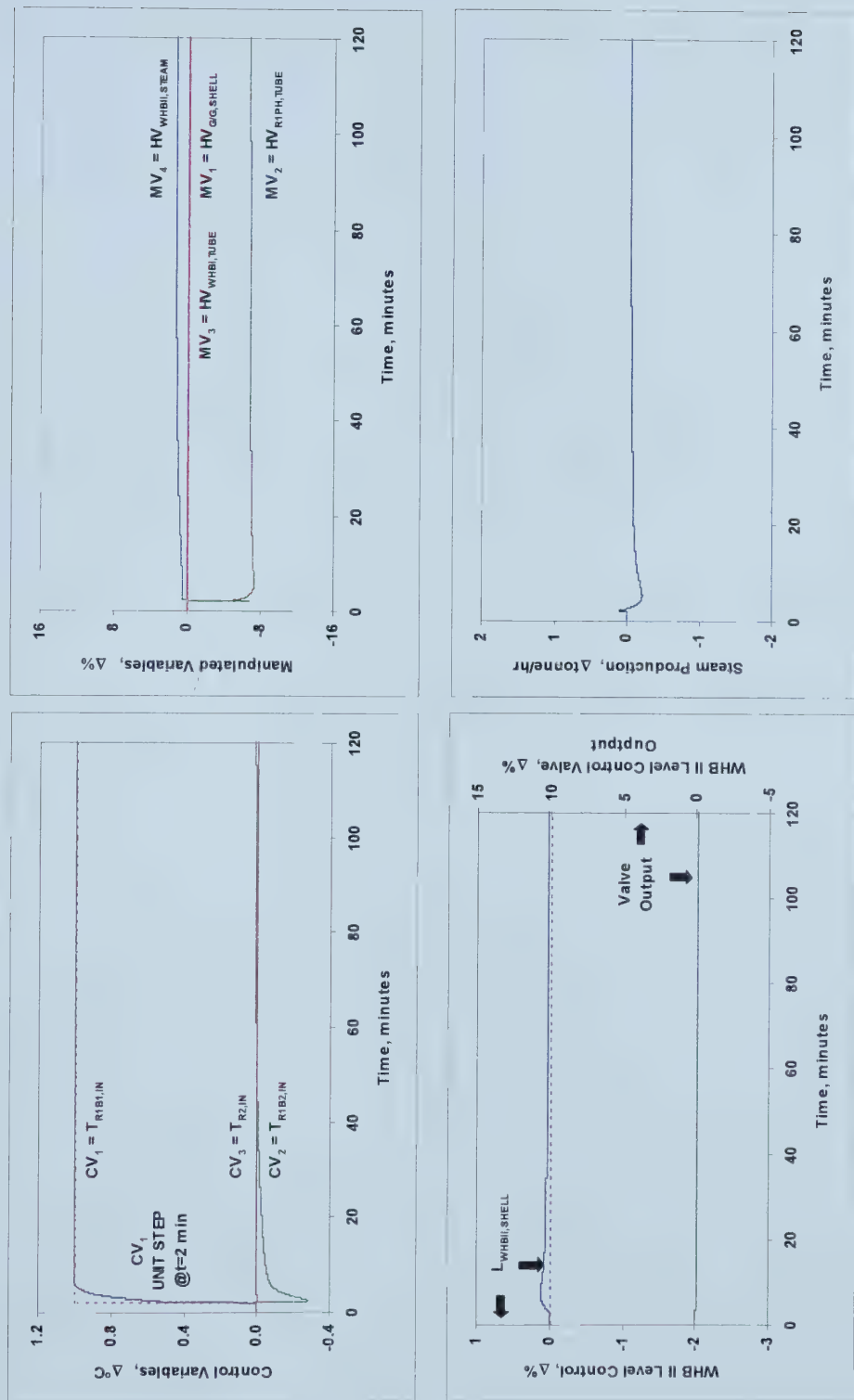
Again the  $T_{R1B1,IN}$  controller satisfies all required criteria. The settling time of 3.3 minutes is about 25 % less than the first case. This is a consequence of the relatively slow control action with  $HV_{WHBII,STEAM}$  and subsequent interaction with  $T_{R1B1,IN}$ . Steam production and level are affected slightly due to the disturbance on  $T_{R1B2,IN}$ . Figure 5-8 demonstrates the  $T_{R1B1,IN}$  control performance.

Figure 5-9 illustrates the response of the  $T_{R1B2,IN}$  controller with  $HV_{WHBII,STEAM}$ . The predominant characteristic of this controller is the settling time of 107 minutes. Detuning of the  $HV_{WHBII,STEAM}/T_{R1B2,IN}$  controller is done to meet constraints in the steam production system. Steam overshoot in this case is 1 tonne/hr per 1°C setpoint change, equal to the constraint imposed. This detuned controller, with respect to the interaction between other CVs, imposes a smaller disturbance compared to  $HV_{G/G,SHELL}$ . This allows  $T_{R1B1,IN}$  and  $T_{R2,IN}$  to return to steady-state more rapidly than when  $T_{R1B2,IN}$  is controlled with  $HV_{G/G,SHELL}$ . However, the controllers' ability to reject disturbances degrades.

The  $T_{R2,IN}$  control performance with  $HV_{WHBII,STEAM}$  controlling  $T_{R1B2,IN}$  is notably different than the  $T_{R2,IN}$  step response with  $HV_{G/G,SHELL}$  controlling  $T_{R1B2,IN}$ . While  $T_{R2,IN}$  reaches steady-state in less than one minute, increased valve action is noted. Also in this case, both the  $T_{R1B1,IN}$  and  $T_{R1B2,IN}$  outputs are manipulated to maintain their setpoints.  $T_{R1B2,IN}$  deviates from setpoint by 0.4°C. It requires about 110 minutes to return to steady-state. An oscillation in the steam system, of 0.97 tonne/hr is within design criteria. These observations are based on Figure 5-10.



**Figure 5-8**  $CV_1$  Step, PID,  $MV_1$  Saturated





**Figure 5-9**  $CV_2$  Step, PID,  $MV_1$  Saturated

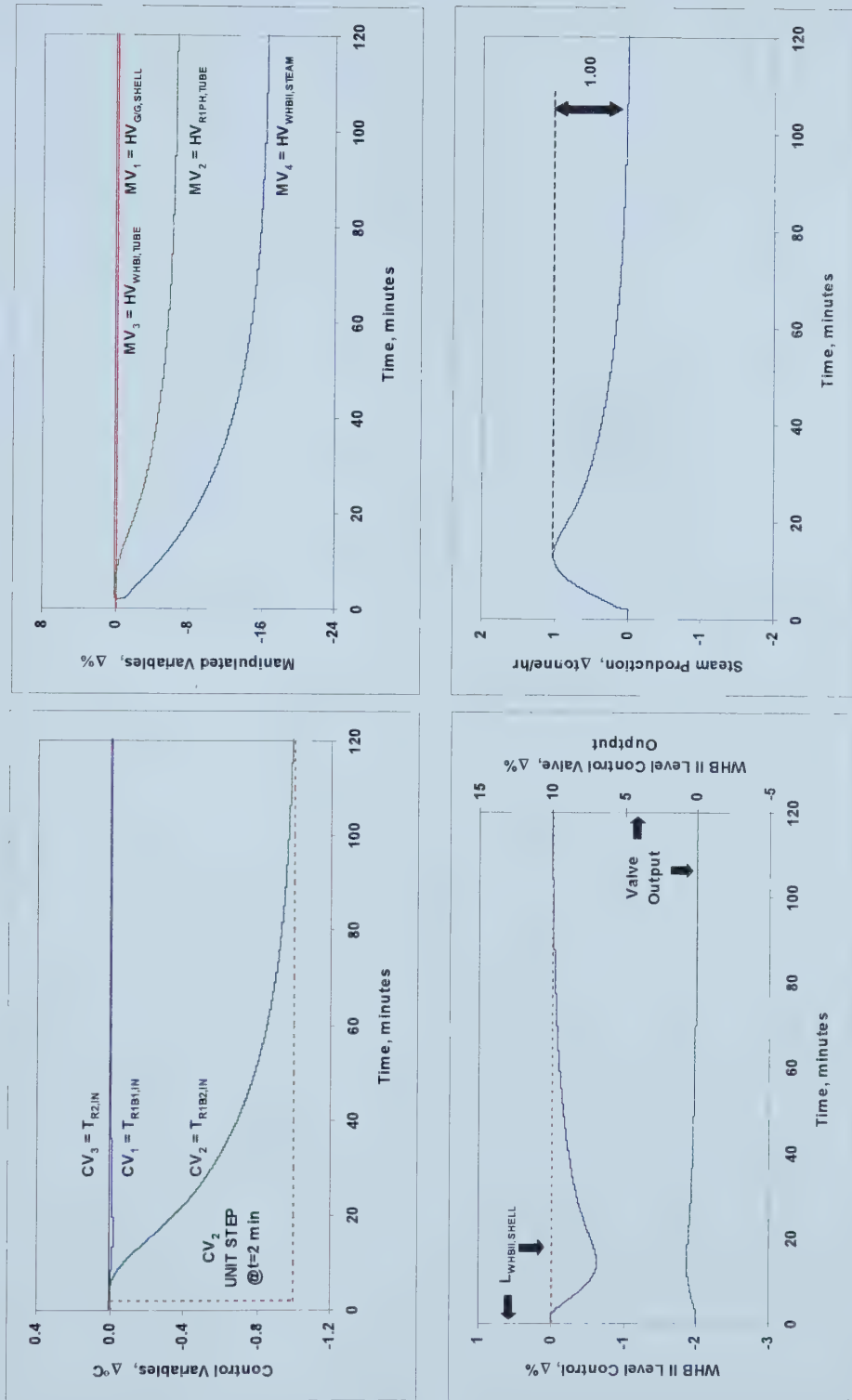
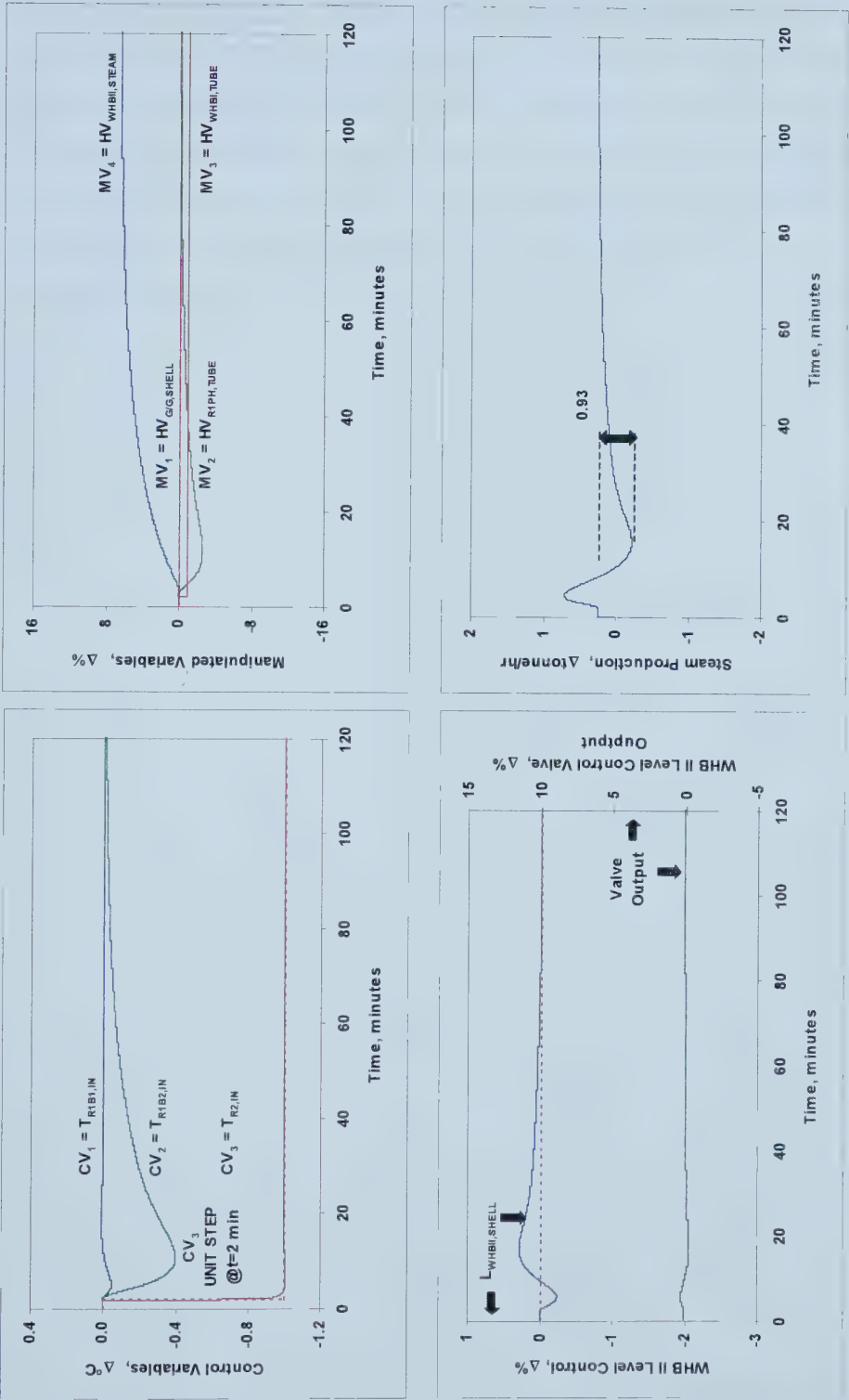






Figure 5-10 CV<sub>3</sub> Step, PID, MV<sub>1</sub> Saturated





### 5.3.3.3. $T_{R1B2,IN}$ Split Range PID Control

To demonstrate the functionality of the split range controller a setpoint change of 5 °C is performed, as shown in Figure 5-11. While controller setpoints are achieved, the transition from  $HV_{WHBII,STEAM}$  to  $HV_{G/G,SHELL}$  introduces additional disturbances in the process, specifically in the steam system. A change in steam production of 6.4 tonne/hr introduces the possibility of oscillations in the steam system. However, the overshoot of about 1.03 tonne/hr steam per 1 °C setpoint change is considered sufficiently close to the criteria set. The transition from  $HV_{G/G,SHELL}$  to  $HV_{WHBII,STEAM}$ , Figure 5-12, produces a smoother response.



Figure 5-11 CV<sub>2</sub> Step Down, Split Range Controller

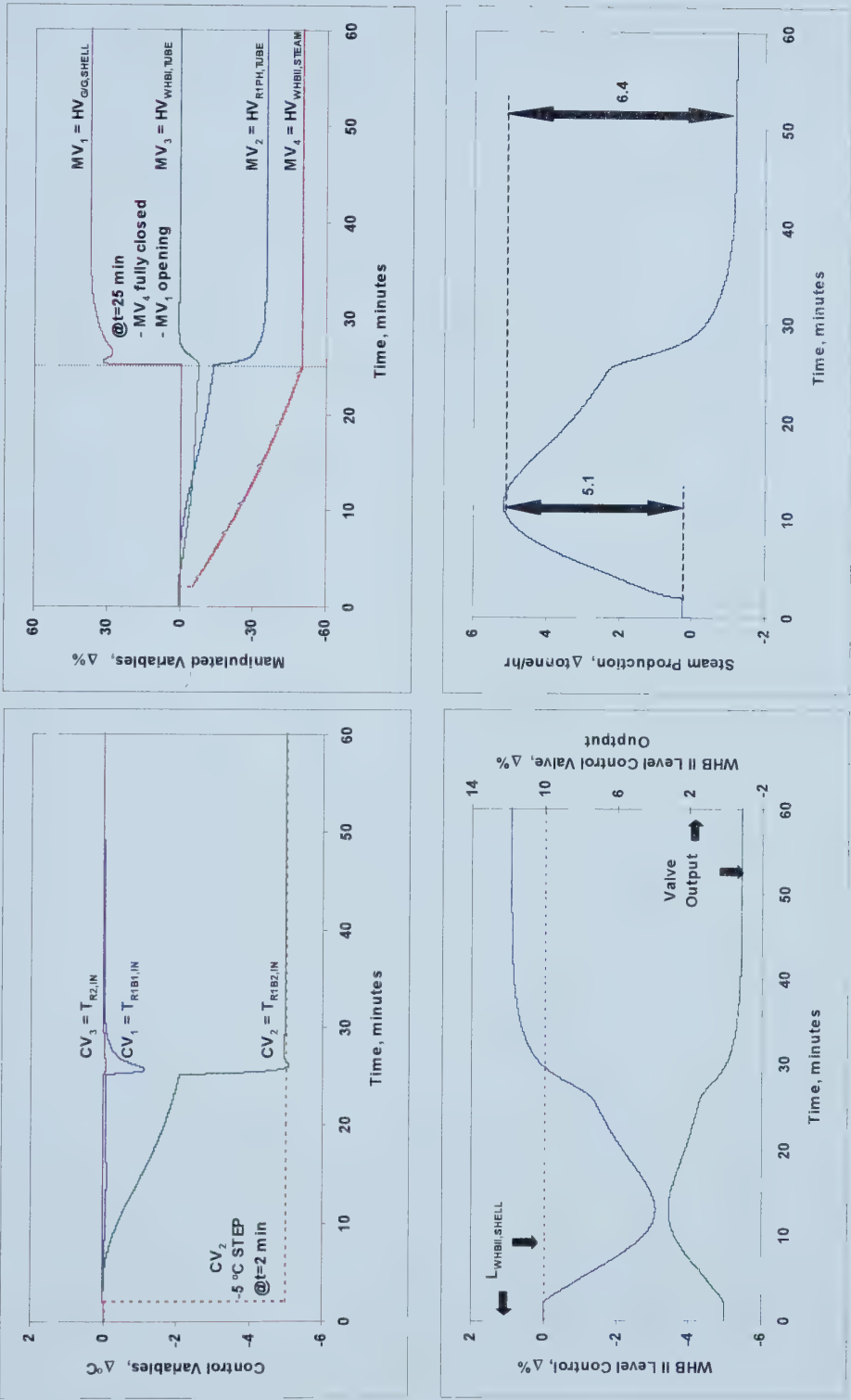
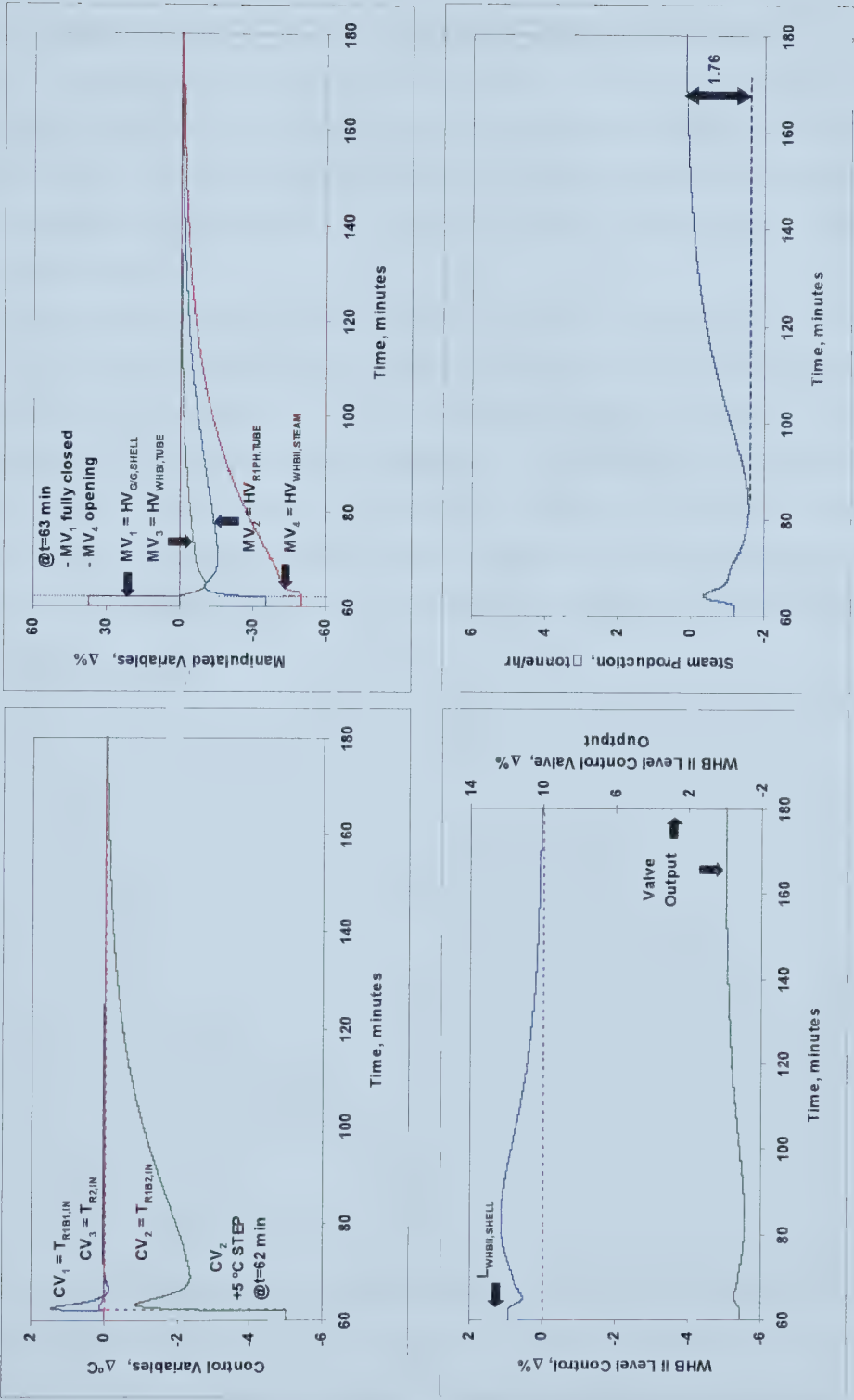




Figure 5-12 CV<sub>2</sub> Step Up, Split Range Controller - CV Response







## 5.4. Linear Multi-Variable Control

While several modifications have been made to the conventional PID form, such as gain-scheduling, nonlinear gains, output characterization, split range controllers, etc., it remains best suited for single input, single output (SISO) systems over a near-linear process. Comparatively, multivariable control (MVC) considers the process as a complete system, allowing a wider range of applicability. While considerable time may be required for implementation, potential returns on the implementation of a multi-input, multi-output (MIMO) system make it an attractive control option relative to PID.

Initially multivariable predictive control (MPC) was considered for MVC control studies. MPC is an industry standard for MVC applications and tools are readily available. However, implementation of this controller type on similar ammonia facilities has successfully been demonstrated<sup>[19],[22]</sup>. Based on this information, it is decided to explore the design and implementation of a linear quadratic regulator (LQR). Although commercial engineering tools are not as available compared to MPC, effort to design the LQR is not considered prohibitive. Further, an LQR algorithm can have a smaller on-line computational cost than MPC.

### 5.4.1. MVC Design

The LQR control problem is an optimal controller that attempts to minimize a user supplied quadratic performance index or cost function ( $J$ )<sup>[8]</sup>. The cost function, Equation 5.20 is designed to drive the state or part of the state of the system to zero without using excessive input energy<sup>[5]</sup>. The weighting matrices for the control variables and process inputs,  $\mathbf{Q}$  and  $\mathbf{R}$ , are tuned by trial and error by the controls engineer to achieve the desired control performance. Knowledge of the process and relative importance of the control variables is used to determine reasonable initial values of the weighting matrix. The performance index is posed to look at the change in valve movement for each controller step made<sup>[9]</sup>. This is done to eliminate steady-state offset from setpoint and is achieved by discretizing the LQR controller with a zero order hold, and a sample period of one second.

$$J = \int_0^{\infty} (\mathbf{x}^T \mathbf{Q} \mathbf{x} + \Delta \mathbf{u}^T \mathbf{R} \Delta \mathbf{u}) dt \quad (5.20)$$

The state feedback control law that results from the solution of the LQR problem has the following form, Equation 5.21.  $\mathbf{u}^*$  is the optimal controller input and  $\mathbf{K}_C$  is the controller gain matrix.

$$\mathbf{u}^* = -\mathbf{K}_C \mathbf{x} \quad (5.21)$$



Solution of the infinite time LQR problem uses the well known algebraic Riccati equation<sup>[5]</sup> and yields Equation 5.22. **S** is the Riccati matrix.

$$\mathbf{K}_C^T = \mathbf{S} \mathbf{B} \mathbf{R}^{-1} \quad (5.22)$$

Since not all of the states are available, a state observer is required to implement this controller. Accordingly, a Kalman Filter is used to estimate the state variables from measured and input variables, **y** and **u**. Refer to Equations 5.23 and 5.24<sup>[21]</sup>.

$$\frac{d\hat{\mathbf{x}}}{dt} = \mathbf{A} \hat{\mathbf{x}} + \mathbf{B} \mathbf{u} + \mathbf{L} (\mathbf{y} - \mathbf{C} \hat{\mathbf{x}}) \quad (5.23)$$

$$\hat{\mathbf{y}} = \mathbf{C} \hat{\mathbf{x}} \quad (5.24)$$

The estimator gain, **L**, is used to drive the error of the estimated states to zero based on a weighting matrix and the Riccati matrix<sup>[21]</sup>. The weighting matrix is equal to the inverse of the measurement covariance matrix, as identified in Equations 3.15 and 3.16. Measurement error is based on the error between the process model and the Kalman Filter estimate.

$$\mathbf{L}^T = \mathbf{W} \mathbf{C}^T \mathbf{S} \quad (5.25)$$

$$\mathbf{e} = \mathbf{y} - \hat{\mathbf{y}} = \mathbf{y} - \mathbf{C} \hat{\mathbf{x}} \quad (5.26)$$

Combining the state estimator with the optimal control vector yields the output feedback linear quadratic Gaussian regulator, LQGR<sup>[21]</sup>, Equations 5.27 and 5.28. LQGR is implemented as a discrete controller, using a zero order hold and a sample period of one second.

$$\frac{d\mathbf{x}}{dt} = \mathbf{A} \mathbf{x} + \mathbf{B} \mathbf{y} \quad (5.27)$$

$$\mathbf{u} = \mathbf{C} \mathbf{x} + \mathbf{D} \mathbf{y} \quad (5.28)$$

### 5.4.2. MVC Tuning

Tuning of the LQR controller is based on a locally linearized model of the process. Consistent with industry practices, the controller is tested and tuned on this same linearized model, prior to implementation<sup>[4]</sup>. This allows for immediate feedback without disrupting operations and in some cases is used for operator training.

As a starting point, noting that all CVs are equally important, the identity matrix is used for the weighting matrices **Q** and **R**. Subsequent tuning of **Q** and **R** is achieved iteratively. The resulting control action and performance yields positive results for each CV. Noting that the PID controller is able to effectively handle the saturation of  $HV_{G/G, SHELL}$ , the performance of the LQR controller under these conditions is also considered. With  $HV_{G/G, SHELL}$  dropped from the control problem the controller is unable to converge to a steady operating point, triggering the process to



become unstable. Iterative tuning of  $\mathbf{Q}$  and  $\mathbf{R}$  proves to be inadequate to identify a suitable controller.

A new term,  $\mathbf{N}$ , designed to promote loop pairings between controller inputs and outputs is introduced into the performance index<sup>[21]</sup>, Equation 5.29. With this information and knowledge of the loop pairing identified in Table 5-1 using the RGA,  $\mathbf{N}$  is used to promote control of  $T_{R1B2,IN}$  with  $HV_{WHBII,STEAM}$ .

$$J = \int_0^{\infty} (\mathbf{x}^T \mathbf{Q} \mathbf{x} + \Delta \mathbf{u}^T \mathbf{R} \Delta \mathbf{u} + 2 \mathbf{x}^T \mathbf{N} \Delta \mathbf{u}) dt \quad (5.29)$$

Using this modified controller with  $HV_{G/G,SHELL}$  saturated,  $T_{R1B2,IN}$  has a settling time of approximately 60 minutes for the linearized process model. This is a significant improvement over the PID control observed in section 4.2. An overshoot in steam production of 0.9 tonne per hour is noted. Validation of these results with the process is explored in Section 5.4.3, with the tuning constants presented in Equation 5.30.

$$\mathbf{Q} = 2 \begin{bmatrix} 1 & 0 & 0 \\ 0 & 1 & 0 \\ 0 & 0 & 1 \end{bmatrix} \quad \mathbf{R} = \begin{bmatrix} 1 & 0 & 0 & 0 \\ 0 & 1 & 0 & 0 \\ 0 & 0 & 1 & 0 \\ 0 & 0 & 0 & 1 \end{bmatrix} \quad \mathbf{N} = \frac{2}{100} \begin{bmatrix} 0 & 0 & 0 & 0 \\ 0 & 0 & 0 & 1 \\ 0 & 0 & 0 & 0 \end{bmatrix} \quad (5.30)$$

### 5.4.3. MVC Results

The LQR controller is then implemented on the process. The process response to the LQR with  $MV_1$  saturated is tested first. The process remains stable with a settling time of 60 minutes, similar to the linear model results. However, steady-state offset in the control variables is observed as well as an overshoot in steam production of 2.3 tonne/hr. Results are presented in Figure 5-13. This behaviour is notably different than the response observed in the linearized process model. The controller is then re-tuned to meet specifications.

$$\mathbf{Q} = 2 \begin{bmatrix} 1 & 0 & 0 \\ 0 & 1 & 0 \\ 0 & 0 & 1 \end{bmatrix} \quad \mathbf{R} = \begin{bmatrix} 1 & 0 & 0 & 0 \\ 0 & 1 & 0 & 0 \\ 0 & 0 & 1 & 0 \\ 0 & 0 & 0 & 1 \end{bmatrix} \quad \mathbf{N} = \frac{1.065}{100} \begin{bmatrix} 0 & 0 & 0 & 0 \\ 0 & 0 & 0 & 1 \\ 0 & 0 & 0 & 0 \end{bmatrix} \quad (5.31)$$

With the revised controller tuning constants, Equation 5.31, a stable process response for all CVs is achieved within controller specifications. The process control response for a step in each CV with  $HV_{G/G,TUBE}$  saturated can be found in Figures 5-14 to 5-16. Comparatively graphical results with  $HV_{WHBII,STEAM}$  are included in Figures 5-17 to 5-19. Significant improvement in settling times compared to PID control results are marked.



Figure 5-13 CV<sub>2</sub> Step, Modified LQR, MV<sub>1</sub> Saturated

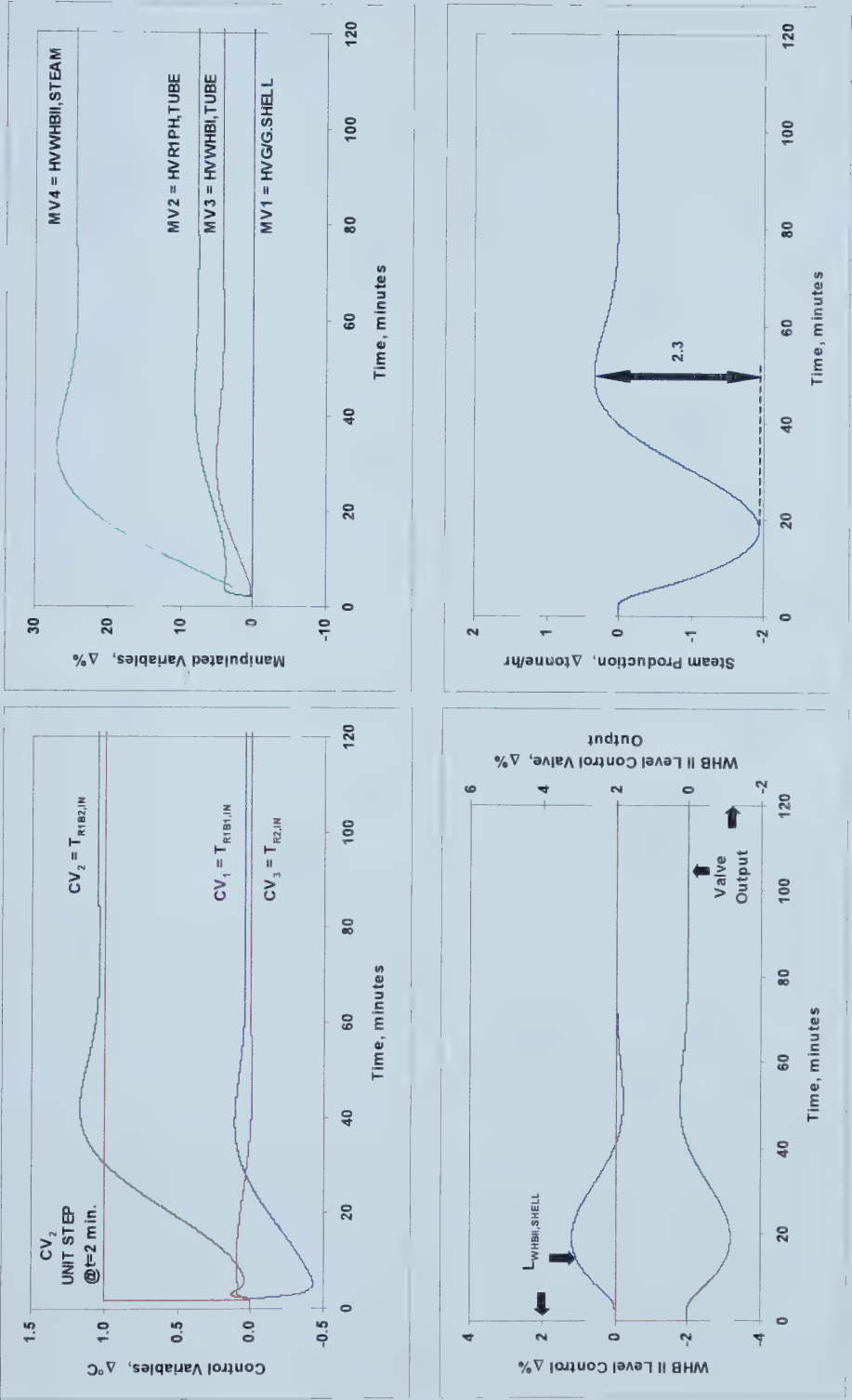






Figure 5-14 CV<sub>1</sub> Step, Final LQR, MV<sub>4</sub> Saturated

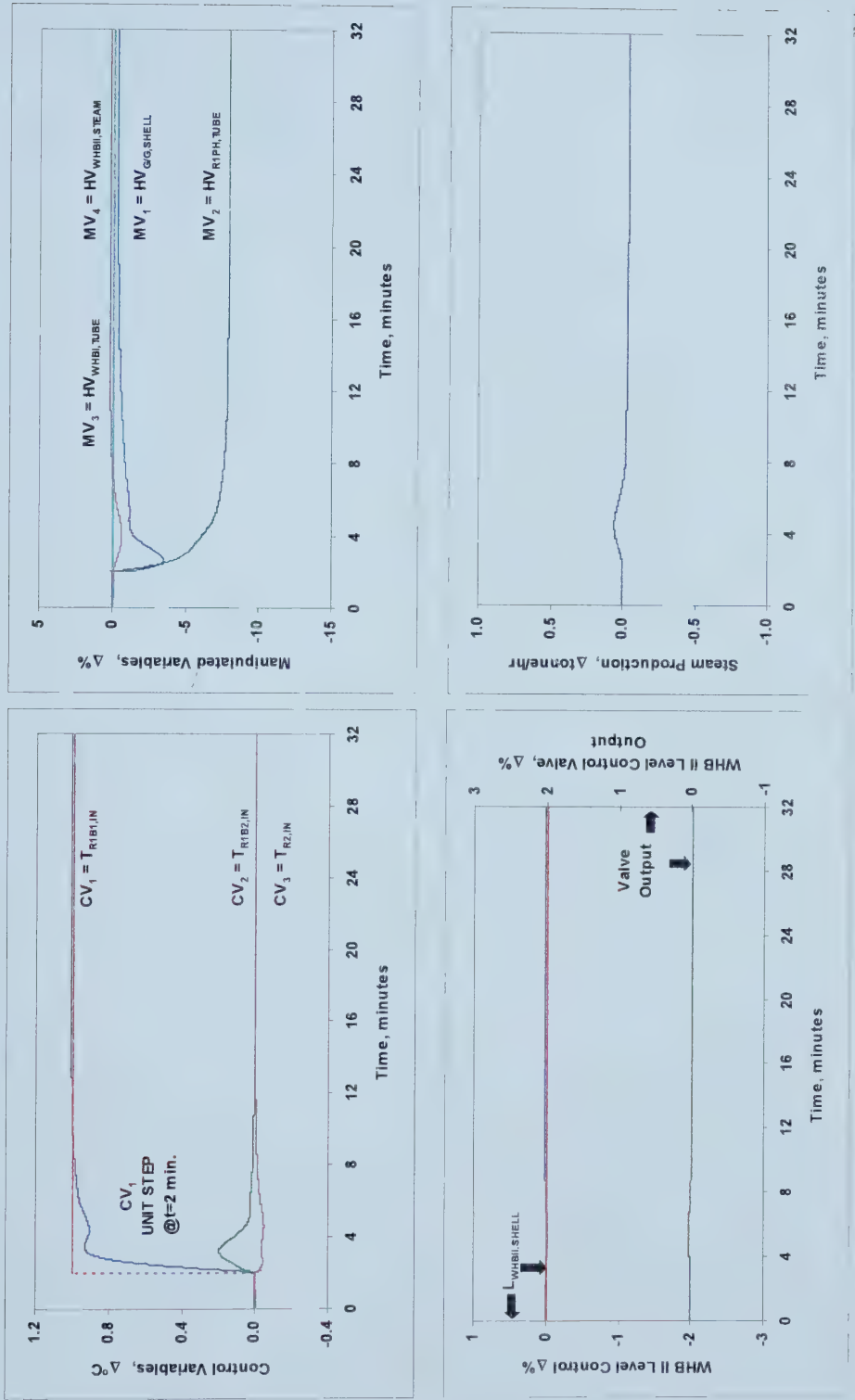




Figure 5-15 CV<sub>2</sub> Step, Final LQR, MV<sub>4</sub> Saturated

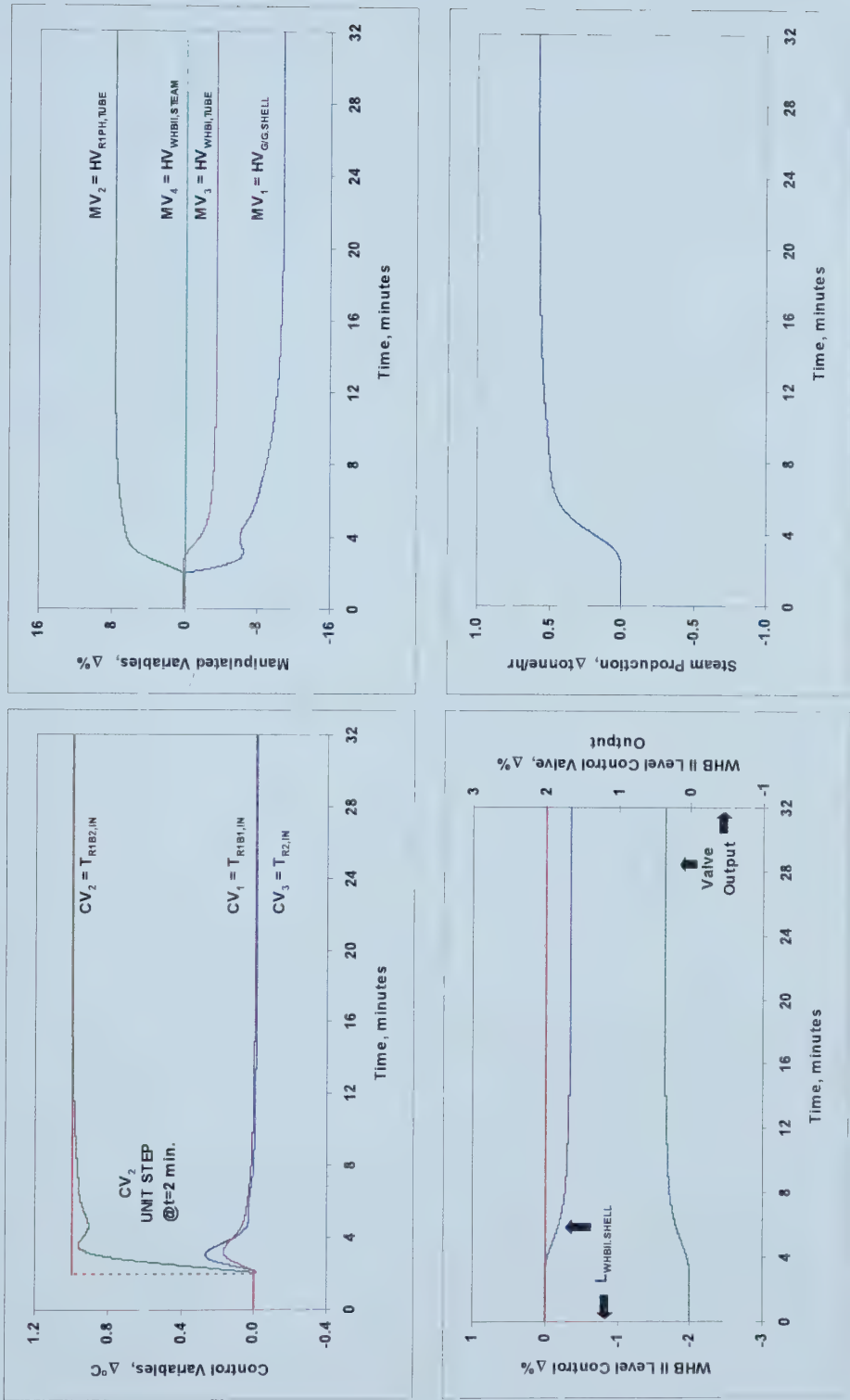




Figure 5-16 CV<sub>3</sub> Step, Final LQR, MV<sub>4</sub> Saturated

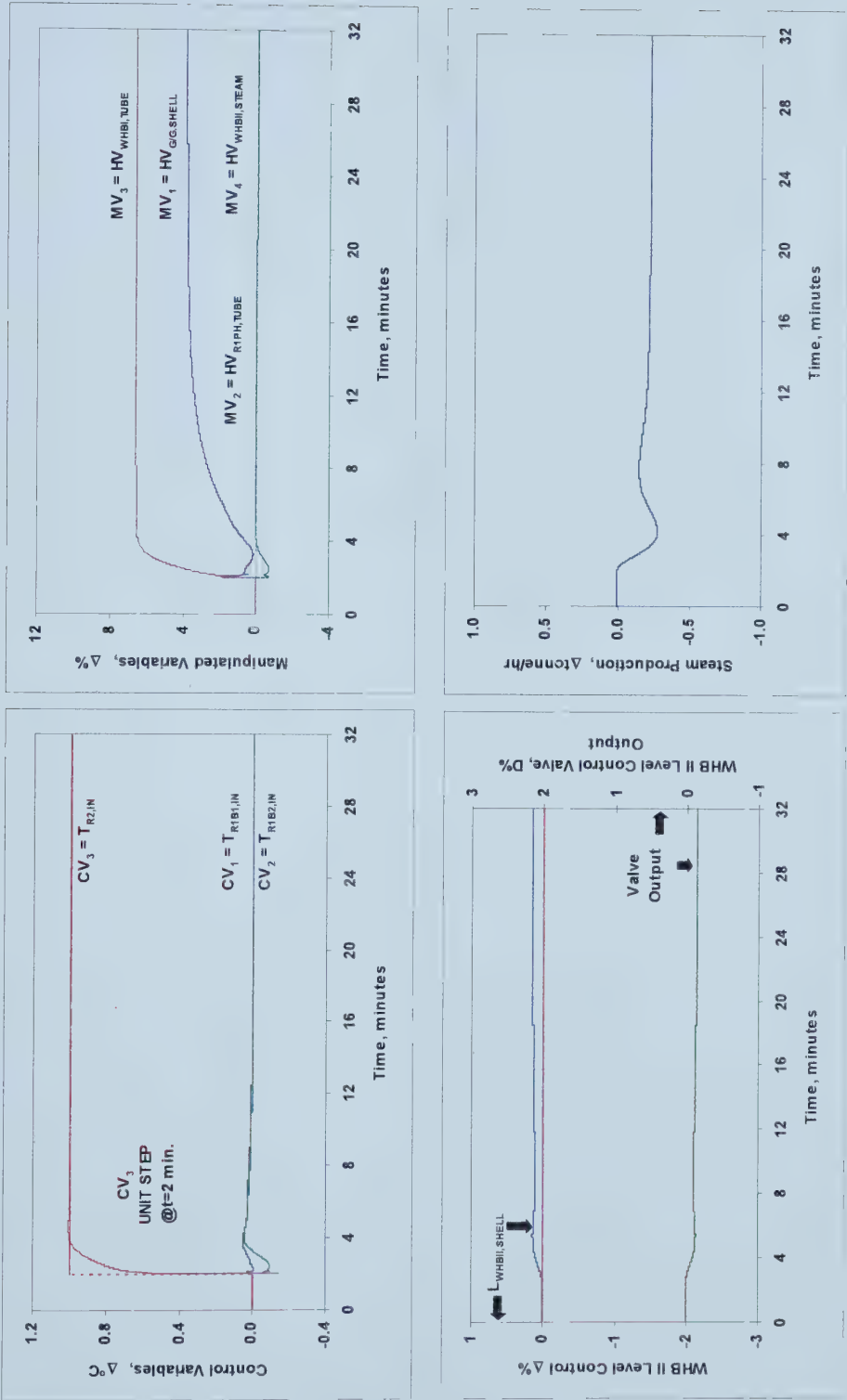




Figure 5-17 CV<sub>1</sub> Step, Final LQR, MV<sub>1</sub> Saturated

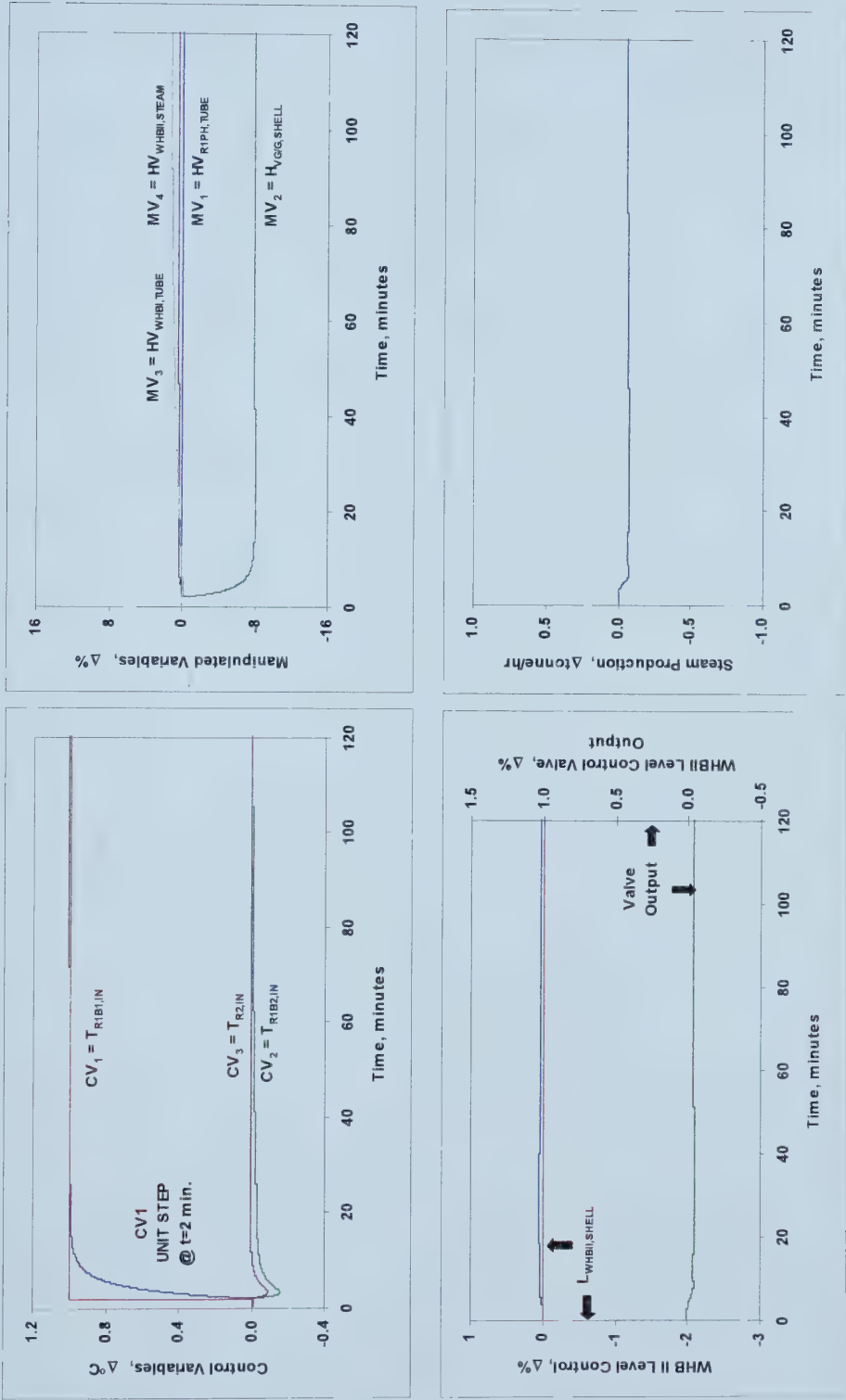






Figure 5-18 CV<sub>2</sub> Step, Final LQR, MV<sub>1</sub> Saturated

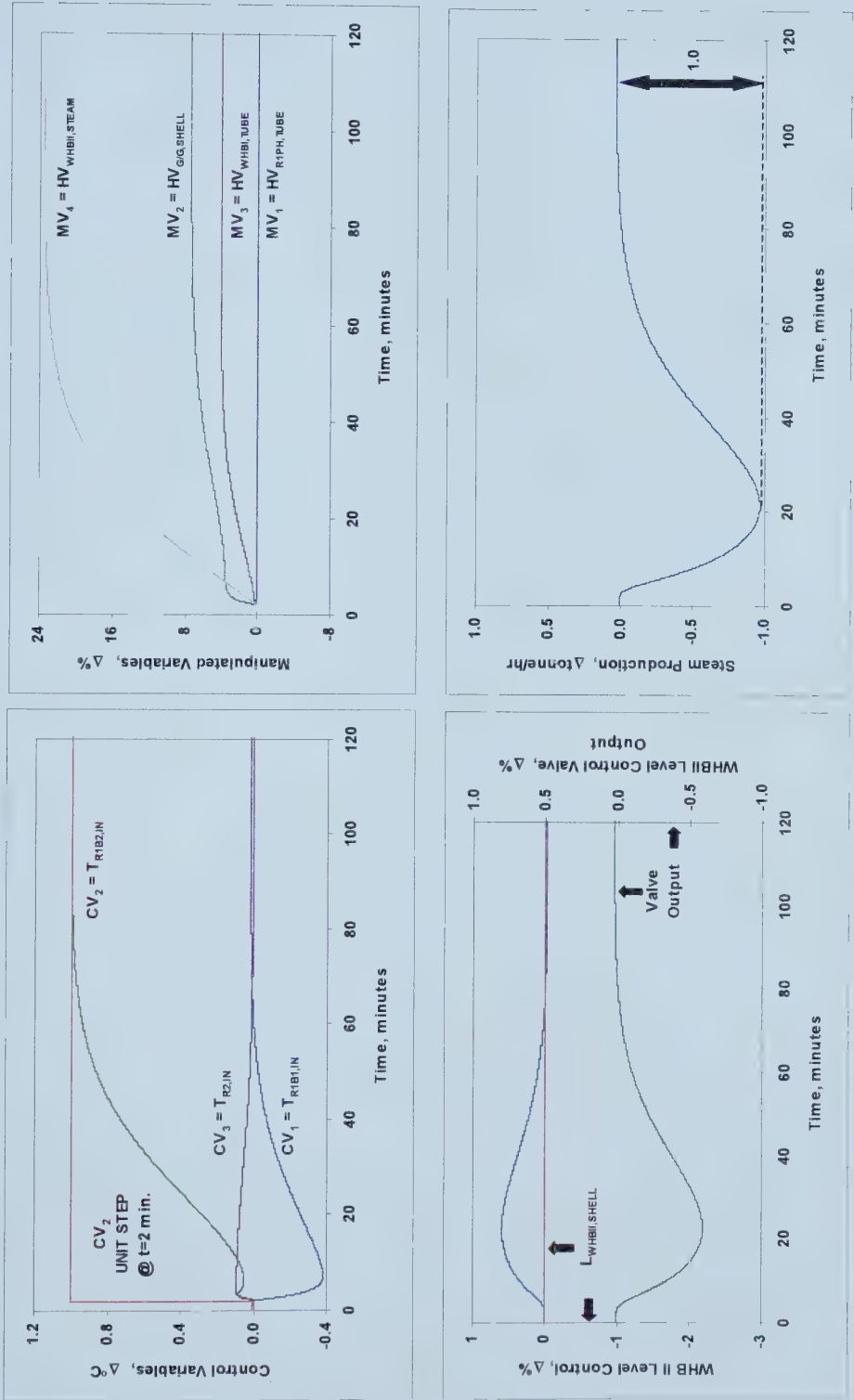
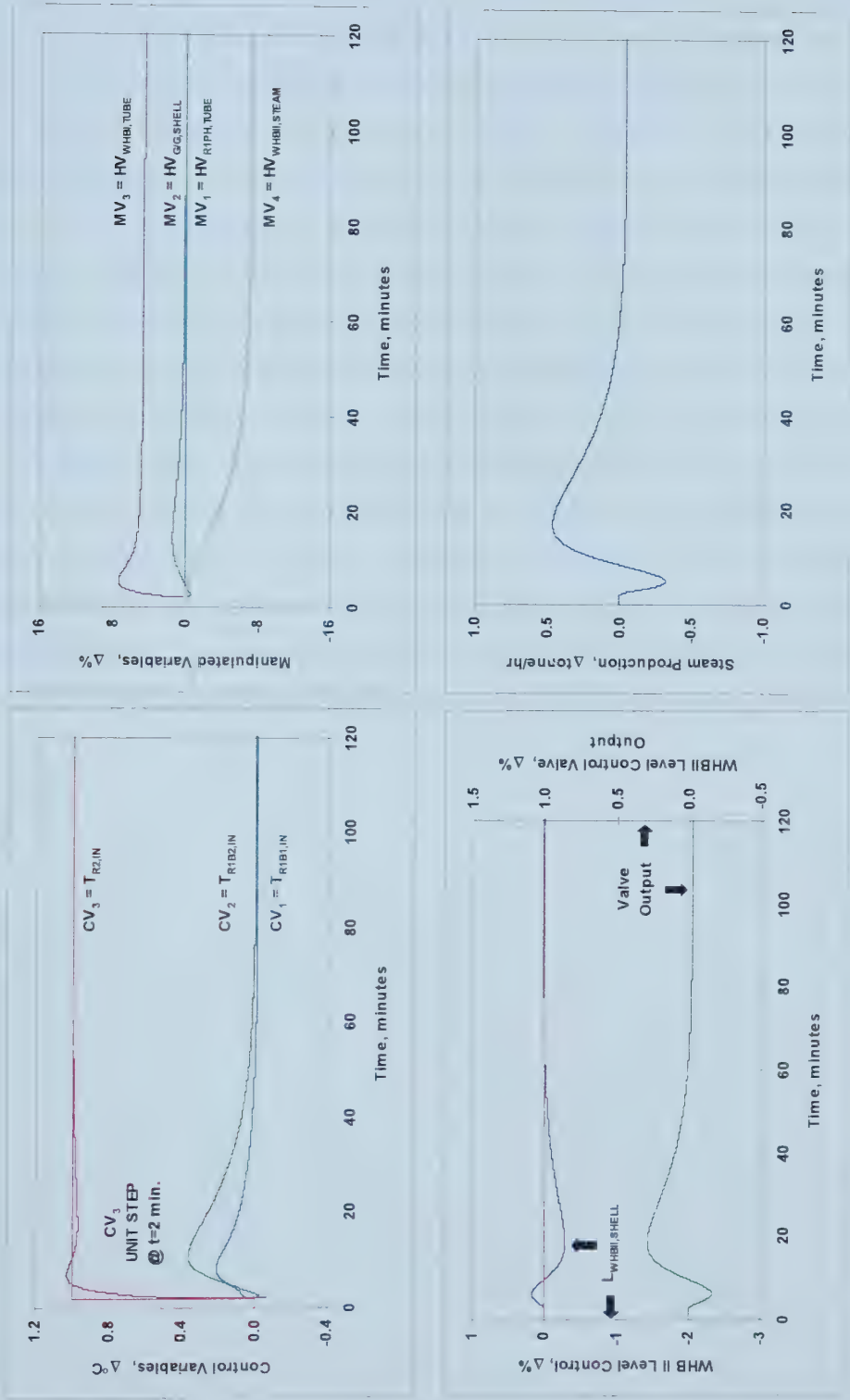




Figure 5-19 CV<sub>3</sub> Step, Final LQR, MV<sub>1</sub> Saturated





## 5.5. Discussion

By careful selection of the control variables, both the linear LQR and PID controllers are able to effectively control a known nonlinear process. Tables 5-3 and 5-4 summarize the PID and LQR controller performance. Comparison of these controllers can be found in Table 5-5.

Table 5-3 looks at the controllers with  $MV_1$ ,  $MV_2$  and  $MV_3$  involved in the control strategy. Performance of both the PID and LQR controllers is exceptionally good. Settling times are fast, process disturbances introduced by changing setpoints are relatively small and steam overshoot is within specifications. Without introducing a quantitative measurement, such as ITAE, with penalties on changing steam production and MV movement, it is difficult to differentiate between the results. Noting that an optimizer may only run a few times per day with a new setpoint, the differences between the two controllers are not considered to be significant.

Similarly, Table 5-4 looks at the control performance with  $MV_2$ ,  $MV_3$  and  $MV_4$ , actively involved in the control matrix.  $MV_4$ , which has a larger impact on steam production and notably slower dynamics than the other MVs, inherently introduces a layer of complexity to the control problem. In all cases, the time required for these highly interactive loops to return to steady-state after a CV unit step is significantly less for the LQR. After a unit step in  $CV_3$ , the settling time for PID control is over 1 hour longer than the time for the LQR controller to reach steady-state.



Table 5-3

Comparative Controller Behaviour with MV<sub>4</sub> Saturated

Control Variable ( $\Delta^{\circ}\text{C}$ )	Control Type	CV Response Time (minutes)	CV Settling Time (minutes)	Process Settling Time (minutes)	CV <sub>1</sub> Dev'n ( $\Delta^{\circ}\text{C}$ )	CV <sub>2</sub> Dev'n ( $\Delta^{\circ}\text{C}$ )	CV <sub>3</sub> Dev'n ( $\Delta^{\circ}\text{C}$ )	$\Delta M_{\text{STEAM}}$ ( $\Delta\text{tonne/hr}$ )
$\Delta\text{CV}_1 = 1$	PID	4.3	4.3	4.3	0.00	0.15	0.00	0.04
	LQR	5.6	5.6	5.6	0.00	0.19	0.05	0.06
$\Delta\text{CV}_2 = 1$	PID	0.5	1.2	4.6	0.43	0.04	0.03	0.58
	LQR	7.5	7.5	7.5	0.26	0.00	0.17	0.57
$\Delta\text{CV}_3 = 1$	PID	1.0	1.0	1.0	0.00	0.01	0.00	0.28
	LQR	1.6	1.6	5.6	0.05	0.09	0.00	0.28

Table 5-4

Comparative Controller Behaviour with MV<sub>1</sub> Saturated

Control Variable ( $\Delta^{\circ}\text{C}$ )	Control Type	Response Time (minutes)	CV Settling Time (minutes)	Process Settling Time (minutes)	CV <sub>1</sub> Dev'n ( $\Delta^{\circ}\text{C}$ )	CV <sub>2</sub> Dev'n ( $\Delta^{\circ}\text{C}$ )	CV <sub>3</sub> Dev'n ( $\Delta^{\circ}\text{C}$ )	$\Delta M_{\text{STEAM}}$ ( $\Delta\text{tonne/hr}$ )
$\Delta\text{CV}_1 = 1$	PID	3.3	3.3	22.8	0.00	0.30	0.01	0.21
	LQR	11.3	11.3	11.3	0.00	-0.16	-0.09	-0.08
$\Delta\text{CV}_2 = 1$	PID	106.5	106.5	106.5	0.02	0.00	0.00	1.00
	LQR	70.5	70.5	70.5	0.38	0.00	0.09	1.00
	LQR-Model	33.4	59.6	59.6	0.41	0.06	0.09	0.90
$\Delta\text{CV}_3 = 1$	PID	0.9	0.9	90.5	0.05	0.40	0.00	0.97
	LQR	3.1	27.4	27.4	0.21	0.36	0.03	0.79





The advantages and disadvantages of the characteristics of each controller are summarized in Table 5-5. The complexity of the two controllers is also a determining factor in selecting the preferred control scheme, PID or LQR. While LQR performance is superior compared to PID control, implementation in this case is not considered practical based on the incremental effort required to develop, maintain and train operations. Further use of  $HV_{WHBII,STEAM}$  in the control strategy demonstrates marginal performance. Prior to implementing a controller with this MV, additional tests should be carried out, including evaluating the controller’s ability to reject noise and process disturbances. Based on these results, PID control is recommended, preferably excluding  $HV_{WHBII,STEAM}$  as a manipulated variable.

**Table 5-5                      Comparative Controller Characteristics**

Control Type	PID	LQR
Advantages	1. Well known industry standard.	1. Inherently considers process as single control problem with CVs to be resolved simultaneously.
	2. Tools and control algorithms readily available.	2. Control algorithm weights MV adjustments.
	3. Single loop tuning relatively simple.	
	4. Model identification based on three control variables.	
	5. Easy to drop single CV from control scheme.	
Disadvantages	1. Considers process as three distinct control problems to be resolved independently.	1. Technology relatively complex.
	2. Tuning of multiple loops with interaction done iteratively.	2. Custom programming required to implement LQR algorithm.
	3. Controller based on a linearized process.	3. Three control matrices tuned iteratively.
		4. Model identification based on 34 state space variables.
		5. Custom programming required to drop CV from control scheme.
		6. Controller based on a linearized process.

Control considerations not included here are controller stability and process noise. Typically the stability of the controller over different operations needs to be explored. Additionally if noise is introduced in the process, controller results may vary slightly, particularly with respect to the steam system.



## CHAPTER 6

### SUMMARY AND CONCLUSIONS

The growing demand for nitrogen fertilizer in agriculture has renewed interest in control applications for ammonia production. The objective of this thesis is to explore these automation prospects and technologies to exploit these opportunities at Saskferco Products Inc. The ammonia synthesis unit is chosen as the focal point of these studies. While some research has been done on similar units, it is neither exhaustive nor entirely clear that other means of control would not achieve similar results, with less overhead required for implementation and maintenance. Additionally, known nonlinearities in the ammonia synthesis unit offer the chance to investigate the applicability of conventional linear control methods to a nonlinear process.

#### 6.1. Area of Study

A dynamic model of the ammonia synthesis unit is developed to provide insight into the process operation and a platform for optimization and control studies. To improve the accuracy of the model for these studies, dynamic update of a reaction fit parameter is investigated using historical data. Parameter estimation is intended to account for model mismatch, changing catalyst activity and diffusion limitations. To this end, a new term referred to as the catalyst effectiveness parameter is introduced into the Temkin-Pyshev reaction equation, biasing the reaction kinetics of the rate-limiting forward reaction. Update of this parameter using variations in the least squares algorithm is studied to determine the most suitable update method.

Based on this model, several optimization studies are performed, including normal operation, seasonal operation and operation during periods of reduced catalyst activity. The objective function is to maximize overall conversion of synthesis gas to ammonia for each pass through the converter beds. Increased conversion potentially allows increased make-up gas feed, and a more efficient process based on reduced synthesis gas recycle. Given the fast dynamics of the process relative to the process disturbance frequency, optimization studies are based on the steady-state operation of the process. Process control to enforce optimization results is investigated for PID and LQR control strategies using 3 CVs and 4 MVs. A maximum overshoot in steam production of 1 tonne/hr per 1 °C setpoint change is imposed. As part of the plant's protection system, the WHB level control is not included in this advanced control application.



This thesis took the standard approach for level control by implementing a proportional controller, despite limitations as a regulatory controller.

## 6.2. Results

Process model results, with fit parameters in the model, reveal a good fit between plant data and model predictions. Nonlinear relationships in the converters and known problems in the control of the WHB level are substantiated.

The results of the parameter update problem found the recursive least squares algorithm, to be the most accurate and practical approach. Using 3 parameters to estimate 4 process measurements, the recursive least squares method demonstrated the best overall accuracy, with the least variation in the parameter results. Computer resources in this case are approximately 6 % of other least squares formulations. Interestingly the weighted least squares method typically sacrificed the R1B1 inlet temperature to achieve results. The major drawback of this method is that it is based on difference variables. Accordingly, it must be coupled with another method, such as the sum of squares, to find reasonable initial conditions and to circumvent model drift. Studies around the sum of squares parameter update method uncover a strong relationship between the parameter update value and the process H/N ratio. These results expose a limitation in the process model, which over-penalizes ammonia conversion at higher H/N ratios.

Results of the optimization studies identified potential benefits of approximately \$180 k/year. In all cases, it is found that the R1 preheater bypass valve is typically constrained in the closed position. It is observed that a reduced optimization model on the last converter bed could achieve 70 % of these benefits.

Analysis of summer versus winter operation reveals some interesting relationships. Typically Saskferco operates at reduced rates in the summer months due to process limitations aggravated by ambient temperatures. Increased ammonia conversion in the summer is partially attributed to a reduction of inerts in the feed and also possibly to the reduction in catalyst diffusion limitations with reduced throughput. Optimal converter temperatures are on average 3 °C, 5 °C and 6 °C colder in beds one, two and three respectively during the summer months compared to winter.

Results of a post optimality analysis indicate a conversion “dead zone” in the region surrounding the optimal reactor inlet temperature. This information can ultimately be used to operate the plant a safe margin above the calculated optimum temperature without significant penalties or to accept/reject changes in the optimization results depending on the magnitude of the change. Results are unable to confirm the optimum H/N ratio given in literature.





Loop pairing for PID control, using the RGA, is contrary to what might have been anticipated given the process layout. The R1B2 inlet temperature is paired with the two valves upstream of R1B1 as a split range controller, while the R1B1 temperature is paired with the converter one preheater bypass valve. PID control on the nonlinear process model is relatively simple to implement and is able to effectively satisfy the control criteria. Performance of the R1B2 inlet temperature with the WHB II BFW split valve is marginal. A settling time of 107 minutes is observed, with an overshoot in steam production of 1 tonne/hour when this CV is perturbed with a unit step.

Design of the optimal controller, LQR, is also straightforward. The main difficulty with this method is to formulate an appropriate performance index to meet the control criterion and to address steady-state errors and controller stability issues. Tuning of this controller encompasses 3 weighting matrices that are solved iteratively. Input saturation of the gas-gas exchanger bypass is handled by dropping this MV from the control matrix. The worst performance is observed in the R1B2 inlet temperature when stepped with the gas-gas exchanger bypass valve saturated, with a settling time of 71 minutes.

### **6.3. Conclusions**

It is concluded that the opportunity exists at Saskferco to improve control and optimization in the ammonia synthesis loop. Implementation based on conventional and modest automation techniques is determined to be the most feasible, achieving the majority of these benefits.

Linear LQR and PID controllers are able to successfully control a known nonlinear process by judicious selection of the control variables. Performance of the LQR for highly interactive loops is considered superior to the PID control strategy, based on controller settling times. However, while LQR control results are encouraging, implementation is not considered to be practical based on the incremental effort required to program, tune, maintain and train operations compared to PID control. Depending on optimization frequency, effective benefits between these servo controllers could be considered financially insignificant.

Based on optimization results, indicating saturation of the R1PH bypass valve, PID control on the R1B1 inlet temperature would be meaningless. Further, PID control of the R1B2 inlet temperature controller is also not considered feasible based on marginal performance of this loop with the WHB BFW split valve. Significant detuning is necessary to reduce impact on the steam system, resulting in long settling times. Control benefits of \$54 k/year are outweighed by potential oscillations in the steam system (and possible plant trip scenarios).





While existing MVC ammonia synthesis controllers have been demonstrated on quench converters, with different MVs available, installation of MVC for ammonia synthesis is questioned, considering the relative benefits of simpler control strategies.

#### **6.4. Recommendations**

Further research to investigate the comparative performance of the PID and LQR controllers, as regulatory controllers, subject to noise and disturbance variables, should be explored. Results and conclusions of this thesis are based on the servo control response of PID and LQR systems.

While this thesis focuses on the ammonia synthesis loop at Saskferco, it is noted that additional control opportunities in the ammonia plant may exist in upstream units. Given rising energy costs, opportunities in the UHDE methane reformer may prove attractive. It is noted that similar reformer control applications have been implemented<sup>[20],[22]</sup>.

As a final submission, the following recommendations are made for Saskferco operations.

1. On-line optimization of the R2 inlet temperature.
2. On-line optimization of the R1 inlet temperatures operated in advisory mode.  
Results would be available as an operational guide and to alarm temperatures below optimal conditions, where potential loss of the reaction exists.
3. Parameter updates to complement process optimizers.  
Implementation would be achieved using a weighted least squares approach augmented with the sum of squares, for initial conditions and to prevent model drift. Ammonia conversion soft sensors through each converter bed would be beneficial by-products of these efforts.
4. R2 inlet temperature PID control operating in conjunction with the R2 optimizer.  
Site issues relating to the WHB I bypass control valve will need to be addressed.
5. Investigation of improved control strategies on the WHB II level controller.



## BIBLIOGRAPHY

- [1] M. Appl. *Ammonia, Principles and Industrial Practice*. Wiley-VCH, Weinheim, 1999.
- [2] H. Bakermeier, T. Huberich, R. Krabetz, W. Liebe, M. Schunk, *Ullmann's Encyclopedia of Industrial Chemistry, Ammonia*. A2, VCH Verlagsgesellschaft, 1996.
- [3] A. Bertucco, M. Barolo and G. Soave. Estimation of Chemical Equilibria in High-Pressure Gaseous Systems by a Modified Redlich-Kwong-Soave Equation of State. *Ind. Eng. Chem. Res.*, 34:3159-3165, 1995.
- [4] B.W. Bequette. *Process Dynamics, Modelling, Analysis and Simulation*. Prentice Hall Inc., Upper Saddle River, NJ, 1998.
- [5] S. Bittanti, A.J. Laub and J.C. Willems. *The Riccati Equation*. Springer-Verlag New York Inc., New York, 1991.
- [6] W.L. Brogan. *Modern Control Theory*. Prentice Hall Inc., Upper Saddle River, NJ, 1991.
- [7] D.R. Coughanowr. *Process Systems Analysis and Control. Second Edition*. McGraw-Hill Inc., New York, 1991.
- [8] J.J. D'Azzo and C.H. Houpis. *Linear Control System Analysis and Design. Conventional and Modern. Second Edition*. McGraw-Hill Inc, New York, 1981.
- [9] J.M. Douglas. *Process Dynamics and Control, Volume 2, Control Systems Synthesis*. pages 291-293, Prentice Hall, Englewood Cliffs, NJ, 1972.
- [10] N. Draper and H. Smith. *Applied Regression Analysis, Second Edition*. John Wiley & Sons, Inc., 1966.
- [11] T.F. Edgar and D.M. Himmelblau. *Optimization of Chemical Processes*. McGraw-Hill Inc., New York, 1988.
- [12] B. Edmondson, Saskferco Products Inc. Technical Director, Belle Plaine, SK. *Personal Communications*, 1999.



- [13] S. S. Elnashaie, M. E. Abashar and A. S. Al-Ulbaid. Simulation and Optimization of an Industrial Ammonia Reactor. *Ind. Eng. Chem. Res.*, 27:2015-2022, 1988.
- [14] B. Friedland. *Control System Design. An Introduction to State-Space Methods*. McGraw-Hill Inc., New York, 1986.
- [15] N. Ganesh, L.T. Biegler. A Reduced Hessian Strategy for Sensitivity Analysis of Optimal Flowsheets. *AIChE Journal*. 33(2):282-296, February 1987.
- [16] J.P. Holman. *Heat Transfer, Seventh Edition*. McGraw-Hill Inc., New York, 1990
- [17] B.R. Hope, P. K. Robertson. *Confidential Disclosure Agreement Between Saskferco and University of Alberta*. Alberta, 2001.
- [18] A. Hugo. *Limitations of Model Predictive Controllers*. Hydrocarbon Processing, pages 83-88, January 2000.
- [19] L. Kane. *Advanced Process Control Strategies 1993*. Hydrocarbon Processing, pages 84-85, September 1993.
- [20] E. Kharbat. Successful Application of Adaptive Technologies to Ammonia Reformers. Ammonia Plant Safety and Related Facilities, 38:279-285, 1998.
- [21] J.N. Little, C.M. Thompson, P. Gahinet, *Control System Toolbox for Use With Matlab, User's Guide*. The MathWorks Inc., Natick MA, 4.2, 1992-1999.
- [22] R. Lin, R. de Boer and B. Poe. Optimize Ammonia Plant Operation. *Hydrocarbon Processing*, pages 91-100, June 1999.
- [23] L. Ljung and T. Soderstrom. *Theory and Practice of Recursive Identification*. The MIT Press, Cambridge, Massachusetts, 1983.
- [24] W.G. Mallard and P.J. Linstrom, Eds. *NIST Chemistry WebBook, NIST Standard Reference Database Number 69*. <http://webbook.nist.gov>. National Institute of Standards and Technology, Gaithersburg MD, February 2000.
- [25] B. Mansson and B. Andresen. Optimal Temperature Profile for an Ammonia Reactor. *Ind. Eng. Chem. Process Des. Dev.*, 25:59-65, 1986.



- [26] J. Markos and M. Barto. Optimization Method for Balance Adjustment in Large Chemical Process Systems. *Chem. Eng. Process.*, 30:45-50, 1991.
- [27] T.E. Marlin. *Process Control Designing Processes for Control Systems for Dynamic Performance*, McGraw-Hill Inc., New York, 1995.
- [28] S.A. Matthews. Process Plant Productivity Improvement through Neural Network Applications. *ISA TECH EXPO Technology Update Conference Proceedings*. 1(2):157-166, ISA, Research Triangle Park, NC, 1997
- [29] A. Mihajlov, B. Djordjevic and A. Tasic. Calculation of Enthalpy and Entropy of Gases by Modified Redlich-Kwong Equation of State. *Hungarian Journal of Industrial Chemistry*, 9:407-416, 1981.
- [30] K. Mishima, J. Sugino, M. Ueno, K. Matsuyama and M. Nagatani. Correlation of Solubilities for CO<sub>2</sub> and NH<sub>3</sub> in H<sub>2</sub>O Using Soave-Redlich-Kwong Equation of State with MHV2 Mixing Rule. *Journal of Chemical Engineering of Japan*. 28(2):144-147, 1995.
- [31] M. Munro. Beware the Green Peril. *National Post*. Hollinger/Canwest Publications, 24-April, 2001
- [32] D.Y. Murzin and A.K. Avetisov. Kinetics of Ammonia Synthesis Close to Equilibrium. *Ind. Eng. Chem. Res.*, 36:4779-4783, 1997.
- [33] L. Naess, A. Mjaavatten and J.O, Li. Using Dynamic Process Simulation from Conception to Normal Operation of Process Plants. *Computers Chem. Engng.*, 17(5/6):585-600, 1993.
- [34] L.M. Patnaik, N. Viswanadham and I.G. Sarma. Design of Multiloop Controllers for an Ammonia Reactor. *IEEE Transactions on Industrial Electronics and Control Instrumentation*, 28(4):253-358, 1981.
- [35] L.M. Patnaik, N. Viswanadham and I.G. Sarma. Hierarchical Control of an Ammonia Reactor. *IEEE Transactions of Systems, Man and Cybernetics*, 12(6):919-924, November/December 1982.
- [36] E. A. Robinson. *Least Square Regression Analysis in Terms of Linear Algebra*. Goose Pond Press., Houston, 1981.





- [37] J. M. Smith and H. C. Van Ness. *Introduction to Chemical Engineering Thermodynamics. Fourth Edition*. McGraw-Hill, Inc. New York, 1987.
- [38] G. Soave. Direct Calculation of Pure-Compound Vapour Pressures through Cubic Equations of State. *Fluid Phase Equilibria*, 31:203-207, 1986.
- [39] G. Soave, M. Barolo and A. Bertucco. Estimation of high-pressure fugacity coefficients of pure gaseous fluids by a modified SRK equation of state. *Fluid Phase Equilibria*, 91:87-100, 1993.
- [40] D. Tilman, J. Fargione, B. Wolff, C. D'Antonio, A. Dobson, R. Howarth, D. Schindler, W. H. Schlesinger, D. Simberloff, and D. Swackhamer. Forecasting Agriculturally Driven Global Environmental Change. *SCIENCE*, 292:281-284, April 2001.
- [41] M. V. Twigg. *Catalyst Handbook. Second Edition*. Manson Publishing, London, 1996.
- [42] S.R. Upreti and K. Deb. Optimal Design of an Ammonia Synthesis Reactor Using Genetic Algorithms. *Computers Chem. Engng.*, 21(1):87-92, 1997.
- [43] N. Viswanadham, L.M. Patnaik and I.G. Sarma. Robust Multivariable Controllers for a Tubular Ammonia Reactor. *Transactions of the ASME*. 101:290-298, December 1979.
- [44] C. Ying and B. Joseph. Performance and Stability Analysis of LP-MPC and QP-MPC Cascade Control Systems. *AIChE Journal*, 34(7):1521-1534, July 1999.



# APPENDIX A

## PLANT DATA

Shift averages for February and March were collected from the Saskferco information system. This data is used to fit the Simulink process model, in the parameter fit evaluations and for comparison of operation to optimization results.

**Table A-1      Plant Data**

Date	V <sub>IN,SG</sub> k-sm <sup>3</sup> /hr	P <sub>IN,SG</sub> MPag	y <sub>IN,NH3</sub> vol %	y <sub>IN,N2</sub> vol %	y <sub>IN,H2</sub> vol %	y <sub>IN,HE</sub> vol %	y <sub>IN,AR</sub> vol %	y <sub>IN,CH4</sub> vol %
01-Feb-99 07:00	729.30	18.90	2.23	20.46	61.85	0.99	2.90	11.27
01-Feb-99 19:00	731.11	18.85	2.23	20.60	61.55	0.99	2.90	11.29
02-Feb-99 07:00	736.00	18.87	2.20	20.48	61.32	0.98	2.88	11.75
02-Feb-99 19:00	731.31	18.79	2.19	20.55	61.64	0.97	2.90	11.36
03-Feb-99 07:00	731.49	18.83	2.19	20.52	61.60	0.97	2.90	11.40
03-Feb-99 19:00	732.93	18.75	2.28	20.63	61.78	1.01	2.91	11.12
04-Feb-99 07:00	721.86	18.60	2.20	20.61	61.85	1.04	2.91	10.97
04-Feb-99 19:00	726.87	18.75	2.23	20.59	61.95	1.06	2.91	10.89
05-Feb-99 07:00	731.18	18.84	2.23	20.63	61.80	1.05	2.90	11.08
05-Feb-99 19:00	733.36	18.73	2.21	20.60	61.79	1.05	2.90	11.12
06-Feb-99 07:00	731.94	18.75	2.19	20.63	61.78	1.05	2.91	11.05
06-Feb-99 19:00	728.10	18.83	2.24	20.55	61.90	1.03	2.91	11.01
07-Feb-99 07:00	728.95	18.89	2.21	20.03	62.07	1.01	2.90	11.32
07-Feb-99 19:00	720.57	19.06	2.24	18.31	63.96	0.99	2.83	11.28
08-Feb-99 07:00	732.44	18.95	2.22	19.96	61.83	1.00	2.87	11.70
08-Feb-99 19:00	734.57	18.82	2.23	20.42	61.34	0.96	2.88	11.75
09-Feb-99 07:00	737.74	18.83	2.22	20.48	61.46	0.95	2.89	11.66
09-Feb-99 19:00	737.54	18.89	2.24	20.46	61.42	0.95	2.88	11.72
10-Feb-99 07:00	733.93	18.93	2.27	20.42	61.32	0.92	2.88	11.72
10-Feb-99 19:00	736.05	18.82	2.24	20.47	61.15	0.94	2.83	12.00
11-Feb-99 07:00	736.98	18.86	2.25	20.38	61.07	1.01	2.82	12.08
11-Feb-99 19:00	741.89	18.88	2.26	20.29	60.95	1.02	2.89	12.11
12-Feb-99 07:00	746.09	18.92	2.26	20.32	60.90	1.07	2.98	12.07
12-Feb-99 19:00	748.77	18.97	2.27	20.20	60.82	1.08	3.00	12.23
13-Feb-99 07:00	745.79	19.05	2.31	20.24	60.86	1.04	2.99	12.24
13-Feb-99 19:00	744.39	19.01	2.31	20.45	60.68	1.03	2.99	12.17
14-Feb-99 07:00	743.93	19.04	2.33	20.39	60.47	1.05	2.97	12.31
14-Feb-99 19:00	742.94	18.92	2.28	20.49	60.50	1.06	2.94	12.28
15-Feb-99 07:00	741.86	18.91	2.27	20.55	60.57	1.06	2.93	12.24
15-Feb-99 19:00	745.40	18.87	2.27	20.49	60.55	1.06	2.92	12.32
16-Feb-99 07:00	741.93	18.90	2.27	20.55	60.66	1.04	2.89	12.21
16-Feb-99 19:00	741.65	18.90	2.29	20.59	60.61	1.02	2.89	12.22
17-Feb-99 07:00	741.19	18.86	2.24	20.52	60.67	1.01	2.87	12.29
17-Feb-99 19:00	738.73	18.87	2.28	20.58	60.81	1.00	2.89	12.05
18-Feb-99 07:00	741.24	18.94	2.26	20.24	60.80	1.00	2.91	12.39
18-Feb-99 19:00	739.42	18.95	2.30	20.04	60.99	1.05	2.94	12.31
19-Feb-99 07:00	737.33	18.99	2.31	20.08	61.13	1.06	2.95	12.10
19-Feb-99 19:00	739.26	19.04	2.34	20.01	61.07	1.14	2.94	12.11



Date	V <sub>IN,SG</sub> k-sm <sup>3</sup> /hr	P <sub>IN,SG</sub> MPag	y <sub>IN,NH3</sub> vol %	y <sub>IN,N2</sub> vol %	y <sub>IN,H2</sub> vol %	y <sub>IN,HE</sub> vol %	y <sub>IN,AR</sub> vol %	y <sub>IN,CH4</sub> vol %
20-Feb-99 07:00	744.15	19.15	2.38	19.79	61.05	1.20	2.92	12.27
20-Feb-99 19:00	743.52	19.14	2.38	19.40	61.23	1.16	2.86	12.56
21-Feb-99 07:00	739.19	19.08	2.34	19.55	61.18	1.15	2.83	12.57
21-Feb-99 19:00	734.56	18.99	2.31	19.62	61.69	1.16	2.88	11.93
22-Feb-99 07:00	737.32	19.11	2.37	19.61	61.52	1.15	2.89	12.07
22-Feb-99 19:00	735.96	18.98	2.28	19.57	61.66	1.15	2.90	12.07
23-Feb-99 07:00	731.47	18.95	2.27	19.56	61.61	1.12	2.87	12.15
26-Feb-99 19:00	729.97	18.75	2.38	21.78	60.72	0.96	2.87	10.91
27-Feb-99 07:00	736.26	18.84	2.28	20.04	62.37	0.94	2.84	11.15
27-Feb-99 19:00	737.44	18.90	2.26	19.57	62.58	0.97	2.83	11.40
28-Feb-99 07:00	733.93	18.82	2.25	19.68	62.83	0.99	2.84	11.02
28-Feb-99 19:00	733.40	18.89	2.27	19.49	62.99	0.98	2.82	11.07
01-Mar-99 07:00	736.66	18.86	2.24	19.64	62.64	0.98	2.81	11.29
01-Mar-99 19:00	737.44	18.87	2.26	19.61	62.52	0.97	2.80	11.45
02-Mar-99 07:00	735.83	18.79	2.23	19.65	62.83	0.96	2.78	11.15
02-Mar-99 19:00	737.45	18.81	2.23	19.63	62.76	0.95	2.79	11.29
03-Mar-99 07:00	740.15	18.83	2.24	19.76	62.37	0.93	2.79	11.54
03-Mar-99 19:00	739.06	18.87	2.29	20.03	62.04	0.92	2.80	11.53
04-Mar-99 07:00	738.20	18.93	2.31	20.02	62.12	0.93	2.77	11.49
04-Mar-99 19:00	742.61	19.05	2.36	19.95	61.87	0.88	2.74	11.83
05-Mar-99 07:00	740.64	18.96	2.33	19.99	61.95	0.88	2.74	11.73
05-Mar-99 19:00	744.95	18.95	2.28	19.87	61.73	0.98	2.77	12.02
06-Mar-99 07:00	738.05	18.92	2.27	19.80	62.49	1.01	2.77	11.30
06-Mar-99 19:00	738.27	18.91	2.28	19.78	62.32	1.01	2.77	11.43
07-Mar-99 07:00	738.00	18.86	2.26	19.74	62.33	1.03	2.76	11.50
07-Mar-99 19:00	734.86	18.90	2.27	19.81	62.51	1.06	2.75	11.20
08-Mar-99 07:00	736.10	18.98	2.33	19.75	62.21	1.07	2.72	11.53
08-Mar-99 19:00	739.16	19.02	2.34	19.61	61.92	1.04	2.70	12.01
09-Mar-99 07:00	738.18	19.01	2.35	19.65	61.96	1.03	2.69	11.94
09-Mar-99 19:00	744.07	19.00	2.44	19.73	63.83	0.91	2.80	9.89
10-Mar-99 07:00	746.64	18.91	2.51	20.43	64.35	0.88	2.95	8.50
10-Mar-99 19:00	743.25	18.90	2.48	19.91	64.89	0.89	2.93	8.51
11-Mar-99 07:00	743.89	18.83	2.47	19.85	64.86	0.93	2.96	8.56
11-Mar-99 19:00	744.77	18.84	2.46	20.30	64.36	0.92	3.00	8.59
12-Mar-99 07:00	751.80	18.93	2.47	20.13	64.33	0.95	3.10	8.63
12-Mar-99 19:00	748.89	18.99	2.51	20.17	64.52	0.91	3.09	8.41
13-Mar-99 07:00	754.32	18.98	2.50	20.07	64.23	0.90	3.09	8.85
13-Mar-99 19:00	755.02	19.05	2.54	20.03	64.09	0.86	3.08	9.01
14-Mar-99 07:00	757.02	19.06	2.52	20.03	63.96	0.85	3.08	9.19
14-Mar-99 19:00	752.85	19.12	2.55	19.61	64.33	0.81	3.06	9.24
15-Mar-99 07:00	750.21	19.19	2.53	19.00	65.04	0.80	3.00	9.24
15-Mar-99 19:00	753.08	19.14	2.52	19.28	64.55	0.83	3.00	9.44
16-Mar-99 07:00	757.08	19.08	2.50	19.44	64.20	0.83	3.03	9.63
16-Mar-99 19:00	738.68	18.92	2.51	19.57	64.77	0.81	3.12	8.83
17-Mar-99 07:00	755.70	19.08	2.51	19.52	64.28	0.87	3.03	9.42
17-Mar-99 19:00	764.68	19.14	2.47	19.39	63.90	0.82	3.01	10.04
18-Mar-99 07:00	764.38	19.12	2.43	19.38	63.94	0.86	3.00	10.02
18-Mar-99 19:00	759.44	19.18	2.46	19.44	64.12	0.90	3.04	9.68
19-Mar-99 07:00	752.73	19.08	2.46	19.51	64.49	0.91	3.04	9.22
19-Mar-99 19:00	754.45	19.20	2.52	19.47	64.23	0.89	3.03	9.48
20-Mar-99 07:00	755.09	19.12	2.48	19.47	64.26	0.87	3.02	9.52
20-Mar-99 19:00	756.03	19.13	2.46	19.08	65.06	0.82	2.99	9.19
21-Mar-99 07:00	758.58	19.07	2.46	18.84	65.89	0.83	2.93	8.66
21-Mar-99 19:00	758.49	19.11	2.43	18.47	66.38	0.78	2.93	8.62





Date	V <sub>IN,SG</sub> k-sm <sup>3</sup> /hr	P <sub>IN,SG</sub> MPag	Y <sub>IN,NH3</sub> vol %	Y <sub>IN,N2</sub> vol %	Y <sub>IN,H2</sub> vol %	Y <sub>IN,HE</sub> vol %	Y <sub>IN,AR</sub> vol %	Y <sub>IN,CH4</sub> vol %
22-Mar-99 07:00	758.42	19.07	2.42	18.43	66.37	0.81	2.93	8.66
22-Mar-99 19:00	761.70	19.12	2.43	18.42	66.26	0.79	2.93	8.78
23-Mar-99 07:00	764.07	19.10	2.44	18.35	66.01	0.83	2.91	9.08
23-Mar-99 19:00	763.06	19.13	2.48	18.34	66.02	0.84	2.93	9.02
24-Mar-99 07:00	761.94	19.02	2.41	18.36	66.13	0.87	2.91	8.96
24-Mar-99 19:00	759.38	19.05	2.43	18.39	66.22	0.88	2.93	8.80
25-Mar-99 07:00	759.50	19.05	2.43	18.37	66.14	0.87	2.93	8.90
25-Mar-99 19:00	757.91	19.13	2.48	18.35	66.24	0.85	2.92	8.79
26-Mar-99 07:00	757.59	19.26	2.55	17.49	67.06	0.88	2.98	8.67
26-Mar-99 19:00	739.92	19.27	2.48	16.32	68.93	0.85	2.82	8.21
27-Mar-99 07:00	719.36	19.09	2.44	15.86	70.28	0.93	2.70	7.43
27-Mar-99 19:00	721.97	19.01	2.44	16.61	69.50	0.89	2.72	7.48
28-Mar-99 07:00	741.92	18.96	2.45	18.33	67.00	0.87	2.79	8.16
28-Mar-99 19:00	748.17	19.01	2.47	18.48	66.49	0.81	2.78	8.61
29-Mar-99 07:00	745.54	18.91	2.45	18.56	66.78	0.78	2.80	8.25
29-Mar-99 19:00	741.59	18.95	2.47	18.21	67.15	0.80	2.81	8.19
30-Mar-99 07:00	742.18	18.97	2.46	17.90	67.30	0.81	2.80	8.34
30-Mar-99 19:00	743.73	19.15	2.48	16.98	67.98	0.81	2.84	8.53
31-Mar-99 07:00	756.58	19.16	2.51	17.96	66.39	0.91	2.95	8.92
31-Mar-99 19:00	768.92	19.20	2.54	18.72	65.61	0.91	3.04	8.81
01-Jul-99 07:00	708.91	18.89	2.57	15.58	68.79	1.30	2.82	8.95
01-Jul-99 19:00	708.31	19.14	2.54	14.21	70.17	1.27	2.75	9.06
02-Jul-99 07:00	705.52	19.05	2.49	14.44	70.02	1.37	2.76	8.92
02-Jul-99 19:00	704.06	19.13	2.59	14.37	69.78	1.37	2.75	9.14
03-Jul-99 07:00	705.02	19.02	2.49	15.34	68.47	1.34	2.74	9.62
03-Jul-99 19:00	703.48	19.22	2.55	14.22	70.07	1.26	2.71	9.19
04-Jul-99 07:00	700.80	19.18	2.47	14.12	70.33	1.29	2.76	9.03
04-Jul-99 19:00	700.19	19.18	2.44	14.09	70.50	1.26	2.67	9.04
05-Jul-99 07:00	707.49	19.24	2.42	14.28	69.91	1.28	2.67	9.44
05-Jul-99 19:00	698.34	19.19	2.62	14.51	69.90	1.25	2.66	9.07
06-Jul-99 07:00	719.74	19.22	2.54	14.56	69.05	1.25	2.70	9.89
06-Jul-99 19:00	712.17	19.25	2.66	14.27	69.77	1.19	2.70	9.41
07-Jul-99 07:00	718.19	19.15	2.55	14.55	69.52	1.23	2.74	9.41
07-Jul-99 19:00	711.63	19.26	2.69	13.91	70.31	1.26	2.71	9.12
08-Jul-99 07:00	712.74	19.21	2.75	14.57	69.19	1.29	2.69	9.50
08-Jul-99 19:00	705.36	19.05	2.57	14.83	69.26	1.26	2.74	9.34
09-Jul-99 07:00	720.70	19.09	2.56	15.11	68.50	1.28	2.79	9.76
09-Jul-99 19:00	713.11	19.05	2.63	15.20	68.92	1.19	2.79	9.28
10-Jul-99 07:00	710.72	19.05	2.53	14.65	69.44	1.31	2.81	9.27
10-Jul-99 19:00	703.11	19.19	2.67	13.81	70.70	1.29	2.74	8.79
11-Jul-99 07:00	703.78	19.10	2.63	14.32	70.14	1.35	2.77	8.80
11-Jul-99 19:00	694.48	19.31	2.78	13.12	71.65	1.37	2.72	8.37
12-Jul-99 07:00	705.80	19.26	2.77	14.51	69.26	1.47	2.97	9.02
12-Jul-99 19:00	694.73	19.18	2.81	14.49	69.66	1.49	2.99	8.56
13-Jul-99 07:00	704.72	19.14	2.75	15.13	68.65	1.50	2.99	8.97
13-Jul-99 19:00	707.54	19.15	2.67	14.83	68.90	1.44	2.92	9.24
14-Jul-99 07:00	709.98	19.20	2.63	14.49	69.18	1.48	2.94	9.29
14-Jul-99 19:00	711.06	19.24	2.70	14.36	69.11	1.52	2.93	9.38
15-Jul-99 07:00	705.91	19.22	2.73	14.35	69.20	1.51	2.91	9.30
15-Jul-99 19:00	625.76	18.20	2.94	15.68	67.87	1.49	3.24	8.77
16-Jul-99 07:00	521.21	17.01	3.11	16.82	66.48	1.92	3.58	8.08
16-Jul-99 19:00	567.32	17.43	3.12	17.77	64.42	2.21	3.74	8.75
17-Jul-99 07:00	649.17	17.90	2.65	18.83	65.06	1.81	3.10	8.55
17-Jul-99 19:00	681.91	18.01	2.57	19.54	63.80	1.52	3.18	9.40





Date	V <sub>IN,SG</sub> k-sm <sup>3</sup> /hr	P <sub>IN,SG</sub> MPag	y <sub>IN,NH3</sub> vol %	y <sub>IN,N2</sub> vol %	y <sub>IN,H2</sub> vol %	y <sub>IN,HE</sub> vol %	y <sub>IN,AR</sub> vol %	y <sub>IN,CH4</sub> vol %
18-Jul-99 07:00	706.28	18.80	2.62	15.86	67.58	1.38	2.89	9.68
18-Jul-99 19:00	709.90	19.14	2.68	14.46	69.12	1.41	2.89	9.44
19-Jul-99 07:00	706.62	18.86	2.67	15.37	68.36	1.51	2.90	9.18
19-Jul-99 19:00	698.34	19.18	2.67	13.99	70.30	1.47	2.78	8.79
20-Jul-99 07:00	699.85	19.14	2.60	14.34	69.61	1.56	2.83	9.06
20-Jul-99 19:00	692.70	19.25	2.80	14.33	69.53	1.51	2.81	9.02
21-Jul-99 07:00	696.05	19.08	2.84	15.07	68.64	1.50	2.86	9.09
21-Jul-99 19:00	684.88	19.13	2.86	14.89	69.36	1.37	2.87	8.65
22-Jul-99 07:00	703.24	19.19	2.75	15.02	68.34	1.42	2.92	9.55
22-Jul-99 19:00	679.11	19.12	2.85	14.67	69.75	1.23	2.80	8.69
23-Jul-99 07:00	701.54	19.08	2.67	15.26	68.45	1.27	2.87	9.47
23-Jul-99 19:00	699.54	19.19	2.85	15.07	68.49	1.26	2.87	9.46
24-Jul-99 07:00	654.16	18.25	2.75	16.62	66.35	1.63	3.76	8.90
24-Jul-99 19:00	695.63	19.17	2.88	15.26	67.82	1.55	2.97	9.52
25-Jul-99 07:00	689.65	18.97	2.83	15.66	68.33	1.35	2.79	9.04
25-Jul-99 19:00	700.35	19.07	2.72	15.34	68.31	1.27	2.84	9.53
26-Jul-99 07:00	712.46	18.87	2.47	16.36	67.10	1.28	2.91	9.86
26-Jul-99 19:00	709.28	19.09	2.57	14.77	68.85	1.24	2.86	9.72
27-Jul-99 07:00	711.78	19.15	2.53	14.53	68.95	1.36	2.86	9.77
27-Jul-99 19:00	699.34	19.21	2.73	14.29	69.35	1.39	2.81	9.43
28-Jul-99 07:00	702.68	19.15	2.66	15.17	68.13	1.37	2.75	9.90
28-Jul-99 19:00	688.71	19.19	2.89	14.40	69.38	1.29	2.67	9.36
29-Jul-99 07:00	686.12	19.05	2.81	15.08	68.94	1.28	2.65	9.23
29-Jul-99 19:00	678.29	19.23	2.89	14.18	70.05	1.20	2.55	9.14
30-Jul-99 07:00	690.95	19.16	2.61	14.71	69.43	1.16	2.55	9.54
30-Jul-99 19:00	697.05	19.21	2.52	14.31	69.73	1.10	2.58	9.76
31-Jul-99 07:00	706.24	19.11	2.40	14.76	69.07	1.13	2.61	10.02
31-Jul-99 19:00	705.65	19.28	2.43	13.90	70.47	1.11	2.60	9.50



**Table A-1**      **Plant Data (cont'd)**

Date	T <sub>IN,SG</sub> °C	T <sub>G/G,SHELL</sub> °C	T <sub>G/G,TUBE</sub> °C	T <sub>G/G,BY</sub> °C	T <sub>TRIPH,BY</sub> °C	T <sub>TRIPH,BY</sub> °C	T <sub>TRIPH,SHELL</sub> °C	T <sub>TRIPH,SHELL</sub> °C
01-Feb-99 07:00	28.75	286.81	55.72	286.29	381.41	386.11	405.36	416.20
01-Feb-99 19:00	28.39	286.90	55.45	286.49	380.26	386.99	405.54	416.41
02-Feb-99 07:00	26.77	286.78	54.14	286.25	380.23	385.92	404.95	415.90
02-Feb-99 19:00	26.86	286.69	54.13	286.10	380.66	385.33	404.86	415.99
03-Feb-99 07:00	27.13	286.80	54.37	286.28	381.92	386.02	405.19	416.40
03-Feb-99 19:00	25.97	286.68	53.60	286.47	380.35	387.40	404.85	416.17
04-Feb-99 07:00	23.71	286.13	51.39	285.86	380.66	386.23	404.85	415.99
04-Feb-99 19:00	26.65	286.58	54.02	286.34	381.74	386.31	405.26	416.41
05-Feb-99 07:00	27.54	286.83	54.43	286.45	381.17	386.00	405.59	416.33
05-Feb-99 19:00	24.69	286.28	52.22	286.28	381.04	387.55	405.04	416.35
06-Feb-99 07:00	25.15	286.49	52.88	285.98	381.45	386.29	405.08	416.21
06-Feb-99 19:00	28.52	286.90	55.84	286.40	381.67	386.38	405.47	416.59
07-Feb-99 07:00	27.76	286.58	54.83	286.11	381.65	385.59	405.33	416.14
07-Feb-99 19:00	29.43	286.97	56.35	286.68	380.84	384.95	404.76	415.59
08-Feb-99 07:00	27.56	286.90	54.80	286.60	380.41	385.20	404.94	415.80
08-Feb-99 19:00	26.73	286.51	54.18	286.42	379.34	387.07	404.53	415.64
09-Feb-99 07:00	25.56	286.46	52.96	286.26	380.44	385.38	404.78	415.83
09-Feb-99 19:00	27.40	286.73	54.87	286.40	381.15	385.30	404.97	415.58
10-Feb-99 07:00	28.67	286.77	55.96	286.46	381.04	384.64	405.02	415.62
10-Feb-99 19:00	26.09	286.66	53.68	286.45	380.06	386.66	404.44	415.52
11-Feb-99 07:00	26.03	286.27	54.17	286.47	379.42	385.78	404.35	415.26
11-Feb-99 19:00	26.16	286.54	54.19	286.45	378.59	386.12	404.45	414.96
12-Feb-99 07:00	24.99	286.44	53.15	286.46	379.38	385.54	404.16	414.93
12-Feb-99 19:00	26.34	286.43	53.96	286.42	379.75	383.48	403.91	414.53
13-Feb-99 07:00	28.05	286.80	55.68	286.50	380.02	384.62	404.27	415.06
13-Feb-99 19:00	28.89	286.85	56.44	286.49	379.74	384.14	404.44	415.09
14-Feb-99 07:00	28.85	286.98	56.41	286.44	379.21	384.57	404.12	415.17
14-Feb-99 19:00	27.43	286.85	55.16	286.25	379.67	385.01	404.08	415.26
15-Feb-99 07:00	26.75	286.69	54.54	286.08	380.60	384.97	404.36	415.78
15-Feb-99 19:00	25.80	286.73	53.59	286.31	380.02	384.34	403.47	415.03
16-Feb-99 07:00	26.80	286.84	54.56	286.43	380.57	385.00	404.24	415.36
16-Feb-99 19:00	27.28	286.95	55.07	286.60	380.24	384.75	403.88	415.23
17-Feb-99 07:00	25.73	286.56	53.65	286.29	380.32	384.71	404.01	415.15
17-Feb-99 19:00	27.48	286.54	55.12	286.40	380.39	384.75	404.17	415.15
18-Feb-99 07:00	26.83	286.62	54.44	286.35	379.99	384.04	403.97	414.85
18-Feb-99 19:00	28.01	286.68	55.52	286.56	379.82	384.25	403.82	414.74
19-Feb-99 07:00	28.74	286.73	56.28	286.41	380.21	384.55	404.25	415.01
19-Feb-99 19:00	29.72	287.00	57.05	286.69	380.16	384.17	404.13	415.06
20-Feb-99 07:00	29.79	287.23	57.22	286.73	379.75	384.43	404.46	415.21
20-Feb-99 19:00	29.70	287.31	57.30	286.78	379.24	383.83	403.61	414.24
21-Feb-99 07:00	29.08	287.02	56.50	286.51	379.57	384.13	403.65	414.76
21-Feb-99 19:00	28.85	286.97	56.09	286.45	380.29	384.79	404.09	415.05
22-Feb-99 07:00	30.08	287.33	57.47	286.88	380.43	385.25	404.06	415.31
22-Feb-99 19:00	28.32	286.81	55.82	286.52	380.23	384.69	404.16	415.34
23-Feb-99 07:00	28.01	286.81	55.37	286.38	380.53	384.61	404.19	415.14
26-Feb-99 19:00	28.45	282.45	55.44	282.04	377.25	378.73	401.95	413.35
27-Feb-99 07:00	27.27	282.64	54.39	282.55	376.94	377.67	401.67	412.99
27-Feb-99 19:00	27.14	282.52	54.38	282.39	376.75	377.13	401.47	412.09
28-Feb-99 07:00	26.52	282.53	53.80	282.26	377.60	378.72	402.56	413.10
28-Feb-99 19:00	27.89	282.23	55.01	281.98	377.06	378.19	401.88	412.09
01-Mar-99 07:00	26.76	282.07	53.91	281.89	376.93	377.44	401.44	412.00
01-Mar-99 19:00	26.66	282.08	53.85	281.97	377.02	377.00	401.08	411.79



Date	T <sub>IN,SG</sub> °C	T <sub>G/G,SHELL</sub> °C	T <sub>G/G,TUBE</sub> °C	T <sub>G/G,BY</sub> °C	T <sub>RIPH,BY</sub> °C	T <sub>RIPH,BY</sub> °C	T <sub>RIPH,SHELL</sub> °C	T <sub>RIPH,SHELL</sub> °C
02-Mar-99 07:00	25.38	281.73	52.57	281.85	376.56	377.55	401.66	412.05
02-Mar-99 19:00	25.23	281.35	52.46	281.28	376.56	376.86	401.07	411.42
03-Mar-99 07:00	25.48	281.62	52.55	281.50	376.84	376.24	400.87	411.21
03-Mar-99 19:00	27.33	281.77	54.33	281.49	376.92	376.36	401.13	411.62
04-Mar-99 07:00	28.65	282.02	55.44	281.61	376.60	376.50	400.98	412.00
04-Mar-99 19:00	29.81	282.42	56.78	281.99	376.03	376.05	400.66	411.88
05-Mar-99 07:00	28.07	282.13	55.39	281.74	376.16	376.16	400.76	412.10
05-Mar-99 19:00	27.08	281.97	54.28	281.57	375.77	375.77	400.55	411.16
06-Mar-99 07:00	27.37	282.20	54.33	281.75	376.96	376.99	401.76	412.18
06-Mar-99 19:00	27.28	281.85	54.11	281.48	376.48	377.65	401.81	411.92
07-Mar-99 07:00	26.45	281.37	53.42	281.23	375.53	376.87	401.40	411.78
07-Mar-99 19:00	27.93	281.35	54.82	281.33	377.24	377.16	401.40	412.11
08-Mar-99 07:00	29.41	281.76	56.07	281.57	376.65	376.23	400.58	411.51
08-Mar-99 19:00	29.22	282.35	56.27	281.79	376.19	376.06	400.37	411.22
09-Mar-99 07:00	29.35	281.72	56.24	281.57	375.88	376.10	400.72	410.78
09-Mar-99 19:00	28.25	281.39	55.32	281.36	376.01	376.72	400.84	411.17
10-Mar-99 07:00	28.64	281.07	55.52	281.00	377.08	377.10	401.79	412.29
10-Mar-99 19:00	28.36	281.00	55.16	280.98	376.98	377.37	401.64	412.00
11-Mar-99 07:00	27.09	281.04	54.14	280.99	376.52	376.82	401.57	411.81
11-Mar-99 19:00	27.02	281.08	54.37	281.13	376.57	376.83	401.59	411.84
12-Mar-99 07:00	27.59	281.71	54.73	281.17	376.80	377.25	401.79	412.14
12-Mar-99 19:00	29.88	281.68	56.79	281.38	376.73	377.96	401.85	412.21
13-Mar-99 07:00	28.30	281.53	55.26	281.22	376.48	376.59	401.32	411.35
13-Mar-99 19:00	29.66	282.01	56.56	281.37	376.02	376.69	400.95	411.38
14-Mar-99 07:00	29.16	281.83	56.29	281.42	375.80	376.49	401.12	411.03
14-Mar-99 19:00	30.52	282.04	57.31	281.50	375.25	377.07	400.86	410.89
15-Mar-99 07:00	30.37	282.05	57.17	281.50	375.70	377.03	400.76	410.60
15-Mar-99 19:00	29.62	284.81	56.75	284.47	376.51	379.27	402.97	413.38
16-Mar-99 07:00	28.25	284.99	55.78	284.52	377.94	379.26	403.11	413.40
16-Mar-99 19:00	29.57	284.79	56.46	284.29	379.64	380.15	402.72	413.78
17-Mar-99 07:00	28.76	284.79	56.12	284.66	377.73	379.68	403.32	413.77
17-Mar-99 19:00	27.43	285.09	54.93	284.70	375.27	378.91	402.26	412.79
18-Mar-99 07:00	26.13	284.75	53.77	284.28	376.99	378.38	402.72	412.71
18-Mar-99 19:00	27.89	284.35	55.37	283.75	377.87	379.38	402.79	413.15
19-Mar-99 07:00	27.63	284.37	54.96	284.07	378.50	380.25	403.84	414.15
19-Mar-99 19:00	29.66	284.66	56.80	284.26	377.28	380.53	403.37	413.85
20-Mar-99 07:00	27.97	284.58	55.27	284.38	377.14	380.08	403.17	414.19
20-Mar-99 19:00	28.08	284.68	55.34	284.34	377.27	380.14	403.34	413.87
21-Mar-99 07:00	27.74	284.78	55.21	284.30	378.41	379.98	403.63	414.32
21-Mar-99 19:00	27.61	284.73	55.01	284.42	378.49	380.14	403.08	414.10
22-Mar-99 07:00	26.61	284.52	54.18	284.08	378.53	380.04	403.23	413.97
22-Mar-99 19:00	27.49	284.73	55.02	284.32	378.20	379.61	402.68	413.43
23-Mar-99 07:00	26.99	284.95	54.60	284.56	377.62	379.18	402.61	412.87
23-Mar-99 19:00	28.31	285.30	55.90	284.97	378.20	379.74	402.43	413.18
24-Mar-99 07:00	26.43	285.18	54.18	284.85	378.09	379.69	403.00	413.25
24-Mar-99 19:00	27.74	285.14	55.27	284.72	378.35	380.03	402.93	413.47
25-Mar-99 07:00	27.71	285.16	55.16	284.69	378.22	379.23	403.17	413.45
25-Mar-99 19:00	29.71	285.39	57.00	284.72	378.14	379.60	403.07	413.44
26-Mar-99 07:00	30.24	285.89	57.45	285.28	378.20	379.56	403.35	413.33
26-Mar-99 19:00	30.33	285.38	57.34	284.86	378.90	380.01	402.68	413.21
27-Mar-99 07:00	30.17	284.90	56.74	284.46	378.95	381.33	403.96	414.27
27-Mar-99 19:00	30.39	285.14	56.95	284.57	378.83	381.38	404.52	414.98
28-Mar-99 07:00	29.06	285.20	56.14	284.60	379.26	381.61	404.57	414.59
28-Mar-99 19:00	29.34	285.28	56.55	284.72	378.42	381.30	403.93	414.27





Date	T <sub>IN,SG</sub> °C	T <sub>G/G,SHELL</sub> °C	T <sub>G/G,TUBE</sub> °C	T <sub>G/G,BY</sub> °C	T <sub>TRIPH,BY</sub> °C	T <sub>TRIPH,BY</sub> °C	T <sub>TRIPH,SHELL</sub> °C	T <sub>TRIPH,SHELL</sub> °C
29-Mar-99 07:00	28.54	284.93	55.77	284.33	379.15	381.92	404.14	414.27
29-Mar-99 19:00	29.78	285.24	56.77	284.55	379.40	381.43	404.10	414.75
30-Mar-99 07:00	29.54	285.25	56.57	284.64	379.37	381.41	404.08	414.49
30-Mar-99 19:00	30.08	285.35	57.12	284.84	378.43	381.05	403.46	413.64
31-Mar-99 07:00	29.79	285.53	57.06	284.93	378.44	379.59	402.83	413.29
31-Mar-99 19:00	29.78	285.65	57.16	285.01	378.66	379.96	403.46	413.85
01-Jul-99 07:00	34.49	290.05	61.17	289.35	382.52	386.30	405.25	416.86
01-Jul-99 19:00	34.78	290.35	61.45	289.43	381.17	385.05	404.78	415.44
02-Jul-99 07:00	34.65	290.16	61.12	289.27	382.22	386.14	405.94	416.50
02-Jul-99 19:00	35.39	290.25	61.91	289.31	381.38	384.93	404.31	415.38
03-Jul-99 07:00	34.52	289.73	61.23	289.04	381.79	384.85	405.14	415.86
03-Jul-99 19:00	35.19	290.14	61.67	289.20	380.98	385.02	405.04	415.07
04-Jul-99 07:00	34.39	289.83	60.93	289.02	381.77	385.55	406.21	416.04
04-Jul-99 19:00	34.21	289.96	60.73	289.08	381.59	386.02	405.81	416.15
05-Jul-99 07:00	34.19	289.90	60.80	289.11	381.58	385.67	405.96	416.13
05-Jul-99 19:00	36.17	289.92	62.50	289.10	379.56	386.07	405.31	415.78
06-Jul-99 07:00	34.64	290.06	61.51	289.42	379.32	384.76	404.66	414.96
06-Jul-99 19:00	35.26	290.16	62.03	289.36	379.72	385.43	404.03	414.42
07-Jul-99 07:00	34.09	290.10	60.94	289.49	381.03	384.82	404.63	415.74
07-Jul-99 19:00	34.95	290.29	61.60	289.44	380.43	384.35	403.72	413.93
08-Jul-99 07:00	35.53	290.30	62.25	289.45	379.77	383.90	403.24	413.68
08-Jul-99 19:00	35.14	289.88	61.72	289.06	380.39	385.16	404.96	415.34
09-Jul-99 07:00	34.99	290.16	61.84	289.22	380.47	384.40	404.51	414.92
09-Jul-99 19:00	35.77	290.33	62.47	289.52	380.81	385.98	404.57	415.64
10-Jul-99 07:00	35.00	290.06	61.56	289.25	381.35	386.22	405.90	415.92
10-Jul-99 19:00	35.94	290.41	62.34	289.23	379.95	385.63	404.15	414.48
11-Jul-99 07:00	35.50	290.01	61.96	289.06	381.25	386.20	405.25	415.56
11-Jul-99 19:00	36.90	290.31	63.12	289.12	378.99	383.99	402.88	413.02
12-Jul-99 07:00	37.05	290.35	63.47	289.32	380.30	384.66	404.54	414.67
12-Jul-99 19:00	37.51	290.18	63.69	289.24	380.88	385.51	404.49	415.05
13-Jul-99 07:00	36.89	290.08	63.20	289.14	381.74	385.26	404.77	415.79
13-Jul-99 19:00	36.41	290.02	62.66	289.26	380.81	385.38	404.58	415.53
14-Jul-99 07:00	35.81	290.17	62.30	289.13	380.10	385.55	404.98	415.55
14-Jul-99 19:00	36.08	290.44	62.69	289.19	380.59	384.29	403.35	414.66
15-Jul-99 07:00	36.55	290.15	62.92	289.12	380.80	384.32	403.39	414.77
15-Jul-99 19:00	33.01	290.74	58.85	289.88	381.36	384.61	402.38	413.73
16-Jul-99 07:00	25.59	291.07	50.66	290.69	381.27	385.17	400.23	411.41
16-Jul-99 19:00	26.86	291.95	52.99	291.69	381.28	386.13	401.46	412.61
17-Jul-99 07:00	31.19	289.16	57.55	288.52	382.07	386.36	404.75	415.62
17-Jul-99 19:00	33.65	288.29	60.04	287.27	381.58	385.53	403.74	415.02
18-Jul-99 07:00	35.35	289.55	61.92	288.53	381.55	384.23	403.94	415.05
18-Jul-99 19:00	36.33	289.86	62.77	288.96	379.89	383.08	403.25	413.92
19-Jul-99 07:00	35.89	289.91	62.24	289.10	381.17	384.97	405.00	415.37
19-Jul-99 19:00	36.01	290.17	62.39	289.06	380.10	385.14	404.08	414.28
20-Jul-99 07:00	35.40	290.19	61.79	289.11	381.59	385.56	405.62	415.86
20-Jul-99 19:00	37.20	290.55	63.46	289.18	379.87	384.28	403.80	414.33
21-Jul-99 07:00	36.28	289.71	62.67	288.53	380.48	384.50	404.11	414.73
21-Jul-99 19:00	37.33	289.90	63.37	288.74	380.41	385.14	404.37	415.15
22-Jul-99 07:00	36.46	290.05	62.96	288.85	380.46	384.17	404.20	414.71
22-Jul-99 19:00	37.70	289.81	63.78	288.55	380.25	384.18	404.28	414.96
23-Jul-99 07:00	36.05	289.71	62.48	288.47	380.55	384.81	404.71	415.39
23-Jul-99 19:00	37.18	290.05	63.65	288.87	379.36	383.54	403.72	414.00
24-Jul-99 07:00	34.96	288.19	60.90	286.99	379.82	383.38	401.85	412.97
24-Jul-99 19:00	37.97	289.60	64.19	288.54	379.91	383.01	402.74	413.56





Date	T <sub>IN,SG</sub> °C	T <sub>G/G,SHELL</sub> °C	T <sub>G/G,TUBE</sub> °C	T <sub>G/G,BY</sub> °C	T <sub>RIPH,BY</sub> °C	T <sub>RIPH,BY</sub> °C	T <sub>RIPH,SHELL</sub> °C	T <sub>RIPH,SHELL</sub> °C
25-Jul-99 07:00	37.27	289.43	63.48	288.43	380.54	384.54	404.81	416.09
25-Jul-99 19:00	36.69	289.76	62.96	288.81	378.90	384.96	404.75	415.42
26-Jul-99 07:00	34.38	289.31	60.99	288.51	380.17	386.14	406.37	417.12
26-Jul-99 19:00	34.80	289.79	61.48	288.91	379.44	385.29	404.90	415.54
27-Jul-99 07:00	34.52	289.92	61.17	288.91	380.64	384.92	405.12	415.67
27-Jul-99 19:00	36.37	289.96	62.65	288.89	379.26	384.20	403.78	414.27
28-Jul-99 07:00	36.01	289.83	62.51	288.72	380.81	384.51	405.33	415.72
28-Jul-99 19:00	37.74	289.84	63.91	288.82	378.78	383.52	402.95	413.16
29-Jul-99 07:00	37.16	289.63	63.39	288.43	381.18	384.75	404.91	415.34
29-Jul-99 19:00	38.06	289.98	64.15	288.71	379.31	384.10	403.60	414.02
30-Jul-99 07:00	36.12	289.62	62.26	288.83	380.92	385.75	405.87	416.72
30-Jul-99 19:00	35.20	289.64	61.51	288.92	379.81	386.05	405.77	416.40
31-Jul-99 07:00	34.10	289.41	60.64	288.69	379.88	385.50	405.81	416.90
31-Jul-99 19:00	34.38	289.64	60.95	288.98	380.01	385.53	405.90	416.60



**Table A-1**      **Plant Data (cont'd)**

Date	T <sub>RIB1</sub> °C	T <sub>RIB1</sub> °C	T <sub>RIB1</sub> °C	T <sub>RIB1</sub> °C	T <sub>RIB2</sub> °C	T <sub>WHB1,TUBE</sub> °C	T <sub>WHB1,BY</sub> °C	T <sub>R2</sub> °C	T <sub>WHB2,TUBE</sub> °C
01-Feb-99 07:00	509.15	519.23	516.92	520.97	469.08	345.92	400.78	444.43	324.42
01-Feb-99 19:00	509.42	519.71	517.18	521.11	469.08	345.91	400.78	444.39	324.47
02-Feb-99 07:00	507.84	518.20	516.01	519.99	467.91	345.69	400.21	443.50	324.55
02-Feb-99 19:00	508.81	518.80	516.49	520.29	468.78	345.78	400.53	444.06	324.48
03-Feb-99 07:00	509.74	519.15	516.64	519.89	469.28	345.85	400.93	444.45	324.53
03-Feb-99 19:00	508.66	518.83	516.45	520.59	468.45	345.95	400.99	444.25	324.46
04-Feb-99 07:00	509.27	519.37	516.66	521.03	468.55	345.50	401.07	444.28	324.13
04-Feb-99 19:00	510.70	519.86	517.36	521.07	469.90	345.77	401.93	445.35	324.37
05-Feb-99 07:00	509.83	519.51	517.31	520.77	469.63	345.91	401.39	444.86	324.61
05-Feb-99 19:00	509.87	519.29	517.15	520.94	468.78	345.70	401.22	444.34	324.44
06-Feb-99 07:00	510.02	519.48	516.96	520.63	469.60	345.81	401.57	445.03	324.43
06-Feb-99 19:00	510.11	519.95	517.72	521.82	469.75	345.92	401.34	445.03	324.54
07-Feb-99 07:00	508.84	519.16	516.39	520.49	468.76	345.43	400.69	444.15	324.29
07-Feb-99 19:00	507.27	518.20	515.18	520.05	467.23	345.51	399.73	442.72	324.43
08-Feb-99 07:00	507.57	517.98	515.37	519.74	467.55	345.68	400.32	443.30	324.62
08-Feb-99 19:00	507.42	517.86	515.33	519.62	467.35	345.50	400.21	443.30	324.36
09-Feb-99 07:00	507.88	518.08	514.97	518.91	467.96	345.55	400.50	443.79	324.44
09-Feb-99 19:00	507.56	517.99	515.21	519.58	467.89	345.77	400.53	443.62	324.56
10-Feb-99 07:00	507.96	517.68	514.81	518.71	468.06	345.51	400.59	443.74	324.37
10-Feb-99 19:00	506.90	517.82	514.71	518.99	467.00	345.52	399.92	443.09	324.42
11-Feb-99 07:00	506.34	517.06	513.99	518.48	466.28	345.16	399.75	442.36	324.14
11-Feb-99 19:00	505.94	516.55	513.89	518.25	466.17	345.22	399.61	442.38	324.43
12-Feb-99 07:00	505.58	516.19	513.33	517.68	466.19	345.40	399.72	442.42	324.46
12-Feb-99 19:00	504.88	515.33	511.54	516.17	465.83	345.20	399.76	442.14	324.32
13-Feb-99 07:00	505.29	516.48	513.24	518.06	466.49	345.55	399.89	442.45	324.41
13-Feb-99 19:00	505.36	516.63	513.37	518.33	466.48	345.50	399.45	442.37	324.59
14-Feb-99 07:00	504.78	516.38	513.07	517.60	466.36	345.56	399.32	442.47	324.58
14-Feb-99 19:00	505.25	516.28	513.02	517.12	466.20	345.49	399.39	442.41	324.63
15-Feb-99 07:00	506.48	517.11	513.78	517.76	466.89	345.61	399.75	442.80	324.57
15-Feb-99 19:00	505.13	516.11	512.17	516.55	466.58	345.65	399.52	442.64	324.62
16-Feb-99 07:00	505.90	516.96	513.12	517.41	467.31	345.65	399.91	443.22	324.58
16-Feb-99 19:00	505.59	516.70	512.85	517.23	467.12	345.73	400.06	443.13	324.72
17-Feb-99 07:00	505.73	516.53	512.81	517.28	466.61	345.33	399.99	442.81	324.42
17-Feb-99 19:00	506.27	516.87	513.37	517.80	467.08	345.25	400.31	442.96	324.24
18-Feb-99 07:00	505.16	516.13	512.19	516.73	466.06	345.26	399.87	442.40	324.31
18-Feb-99 19:00	504.74	515.63	511.73	516.26	466.05	345.18	399.70	442.32	324.26
19-Feb-99 07:00	505.66	516.38	512.70	517.17	466.78	345.35	400.08	442.79	324.26
19-Feb-99 19:00	505.22	516.13	512.21	516.52	466.71	345.22	399.90	442.71	324.34
20-Feb-99 07:00	504.27	515.65	512.22	516.21	466.16	345.48	399.40	442.32	324.80
20-Feb-99 19:00	502.47	514.45	510.48	515.06	465.03	345.54	398.82	441.58	324.77
21-Feb-99 07:00	503.54	515.33	511.55	516.54	465.51	345.45	398.89	441.68	324.56
21-Feb-99 19:00	505.42	516.63	512.92	517.36	466.80	345.24	399.92	442.92	324.32
22-Feb-99 07:00	505.07	516.50	512.67	517.21	466.92	345.57	399.75	443.17	324.63
22-Feb-99 19:00	505.36	516.77	512.77	517.03	466.66	345.49	399.67	442.68	324.59
23-Feb-99 07:00	505.58	516.88	513.13	517.28	466.43	345.44	399.90	442.69	324.43
26-Feb-99 19:00	505.95	517.75	514.34	518.93	465.72	344.88	398.83	443.57	319.58
27-Feb-99 07:00	503.93	516.49	512.25	517.68	464.53	345.17	398.62	442.61	320.10
27-Feb-99 19:00	502.74	515.10	510.72	516.16	463.53	345.17	398.32	442.12	319.97
28-Feb-99 07:00	504.24	516.86	512.38	517.01	465.25	345.75	399.23	443.38	320.22
28-Feb-99 19:00	503.19	515.71	511.27	516.68	464.40	344.73	398.16	442.79	319.52
01-Mar-99 07:00	503.15	515.23	510.84	515.99	463.80	344.74	398.21	442.42	319.60
01-Mar-99 19:00	502.71	514.76	510.05	515.33	463.33	344.76	398.18	442.11	319.49



Date	T <sub>RI1</sub> °C	T <sub>RI1</sub> °C	T <sub>RI1</sub> °C	T <sub>RI1</sub> °C	T <sub>RI2</sub> °C	T <sub>WH1,TUBE</sub> °C	T <sub>WH1,BY</sub> °C	T <sub>R2</sub> °C	T <sub>WH1,TUBE</sub> °C
02-Mar-99 07:00	503.21	515.41	511.31	516.60	463.43	344.66	398.51	442.24	319.27
02-Mar-99 19:00	503.07	514.78	510.10	515.49	463.37	344.26	397.91	441.88	319.00
03-Mar-99 07:00	502.06	514.10	508.98	514.45	463.22	344.01	397.86	442.01	319.02
03-Mar-99 19:00	502.74	514.92	510.30	515.67	463.73	344.36	398.24	442.51	318.90
04-Mar-99 07:00	502.01	515.20	510.40	515.94	463.73	344.41	398.04	442.41	319.06
04-Mar-99 19:00	500.57	514.24	508.98	514.95	463.11	344.68	397.57	442.03	319.31
05-Mar-99 07:00	501.00	514.69	509.73	515.30	463.33	344.72	397.87	442.28	319.25
05-Mar-99 19:00	500.47	513.54	508.15	513.92	462.23	344.56	397.57	441.59	319.28
06-Mar-99 07:00	502.90	515.45	510.48	515.62	464.31	345.10	398.75	443.01	319.38
06-Mar-99 19:00	502.32	514.88	510.72	515.55	463.71	344.73	398.20	442.58	319.05
07-Mar-99 07:00	502.04	514.58	510.92	515.53	463.14	344.20	397.90	441.77	318.84
07-Mar-99 19:00	503.87	515.83	510.91	515.85	463.76	344.30	398.40	442.32	318.60
08-Mar-99 07:00	501.93	514.45	508.87	514.34	463.04	344.17	397.93	442.11	318.81
08-Mar-99 19:00	500.26	513.18	507.59	512.94	462.31	344.51	397.62	441.89	319.07
09-Mar-99 07:00	499.71	512.72	507.10	512.45	461.78	343.95	397.63	441.54	318.68
09-Mar-99 19:00	501.33	513.81	509.01	514.17	462.81	343.92	398.46	442.05	318.60
10-Mar-99 07:00	504.32	516.03	511.69	516.48	464.93	344.01	399.33	443.72	318.23
10-Mar-99 19:00	504.21	515.97	511.41	516.42	464.36	344.05	399.20	443.43	318.35
11-Mar-99 07:00	503.66	515.73	510.93	515.90	464.23	344.00	399.15	443.25	318.32
11-Mar-99 19:00	503.85	515.66	511.38	515.72	464.39	344.01	398.94	443.22	318.38
12-Mar-99 07:00	503.45	515.56	510.67	515.41	464.38	344.67	399.27	443.46	318.96
12-Mar-99 19:00	504.01	515.67	511.07	516.08	464.70	344.37	399.51	443.76	318.53
13-Mar-99 07:00	502.25	514.48	509.45	514.86	463.46	344.37	398.87	442.97	318.99
13-Mar-99 19:00	501.64	514.10	508.96	514.37	463.19	344.54	398.62	442.90	319.19
14-Mar-99 07:00	500.25	513.49	508.24	513.57	462.62	344.29	398.19	442.35	318.90
14-Mar-99 19:00	500.03	513.40	508.63	514.16	462.09	344.37	397.54	441.72	318.88
15-Mar-99 07:00	499.26	512.54	507.57	513.92	461.81	344.27	397.44	441.45	319.18
15-Mar-99 19:00	502.35	514.94	510.92	515.94	464.39	344.59	398.87	442.87	322.12
16-Mar-99 07:00	502.21	514.59	509.92	514.55	464.49	344.57	398.96	442.80	322.54
16-Mar-99 19:00	505.08	516.47	511.73	516.68	465.30	344.14	399.20	443.16	321.95
17-Mar-99 07:00	503.20	515.74	511.34	516.29	464.73	344.41	399.31	442.83	322.41
17-Mar-99 19:00	500.29	513.59	509.06	514.21	463.15	344.68	398.33	441.74	322.71
18-Mar-99 07:00	500.32	513.35	508.60	513.77	463.57	344.47	398.43	441.85	322.43
18-Mar-99 19:00	502.83	514.94	510.92	515.75	464.55	343.92	398.86	442.48	321.86
19-Mar-99 07:00	504.51	516.69	512.87	517.20	466.33	344.35	399.65	443.77	322.10
19-Mar-99 19:00	503.87	515.95	512.38	517.40	465.39	344.33	399.18	443.11	322.09
20-Mar-99 07:00	503.54	516.26	512.56	517.03	465.13	344.21	398.99	442.99	322.15
20-Mar-99 19:00	503.81	515.72	512.34	516.82	465.13	344.29	399.13	443.15	322.23
21-Mar-99 07:00	504.00	515.84	511.88	515.90	466.02	344.69	399.60	443.62	322.45
21-Mar-99 19:00	503.94	516.06	511.79	516.03	465.69	344.53	399.63	443.54	322.41
22-Mar-99 07:00	503.47	515.75	511.54	515.80	465.61	344.33	399.50	443.50	322.26
22-Mar-99 19:00	503.05	514.70	510.15	514.69	464.83	344.41	399.01	443.10	322.24
23-Mar-99 07:00	500.87	513.76	508.47	513.45	463.72	344.57	398.64	442.42	322.64
23-Mar-99 19:00	501.52	514.03	508.78	513.79	464.15	344.97	399.05	442.79	323.04
24-Mar-99 07:00	501.87	514.45	509.55	514.58	464.37	345.10	399.40	442.77	323.00
24-Mar-99 19:00	502.96	515.15	510.32	515.25	464.72	344.99	399.63	443.34	322.88
25-Mar-99 07:00	502.46	515.06	510.33	515.36	464.58	345.09	399.59	443.13	322.94
25-Mar-99 19:00	503.02	515.07	510.12	515.28	464.90	345.03	399.77	443.31	322.99
26-Mar-99 07:00	501.36	514.35	508.94	513.72	464.46	345.30	399.51	443.22	323.27
26-Mar-99 19:00	502.20	514.87	509.61	514.65	464.40	344.71	398.87	442.77	322.74
27-Mar-99 07:00	505.85	518.59	514.22	519.34	466.53	344.57	399.61	443.57	322.20
27-Mar-99 19:00	507.33	519.22	515.60	519.89	467.54	344.80	400.23	444.53	322.29
28-Mar-99 07:00	506.36	517.87	514.56	518.83	467.36	345.32	400.56	444.73	322.72
28-Mar-99 19:00	504.78	516.57	513.00	517.35	466.20	345.18	399.98	444.09	322.81





Date	T <sub>R1B1</sub> °C	T <sub>R1B1</sub> °C	T <sub>R1B1</sub> °C	T <sub>R1B1</sub> °C	T <sub>R1B2</sub> °C	T <sub>WHB1,TUBE</sub> °C	T <sub>WHB1,BY</sub> °C	T <sub>R2</sub> °C	T <sub>WHB2,TUBE</sub> °C
29-Mar-99 07:00	505.56	517.49	513.62	518.63	466.76	345.17	400.19	444.19	322.52
29-Mar-99 19:00	506.21	517.72	514.26	518.28	467.13	345.12	400.24	444.61	322.63
30-Mar-99 07:00	505.27	517.38	513.42	517.91	466.59	345.01	400.17	444.18	322.67
30-Mar-99 19:00	502.87	515.64	511.11	515.72	464.64	344.85	398.92	442.96	322.78
31-Mar-99 07:00	502.39	514.70	509.56	514.32	464.63	345.18	399.27	442.91	322.84
31-Mar-99 19:00	503.39	515.11	510.24	514.77	465.47	345.38	399.78	443.55	323.11
01-Jul-99 07:00	506.62	518.25	513.52	517.65	468.59	345.58	398.49	442.47	327.35
01-Jul-99 19:00	502.38	516.04	510.68	515.12	466.42	345.39	397.37	440.59	327.47
02-Jul-99 07:00	504.44	518.07	512.81	516.80	467.70	345.38	397.89	441.21	327.40
02-Jul-99 19:00	502.84	516.26	510.26	514.77	466.09	345.11	397.01	440.36	327.45
03-Jul-99 07:00	506.12	517.72	512.07	516.56	467.87	345.15	397.96	441.45	327.15
03-Jul-99 19:00	503.60	516.77	510.45	515.51	466.61	345.15	397.20	440.54	327.25
04-Jul-99 07:00	505.67	518.24	512.20	516.92	467.62	345.30	397.87	440.92	327.05
04-Jul-99 19:00	505.58	518.17	513.26	517.46	467.55	345.18	397.72	440.88	327.18
05-Jul-99 07:00	504.56	518.14	512.50	517.15	466.86	345.35	397.66	440.32	327.28
05-Jul-99 19:00	504.47	517.99	511.98	516.66	467.18	345.07	397.16	441.06	327.00
06-Jul-99 07:00	500.56	514.68	509.37	514.48	465.26	345.07	396.59	439.91	327.60
06-Jul-99 19:00	499.58	514.38	508.65	513.40	464.47	345.03	396.30	439.66	327.39
07-Jul-99 07:00	502.16	515.95	509.94	514.41	466.13	345.35	397.26	440.35	327.68
07-Jul-99 19:00	499.01	513.82	506.77	512.16	464.51	345.03	396.42	439.72	327.56
08-Jul-99 07:00	498.63	513.28	506.51	512.38	464.34	344.91	396.21	439.71	327.21
08-Jul-99 19:00	503.69	516.60	511.58	516.51	466.62	345.05	397.14	440.62	327.25
09-Jul-99 07:00	501.25	514.68	508.94	513.67	465.33	345.24	396.93	439.91	327.42
09-Jul-99 19:00	502.70	516.10	510.61	514.90	466.24	345.35	396.99	440.85	327.37
10-Jul-99 07:00	503.95	516.80	512.51	516.54	467.00	345.31	397.81	441.02	327.48
10-Jul-99 19:00	500.20	514.67	509.40	514.71	465.13	345.24	396.36	439.74	327.21
11-Jul-99 07:00	502.76	516.92	511.94	517.09	466.59	345.33	397.38	440.56	327.28
11-Jul-99 19:00	496.52	512.71	506.09	511.98	463.26	344.69	395.06	438.36	327.08
12-Jul-99 07:00	500.58	514.93	508.31	513.39	465.65	344.99	396.36	440.07	327.14
12-Jul-99 19:00	503.20	516.51	510.69	515.05	466.75	344.99	396.91	441.13	326.83
13-Jul-99 07:00	503.96	516.92	510.62	514.92	467.38	345.29	397.09	441.43	327.17
13-Jul-99 19:00	502.64	516.19	510.80	515.07	466.31	345.03	396.97	440.53	327.22
14-Jul-99 07:00	502.29	515.99	511.26	515.46	466.40	345.11	397.13	440.65	327.29
14-Jul-99 19:00	500.27	514.30	508.12	512.42	464.95	345.07	396.08	439.70	327.33
15-Jul-99 07:00	500.12	514.97	508.16	513.02	464.88	344.87	396.02	439.45	327.02
15-Jul-99 19:00	503.15	514.41	509.45	512.90	464.97	341.85	394.48	438.67	327.42
16-Jul-99 07:00	504.15	512.58	510.78	513.35	464.30	337.89	392.21	436.34	328.02
16-Jul-99 19:00	504.18	512.79	510.42	513.41	465.02	339.01	392.90	437.23	329.23
17-Jul-99 07:00	509.07	518.35	516.27	518.66	469.24	342.92	397.19	442.31	326.64
17-Jul-99 19:00	507.30	517.66	514.14	517.28	467.75	343.76	396.93	441.89	325.55
18-Jul-99 07:00	503.40	516.17	510.13	514.75	465.97	344.48	396.68	440.38	326.67
18-Jul-99 19:00	499.69	514.36	506.94	512.04	464.64	344.29	396.03	439.37	326.66
19-Jul-99 07:00	503.42	516.72	511.33	515.81	466.89	344.91	397.52	441.36	326.94
19-Jul-99 19:00	501.50	515.34	509.54	515.26	465.62	344.67	396.70	440.42	327.29
20-Jul-99 07:00	504.00	517.34	512.07	516.53	467.43	344.97	397.97	441.43	327.31
20-Jul-99 19:00	500.75	514.99	508.68	513.55	465.39	344.87	396.53	440.45	327.20
21-Jul-99 07:00	501.66	516.05	509.63	514.88	466.21	344.76	396.72	440.88	326.72
21-Jul-99 19:00	504.30	517.02	511.22	515.56	467.41	344.43	397.12	441.70	326.57
22-Jul-99 07:00	501.76	515.83	509.31	514.08	466.01	344.72	396.68	440.70	326.81
22-Jul-99 19:00	503.71	516.82	510.48	515.94	467.09	344.21	396.53	441.37	326.05
23-Jul-99 07:00	503.36	516.90	511.33	516.50	466.99	344.67	397.19	441.31	326.81
23-Jul-99 19:00	500.58	514.70	508.21	513.32	465.33	344.66	396.22	440.46	326.93
24-Jul-99 07:00	503.69	515.61	509.76	513.65	464.91	342.95	395.35	439.73	324.90
24-Jul-99 19:00	500.79	514.53	506.71	511.89	465.13	343.90	395.93	440.34	326.45





Date	T <sub>R1B1</sub> °C	T <sub>R1B1</sub> °C	T <sub>R1B1</sub> °C	T <sub>R1B1</sub> °C	T <sub>R1B2</sub> °C	T <sub>WHB1,TUBE</sub> °C	T <sub>WHB1,BY</sub> °C	T <sub>R2</sub> °C	T <sub>WHBII,TUBE</sub> °C
25-Jul-99 07:00	504.85	517.32	512.37	516.33	467.87	344.25	397.12	442.16	326.19
25-Jul-99 19:00	504.07	517.51	511.49	516.45	467.39	344.68	397.11	441.54	326.63
26-Jul-99 07:00	508.20	519.58	515.69	519.47	469.30	344.76	398.71	442.89	326.74
26-Jul-99 19:00	503.04	516.71	511.78	516.36	466.43	344.80	396.99	440.90	327.19
27-Jul-99 07:00	502.82	516.41	511.50	515.96	466.58	344.84	397.51	440.90	327.21
27-Jul-99 19:00	500.23	514.57	508.96	514.04	464.80	344.36	396.30	439.95	326.64
28-Jul-99 07:00	503.79	517.16	511.27	515.59	467.01	344.83	397.33	441.13	326.83
28-Jul-99 19:00	499.07	513.63	506.47	511.63	463.83	344.06	395.47	439.59	326.52
29-Jul-99 07:00	503.77	517.19	511.27	515.33	467.24	344.46	397.05	441.50	326.53
29-Jul-99 19:00	501.11	515.30	508.44	513.90	465.61	344.21	396.55	440.90	326.49
30-Jul-99 07:00	506.60	519.35	514.05	517.89	468.65	344.26	398.57	442.63	326.66
30-Jul-99 19:00	506.25	519.10	513.47	517.98	468.01	344.42	398.41	442.14	326.62
31-Jul-99 07:00	506.89	519.33	514.25	518.97	468.37	344.44	398.88	442.43	326.79
31-Jul-99 19:00	505.89	519.15	513.77	518.01	467.75	344.43	398.38	441.87	326.84



**Table A-1**      **Plant Data (cont'd)**

Date	M <sub>NH3,RECV,1</sub> tonne/hr	M <sub>NH3,RECV,2</sub> m <sup>3</sup> /hr	HV <sub>G/G,SHELL</sub> %	HV <sub>RIPH,TUBE</sub> %	HV <sub>WHBI,TUBE</sub> %	HV <sub>WHBI,STEAM</sub> %	L <sub>WHBI</sub> %	LV <sub>WHBI</sub> %
01-Feb-99 07:00	76.71	1.70	0.00	0.00	84.00	5.00	61.03	75.35
01-Feb-99 19:00	76.72	1.55	0.00	0.00	84.00	5.00	60.96	74.81
02-Feb-99 07:00	76.73	1.76	0.00	0.00	84.00	5.00	61.02	74.64
02-Feb-99 19:00	76.72	1.74	0.00	0.00	84.00	5.00	60.99	74.96
03-Feb-99 07:00	76.74	1.65	0.00	0.00	84.00	5.00	61.13	74.64
03-Feb-99 19:00	76.76	1.81	0.00	0.00	84.00	5.00	60.98	72.64
04-Feb-99 07:00	76.22	1.87	0.00	0.00	84.00	5.00	61.00	73.77
04-Feb-99 19:00	76.86	1.73	0.00	0.00	85.53	5.00	61.01	75.89
05-Feb-99 07:00	77.05	1.42	0.00	0.00	87.00	5.00	61.05	75.22
05-Feb-99 19:00	77.05	1.71	0.00	0.00	87.00	5.00	61.02	74.80
06-Feb-99 07:00	77.08	1.72	0.00	0.00	87.00	5.00	61.25	74.61
06-Feb-99 19:00	76.94	1.87	0.00	0.00	87.00	5.00	60.97	75.24
07-Feb-99 07:00	76.89	1.95	0.00	0.00	87.00	5.00	61.09	74.77
07-Feb-99 19:00	76.77	1.68	0.00	0.00	87.00	5.00	61.01	75.54
08-Feb-99 07:00	76.80	1.70	0.00	0.00	87.00	5.00	61.06	75.67
08-Feb-99 19:00	76.58	1.94	0.00	0.00	87.00	5.00	61.04	74.67
09-Feb-99 07:00	76.90	1.75	0.00	0.00	87.00	5.00	60.98	74.89
09-Feb-99 19:00	76.93	1.63	0.00	0.00	87.00	5.00	60.98	75.66
10-Feb-99 07:00	76.75	1.77	0.00	0.00	87.00	5.00	61.06	75.73
10-Feb-99 19:00	76.57	1.36	0.00	0.00	87.00	5.00	61.05	74.16
11-Feb-99 07:00	76.52	1.49	0.00	0.00	87.00	5.00	60.96	74.37
11-Feb-99 19:00	76.67	1.83	0.00	0.00	87.00	5.00	60.94	74.62
12-Feb-99 07:00	76.91	1.68	0.00	0.00	87.00	5.00	60.99	74.43
12-Feb-99 19:00	76.97	1.90	0.00	0.00	87.00	5.00	61.01	75.14
13-Feb-99 07:00	76.85	1.77	0.00	0.00	87.00	5.00	61.03	75.76
13-Feb-99 19:00	76.49	1.82	0.00	0.00	87.00	5.00	60.99	75.60
14-Feb-99 07:00	76.45	1.88	0.00	0.00	87.00	5.00	61.07	75.12
14-Feb-99 19:00	76.43	1.57	0.00	0.00	87.00	5.00	61.01	75.26
15-Feb-99 07:00	76.43	1.88	0.00	0.00	87.00	5.00	61.04	75.12
15-Feb-99 19:00	76.62	1.79	0.00	0.00	87.00	5.00	60.96	74.98
16-Feb-99 07:00	76.61	1.77	0.00	0.00	87.00	5.00	61.02	75.35
16-Feb-99 19:00	76.68	1.73	0.00	0.00	87.00	5.00	61.02	75.18
17-Feb-99 07:00	76.53	1.75	0.00	0.00	87.00	5.00	61.01	74.67
17-Feb-99 19:00	76.66	1.70	0.00	0.00	87.00	5.00	60.90	75.10
18-Feb-99 07:00	76.58	1.43	0.00	0.00	87.00	5.00	61.06	75.16
18-Feb-99 19:00	76.47	1.74	0.00	0.00	87.00	5.00	61.07	74.89
19-Feb-99 07:00	76.55	1.02	0.00	0.00	87.00	5.00	61.01	75.17
19-Feb-99 19:00	76.58	1.17	0.00	0.00	87.00	5.00	61.00	75.39
20-Feb-99 07:00	76.72	1.92	0.00	0.00	87.00	5.00	61.00	75.74
20-Feb-99 19:00	76.59	2.22	0.00	0.00	87.00	5.00	61.04	75.46
21-Feb-99 07:00	76.37	1.70	0.00	0.00	87.00	5.00	61.02	75.03
21-Feb-99 19:00	76.64	2.11	0.00	0.00	87.00	5.00	61.02	75.59
22-Feb-99 07:00	76.61	1.46	0.00	0.00	87.00	5.00	61.03	76.09
22-Feb-99 19:00	76.58	1.23	0.00	0.00	87.00	5.00	61.08	75.65
23-Feb-99 07:00	76.23	2.40	0.00	0.00	87.00	5.00	61.07	74.82
26-Feb-99 19:00	75.67	1.48	0.00	0.00	86.00	5.00	61.35	73.97
27-Feb-99 07:00	77.21	1.48	0.00	0.00	86.00	5.00	60.00	75.32
27-Feb-99 19:00	77.24	2.12	0.00	0.00	87.99	5.00	60.04	75.26
28-Feb-99 07:00	77.46	1.56	0.00	0.00	88.00	5.00	59.99	74.90
28-Feb-99 19:00	77.45	2.17	0.00	0.00	88.00	5.00	59.99	76.10
01-Mar-99 07:00	77.50	2.03	0.00	0.00	88.00	5.00	60.02	77.31
01-Mar-99 19:00	77.48	2.30	0.00	0.00	88.00	5.00	60.06	77.11



Date	M <sub>NH3,RECVR,1</sub> tonne/hr	M <sub>NH3,RECVR,2</sub> m <sup>3</sup> /hr	HV <sub>G/G,SHELL</sub> %	HV <sub>RIPH,TUBE</sub> %	HV <sub>WHBI,TUBE</sub> %	HV <sub>WHBI,STEAM</sub> %	L <sub>WHBI</sub> %	LV <sub>WHBI</sub> %
02-Mar-99 07:00	77.60	1.93	0.00	0.00	88.00	5.00	60.06	76.31
02-Mar-99 19:00	77.67	1.48	0.00	0.00	88.00	5.00	60.03	75.40
03-Mar-99 07:00	77.64	1.87	0.00	0.00	88.00	5.00	60.05	75.62
03-Mar-99 19:00	77.52	1.86	0.00	0.00	88.00	5.00	60.07	75.87
04-Mar-99 07:00	77.47	1.46	0.00	0.00	88.00	5.00	60.05	75.77
04-Mar-99 19:00	77.50	2.17	0.00	0.00	88.00	5.00	60.01	76.05
05-Mar-99 07:00	77.52	1.67	0.00	0.00	88.00	5.00	60.04	76.03
05-Mar-99 19:00	77.55	1.72	0.00	0.00	88.00	5.00	59.97	76.15
06-Mar-99 07:00	77.72	2.05	0.00	0.00	88.00	5.00	60.04	76.54
06-Mar-99 19:00	77.58	2.49	0.00	0.00	89.81	5.00	60.07	76.58
07-Mar-99 07:00	77.68	1.54	0.00	0.00	90.00	5.00	60.02	76.05
07-Mar-99 19:00	77.62	2.19	0.00	0.00	90.00	5.00	60.04	76.42
08-Mar-99 07:00	77.25	1.09	0.00	0.00	91.81	5.00	60.05	76.56
08-Mar-99 19:00	77.12	2.37	0.00	0.00	94.00	5.00	60.05	76.55
09-Mar-99 07:00	77.14	1.76	0.00	0.00	94.00	5.00	60.00	76.49
09-Mar-99 19:00	77.26	2.17	0.00	0.00	94.00	5.00	60.02	76.60
10-Mar-99 07:00	77.51	2.31	0.00	0.00	94.00	5.00	60.07	76.89
10-Mar-99 19:00	77.52	1.70	0.00	0.00	94.00	5.00	60.03	76.97
11-Mar-99 07:00	77.57	1.79	0.00	0.00	94.00	5.00	60.05	76.57
11-Mar-99 19:00	77.12	1.55	0.00	0.00	94.00	5.00	61.46	76.01
12-Mar-99 07:00	77.59	2.22	0.00	0.00	94.00	5.00	62.98	75.91
12-Mar-99 19:00	77.56	1.61	0.00	0.00	94.00	5.00	62.98	77.12
13-Mar-99 07:00	77.64	1.33	0.00	0.00	94.00	5.00	62.01	77.01
13-Mar-99 19:00	77.45	1.10	0.00	0.00	94.00	5.00	61.98	77.14
14-Mar-99 07:00	77.47	2.09	0.00	0.00	94.00	5.00	62.00	77.05
14-Mar-99 19:00	77.19	1.96	0.00	0.00	94.00	5.00	61.99	77.25
15-Mar-99 07:00	77.33	2.20	0.00	0.00	94.00	5.00	62.02	77.52
15-Mar-99 19:00	77.16	1.57	0.00	0.00	94.00	5.00	62.06	76.34
16-Mar-99 07:00	77.25	2.12	0.00	0.00	94.00	5.00	62.00	76.34
16-Mar-99 19:00	76.09	1.84	0.00	0.00	94.00	5.00	62.02	75.05
17-Mar-99 07:00	77.30	2.32	0.00	0.00	94.00	5.00	61.98	76.39
17-Mar-99 19:00	77.27	2.31	0.00	0.00	94.00	5.00	62.00	76.42
18-Mar-99 07:00	77.27	1.93	0.00	0.00	94.00	5.00	62.08	75.88
18-Mar-99 19:00	77.28	2.05	0.00	0.00	94.00	5.00	61.99	75.33
19-Mar-99 07:00	77.33	2.22	0.00	0.00	94.00	5.00	62.00	75.95
19-Mar-99 19:00	77.11	2.23	0.00	0.00	94.00	5.00	62.01	75.88
20-Mar-99 07:00	77.25	1.31	0.00	0.00	94.00	5.00	62.04	75.50
20-Mar-99 19:00	77.27	1.81	0.00	0.00	94.00	5.00	61.99	76.14
21-Mar-99 07:00	77.33	1.86	0.00	0.00	94.00	5.00	62.04	76.34
21-Mar-99 19:00	77.39	2.36	0.00	0.00	94.00	5.00	61.98	76.39
22-Mar-99 07:00	77.51	2.12	0.00	0.00	94.00	5.00	62.05	75.99
22-Mar-99 19:00	77.47	2.24	0.00	0.00	94.00	5.00	62.01	76.39
23-Mar-99 07:00	77.36	2.20	0.00	0.00	94.00	5.00	61.96	76.72
23-Mar-99 19:00	77.26	1.84	0.00	0.00	94.00	5.00	61.95	78.01
24-Mar-99 07:00	77.45	1.61	0.00	0.00	94.00	5.00	62.02	77.49
24-Mar-99 19:00	77.34	1.91	0.00	0.00	94.00	5.00	61.97	77.63
25-Mar-99 07:00	77.36	1.63	0.00	0.00	94.00	5.00	62.02	77.59
25-Mar-99 19:00	77.31	1.82	0.00	0.00	94.00	5.00	61.98	78.41
26-Mar-99 07:00	77.38	1.33	0.00	0.00	94.00	5.00	62.08	76.68
26-Mar-99 19:00	77.04	2.20	0.00	0.00	94.00	5.00	61.98	76.53
27-Mar-99 07:00	76.99	2.21	0.00	0.00	94.00	5.00	62.03	77.62
27-Mar-99 19:00	76.97	1.42	0.00	0.00	94.00	5.00	61.98	78.38
28-Mar-99 07:00	77.18	1.49	0.00	0.00	94.00	5.00	62.00	78.97
28-Mar-99 19:00	77.05	1.99	0.00	0.00	94.00	5.00	61.98	78.99





Date	M <sub>NH3,RECVR,1</sub> tonne/hr	M <sub>NH3,RECVR,2</sub> m <sup>3</sup> /hr	HV <sub>G/G,SHELL</sub> %	HV <sub>RIPIH,TUBE</sub> %	HV <sub>WHBI,TUBE</sub> %	HV <sub>WHBI,STEAM</sub> %	L <sub>WHBI</sub> %	LV <sub>WHBI</sub> %
29-Mar-99 07:00	77.26	1.84	0.00	0.00	94.00	5.00	62.07	78.55
29-Mar-99 19:00	77.12	2.29	0.00	0.00	94.00	5.00	62.00	78.96
30-Mar-99 07:00	77.26	2.42	0.00	0.00	94.00	5.00	61.96	78.94
30-Mar-99 19:00	77.12	2.25	0.00	0.00	94.00	5.00	62.07	79.01
31-Mar-99 07:00	77.19	1.85	0.00	0.00	94.00	5.00	61.96	78.67
31-Mar-99 19:00	77.73	2.03	0.00	0.00	94.00	5.00	61.98	80.17
01-Jul-99 07:00	75.26	2.07	0.00	0.00	88.00	5.00	62.92	74.85
01-Jul-99 19:00	75.21	2.11	0.00	0.00	88.00	5.00	63.04	75.01
02-Jul-99 07:00	75.48	2.05	0.00	0.00	88.00	5.00	63.00	74.92
02-Jul-99 19:00	74.58	2.14	0.00	0.00	88.00	5.00	63.08	73.99
03-Jul-99 07:00	74.51	2.02	0.00	0.00	88.00	5.00	62.99	73.50
03-Jul-99 19:00	74.50	2.13	0.00	0.00	88.00	5.00	63.04	74.04
04-Jul-99 07:00	74.92	2.02	0.00	0.00	88.00	5.00	62.90	74.14
04-Jul-99 19:00	75.01	2.02	0.00	0.00	88.00	5.00	63.05	74.70
05-Jul-99 07:00	75.29	2.02	0.00	0.00	88.00	5.00	63.03	74.90
05-Jul-99 19:00	74.24	2.20	0.00	0.00	88.00	5.00	63.02	73.87
06-Jul-99 07:00	75.57	2.12	0.00	0.00	88.00	5.00	62.97	75.28
06-Jul-99 19:00	74.87	2.23	0.00	0.00	88.00	5.00	63.08	74.63
07-Jul-99 07:00	75.98	2.12	0.00	0.00	88.00	5.00	62.87	76.01
07-Jul-99 19:00	75.03	2.25	0.00	0.00	88.00	5.00	63.16	75.12
08-Jul-99 07:00	74.58	2.27	0.00	0.00	88.00	5.00	63.02	74.17
08-Jul-99 19:00	74.68	2.10	0.00	0.00	88.00	5.00	63.01	74.33
09-Jul-99 07:00	75.34	2.10	0.00	0.00	88.00	5.00	63.00	75.29
09-Jul-99 19:00	74.87	2.15	0.00	0.00	88.00	5.00	63.04	74.65
10-Jul-99 07:00	75.58	2.07	0.00	0.00	88.00	5.00	62.98	75.58
10-Jul-99 19:00	74.53	2.22	0.00	0.00	88.00	5.00	63.09	74.37
11-Jul-99 07:00	75.00	2.15	0.00	0.00	88.00	5.00	62.93	74.63
11-Jul-99 19:00	73.39	2.30	0.00	0.00	88.00	5.00	63.15	72.90
12-Jul-99 07:00	73.71	2.19	0.00	0.00	88.00	5.00	62.94	72.78
12-Jul-99 19:00	72.92	2.21	0.00	0.00	88.00	5.00	63.09	72.46
13-Jul-99 07:00	73.79	2.16	0.00	0.00	88.00	5.00	62.93	73.36
13-Jul-99 19:00	74.20	2.14	0.00	0.00	88.00	5.00	63.07	74.24
14-Jul-99 07:00	74.69	2.10	0.00	0.00	88.00	5.00	62.92	74.61
14-Jul-99 19:00	74.04	2.16	0.00	0.00	88.00	5.00	63.12	74.30
15-Jul-99 07:00	73.88	2.18	0.00	0.00	88.00	5.00	62.96	73.47
15-Jul-99 19:00	63.91	1.72	0.00	0.00	88.00	5.00	64.30	63.79
16-Jul-99 07:00	51.34	1.01	0.00	0.00	88.01	5.00	64.93	52.95
16-Jul-99 19:00	53.98	1.03	0.00	0.00	88.42	5.00	64.85	56.73
17-Jul-99 07:00	66.10	1.55	0.00	0.00	89.00	5.00	64.88	67.29
17-Jul-99 19:00	69.59	1.72	0.00	0.00	89.00	5.00	62.85	68.64
18-Jul-99 07:00	73.49	2.06	0.00	0.00	89.00	5.00	62.02	73.69
18-Jul-99 19:00	73.84	2.16	0.00	0.00	89.00	5.00	62.02	74.37
19-Jul-99 07:00	74.19	2.10	0.00	0.00	89.00	5.00	61.96	74.68
19-Jul-99 19:00	73.68	2.19	0.00	0.00	89.42	5.00	62.12	74.27
20-Jul-99 07:00	74.03	2.10	0.00	0.00	90.00	5.00	61.98	74.22
20-Jul-99 19:00	72.12	2.25	0.00	0.00	90.00	5.00	62.11	71.49
21-Jul-99 07:00	72.33	2.26	0.00	0.00	90.00	5.00	63.54	71.53
21-Jul-99 19:00	71.46	2.23	0.00	0.00	90.00	5.00	67.93	70.89
22-Jul-99 07:00	72.77	2.17	0.00	0.00	90.00	5.00	67.92	71.55
22-Jul-99 19:00	71.11	2.25	0.00	0.00	90.00	5.00	68.04	70.63
23-Jul-99 07:00	73.10	2.13	0.00	0.00	90.00	5.00	67.90	72.52
23-Jul-99 19:00	71.87	2.27	0.00	0.00	90.00	5.00	68.09	71.29
24-Jul-99 07:00	66.51	1.71	0.00	0.00	90.00	5.00	68.06	65.54
24-Jul-99 19:00	70.91	2.30	0.00	0.00	90.00	5.00	67.11	70.14





Date	M <sub>NH3,RECVR,1</sub> tonne/hr	M <sub>NH3,RECVR,2</sub> m <sup>3</sup> /hr	HV <sub>G/G,SHELL</sub> %	HV <sub>R1PH,TUBE</sub> %	HV <sub>WHBI,TUBE</sub> %	HV <sub>WHBII,STEAM</sub> %	L <sub>WHBII</sub> %	LV <sub>WHBII</sub> %
25-Jul-99 07:00	72.03	2.25	0.00	0.00	90.00	5.00	66.91	71.56
25-Jul-99 19:00	73.01	2.19	0.00	0.00	90.00	5.00	66.98	72.71
26-Jul-99 07:00	74.63	1.94	0.00	0.00	90.00	5.00	66.89	74.53
26-Jul-99 19:00	74.10	2.09	0.00	0.00	90.00	5.00	67.04	74.35
27-Jul-99 07:00	74.58	2.05	0.00	0.00	90.00	5.00	66.90	74.71
27-Jul-99 19:00	72.71	2.23	0.00	0.00	90.00	5.00	64.44	73.10
28-Jul-99 07:00	73.11	2.17	0.00	0.00	90.00	5.00	62.96	73.01
28-Jul-99 19:00	71.26	2.37	0.00	0.00	90.00	5.00	63.13	71.25
29-Jul-99 07:00	71.82	2.28	0.00	0.00	90.00	5.00	62.94	71.29
29-Jul-99 19:00	70.80	2.40	0.00	0.00	91.68	5.00	63.09	70.71
30-Jul-99 07:00	72.91	2.20	0.00	0.00	92.00	5.00	62.92	72.75
30-Jul-99 19:00	73.62	2.14	0.00	0.00	92.00	5.00	63.03	73.56
31-Jul-99 07:00	74.88	2.01	0.00	0.00	92.00	5.00	62.88	74.65
31-Jul-99 19:00	75.07	2.08	0.00	0.00	92.00	5.00	63.05	75.89



**Table A-1      Plant Data (*cont'd*)**

Date	M <sub>WHBII,BFW</sub> tonne/hr	M <sub>WHB,STEAM</sub> tonne/hr	P <sub>WHB,STEAM</sub> MPag	P <sub>STEAM</sub> MPag	T <sub>IN,WHBII,BFW</sub> °C
01-Feb-99 07:00	109.92	103.63	12.17	10.89	181.58
01-Feb-99 07:00	109.92	103.63	12.17	10.89	181.58
01-Feb-99 19:00	109.42	103.19	12.18	10.90	181.52
02-Feb-99 07:00	109.13	102.88	12.17	10.90	181.72
02-Feb-99 19:00	109.50	103.34	12.15	10.87	181.71
03-Feb-99 07:00	109.65	103.29	12.17	10.91	181.63
03-Feb-99 19:00	109.09	102.40	12.23	10.98	181.66
04-Feb-99 07:00	108.04	101.57	12.22	10.98	181.69
04-Feb-99 19:00	109.61	102.92	12.24	10.98	181.45
05-Feb-99 07:00	110.16	103.65	12.23	10.94	181.71
05-Feb-99 19:00	109.65	103.02	12.21	10.93	181.38
06-Feb-99 07:00	110.07	103.27	12.22	10.95	181.64
06-Feb-99 19:00	110.16	103.68	12.19	10.90	181.64
07-Feb-99 07:00	110.06	103.73	12.14	10.87	181.47
07-Feb-99 19:00	109.48	103.30	12.17	10.92	181.40
08-Feb-99 07:00	109.49	102.85	12.23	10.96	181.29
08-Feb-99 19:00	109.03	102.60	12.18	10.93	181.37
09-Feb-99 07:00	109.70	103.08	12.21	10.95	181.55
09-Feb-99 19:00	110.05	103.50	12.19	10.92	181.40
10-Feb-99 07:00	110.03	103.42	12.19	10.90	181.19
10-Feb-99 19:00	108.50	102.20	12.16	10.90	181.55
11-Feb-99 07:00	108.52	102.14	12.18	10.92	181.36
11-Feb-99 19:00	108.92	102.55	12.15	10.90	181.61
12-Feb-99 07:00	109.28	102.83	12.17	10.92	181.66
12-Feb-99 19:00	109.82	103.32	12.17	10.90	181.36
13-Feb-99 07:00	109.88	103.42	12.17	10.90	181.34
13-Feb-99 19:00	109.38	103.19	12.15	10.88	181.37
14-Feb-99 07:00	109.02	102.83	12.15	10.89	181.38
14-Feb-99 19:00	109.14	102.82	12.15	10.89	181.59
15-Feb-99 07:00	109.37	102.92	12.17	10.91	181.48
15-Feb-99 19:00	109.32	102.83	12.16	10.90	181.59
16-Feb-99 07:00	109.40	102.93	12.17	10.91	181.55
16-Feb-99 19:00	109.43	102.90	12.18	10.92	181.63
17-Feb-99 07:00	109.13	102.55	12.18	10.93	181.51
17-Feb-99 19:00	109.42	102.90	12.16	10.90	181.35
18-Feb-99 07:00	109.17	102.74	12.17	10.91	181.45
18-Feb-99 19:00	109.12	102.68	12.17	10.92	181.42
19-Feb-99 07:00	109.45	102.98	12.16	10.91	181.40
19-Feb-99 19:00	109.63	103.19	12.15	10.89	181.47
20-Feb-99 07:00	109.88	103.36	12.16	10.89	181.64
20-Feb-99 19:00	109.60	103.22	12.13	10.89	181.68
21-Feb-99 07:00	109.18	102.82	12.14	10.87	181.63
21-Feb-99 19:00	109.71	103.30	12.13	10.87	181.55
22-Feb-99 07:00	109.71	103.19	12.16	10.88	181.67
22-Feb-99 19:00	109.42	102.93	12.16	10.89	181.52
23-Feb-99 07:00	108.86	102.46	12.17	10.92	181.57
26-Feb-99 19:00	108.99	102.53	12.08	10.84	182.02
27-Feb-99 07:00	110.58	103.49	12.16	10.88	181.44
27-Feb-99 19:00	111.03	103.67	12.19	10.94	181.24
28-Feb-99 07:00	111.62	103.99	12.22	10.95	181.56
28-Feb-99 19:00	111.80	104.82	12.11	0.00	181.25



Date	M <sub>WHBIL,BFW</sub> tonne/hr	M <sub>WHB,STEAM</sub> tonne/hr	P <sub>WHB,STEAM</sub> MPag	P <sub>STEAM</sub> MPag	T <sub>IN,WHBIL,BFW</sub> °C
01-Mar-99 07:00	111.63	104.50	12.13	10.85	181.33
01-Mar-99 19:00	111.50	104.25	12.15	10.88	181.14
02-Mar-99 07:00	111.58	104.24	12.18	10.92	181.07
02-Mar-99 19:00	111.70	104.79	12.09	10.81	181.27
03-Mar-99 07:00	111.66	104.87	12.06	10.79	181.39
03-Mar-99 19:00	111.56	104.73	12.07	10.80	181.36
04-Mar-99 07:00	111.36	104.76	12.05	10.78	181.50
04-Mar-99 19:00	111.36	104.72	12.05	10.76	181.70
05-Mar-99 07:00	111.30	104.56	12.07	10.80	181.69
05-Mar-99 19:00	111.49	104.68	12.07	10.78	181.73
06-Mar-99 07:00	112.17	104.79	12.16	10.90	181.75
06-Mar-99 19:00	112.03	104.81	12.12	10.86	181.55
07-Mar-99 07:00	111.86	104.83	12.09	10.80	181.56
07-Mar-99 19:00	112.14	105.23	12.07	10.79	181.33
08-Mar-99 07:00	111.78	104.87	12.06	10.78	181.34
08-Mar-99 19:00	111.81	104.85	12.06	10.78	181.73
09-Mar-99 07:00	111.93	105.00	12.04	10.78	181.37
09-Mar-99 19:00	112.06	105.11	12.05	10.78	181.29
10-Mar-99 07:00	112.63	105.66	12.04	10.76	181.20
10-Mar-99 19:00	112.63	105.67	12.03	10.77	181.24
11-Mar-99 07:00	112.51	105.45	12.05	10.78	181.31
11-Mar-99 19:00	111.76	104.82	12.05	10.77	181.44
12-Mar-99 07:00	112.54	105.11	12.12	10.85	181.54
12-Mar-99 19:00	112.97	105.72	12.09	10.83	181.23
13-Mar-99 07:00	112.79	105.55	12.08	10.80	181.40
13-Mar-99 19:00	112.65	105.42	12.08	10.80	181.57
14-Mar-99 07:00	112.61	105.51	12.06	10.77	181.47
14-Mar-99 19:00	112.26	105.43	12.03	10.75	181.63
15-Mar-99 07:00	112.79	105.76	12.03	10.76	182.27
15-Mar-99 19:00	111.47	104.68	12.06	10.81	182.26
16-Mar-99 07:00	111.65	104.91	12.04	10.78	182.34
16-Mar-99 19:00	110.08	103.75	12.01	10.77	182.40
17-Mar-99 07:00	111.36	104.65	12.04	10.77	182.17
17-Mar-99 19:00	110.95	104.17	12.06	10.82	182.20
18-Mar-99 07:00	111.36	104.69	12.02	10.77	182.32
18-Mar-99 19:00	111.83	105.79	11.91	10.65	182.27
19-Mar-99 07:00	112.00	105.54	11.98	10.72	182.40
19-Mar-99 19:00	111.59	105.27	11.98	10.71	182.41
20-Mar-99 07:00	111.17	104.89	11.98	10.70	182.53
20-Mar-99 19:00	111.74	105.17	12.00	10.74	182.40
21-Mar-99 07:00	111.96	105.22	12.02	10.76	182.39
21-Mar-99 19:00	111.99	105.31	12.03	10.75	182.22
22-Mar-99 07:00	112.05	105.42	12.01	10.73	182.20
22-Mar-99 19:00	112.25	105.55	12.01	10.73	182.22
23-Mar-99 07:00	111.80	104.82	12.05	10.80	182.29
23-Mar-99 19:00	111.82	104.49	12.12	10.86	182.23
24-Mar-99 07:00	111.66	104.27	12.14	10.88	182.32
24-Mar-99 19:00	111.83	104.59	12.12	10.86	182.27
25-Mar-99 07:00	111.84	104.61	12.12	10.86	182.23
25-Mar-99 19:00	112.16	104.92	12.12	10.84	182.24
26-Mar-99 07:00	112.53	104.92	12.17	10.92	182.51
26-Mar-99 19:00	112.06	104.99	12.09	10.86	182.50
27-Mar-99 07:00	111.24	104.72	12.04	10.80	182.49



Date	M <sub>WHBIL,BFW</sub> tonne/hr	M <sub>WHB,STEAM</sub> tonne/hr	P <sub>WHB,STEAM</sub> MPag	P <sub>STEAM</sub> MPag	T <sub>IN,WHBIL,BFW</sub> °C
27-Mar-99 19:00	111.45	104.70	12.07	10.80	182.36
28-Mar-99 07:00	112.04	104.76	12.13	10.89	182.42
28-Mar-99 19:00	111.81	104.60	12.13	10.87	182.39
29-Mar-99 07:00	112.14	105.09	12.10	10.84	182.54
29-Mar-99 19:00	112.26	105.10	12.10	10.85	182.55
30-Mar-99 07:00	112.27	105.10	12.10	10.84	182.48
30-Mar-99 19:00	112.19	105.09	12.08	10.81	182.46
31-Mar-99 07:00	112.13	104.85	12.10	10.84	182.51
31-Mar-99 19:00	113.24	105.65	12.13	10.87	182.50
01-Jul-99 07:00	107.88	101.67	12.13	10.88	183.31
01-Jul-99 19:00	107.81	101.85	12.08	10.86	183.57
02-Jul-99 07:00	108.03	101.97	12.10	10.86	183.37
02-Jul-99 19:00	106.86	101.10	12.06	10.88	183.64
03-Jul-99 07:00	106.82	100.72	12.08	10.85	183.40
03-Jul-99 19:00	107.06	100.94	12.07	10.86	183.67
04-Jul-99 07:00	107.40	101.21	12.08	10.89	183.56
04-Jul-99 19:00	107.59	101.39	12.08	10.85	183.60
05-Jul-99 07:00	107.76	101.56	12.08	10.85	183.50
05-Jul-99 19:00	106.39	100.40	12.05	10.87	183.51
06-Jul-99 07:00	108.10	101.82	12.08	10.85	183.49
06-Jul-99 19:00	107.42	101.27	12.06	10.86	183.40
07-Jul-99 07:00	108.78	102.36	12.10	10.85	183.32
07-Jul-99 19:00	107.65	101.38	12.08	10.85	183.34
08-Jul-99 07:00	106.85	100.75	12.06	10.86	183.18
08-Jul-99 19:00	106.91	100.85	12.06	10.85	183.42
09-Jul-99 07:00	107.86	101.49	12.09	10.86	183.31
09-Jul-99 19:00	107.57	101.35	12.07	10.85	183.68
10-Jul-99 07:00	108.43	101.93	12.12	10.87	183.20
10-Jul-99 19:00	107.23	101.15	12.06	10.85	183.61
11-Jul-99 07:00	107.63	101.43	12.09	10.88	183.31
11-Jul-99 19:00	105.55	99.87	12.02	10.83	183.77
12-Jul-99 07:00	105.98	100.03	12.07	10.88	183.55
12-Jul-99 19:00	105.27	99.32	12.06	10.87	183.64
13-Jul-99 07:00	106.71	99.94	12.06	10.90	183.54
13-Jul-99 19:00	107.18	99.98	12.07	10.86	183.51
14-Jul-99 07:00	107.72	100.46	12.09	10.85	183.59
14-Jul-99 19:00	107.07	100.02	12.06	10.86	183.67
15-Jul-99 07:00	106.62	99.81	12.03	10.83	183.71
15-Jul-99 19:00	92.19	86.82	11.82	10.91	184.01
16-Jul-99 07:00	73.48	70.02	11.50	10.92	184.39
16-Jul-99 19:00	77.20	73.37	11.56	10.93	184.50
17-Jul-99 07:00	96.07	90.22	11.88	10.93	183.77
17-Jul-99 19:00	101.41	94.69	11.92	10.88	183.49
18-Jul-99 07:00	106.90	99.42	11.99	10.85	183.27
18-Jul-99 19:00	107.11	100.15	11.96	10.80	183.09
19-Jul-99 07:00	107.46	100.44	12.05	10.88	182.98
19-Jul-99 19:00	107.08	100.14	12.04	10.89	183.60
20-Jul-99 07:00	107.56	100.46	12.07	10.91	183.55
20-Jul-99 19:00	105.18	98.36	12.05	10.88	183.86
21-Jul-99 07:00	105.78	98.64	12.00	10.86	183.79
21-Jul-99 19:00	105.04	97.87	11.99	10.84	183.96
22-Jul-99 07:00	106.41	99.22	11.98	10.82	183.98
22-Jul-99 19:00	104.41	97.68	11.92	10.79	184.18





Date	M <sub>WHBII,BFW</sub> tonne/hr	M <sub>WHB,STEAM</sub> tonne/hr	P <sub>WHB,STEAM</sub> MPag	P <sub>STEAM</sub> MPag	T <sub>IN,WHBII,BFW</sub> °C
23-Jul-99 07:00	106.95	99.71	11.98	10.85	183.92
23-Jul-99 19:00	105.41	98.25	11.98	10.89	184.12
24-Jul-99 07:00	97.03	90.68	11.89	10.93	184.26
24-Jul-99 19:00	104.21	97.42	11.92	10.84	184.01
25-Jul-99 07:00	105.55	98.71	11.92	10.79	184.04
25-Jul-99 19:00	106.55	99.38	11.95	10.82	183.81
26-Jul-99 07:00	108.62	101.18	11.97	10.78	183.76
26-Jul-99 19:00	108.08	100.59	12.00	10.79	183.96
27-Jul-99 07:00	108.86	100.93	12.03	10.80	183.87
27-Jul-99 19:00	106.67	98.90	11.98	10.82	183.97
28-Jul-99 07:00	107.18	99.45	11.97	10.80	183.98
28-Jul-99 19:00	104.95	97.69	11.92	10.81	184.07
29-Jul-99 07:00	105.64	98.24	11.95	10.85	184.14
29-Jul-99 19:00	104.45	97.19	11.93	10.83	184.17
30-Jul-99 07:00	107.01	99.45	11.95	10.81	183.93
30-Jul-99 19:00	107.82	100.29	11.94	10.80	183.93
31-Jul-99 07:00	108.88	101.46	11.97	10.77	183.91
31-Jul-99 19:00	109.42	102.11	11.94	10.75	184.10



APPENDIX B

GAS CONSTANTS AND EQUATIONS

The RKS EOS is used to model the process. Specifics of this EOS and the Shomate Equation can be found in the following tables and equations.

Table B-1 Gas Component Properties

Gas	T <sub>C</sub> K	P <sub>C</sub> *10 <sup>-6</sup> Paa	MWT	σ reduced volume shift	p RKS param	Δh <sup>o</sup> <sub>f,298</sub>
NH <sub>3</sub>	405.6	11.28	17.0304	0.0380	0.8779	-45.89806
N <sub>2</sub>	126.2	3.39	28.0134	-0.0111	0.3631	0
H <sub>2</sub>	33.2	1.3	2.0158	-0.0111	0.1061	0
He	5.2	0.227	4.00260	-0.0028	-0.1318	0
Ar	150.8	4.87	39.948	-0.0028	0.3632	0
CH <sub>4</sub>	190.6	4.6	16.0426	-0.0014	0.4068	-74.87310

Table B-2 Gas Component Shomate Constants from 298 K to 1400K

Gas	Ã	Ã	Ã	Ã	Ã	Ã
NH <sub>3</sub>	19.99563	49.77119	-15.37599	1.921168	0.189174	-53.30667
N <sub>2</sub>	26.09200	8.218801	-1.976141	0.159274	0.044434	-7.989230
H <sub>2</sub>	33.10780	-11.50800	11.60930	-2.844400	-0.159665	-9.991971
He	20.79331	0	0	0	0	0
Ar	20.79331	0	0	0	0	0
CH <sub>4</sub>	-0.703029	108.4773	-42.52157	5.862788	0.678565	-76.84376

$$a_{C,i} = \frac{\Omega_a R^2 T_{C,i}^2}{P_{C,i}}$$

(B.1)

$$b_i = \frac{\Omega_b R T_{C,i}}{P_{C,i}}$$

(B.2)

$$c_i = \frac{\sigma_i R T_{C,i}}{P_{C,i}}$$

(B.3)

$$a_i = a_{C,i} \alpha_i$$

(B.4)

$$a = \sum_i \sum_j y_i y_j \sqrt{a_i a_j} (1-k_{ij})$$

(B.5a)



$$= K_0 + K_1 \sqrt{T} + K_2 T \quad (\text{B.5b})$$

$$b = \sum_i y_i b_i \quad (\text{B.6})$$

$$c = \sum_i y_i c_i \quad (\text{B.7})$$

$$A_i = \frac{\Omega_a \alpha_i P_{R,i}}{T_{R,i}^2} \quad (\text{B.8})$$

$$B_i = \frac{\Omega_b P_{R,i}}{T_{R,i}} \quad (\text{B.9})$$

$$C_i = \frac{\sigma_i P_{R,i}}{T_{R,i}} \quad (\text{B.10})$$

$$A = \frac{a P}{(R T)^2} \quad (\text{B.11})$$

$$B = \frac{b P}{R T} \quad (\text{B.12})$$

$$C = \frac{c P}{R T} \quad (\text{B.13})$$

$$\sqrt{\alpha_i} = 1 + p_i (1 - \sqrt{T_{R,i}}) \quad (\text{B.14})$$

$$\sigma_i = \frac{c_i P_{C,i}}{R T_{C,i}} \quad (\text{B.15})$$

$$p_i = 0.480 + 1.574 \omega_i - 0.176 \omega_i^2 \quad (\text{B.16})$$

$$k_{i,j} \approx 0^{[25]} \quad (\text{B.17})$$

$$K_0 = \sum_i \sum_j \left( y_i y_j \sqrt{a c_i a c_j} (1 - k_{i,j}) (1 + p_j + p_i + p_i p_j) \right) \quad (\text{B.18})$$

$$K_1 = \sum_i \sum_j \left( y_i y_j \sqrt{a c_i a c_j} (1 - k_{i,j}) \left( \frac{p_i + p_i p_j}{\sqrt{T_{C,i}}} + \frac{p_j + p_i p_j}{\sqrt{T_{C,j}}} \right) \right) \quad (\text{B.19})$$

$$K_2 = \sum_i \sum_j y_i y_j \sqrt{a c_i a c_j} (1 - k_{i,j}) \frac{p_i p_j}{\sqrt{T_{C,i} T_{C,j}}} \quad (\text{B.20})$$



# APPENDIX C

## MATLAB<sup>®</sup>, SIMULINK<sup>®</sup> AND MAPLE<sup>®</sup> CODE

Matlab<sup>®</sup>, Simulink<sup>®</sup> and Maple<sup>®</sup> files used throughout this thesis, for model development and case studies, are listed here for convenience. Actual coding details, which include process design parameters, are covered by the Saskferco and University of Alberta secrecy agreement<sup>[17]</sup> and are not included here

**Table C-1      Process Simulation Files**

#	Filename	Description
1	WHBI.m	S-Function for WHB I
2	WHBII.m	S-Function for WHB II
3	GG.m	S-Function for Gas-Gas Exchanger
4	R1.m	S-Function for Reactor 1 (includes R1B1, R1B2 & R1PH)
5	R2.m	S-Function for Reactor 2
6	dataWHBI.m	Data File for E1.m s-function
7	dataWHBII.m	Data File for E2.m s-function
8	dataGG.m	Data File for E3.m s-function
9	dataR1.m	Data File for R1.m s-function
10	dataR2.m	Data File for R2.m s-function
11	init.m	Initialize all state variables @ t=0, for s-functions
12	flowarea.m	Subroutine for calculating available flow area
13	conversion.m	Subroutine for calculating ammonia conversion
14	kinetics.m	Subroutine for calculating reaction kinetics
15	mwt.m	Subroutine for calculating the molecular weight of the synthesis gas
16	rks_act.m	Subroutine for RKS fugacity calculations
17	rks_dh.m	Subroutine for RKS enthalpy changes of ammonia system
18	rks_dh2.m	Subroutine for RKS enthalpy changes of ammonia system with different inlet and outlet pressures
19	rks_rho.m	Subroutine for RKS EOS density calculation
20	steam.m	Subroutine for steam tables fit equations
21	ammonia.mdl	Ammonia process simulation





Figure C-1 Simulink Block Diagram

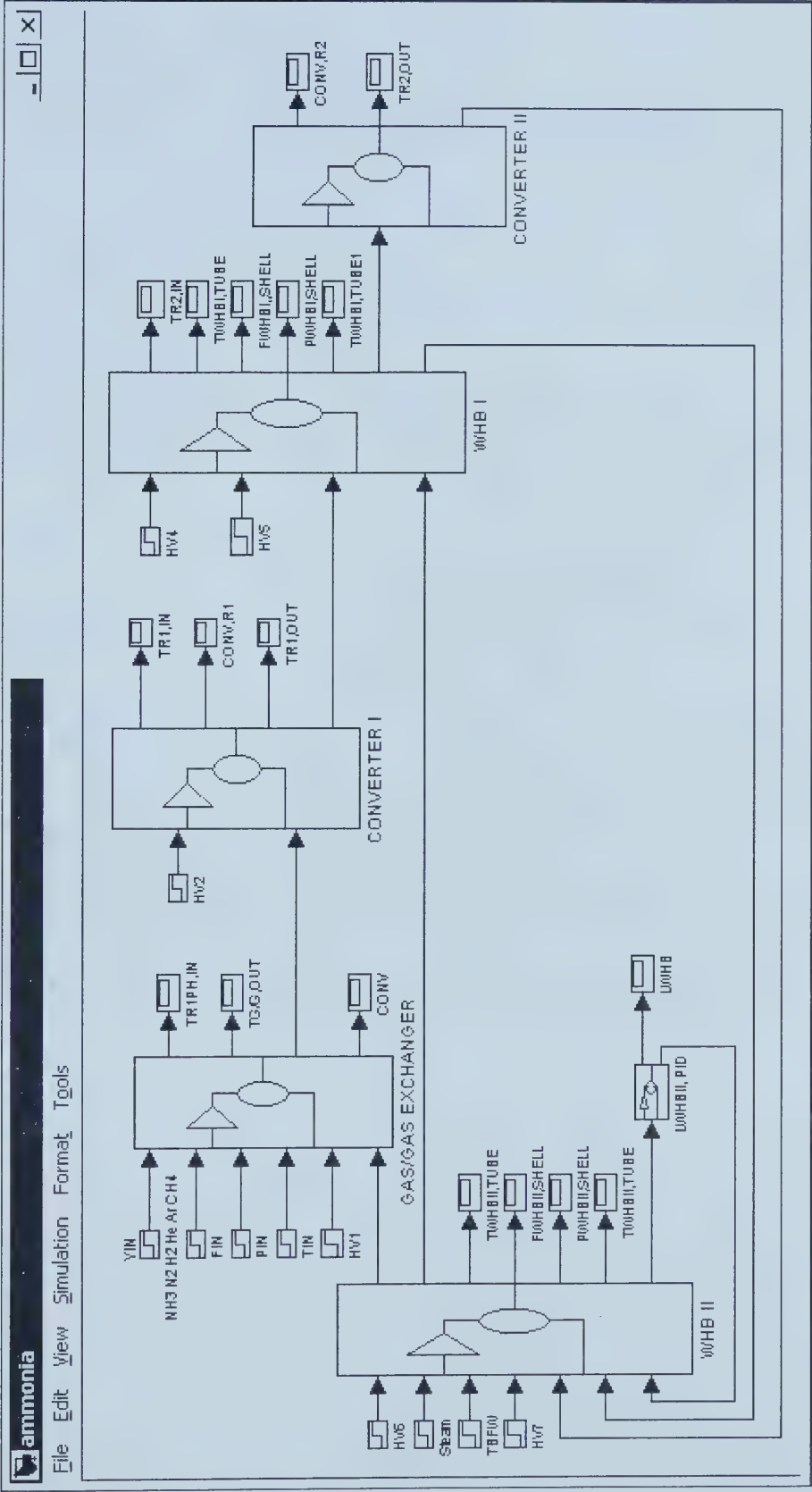




**Table C-2      RKS EOS Calculations**

#	Filename	Description
1	HR.mws	Calculate residual enthalpy symbolically
2	HR.txt	Calculate residual enthalpy symbolically

**Table C-3      Catalyst Effectiveness Parameter Update Files**

#	Filename	Description
1	param_solve.m	Invoke parameter update problem, plot solution
2	loadrx.m	Subroutine to read plant data
3	rxdata.txt	Plant data
4	param_update.m	Initialize parameter update problem
5	set_options.m	Subroutine to set options to solve Matlab functions
6	param_xo.m	Subroutine to scale variables and set upper and lower limits
7	rks_abc.m	Subroutine to calculate RKS thermodynamic properties for initialization
8	rks_abc2.m	Subroutine to calculate RKS thermodynamic properties for initialization (excluding fugacity)
9	rks_act.m	Subroutine for RKS fugacity calculations
10	rks_dh2.m	Subroutine for RKS enthalpy changes of ammonia system with different inlet and outlet pressures
11	rks_rho.m	Subroutine for RKS EOS density calculation
12	mwt.m	Subroutine for calculating the synthesis gas molecular weight
13	fnh3_out.m	Subroutine to calculate reaction variables for initialization
14	fbal.m	Subroutine to calculate variable estimates for initialization
15	param_con.m	Equality and inequality constraints for parameter updates
16	param_opt.m	Objective function for parameter updates
17	param_results.m	Convert solved variables to appropriate units and scaling
18	Hmatrix.mws	Calculate $\Phi$ as a function of process inputs
19	Hmatrix.txt	Process calculations for parameter update matrix
20	Hvalues.txt	Process values for parameter update matrix



**Table C-4      Process Optimization Files**

#	Filename	Description
1	nh3_solve.m	Invoke optimization update problem, plot solution
2	loadnh3.m	Subroutine to read plant data
3	nh3data.txt	Plant data
4	nh3_update.m	Initialize optimization update problem
5	set_options.m	Subroutine to set options to solve Matlab functions
6	nh3_xo.m	Subroutine to Scale variables and set upper and lower limits
7	rks_abc.m	Subroutine to calculate RKS thermodynamic properties for initialization
8	rks_abc2.m	Subroutine to calculate RKS thermodynamic properties for initialization (excluding fugacity)
9	rks_act.m	Subroutine for RKS fugacity calculations
10	rks_dh.m	Subroutine for RKS enthalpy changes of ammonia system
11	rks_rho.m	Subroutine for RKS EOS density calculation
12	mwt.m	Subroutine for calculating the synthesis gas molecular weight
13	flowarea.m	Subroutine for calculating available flow area
14	fbal.m	Subroutine to calculate variable estimates for initialization
15	steam.m	Subroutine for steam tables fit equations
16	steam_tables.m	Subroutine for steam table lookup values
17	ynh3_out2.m	Subroutine for converter output variables
18	nh3_con.m	Equality and inequality constraints for parameter updates
19	nh3_opt.m	Objective function for parameter updates
20	nh3_results.m	Subroutine to convert solved variables to appropriate units and scaling

**Table C-5      State Space Matrices**

#	Filename	Description
1	StateSpace.mws	Calculate state space matrices
2	nh3_m1.txt	State space equations
3	nh3_v1.txt	Process values to determine local state space
4	obs_ctrl.m	Check controllability and observability of full and reduced matrix
5	nh3_tf.m	Evaluate state space properties – check stability, controller gain, etc.

**Table C-6      Process Control Simulations**

#	Filename	Description
1	ammonia_PID.mdl	Ammonia process with PID control
2	ammonia_LQP.mdl	Ammonia process with LQR control



## APPENDIX D

### PROCESS MODEL

Calculations and results of the process model not presented in Chapter 2 can be found in the following sections.

#### D.1 Calculations

Equations D.1 to D.16 comprise the synthesis gas enthalpy, average heat capacity and average density calculations as function of Equations 2.32, 2.33 and 2.41.

$$\left[ \Delta h_{G/G,TUBE}, C_{P,G/G,TUBE}, \rho_{G/G,TUBE} \right] = f(T_{WHBI,TUBE}, T_{G/G,TUBE}, P_{R2}, y_{R2}) \quad (D.1)$$

$$\left[ \Delta h_{G/G,SHELL}, C_{P,G/G,SHELL}, \rho_{G/G,SHELL} \right] = f(T_{G/G,SHELL,IN}, T_{G/G,SHELL}, P_{IN,SG}, y_{IN}) \quad (D.2)$$

$$\left[ \Delta h_{G/G,BY1}, C_{P,G/G,BY1}, \rho_{G/G,BY1} \right] = f(T_{G/G,SHELL,IN}, T_{G/G,BY}, P_{IN,SG}, y_{IN}) \quad (D.3)$$

$$\left[ \Delta h_{G/G,BY2}, C_{P,G/G,BY2}, \rho_{G/G,BY2} \right] = f(T_{G/G,SHELL}, T_{G/G,BY}, P_{IN,SG}, y_{IN}) \quad (D.4)$$

$$\left[ \Delta h_{R1PH,TUBE}, C_{P,R1PH,TUBE}, \rho_{R1PH,TUBE} \right] = f(T_{G/G,BY}, T_{R1PH,TUBE}, P_{IN,SG}, y_{IN}) \quad (D.5)$$

$$\left[ \Delta h_{R1PH,SHELL}, C_{P,R1PH,SHELL}, \rho_{R1PH,SHELL} \right] = f(T_{R1B1}, T_{R1PH,SHELL}, P_{R1B1}, y_{R1B1}) \quad (D.6)$$

$$\left[ \Delta h_{R1PH,BY1}, C_{P,R1PH,BY1}, \rho_{R1PH,BY1} \right] = f(T_{G/G,BY}, T_{R1PH,B}, P_{IN,SG}, y_{IN}) \quad (D.7)$$

$$\left[ \Delta h_{G/G,BY2}, C_{P,G/G,BY2}, \rho_{R1PH,BY1} \right] = f(T_{R1PH,TUBE}, T_{R1PH,BY}, P_{IN,SG}, y_{IN}) \quad (D.8)$$

$$\left[ \Delta h_{R1B1}, C_{P,R1B1}, \rho_{R1B1} \right] = f(T_{R1PH,B}, T_{R1B1}, P_{IN,SG}, P_{R1B1}, y_{IN}) \quad (D.9)$$

$$\left[ \Delta h_{R1B2}, C_{P,R1B2}, \rho_{R1B2} \right] = f(T_{R1PH,SHELL}, T_{R1B2}, P_{R1B1}, P_{R1B2}, y_{R1B1}) \quad (D.10)$$

$$\left[ \Delta h_{WHBI,TUBE}, C_{P,WHBI,TUBE}, \rho_{WHBI,TUBE} \right] = f(T_{R1B2}, T_{WHBI,TUBE}, P_{R1B2}, y_{R1B2}) \quad (D.11)$$

$$\left[ \Delta h_{WHBI,BY1}, C_{P,WHBI,BY1}, \rho_{WHBI,BY1} \right] = f(T_{R1B2}, T_{WHBI,BY}, P_{R1B2}, y_{R1B2}) \quad (D.12)$$

$$\left[ \Delta h_{WHBI,BY2}, C_{P,WHBI,BY2}, \rho_{WHBI,BY2} \right] = f(T_{WHBI,TUBE}, T_{WHBI,BY}, P_{R1B2}, y_{R1B2}) \quad (D.13)$$

$$\left[ \Delta h_{R2}, C_{P,R2}, \rho_{R2} \right] = f(T_{WHBI,B}, T_{R2}, P_{R1B2}, P_{R2}, y_{R1B2}) \quad (D.14)$$

$$\left[ \Delta h_{WHBI,TUBE}, C_{P,WHBI,TUBE}, \rho_{WHBI,TUBE} \right] = f(T_{R2}, T_{WHBI,TUBE}, P_{R2}, y_{R2}) \quad (D.15)$$

$$\rho_{IN,SG,STP} = f(0.101325 \text{ MPa}, 293.15 \text{ K}, y_{IN}) \quad (D.16)$$





Steam properties are expressed as a function of temperature in Equations D.17 to D.21

$$\left[ H_{\text{WHBI,BFW}}, H_{\text{WHBI,STEAM}}, C_{\text{P,WHBI,BFW}}, \rho_{\text{WHBI,BFW}}, \rho_{\text{WHBI,STEAM}}, P_{\text{WHBI,STEAM}} \right] = f(T_{\text{WHBI,SHELL}}) \quad (\text{D.17})$$

$$\left[ H_{\text{WHBI,BFW-IN}}, \rho_{\text{WHBI,BFW-IN}} \right] = f(T_{\text{WHBI,BFW-IN}}) \quad (\text{D.18})$$

$$\left[ H_{\text{WHBI,BFW-B}}, C_{\text{P,WHBI,BFW-B}}, \rho_{\text{WHBI,BFW-B}} \right] = f(T_{\text{WHBI,SHELL-B}}) \quad (\text{D.19})$$

$$\left[ H_{\text{WHBI,BFW-M}}, C_{\text{P,WHBI,BFW-M}}, \rho_{\text{WHBI,BFW-M}} \right] = f(T_{\text{WHBI,SHELL-M}}) \quad (\text{D.20})$$

$$\left[ H_{\text{WHBI,BFW-T}}, H_{\text{WHBI,STEAM}}, C_{\text{P,WHBI,BFW-T}}, \rho_{\text{WHBI,BFW-T}}, \rho_{\text{WHBI,STEAM}}, P_{\text{WHBI,STEAM}} \right] = f(T_{\text{WHBI,SHELL-T}}) \quad (\text{D.21})$$

Using Equation 2.54, the available flow area can be determined as follows in Equations D.22 to D.33. Process valve and piping radii were provided by Saskferco<sup>[17]</sup>.

$$Av_{\text{G/G,SHELL}} = f(r_{\text{G/G,SHELL}}, HV = 100 \%) \quad (\text{D.22})$$

$$Av_{\text{G/G,BY}} = f(r_{\text{G/G,BY}}, HV_{\text{G/G,SHELL}}) \quad (\text{D.23})$$

$$Av_{\text{RIPH,TUBE}} = f(r_{\text{RIPH,TUBE}}, HV = 100 \%) \quad (\text{D.24})$$

$$Av_{\text{RIPH,BY}} = f(R_{\text{RIPH,BY}}, HV_{\text{RIPH,BY}}) \quad (\text{D.25})$$

$$Av_{\text{WHBI,TUBE}} = f(R_{\text{WHBI,TUBE}}, HV = 100 \%) \quad (\text{D.26})$$

$$Av_{\text{WHBI,BY}} = f(R_{\text{WHBI,BY}}, HV_{\text{WHBI,BY}}) \quad (\text{D.27})$$

$$Av_{\text{WHBI,BFW}} = f(r_{\text{WHBI,BFW}}, HV = 100 \%) \quad (\text{D.28})$$

$$Av_{\text{WHBI,STEAM}} = f(r_{\text{WHBI,STEAM}}, HV = 100 \%) \quad (\text{D.29})$$

$$Av_{\text{WHBI,BFW}} = f(r_{\text{WHBI,BFW}}, HV_{\text{WHBI,BFW}}) \quad (\text{D.30})$$

$$Av_{\text{WHBI,BFW-T}} = f(r_{\text{WHBI,BFW-T}}, HV_{\text{WHBI,BFW-T}}) \quad (\text{D.31})$$

$$Av_{\text{WHBI,BFW-B}} = f(r_{\text{WHBI,BFW-B}}, HV = 100 \%) \quad (\text{D.32})$$

$$Av_{\text{WHBI,STEAM}} = f(r_{\text{WHBI,STEAM}}, HV = 100 \%) \quad (\text{D.33})$$

## D.2 Results

Results of the process model compared to actual plant operation are presented in Figures D-1 to D-10.



**Figure D-1**      **Converter One Preheat Exchanger Fitted Data**

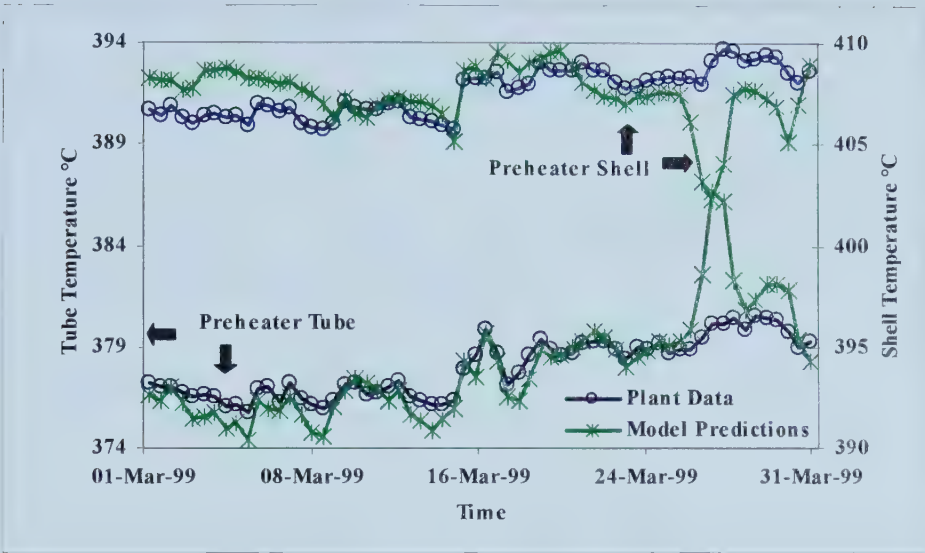


**Figure D-2**      **Converter One Preheat Exchanger Results**

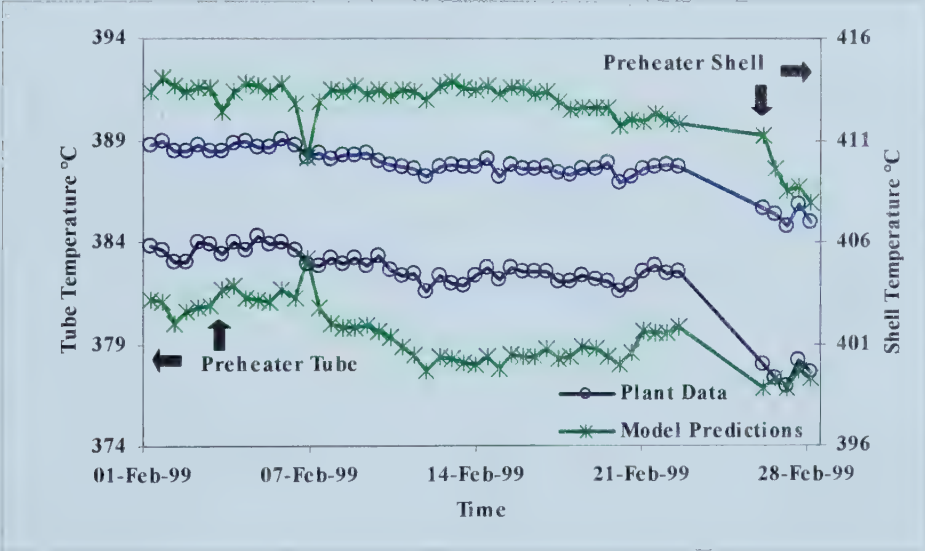




**Figure D-3      Converter One Bed Two Fitted Data**

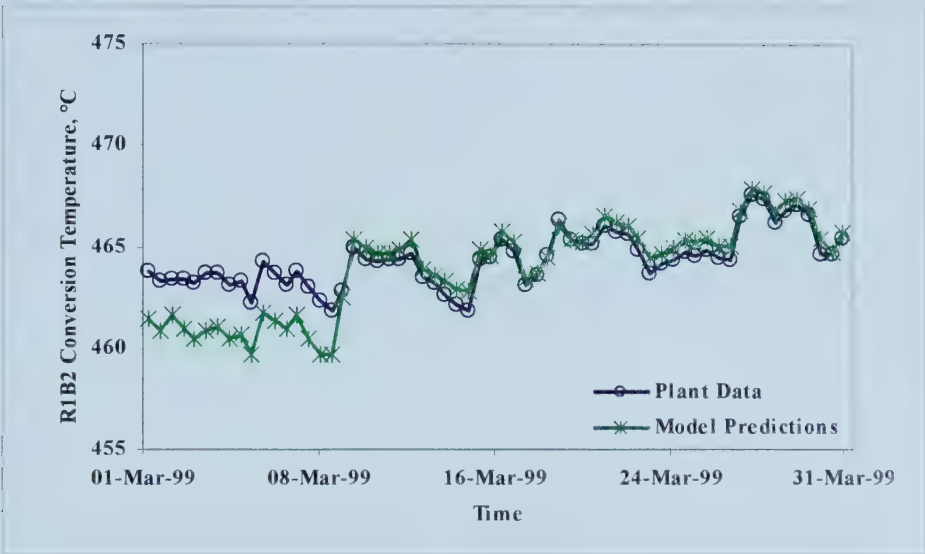


**Figure D-4      Converter One Bed Two Results**

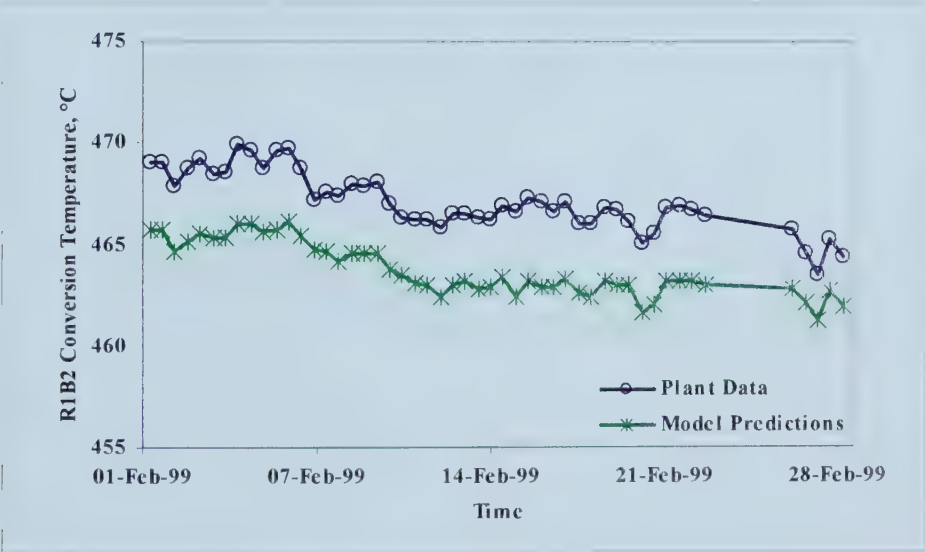




**Figure D-5**      Converter Two Fitted Data

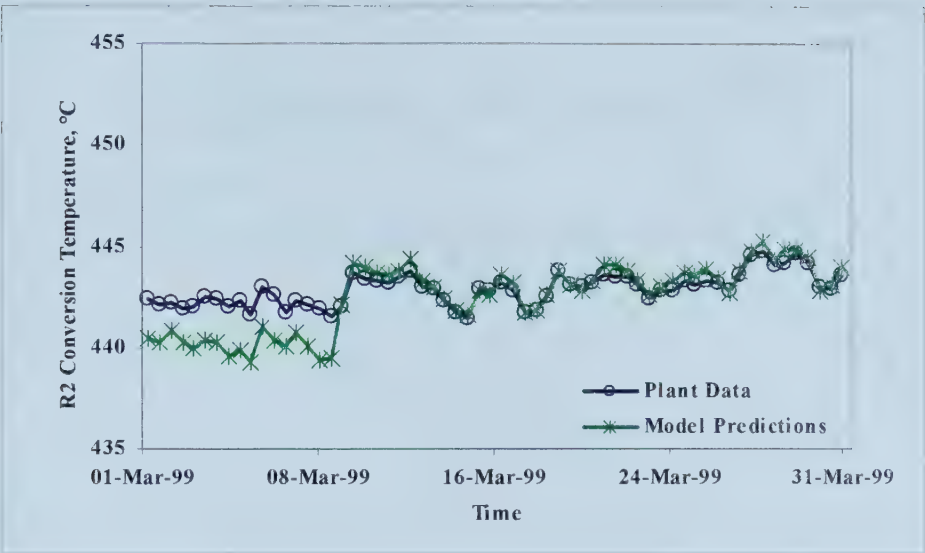


**Figure D-6**      Converter Two Results

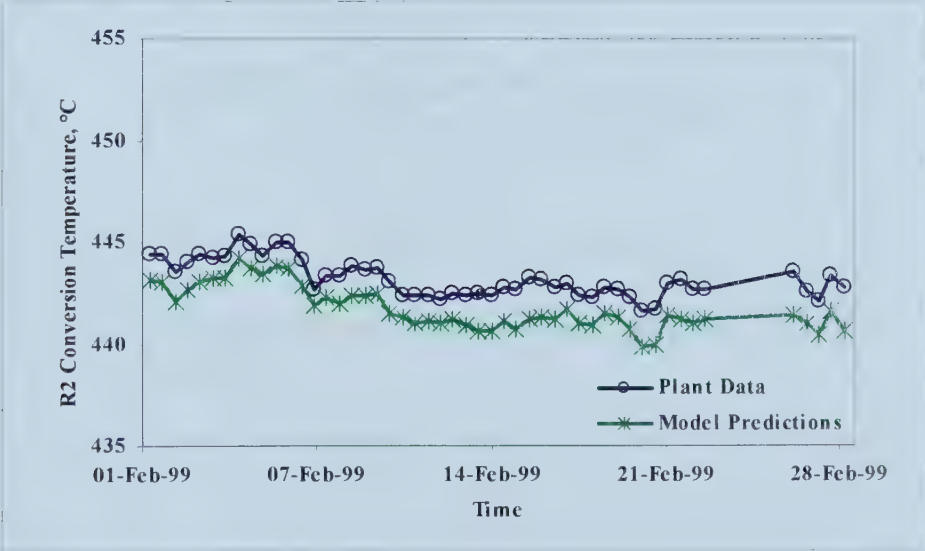






**Figure D-7**      **Waste Heat Boiler I Fitted Data**

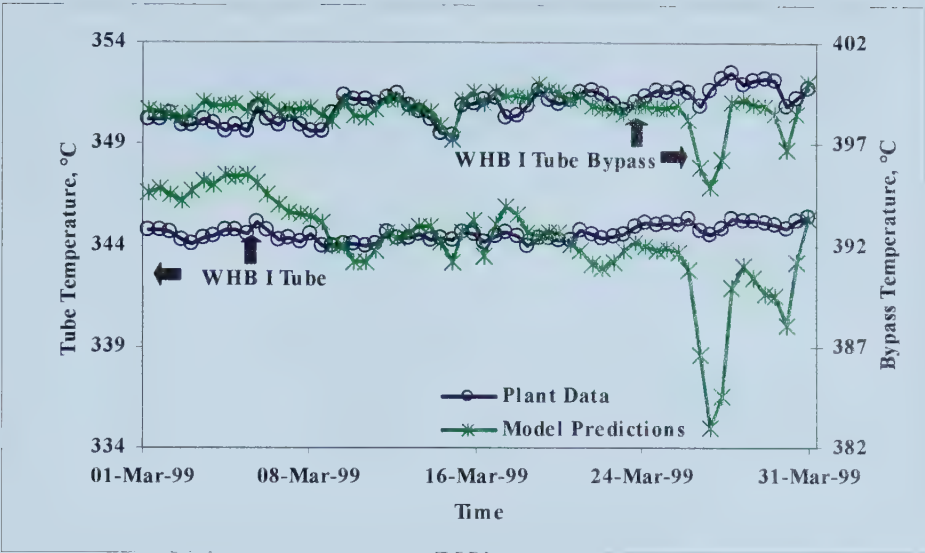


**Figure D-8**      **Waste Heat Boiler I Results**

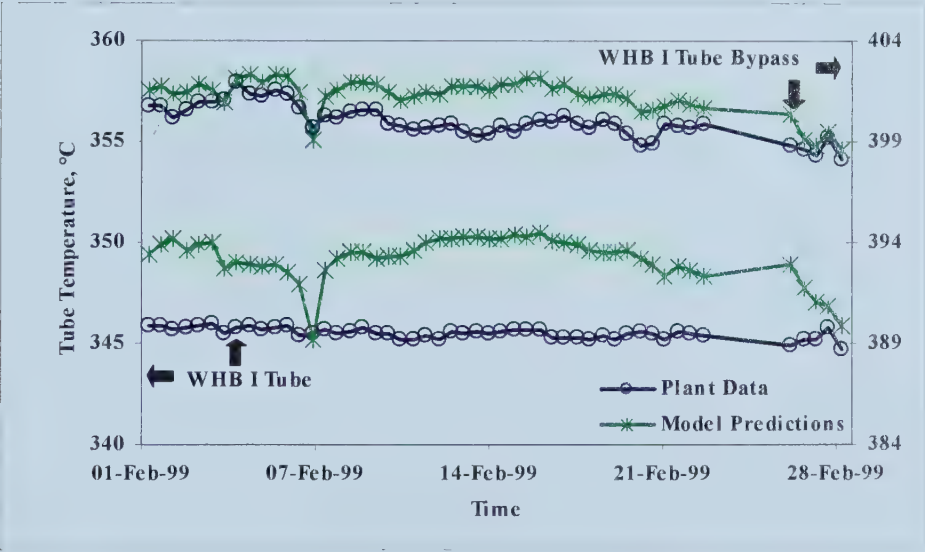




**Figure D-9      Waste Heat Boiler II Fitted Data**

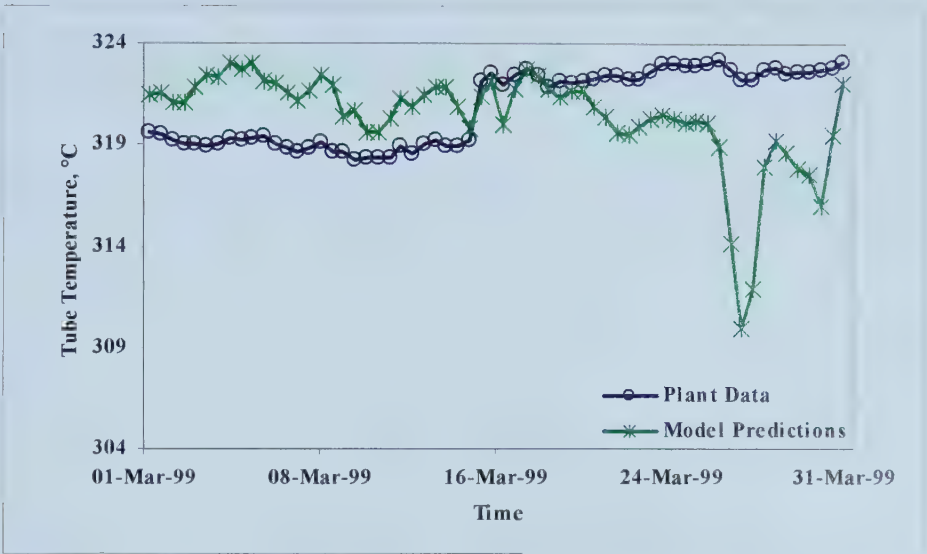
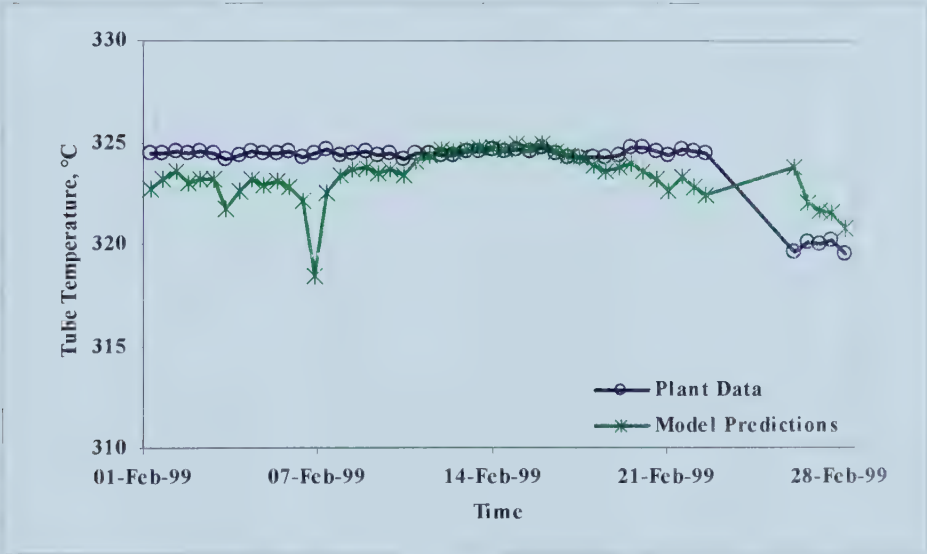


**Figure D-10      Waste Heat Boiler II Results**





# APPENDIX E

## PARAMETER UPDATE RESULTS

The parameter update problems consist of 123 dependent variables, and 3 independent variables. The objective function is posed to minimize the error between 4 measured plant variables and process model predictions.

### E.1 Dependent Variables

Three different cases of the parameter update problem are studied. Table E-1 lists the dependent variables used in case one, the sum of squares.

**Table E-1**      **Parameter Update Constraint Variables**

Equation #	Variable	Equation #	Variable	Equation #	Variable
1	$T_{R1B1}$	27	$C_{R2,IN}$	58 – 63	$a_{R1B2}$
2	$T_{R1B2}$	28	$C_{R1B1,OUT}$	64 – 69	$a_{R2}$
3	$T_{R2}$	29	$C_{R1B2,OUT}$	70 – 75	$y_{R1B1}$
4	$rxn_{R1B1}$	30	$C_{R2,OUT}$	76 – 81	$y_{R1B2}$
5	$rxn_{R1B2}$	31	$C_{R1B1,OUT2}$	82 – 87	$y_{R2}$
6	$rxn_{R2}$	32	$C_{R1B2,OUT2}$	88 – 93	$y_{A_{R1B1}}^2$
7	$A_{R1B1,IN}$	33	$C_{R2,OUT2}$	94 – 99	$y_{A_{R1B2}}^2$
8	$A_{R1B2,IN}$	34	$Z_{R1B1,IN}$	100 – 105	$y_{A_{R2}}^2$
9	$A_{R2,IN}$	35	$Z_{R1B2,IN}$	106	$h_{R_{R1B1,IN}}$
10	$A_{R1B1,OUT}$	36	$Z_{R2,IN}$	107	$h_{R_{R1B2,IN}}$
11	$A_{R1B2,OUT}$	37	$Z_{R1B1,OUT}$	108	$h_{R_{R2,IN}}$
12	$A_{R2,OUT}$	38	$Z_{R1B2,OUT}$	109	$h_{R_{R1B1,OUT}}$
13	$A_{R1B1,OUT2}$	39	$Z_{R2,OUT}$	110	$h_{R_{R1B2,OUT}}$
14	$A_{R1B2,OUT2}$	40	$Z_{R1B1,OUT2}$	111	$h_{R_{R2,OUT}}$
15	$A_{R2,OUT2}$	41	$Z_{R1B2,OUT2}$	112	$\Delta h_{R1B1}$
16	$B_{R1B1,IN}$	42	$Z_{R2,OUT2}$	113	$\Delta h_{R1B2}$
17	$B_{R1B2,IN}$	43	$\phi_{NH3,R1B1}$	114	$\Delta h_{R2}$
18	$B_{R2,IN}$	44	$\phi_{NH3,R1B2}$	115	$k_{R1B1}$



Equation #	Variable	Equation #	Variable	Equation #	Variable
19	B <sub>R1B1,OUT</sub>	45	$\phi_{NH3,R2}$	116	k <sub>_R1B2</sub>
20	B <sub>R1B2,OUT</sub>	46	$\phi_{N2,R1B1}$	117	k <sub>_R2</sub>
21	B <sub>R2,OUT</sub>	47	$\phi_{N2,R1B2}$	118	K <sub>pR1B1</sub>
22	B <sub>R1B1,OUT2</sub>	48	$\phi_{N2,R2}$	119	K <sub>pR1B2</sub>
23	B <sub>R1B2,OUT2</sub>	49	$\phi_{H2,R1B1}$	120	K <sub>pR2</sub>
24	B <sub>R2,OUT2</sub>	50	$\phi_{H2,R1B2}$	121	H <sub>rxnR1B1</sub>
25	C <sub>R1B1,IN</sub>	51	$\phi_{H2,R2}$	122	H <sub>rxnR1B2</sub>
26	C <sub>R1B2,IN</sub>	52 – 57	a <sub>R1B1</sub>	123	H <sub>rxnR2</sub>

## E.2 Intermediate Variables

Variables in Table E-1 are calculated using a steady-state form of the process equations identified in Chapter 2. The exception to this is the use of the intermediate variables defined in Equations E.1 to E.3

$$y_{\_R1B1,i}^2 = y_{R1B1,i} A_{R1B1,OUT2,i}^2 \quad (\text{E.1})$$

$$y_{\_R1B2,i}^2 = y_{R1B2,i} A_{R1B2,OUT2,i}^2 \quad (\text{E.2})$$

$$y_{\_R2,i}^2 = y_{R2,i} A_{R2,OUT2,i}^2 \quad (\text{E.3})$$

## E.3 Results

Results of the parameter update problem for R1B2 and R2 can be referenced in Figures E-1 to E-4.





**Figure E-1** R1B2 Dynamic Parameter Update

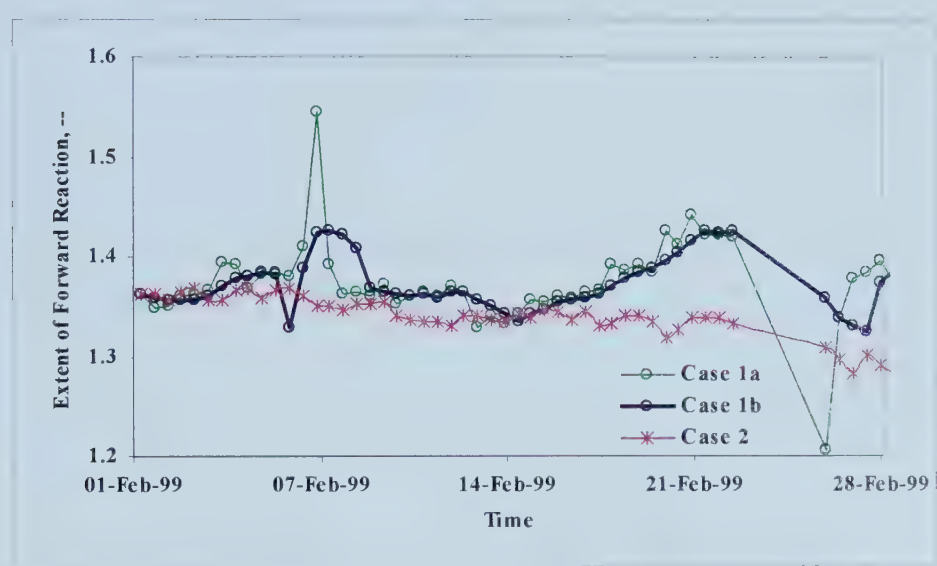


**Figure E-2** R2 Dynamic Parameter Update

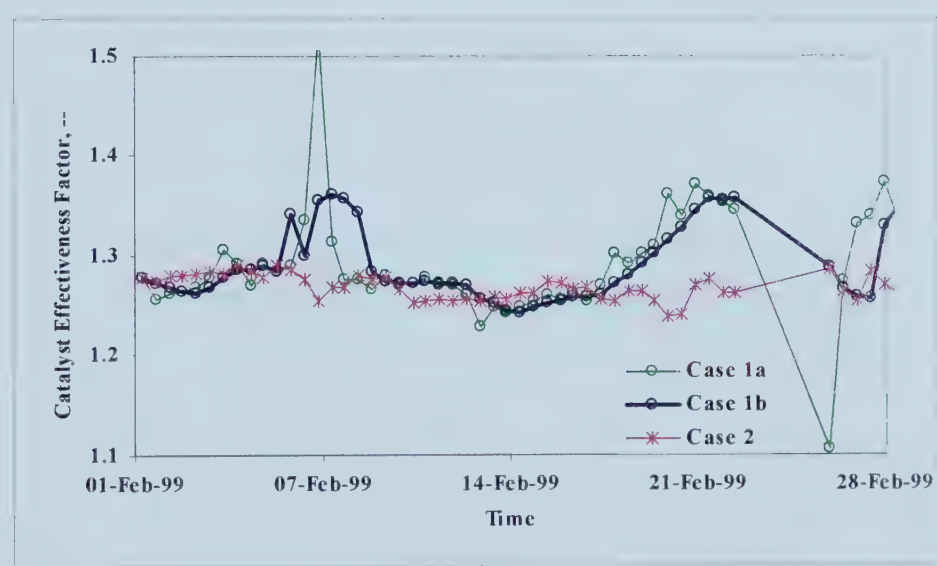




**Figure E-3** R1B2 Conversion Temperature Error

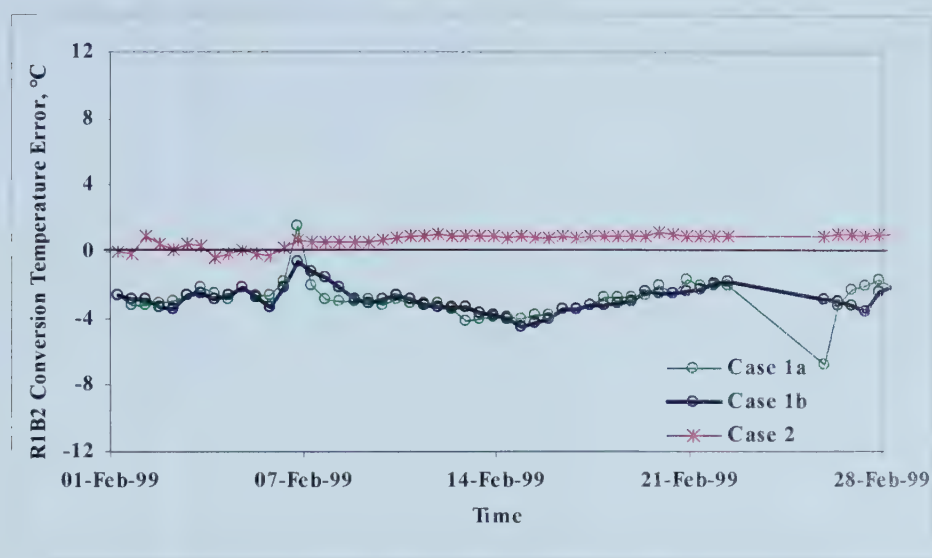
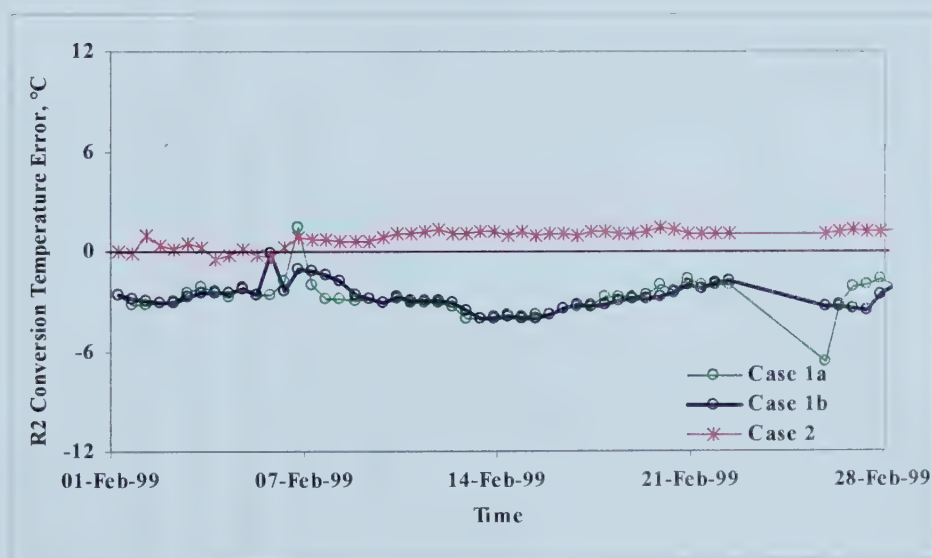


**Figure E-4** R2 Conversion Temperature Error





APPENDIX F

PROCESS OPTIMIZATION

Optimization of the process unit is implemented on the process model using 249 variables, subject to 245 equality constraints and 8 inequality constraints. Barring active constraints, the problem contains a minimum of 4 degrees of freedom. Table F-1 lists the dependent variables used.

Table F-1 Dependent Variables per Equality Equations

Equation #	Variable	Equation #	Variable	Equation #	Variable
1	T <sub>G/G,SHELL</sub>	17	Δh <sub>G/G,SHELL</sub>	29-34	a <sub>G/G,SHELL</sub>
2	T <sub>G/G,BY</sub>	18	Δh <sub>G/G,BY</sub>	35-40	a <sub>G/G,BY</sub>
3	T <sub>R1PH,TUBE</sub>	19	Δh <sub>R1PH,TUBE</sub>	41-46	a <sub>R1PH,TUBE</sub>
4	T <sub>R1PH,BY</sub>	20	Δh <sub>R1PH,BY</sub>	47-52	a <sub>R1PH,BY</sub>
5	T <sub>R1BI</sub>	21	Δh <sub>R1BI,OUT</sub>	53-58	a <sub>R1BI,OUT</sub>
6	T <sub>R1PH,SHELL</sub>	22	Δh <sub>R1PH,SHELL</sub>	59-64	a <sub>R1PH,SHELL</sub>
7	T <sub>R1B2</sub>	23	Δh <sub>R1B2,OUT</sub>	65-70	a <sub>R1B2,OUT</sub>
8	T <sub>WHBI,TUBE</sub>	24	Δh <sub>WHBI,TUBE</sub>	71-76	a <sub>WHBI,TUBE</sub>
9	T <sub>WHB,BY</sub>	25	Δh <sub>WHBI,BY</sub>	77-82	a <sub>WHBI,B</sub>
10	T <sub>R2</sub>	26	Δh <sub>R2,OUT</sub>	83-88	a <sub>R2,OUT</sub>
11	T <sub>WHBI,TUBE</sub>	27	Δh <sub>WHBI,TUBE</sub>	89-94	a <sub>WHBI,TUBE</sub>
12	T <sub>G/G,SHELL</sub>	28	Δh <sub>G/G,TUBE</sub>	95-100	a <sub>G/G,TUBE</sub>
13	T <sub>WHBI,SHELL</sub>				
14	T <sub>WHBI,SHELL-B</sub>				
15	T <sub>WHBI,SHELL-M</sub>				
16	T <sub>WHBI,SHELL-T</sub>				



**Table F-1 Dependent Variables per Equality Equations (cont'd)**

Equation #	Variable	Equation #	Variable	Equation #	Variable	Equation #	Variable	Equation #	Variable
101	A <sub>SG,IN</sub>	117	B <sub>SG,IN</sub>	133	C <sub>SG,IN</sub>	149	Z <sub>SG,IN</sub>	165	hR <sub>SG,IN</sub>
102	A <sub>G/G,SHELL</sub>	118	B <sub>G/G,SHELL</sub>	134	C <sub>G/G,SHELL</sub>	150	Z <sub>G/G,SHELL</sub>	166	hR <sub>G/G,SHELL</sub>
103	A <sub>G/G,BY</sub>	119	B <sub>G/G,BY</sub>	135	C <sub>G/G,BY</sub>	151	Z <sub>G/G,BY</sub>	167	hR <sub>G/G,B</sub>
104	A <sub>RIPH,TUBE</sub>	120	B <sub>RIPH,TUBE</sub>	136	C <sub>RIPH,TUBE</sub>	152	Z <sub>RIPH,TUBE</sub>	168	hR <sub>RIPH,TUBE</sub>
105	A <sub>RIPH,BY</sub>	121	B <sub>RIPH,BY</sub>	137	C <sub>RIPH,BY</sub>	153	Z <sub>RIPH,BY</sub>	169	hR <sub>RIPH,BY</sub>
106	A <sub>RIBI,OUT</sub>	122	B <sub>RIBI,OUT</sub>	138	C <sub>RIBI,OUT</sub>	154	Z <sub>RIBI,OUT</sub>	170	hR <sub>RIBI,OUT</sub>
107	A <sub>RIBI,OUT2</sub>	123	B <sub>RIBI,OUT2</sub>	139	C <sub>RIBI,OUT2</sub>	155	Z <sub>RIBI,OUT2</sub>	171	hR <sub>RIBI,OUT2</sub>
108	A <sub>RIPH,SHELL</sub>	124	B <sub>RIPH,SHELL</sub>	140	C <sub>RIPH,SHELL</sub>	156	Z <sub>RIPH,SHELL</sub>	172	hR <sub>RIPH,SHELL</sub>
109	A <sub>RIB2,OUT</sub>	125	B <sub>RIB2,OUT</sub>	141	C <sub>RIB2,OUT</sub>	157	Z <sub>RIB2,OUT</sub>	173	hR <sub>RIB2,OUT</sub>
110	A <sub>RIB2,OUT2</sub>	126	B <sub>RIB2,OUT2</sub>	142	C <sub>RIB2,OUT2</sub>	158	Z <sub>RIB2,OUT2</sub>	174	hR <sub>RIB2,OUT2</sub>
111	A <sub>WHBI,TUBE</sub>	127	B <sub>WHBI,TUBE</sub>	143	C <sub>WHBI,TUBE</sub>	159	Z <sub>WHBI,TUBE</sub>	175	hR <sub>WHBI,TUBE</sub>
112	A <sub>WHBI,BY</sub>	128	B <sub>WHBI,BY</sub>	144	C <sub>WHBI,BY</sub>	160	Z <sub>WHBI,BY</sub>	176	hR <sub>WHBI,BY</sub>
113	A <sub>R2,OUT</sub>	129	B <sub>R2,OUT</sub>	145	C <sub>R2,OUT</sub>	161	Z <sub>R2,OUT</sub>	177	hR <sub>R2,OUT</sub>
114	A <sub>R2,OUT2</sub>	130	B <sub>R2,OUT2</sub>	146	C <sub>R2,OUT2</sub>	162	Z <sub>R2,OUT2</sub>	178	hR <sub>R2,OUT2</sub>
115	A <sub>WHBI,TUBE</sub>	131	B <sub>WHBI,TUBE</sub>	146	C <sub>WHBI,TUBE</sub>	163	Z <sub>WHBI,TUBE</sub>	179	hR <sub>WHBI,TUBE</sub>
116	A <sub>G/G,TUBE</sub>	132	B <sub>G/G,TUBE</sub>	148	C <sub>G/G,TUBE</sub>	164	Z <sub>G/G,TUBE</sub>	180	hR <sub>G/G,TUBE</sub>





**Table F-1**      **Dependent Variables per Equality Equations (cont'd)**

Equation #	Variable	Equation #	Variable	Equation #	Variable	Equation #	Variable	Equation #	Variable
181	$\Gamma_{\text{XRIB1}}$	184	$K_{\text{PRIB1}}$	187	$k_{\text{RIB1}}$	190-195	$y_{\text{RIB1}}$	208	$\text{HrXRIB1}$
182	$\Gamma_{\text{XRIB2}}$	185	$K_{\text{PRIB2}}$	188	$k_{\text{RIB2}}$	196-201	$y_{\text{RIB2}}$	209	$\text{HrXRIB2}$
183	$\Gamma_{\text{XR2}}$	186	$K_{\text{PR2}}$	189	$k_{\text{R2}}$	202-207	$y_{\text{R2}}$	210	$\text{HrXR2}$
211	$\phi_{\text{NH3,RIB1}}$	214	$\phi_{\text{N2,RIB1}}$	217	$\phi_{\text{H2,RIB1}}$	220-225	$y_{\text{A}_{\text{RIB1}}}^2$		
212	$\phi_{\text{NH3,RIB2}}$	215	$\phi_{\text{N2,RIB2}}$	218	$\phi_{\text{H2,RIB2}}$	226-231	$y_{\text{A}_{\text{RIB2}}}^2$		
213	$\phi_{\text{NH3,R2}}$	216	$\phi_{\text{N2,R2}}$	219	$\phi_{\text{H2,R2}}$	232-237	$y_{\text{A}_{\text{R2}}}^2$		
238	$Q_{\text{G/G}}$	242	$\text{ff}_{\text{G/G,SHELL}}$						
239	$Q_{\text{RIPH}}$	243	$\text{ff}_{\text{RIPH,TUBE}}$						
240	$Q_{\text{WHBI}}$	244	$\text{ff}_{\text{WHBI,TUBE}}$						
241	$Q_{\text{WHBI}}$	245	$\text{ff}_{\text{WHBI,SHELL-B}}$						



# APPENDIX G

## CONTROLLER SYNTHESIS RESULTS

Appendix G is used to describe details of the control structure and to present results for the WHB level control and the converter open loop and closed loop responses. Local values of the state space matrices are included as a point of interest.

### G.1 Controller Variables

Tables G-1 to G-4 catalog the controller design variables.

**Table G-1 State Space Variables**

#	x	units	#	x	units	#	x	units
1	T <sub>G/G,SHELL</sub>	°C	13	G <sub>H2,R1B2</sub>	mol	25	G <sub>N2,R2</sub>	mol
2	T <sub>G/G,BY</sub>	°C	14	G <sub>He,R1B2</sub>	mol	26	G <sub>H2,R2</sub>	mol
3	T <sub>G/G,TUBE</sub>	°C	15	G <sub>AR,R1B2</sub>	mol	27	G <sub>He,R2</sub>	mol
4	G <sub>NH3,R1B1</sub>	mol	16	G <sub>CH4,R1B2</sub>	mol	28	G <sub>AR,R2</sub>	mol
5	G <sub>N2,R1B1</sub>	mol	17	T <sub>R1B2,OUT</sub>	°C	29	G <sub>CH4,R2</sub>	mol
6	G <sub>H2,R1B1</sub>	mol	18	T <sub>R1PH,BY</sub>	°C	30	T <sub>R2,OUT</sub>	°C
7	G <sub>He,R1B1</sub>	mol	19	T <sub>R1PH,SHELL</sub>	°C	31	T <sub>WHBII,TUBE</sub>	°C
8	G <sub>AR,R1B1</sub>	mol	20	T <sub>R1PH,TUBE</sub>	°C	32	T <sub>WHBII,SHELL-B</sub>	°C
9	G <sub>CH4,R1B1</sub>	mol	21	T <sub>WHBI,TUBE</sub>	°C	33	T <sub>WHBII,SHELL-M</sub>	°C
10	T <sub>R1B1,OUT</sub>	°C	22	T <sub>WHBI,B</sub>	°C	34	T <sub>WHBII,SHELL-T</sub>	°C
11	G <sub>NH3,R1B2</sub>	mol	23	T <sub>WHBI,SHELL</sub>	°C			
12	G <sub>N2,R1B2</sub>	mol	24	G <sub>NH3,R2</sub>	mol			

**Table G-2 Manipulated Variables**

#	u	units
1	HV <sub>G/G,SHELL</sub>	%
2	HV <sub>R1PH,TUBE</sub>	%
3	HV <sub>WHBI,TUBE</sub>	%
4	HV <sub>WHBII,STEAM</sub>	%



**Table G-3**      **Control Variables**

#	y	units
1	$T_{R1PH,BY}$	°C
2	$T_{R1PH,SHELL}$	°C
3	$T_{WHBI,B}$	°C

**Table G-4**      **Disturbance Variables**

#	w	units	#	w	units	#	w	units
1	$F_{GAS,IN}$	C	5	$y_{H2,IN}$	mol %	9	$T_{G/G,SHELL,IN}$	C
2	$P_{GAS,IN}$	C	6	$y_{He,IN}$	mol %	10	$T_{WHBII,BFW,IN}$	C
3	$y_{NH3,IN}$	C	7	$y_{AR,IN}$	mol %			
4	$y_{N2,IN}$	mol %	8	$y_{CH4,IN}$	mol %			



G.2 Open Loop Responses

RGA analysis and PID tuning are accomplished by observing the open loop response of the control variables to perturbations in the manipulated variables. Results can be found in Figures G-1 to G-5.

Figure G-1 CV<sub>1</sub> Step, Open Loop

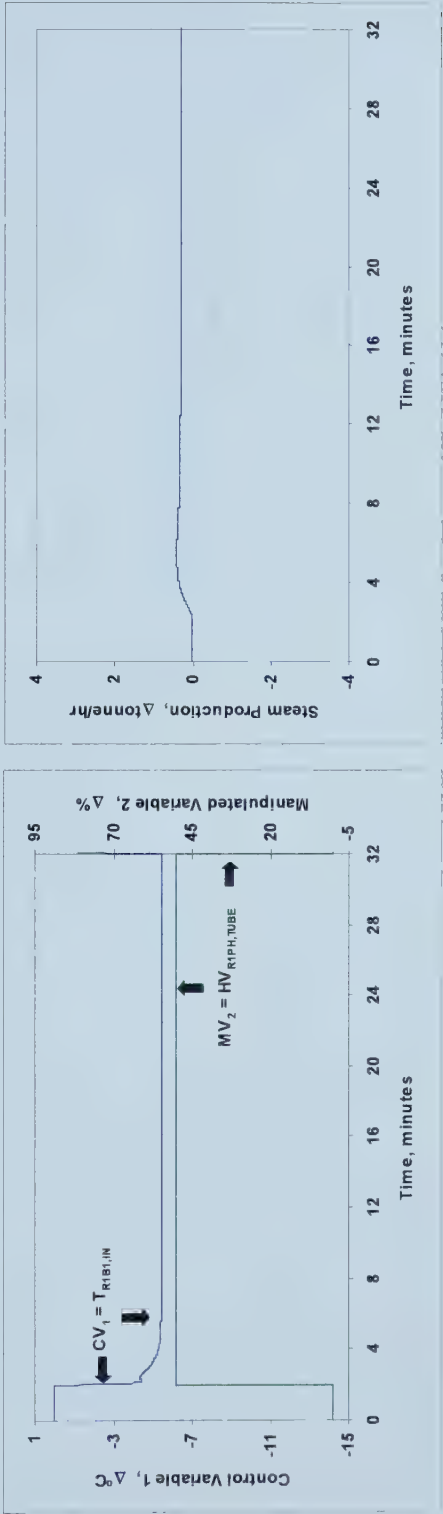






**Figure G-2**  $CV_2$  Step with  $MV_1$ , Open Loop

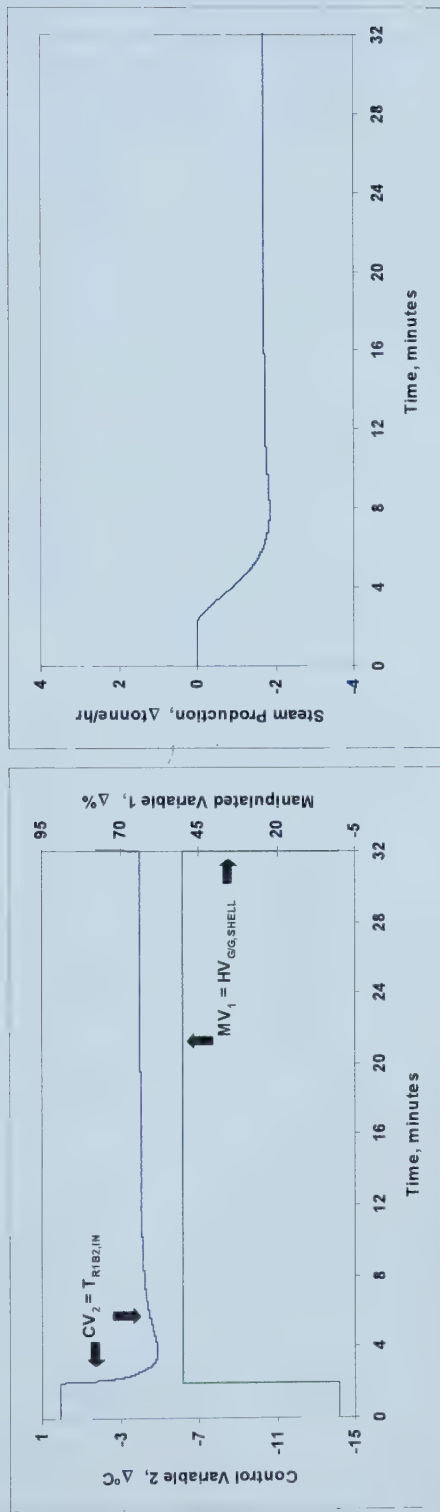


**Figure G-3**  $CV_2$  Step Up with  $MV_4$ , Open Loop

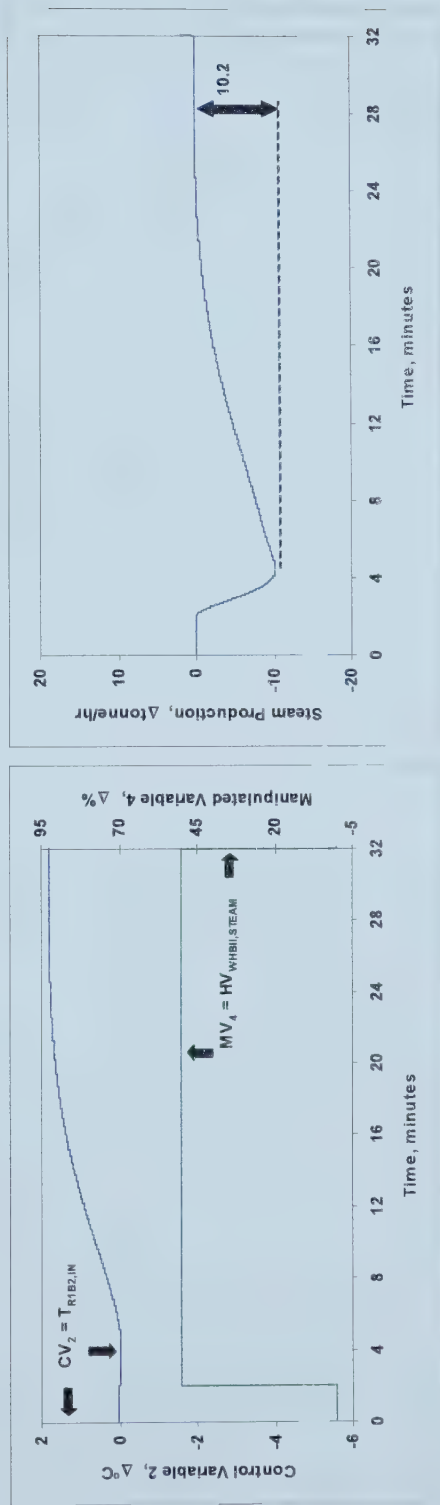




**Figure G-4** CV<sub>2</sub> Step Down with MV<sub>4</sub>, Open Loop

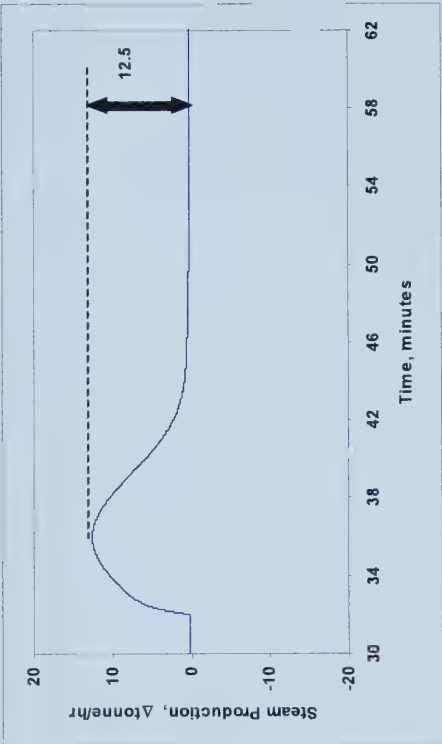


**Figure G-5** CV<sub>3</sub> Step, Open Loop





## G.3 State Space Matrices

Local analysis of controller observability and controllability is evaluated from the following state space matrices. Tables G-5 to G-8 represent the local state space with 34 state variables. Eliminating composition from the state space to remove near-zero eigenvalues resulted in 16 state space variables. The corresponding state space matrices are presented in Table G-9 to G-11.

### Table G-5 Local Value of $A(x,u,w)$ Matrix

61  
A

[illegible]



**Table G-6      Local Value of B(x,u,w) Matrix**

**B=**

0.063	0	0	0
-15.287	0	0	0
0	0	0	0
0	0	0	0
0	0	0	0
0	0	0	0
0	0	0	0
0	0	0	0
0	0	0	0
0	0	0	0
0	0	0	0
0	0	0	0
0	0	0	0
0	0	0	0
0	0	0	0
0	0	0	0
0	0	0	0
0	0	0	0
0	0	0	0
0	-2.191	0	0
0	0	0	0
0	5.076	0	0
0	0	-1.733	0
0	0	0.027	0
0	0	0	0
0	0	0	0
0	0	0	0
0	0	0	0
0	0	0	0
0	0	0	0
0	0	0	0
0	0	0	0
0	0	0	0.011
0	0	0	-0.044
0	0	0	-0.001









**Table G-8      Local Value of G(x,u,w) Matrix**

**G=**

-0.1	-147.7	-102.4	-95.2	-66.8	-75.0	-145.8	-0.2	-1.2	0
0.0	0.0	0	0	0	0	0.0	0	0	0
0.5	615.6	1012.6	72.9	144.7	1443.9	579.9	1.1	5.6	0
-55.6	458402.0	-156989.4	-11296.7	-22430.9	-223871.9	-89904.1	6425.5	0	0
27.8	-145794.8	314023.1	-17257.0	-34265.7	-341989.0	-137338.4	-3212.8	0	0
83.4	-472024.8	-776436.3	497970.6	-110938.5	-1107222.8	-444646.4	-9638.3	0	0
0.0	-9118.4	-14998.8	-1079.3	551698.7	-21388.8	-8589.5	0	0	0
0.0	-26207.7	-43109.3	-3102.1	-6159.5	492366.6	-24687.6	0	0	0
0.0	-105195.5	-173036.7	-12451.4	-24723.8	-246755.9	454747.8	0	0	0
-0.1	-172.1	-108.2	-100.7	-70.8	-73.5	-201.4	16.7	0	0
-22.8	-30550.2	-50252.2	-3616.1	-7180.1	-71661.2	-28778.2	2797.9	0	0
11.4	15275.1	25126.1	1808.0	3590.1	35830.6	14389.1	-1399.0	0	0
34.2	45825.3	75378.3	5424.1	10770.2	107491.8	43167.3	-4196.9	0	0
0.0	0.0	0.0	0.0	0.0	0.0	0.0	0	0	0
0	0.0	0.0	0.0	0.0	0.0	0.0	0	0	0
0.0	0.0	0.0	0.0	0.0	0.0	0.0	0	0	0
0.0	-55.6	-91.4	-6.6	-13.1	-130.4	-52.4	5.2	0	0
0.0	0.0	0	0	0	0	0	0	0	0
1.1	1428.9	2350.4	169.1	335.8	3351.7	1346.0	0.6	0	0
-1.6	-1916.0	-1256.6	-1177.8	-830.2	-874.8	-2134.5	-0.9	0	0
0.4	584.3	961.2	69.2	137.3	1370.7	550.4	0.3	0	0
0.0	0.0	0.0	0.0	0.0	0.0	0.0	0.0	0	0
0	0	0	0	0	0	0	0	0	0
-17.5	-23444.7	-38564.3	-2775.0	-5510.1	-54993.9	-22084.8	2353.7	0	0
8.7	11722.3	19282.1	1387.5	2755.1	27497.0	11042.4	-1176.8	0	0
26.2	35167.0	57846.4	4162.5	8265.2	82490.9	33127.3	-3530.5	0	0
0.0	0.0	0.0	0.0	0.0	0.0	0.0	0	0	0
0.0	0.0	0.0	0.0	0.0	0.0	0.0	0	0	0
0.0	0	0	0	0	0.0	0.0	0	0	0
0.0	-25.6	-42.1	-3.0	-6.0	-60.0	-24.1	2.6	0	0
0.6	826.3	1359.1	97.8	194.2	1938.1	778.3	0.6	0	1.9
0	0	0	0	0	0	0	0	0	0.0
0	0	0	0	0	0	0	0	0	0.0
0	0	0	0	0	0	0	0	0	0







**Table G-10**      Local Value of B(x,u,w) Matrix – Reduced and Scaled

**B=**

1.058E-03	0	0	0
-2.548E-01	0	0	0
0	0	0	0
0	0	0	0
0	0	0	0
0	-3.652E-02	0	0
0	0	0	0
0	8.461E-02	0	0
0	0	-2.889E-02	0
0	0	4.582E-04	0
0	0	0	0
0	0	0	0
0	0	0	0
0	0	0	1.822E-04
0	0	0	-7.398E-04
0	0	0	-2.177E-05

**Table G-11**      C Matrix – Reduced and Scaled

**C=**

0	0	0	0	0	1	0	0	0	0	0	0	0	0	0	0
0	0	0	0	0	0	1	0	0	0	0	0	0	0	0	0
0	0	0	0	0	0	0	0	0	1	0	0	0	0	0	0

















University of Alberta Library



0 1620 1493 8250

**B45564**